Developing a Primary Concentration Method Using Antibody Fragments to Capture Enteric Viruses in Source Waters

by

Nahed N. Mahrous

A Thesis

presented to

The University of Guelph

In partial fulfilment of requirements
for the degree of

Doctor of Philosophy

in

Environmental Sciences and Toxicology

Guelph, Ontario, Canada

ABSTRACT

Developing a Primary Concentration Method Using Antibody Fragments

to Capture Enteric Viruses in Source Waters

Nahed Mahrous
University of Guelph, 2019

Advisor(s):
Professor Marc Habash

Human enteric viruses (EVs) are the commonest causes of waterborne gastroenteritis. Principal challenges to monitoring EVs from water sources include filtering large volumes of water and low recoveries, which can negatively affect downstream applications for detection. Bioactive paper is a low-cost and easy-to-use paper-based sensor that can rapidly and specifically capture and detect pathogens from a sample. We developed antibody-based technologies using cellulose filters and magnetic beads for the capture and detection of EVs from water samples. As a proof-of-concept, RV group A strains, published monomeric single domain antibodies (sdAbs, RV-2KD1 and RV-3B2) and full-length IgG (RV-IgG 26) specific to the RV capsid protein VP_6 were selected. For the antibody-cellulose filter technology, the sdAbs were linked to a cellulose binding module (CBM2a) for attachment to cellulose filter paper. For the antibody-bead technology, the sdAbs and RV-IgG 26 were chemically conjugated to magnetic beads. Western blot and enzyme-linked immunosorbent assay (ELISA) confirmed all RV-mAbs specifically bound RV strains from human and bovine sources. ELISA indicated that the N-terminal linking of 2KD1 to CBM2a was shown to be the most effective. RV recovery by both technologies

from spiked tap and river water was analyzed via quantitative PCR and scanning electron microscopy. RV recoveries of 27.44 ± 22.93% and 26.72 ± 19.66% with RV alone and 29.18 ± 2.38% and 32.66 ± 8.74% in competition with adenovirus from tap and river waters, respectively, were obtained using the filter-based technology. RV recoveries from river water in competition with adenovirus were 1.85 ± 1.46% and 0.87 ± 0.4% using RV-IgG 26- and RV-2KD1-coupled beads, respectively, using the magnetic bead-based technology. SEM confirmed the attachment of RV on the antibody-linked filter and the beads. Both technologies yielded non-specific binding which is a well-known challenge with antibody-based assays (e.g., ELISA). More optimization steps are needed to improve the capturing of the virus by these developed technologies and minimize non-specific binding. The successful development of a filter-based capture technology for the detection of EVs will provide a critical tool for rapid and cost-effective routine monitoring of critical human pathogens to inform water safety and treatment.

Key Words: Antibody, Enteric viruses, Carbohydrate-binding module, Rotavirus, VP_6, Cellulose filter, Magnetic beads.

CO-AUTHORSHIP STATEMENT

This thesis is written in a monograph format and includes 6 chapters. The first chapter represents an extensive literature review on the presence of EVs in water environments and challenges of their detection. The review also focuses on applications of the recombinant antibody and the CBM-fusion technologies in detecting microorganisms. This chapter is currently being prepared for publication and entitled as “A review: Challenges in Analysis of Enteric Viruses in Water Environment”. The manuscript is co-authored with Dr. Marc Habash (supervisor). I wrote the manuscript and Dr. Habash provided guidance in manuscript preparation and revision. I will be the first author of this publication, which is aimed to be submitted to one of the following journals: Critical Reviews in Environmental Science and Technology, Critical Reviews in Microbiology, Applied and Environmental Microbiology or Environmental Science and Pollution Research.

The second chapter represents the rationale beyond RV selection as a surrogate in this proof-of-principle project along with goal, hypotheses and objectives of this study. The third chapter describes the material and the methods that were used to obtain the objectives and test hypotheses of this research. The fourth chapter of the thesis, however, elucidates the obtained results, which are further discussed in the fifth chapter. Finally, general conclusions of the topic along with recommendations for potential future work are provided in chapter six of this thesis. Supplemented data are provided in 6 appendices.

The work and findings from this work are planned to be prepared for publications into two articles. The first manuscript entitled initially as “Developing a Bioactive Paper Using Single Domain Antibody Fragment to Capture Rotavirus in Water Sources”. This

manuscript is planned to include the design and production of the CBM-V_HHs in *E. coli* in addition to their usage in developing a bioactive cellulose filter paper to capture RV from water sources. The second manuscript entitled initially as “One Step Capturing of Rotavirus in Water Using IgG- and V_HH-coupled Magnetic Beads”. This manuscript is planned to include the production of RV full-length IgG in plant, conjugation of the magnetic beads with the RV-IgG 26 and the RV-2KD1 and their ability to capture RV in water in compare to the RV-HA-2KD1-CBM2a-cellulose filter paper. These manuscripts are co-authored with Dr. Marc Habash and Dr. J. Christopher Hall (supervisors). I designed and conducted the experiments, collected and analyzed all the data. I will write the manuscripts as I will be the first author on both of these publications. Laboratory support and guidance in data interpretation were provided by Dr. Habash while Dr. Hall provided financial support and guidance in engineering the antibodies. Funding support for this work was also provided by the Saudi Cultural Bureau in Ottawa.

DEDICATION

This dissertation is dedicated to those that went through the day without a clean glass of safe and healthy water.

ACKNOWLEDGEMENTS

I would like to express my sincerest gratitude to my supervisors, Dr. Marc Habash and Dr. J. Chirstopher Hall, for providing me with opportunity to be a part of their research group. I thank you for all the challenges that you have given me. These experiences have made me even more determined and skilled than I could ever imagine.

I sincerely thank the members of my advisory committee, Dr. Keith Warriner and Dr. Jamshid Tanha, for their feedback and sense of humor.

I am also grateful to Dr. Wing-Fai for sharing knowledge and advices at various time points, Mr. John Teat for assistance with orders for cloning and protein experiments and Mr. Robert Harris for assistance with electron microscope analysis.

I would also like to express my gratitude to the Ministry of Education in the Kingdom of Saudi Arabia for awarded me with the custodian of the two holy mosques' scholarship to pursue a doctorate degree from a Canadian university. I would specially like to thank my advisor at the Saudi Cultural Bureau in Ottawa, Dr. Samia Osman who is always understanding and supportive.

Much gratitude is extended to my parents and sister for making me always want to keep things in perspective and showing me what matters most in life.

TABLE OF CONTENT

Abstract i

Co-Authorship Statement iv

Dedication vi

Acknowledgements vii

Table of Content viii

List of Tables xiv

List of Figures xvi

List of Appendices xix

List of Symbols AND Abbreviations xx

1 LITERATURE REVIEW 1

1.1 Enteric Viruses in Water Environment 1

1.1.1 Challenges in Enteric Viruses Analysis 5

1.1.1.1 Concentration Step 5

1.1.1.1.1 Membrane Filter Methods 7

1.1.1.1.2 Limitations of Membrane Filter Methods 14

1.1.1.2 Detection Step 18

1.1.1.2.1 Limitations of Detection Methods 20

1.1.2 Recommendations for Analysis of Enteric Viruses in Waters 23

1.2 Antibody Engineering Technology 24

1.2.1 Conventional Antibodies 24

1.2.2 Camelid Heavy Chain Antibodies 27

1.2.3 Applications of Recombinant Antibody Technology 30

1.3 Recombinant CBM-Fusion Technology 33

1.3.1 Applications of CBM-Fusion Technology 34

2 RATIONALE, GOAL, HYPOTHESES AND OBJECTIVES 38

2.1 Rational of the Research 38

2.1.1 Rotavirus 39

2.1.1.1 Structure 40

2.1.1.2 Classification 43

2.1.1.3 Diversity and Prevalence 44

2.1.1.4 Biology of RV-VP_6 45

2.2 Goal of the Research 48

2.3 Hypotheses of the Research 51

2.1.2 Cellulose Filter-V_HH Capture Technology 51

2.1.3 Immuno-Magnetic Bead Capture Technology 51

2.4 Objectives of the Research 51

3 MATERIALS AND METHODS 53

3.1 Gene Constructs of Recombinant RV-Single Domain Antibodies 54

3.1.1 Preparation of V_HH-His DNA Constructs 54

3.1.2 Preparation of HA-CBM2a-$([PT]_3T)_{3x}$S-V_HH-His DNA Construct 56

3.1.3 Preparation of HA-CBM2a DNA Constructs 60

3.1.4 Preparation of HA-CBM2a-Linker-2KD1 DNA Constructs at C- & N-Terminals 63

3.1.5 Preparation of Recombinant RV-IgG 26 DNA Construct for Expression in Planta 65

3.1.6 Recombinant RV-Capsid Protein VP_6 70

3.2 Transformation 74

3.2.1 Preparation of Chemically Competent Cells and Heat-Shock Protocol 75

3.2.2 Preparation of Electro-Competent Cells and Electroporation Protocol 76

3.3 Plasmid DNA Analysis 77

3.3.1 Polymerase Chain Reaction Amplification 77

3.3.2 DNA Extraction 79

3.3.3 Restriction Digestion 80
3.3.4 Plasmid DNA Sequencing 80
3.4 Proteins Expression and Extraction 81
3.4.1 Recombinant RV-V_HH Antibodies 81
3.4.2 Agroinfiltration of RV-IgG 26 and Protein Expression 83
3.4.3 Recombinant RV-VP_6 Protein Expression 85
3.4.3.1 Recombinant SUMO-Protease Protein Expression 86
3.5 Protein Purification 87
3.5.1 Soluble Proteins with 6x-His Tag 87
3.5.1.1 Cleavage of SUMO-VP_6 88
3.5.2 Soluble RV-IgG 26 89
3.6 Soluble Protein Characterization 89
3.6.1 Gel Electrophoresis and Western Blotting 89
3.6.2 Protein Concentration 92
3.7 Production of Virus Strains 92
3.7.1 Cell Lines Propagation 92
3.7.2 Viruses Harvesting 95
3.7.3 Quantification of Viruses 95
3.7.3.1 Plaque Assay 95
3.7.3.2 Tissue Culture Infective Dose (TCID) 50% 97
3.7.3.3 Quantitative PCR 98
3.8 Functional Analysis of Antibodies 103
3.8.1 Confirmation of RV-mAbs Binding 103
3.8.2 Enzyme-Linked Immunosorbent Assay 104
3.9 Antibody Capture Technology Development 106
3.9.1 Cellulose Filter Paper Capture System 106
3.9.1.1 Binding RV on RV-mAb Coated Cellulose Filter Paper 106

3.9.1.2 Removal of RV by RV-mAb Coated Cellulose Filter Paper 107
3.9.2 Immuno-Magnetic Capture System 109
3.9.2.1 Magnetic Beads-Antibody Conjugation 109
3.9.2.2 Removal of RV by RV-mAbs Coated Magnetic Beads 110
3.10 Electron Microscopy Analysis 110
3.10.1 Transmission Electron Microscopy 111
3.10.2 Scanning Electron Microscopy 111
3.11 Statistical Data Analysis 112
3.11.1 Data from ELISA 112
3.11.2 Data from qPCR 112
4 RESULTS 114
4.1 Cloning and Transformation of Expression Cassettes 115
4.2 Protein Expression and Purification 115
4.2.1 Recombinant RV-V_HHs 115
4.2.2 Recombinant RV-CBM2a with and without V_HHs 116
4.2.3 Recombinant RV-IgG 26 120
4.2.4 Recombinant RV-VP_6 125
4.3 Virus Propagation and Quantification 127
4.3.1 Infectivity in Cell Types 127
4.3.2 Quantification of the Virus 130
4.3.2.1 Quantification by qPCR 130
4.4 Functionality of RV-Antibodies 133
4.4.1 Detection by Western Blot 133
4.4.2 Detection by ELISA 135
4.4.2.1 Indirect ELISA 135
4.4.2.2 Sandwich ELISA 135

4.5 Antibody Capture Technology Development....144
4.5.1 Cellulose Filter Capture System....144
4.5.2 Immuno-Magnetic Capture System....152
4.6 Electron Microscopy....158
5 DISCUSSION....163
6 CONCLUSIONS AND RECOMMENDATIONS....180
6.1 Conclusions....180
6.2 Recommendations....182
6.2.1 Broader Use of Cellulose Filter Paper Capture System....182
6.2.2 Visualizing and Determining the Binding of RV-mAbs on the Virus....184
REFERENCES....187
APPENDICES....231
Appendix 1. Composition and Preparation of Reagents....231
Appendix 2. Cloning and Transformation of Expression Cassettes....239
1. Competent Bacterial Cells....239
2. Recombinant RV-V_HHs and RV-V_HHs with CBM2a....239
3. Recombinant RV-HA-CBM2a....244
4. Recombinant RV-IgG 26....247
5. Recombinant Protein RV-VP_6....250
Appendix 3. Purification of RV-V_HHs from Long Expression Protocol....254
Appendix 4. Analysis of RV-VP_6 Expression and Purification....256
1. Analysis of Recombinant RV-VP_6....256
2. Discussion....260
Appendix 5. Expression and Purification of SUMO-Protease....262
Appendix 6. Quantification of Enteric Viruses....264

1. Plaque Assay 264
2. Tissue Culture Infective Dose (TCID) 50% 266

LIST OF TABLES

Table 1.1. Features of common human enteric viruses associated with waterborne transmission. 3

Table 1.2. Comparison of common methods used for the concentrating of enteric viruses in water samples. 8

Table 1.3. Comparison of common electropositive-charged filters used for concentrating enteric viruses in water samples. 10

Table 1.4. Comparison of common electronegative-charged filters used for concentrating enteric viruses in water samples. 13

Table 1.5. Comparison of common ultrafilter membranes used for the concentrating of enteric viruses in water samples based on size. 15

Table 1.6. Comparison of common methods used for the analysis and detection of enteric viruses in different environments. 19

Table 1.7. Published enteric virus recovery rates estimated by cell culture- and PCR-based methods after concentrating the viruses from water sources by adsorption and elution methods (modified from Kunze et al., 2015). 22

Table 1.8. Various published monoclonal recombinant antibodies against enteric viruses targeting extracellular protein (Modified from Wu et al., 2017). 31

Table 2.1. Rotavirus proteins characterization (modified from Ward, 2008). 41

Table 3.1. Oligonucleotide primers and PCR product information for sequence confirmation of positive colonies. 78

Table 3.2. Secondary antibodies used in Western blot for the detection of rotavirus and RV-VP6 on PVDF membrane. 91

Table 3.3. Primary and Secondary antibodies used in ELISA for the detection of rotavirus antigen present in a sample. 105

Table 4.1. Removal of enteric viruses from spiked serum free medium (SFM) at different conditions using developed RV-HA-2KD1-$(G_4S)_{3x}$-CBM2a- and HA-CBM2a-cellulose-based filter systems. 147

Table 4.2. Removal of enteric viruses from spiked water samples at different conditions using developed 2KD-cellulose- and CBM2a-based filtration. 150

Table 4.3. Removal of human rotavirus (hRV) using RV-IgG 26-coupled-magnetic beads from spiked serum free medium (SFM) with different concentrations of human rotavirus. 155

Table 4.4. Removal of enteric viruses from spiked river water samples at lowest abundance of human rotavirus (hRV) with highest abundance of human adenovirus (hAdenoV) using developed RV-monoclonal antibodies-coupled-magnetic beads.....157

LIST OF FIGURES

Figure 1.1. Schematically representation of the structure of conventional and camelid heavy-chain antibodies with possible antigen binding fragments and amino acid sequences of the V_H in the conventional IgG and the V_HH in the camelid heavy chain IgG. 26

Figure 2.1. Structure of rotavirus virion. The virus consists of three layers. External layers consist of VP_7 and VP_4 (VP_{8*} and VP_{5*}). 42

Figure 2.2. Structure of VP_6. The VP_6 consists of two domain B and H. 46

Figure 3.1. Framework (FR) and complementarity determining regions (CDR) in the amino acids sequence of (A) 2KD1 and (B) 3B2 in the pITKan expression vector. 55

Figure 3.2. Schematic representation of the expression vector pITKan. 57

Figure 3.3. Schematic representation of V_HH gene constructs in pIT2Kan plasmid used for protein expression in *E. coli*. 58

Figure 3.4. Amino acid sequences of native family 2a carbohydrate binding models (CBM2a) from the enzyme xylanase 10A found in *Cellulomonas fimi*. 59

Figure 3.5. Amino acid sequences of modified 2KD1, expressed in this study, fused in two orintations via different linkers to native family 2a catrbohydrate binding models (CBM2a) from the enzyme xylanase 10A found in the bacteria *Cellulomonas fimi*. 64

Figure 3.6. Amino acid and nucleotide sequences of anti-VP_6 heavy varible (H_V) (A) and anti-VP_6 light variable (L_V) (B) domains expressed in this study as full RV-IgG 26. 66

Figure 3.7. Optimized nucleotides sequence of (A) Anti-VP_6-26 H_C (1,433 bp) and (B) Anti-VP_6-26 L_C (725 bp) in pPFC0205 for expression in *N. benthamiana*. 67

Figure 3.8. Schematic representation of RV-IgG 26 gene construct in pPFC0205 expression vector. 68

Figure 3.9. Schematic representation of the plant expression vector pPFC0205. 69

Figure 3.10. Amino acid and nucleotides sequences of capsid protein VP_6 from human rotavirus (hRV-VP6) group A (RV-VP_6). 71

Figure 3.11. Complete sequence alignment for non-structural protein NSP3 gene (1049 bp) from human and bovine rotavirus group A strains. 101

Figure 4.1. Affinity 6x-His tag chromatography purification profile of RV-2KD1 expressed with rapid protocol (*E. coli HB2151*; pITKan/2KD1) culture induced with 0.5 mM IPTG at 24^0C for 16 h). 117

Figure 4.2. Affinity 6x-His tag chromatography purification profile of RV-3B2 expressed with rapid protocol (*E. coli HB2151*; pITKan/3B2) culture induced with 0.5 mM IPTG at 24^0C for 16 h). 118

Figure 4.3. Western blot analysis of expressed and purified RV-3B2 and RV-2KD1 as presented in Figures 4.1 and 4.2. 119

Figure 4.4. Fusion protein expression and purification of RV-V_HHs linked to HA-CBM2a at N-terminal and His-tag at C-terminal. 121

Figure 4.5. Fusion protein expression of RV-V_HHs linked to HA-CBM2a at N- and C-terminal on 12% SDS-PAGE gels (A) and Western blot (B) of TSP from induced cultures 122

Figure 4.6. Protein A affinity chromatography purification profile of RV-IgG 26. 123

Figure 4.7. Qualitative analysis of RV-IgG 26 expression in *N. benthamiana* under reducing and non-reducing conditions. 124

Figure 4.8. Affinity 6x-His tag chromatography purification profile of RV-SUMO/VP_6. .126

Figure 4.9. Proteolytic cleavage of SUMO-VP_6 with SUMO-protease....128

Figure 4.10. Visualization of cytopathic effects by enteric viruses in cell lines. 129

Figure 4.11. Standard quantification curves of qPCR assays for (A) human adenovirus type 41 and (B) human rotavirus group A. 132

Figure 4.12. Detection of different rotavirus strains on Western blot using V_HHs with and without CBM-V_HHs and full-length IgG 26. 134

Figure 4.13. Characterization of rotavirus monoclonal antibodies binding specificity and sensitivity to rotavirus in indirect ELISA. 136

Figure 4.14. Characterization of rotavirus monoclonal antibodies binding specificity and sensitivity to rotavirus in sandwich ELISA. 138

Figure 4.15. Characterization of RV-V_HHs binding specificity and sensitivity to rotavirus in sandwich ELISA.. 139

Figure 4.16. Characterization of RV-V_HHs fusion to CBM2a binding specificity and sensitivity to rotavirus in sandwich ELISA. 141

Figure 4.17. Characterization of RV-2KD1-fusion to CBM2a binding specificity and sensitivity to rotavirus in sandwich ELISA. T....143

Figure 4.18. Immobilization of HA-CBM2a and RV-HA-2KD1-$(G_4S)_{3x}$-CBM2a on a cellulose disc for the detection of RV strains by sandwich ELISA. 145

Figure 4.19. Detection of RV-VP_6 on SDS-PAGE using antibody-coupled magentic beads. 153

Figure 4.20.Examination of isolated rotavirus (bRV-B223) by transmission electron microscopy shows a typical rotavirus particle. 159

Figure 4.21. Scanning electron microscope micrographs highlighting the attachment of rotavirus on a cellulose filter paper.....160

Figure 4.22. Scanning electron microscope micrographs highlighting the dis-attachment of rotavirus on a magnetic bead only (A), bead-coupled RV-IgG 26 (B-C) and bead-couple RV-2KD1 (D-E).....161

LIST OF APPENDICES

Appendix 1. Composition and Preparation of Reagents 231

Appendix 2. Cloning and Transformation of Expression Cassettes 239

Appendix 3. Purification of RV-V_{HH} from Long Expression Protocol 254

Appendix 4. Analysis of RV-VP_6 Expression and Purification 265

Appendix 5. Expression and Purification of SUMO-Protease 262

Appendix 6. Quantification of Enteric Viruses 264

LIST OF SYMBOLS AND ABBREVIATIONS

AdenoV	Adenovirus
AGI	Acute gastrointestinal illness
AIC	*Agrobacterium* infiltration cocktail
Amp	Ampicillin
A. thaliana	*Arabidopsis thaliana*
AstroV	Astrovirus
A. tumefaciens	*Agrobacterium tumefaciens*
AP	Alkaline phosphatase
bp	Base pair
bRV	Bovine rotavirus
ºC	Celsius
Carb	Carbenicillin
$CaCl_2$	Calcium chloride
CBDs	Cellulose binding domains
CBM/s	Carbohydrate or cellulose binding module/s
CO_2	Carbon dioxide
CC	Cell culture
CDRs	Complementarity determining regions
C. fimi	*Cellulomonas fimi*
cfu	Colony forming unit
C_H	Variable heavy constant domain
C_L	Variable light constant domain
CN	Copy number
CPE	Cytopathic effect
Cys	Cysteine
DLP	Double-layered particle
DMSO	Dimethyl sulfoxide
3D-structure	Three-dimensional structures
dsDNA	Double strand deoxyribonucleic acid
dsRNA	Double strand ribonucleic acid
DTT	Dithiothreitol
ε	Molar extinction coefficient
E. coil	*Escherichia coli*
EDTA	Ethylenediaminetetraacetic acid
ELISA	Enzyme-linked immunosorbent assay
ENF	Electronegative charged filter
EnteroV	Enterovirus
EPD	End point dilution
EPF	Electropositive charged filter
EVs	Enteric viruses
F_{ab}	Fragment antigen-binding
FBS	Fetal bovine serum
F_C	Fragment crystallizable
FRs	Framework regions
Gly	Glycine

h	Hour/s
hAdenoV	Human adenoviruses
HBGAs	Histoblood group antigens
H_C	Heavy polypeptide chains
H_CAbs	Heavy-chain antibodies
HRP	Horseradish peroxidase
hRV	Human rotavirus
H_2SO_4	Sulfuric acid
ICC-PCR	Integrated cell culture-polymerase chain reaction
ICTV	International committee on taxonomy of viruses
Ig	Immunoglobulins
IgC	Ig constant domain
IgV	Ig variable domain
IMAC	Immobilized metal affinity chromatography
Kan	Kanamycin
kDa	Kilodalton
kPa	Kilopascals
L/s	Litre/s
LB	Luria-Bertani Miller broth medium
L_C	Antibody light chain
M	Molar
mAbs	Monoclonal antibodies
MES	Morpholino-ethanesulfonic acid
MF	Microfiltration
Mg^{2+}	Magnesium
µg	Microgram
$MgCl_2$	Magnesium chloride
$MgSO_4$	Magnesium sulfate
min	Minute/s
ml	Milliliter/s
µl	Microliter
mM	Millimolar
$\mu mol/m^{-2}s$	Micromole per second
µS/cm	Micro-Siemens per centimeter
mNV	Murine norovirus
MWCO	Molecular weight cut-off
NaCl	Sodium chloride
NaOH	Sodium hydroxide
$NaPO_4$	Sodium phosphate
Na_2PO_4	Disodium phosphate
Na_3PO_4	Trisodium phosphate
NASBA	Nucleic acid sequence-based amplification
Nb	Nanobody
nm	Nanometer
NF	Nanofiltration
Ni^{+2}	Nickel

NoroV	Norovirus
NTU	Nephelometric turbidity unit
OD_{600}	Optical density at 600 nm
PBS	Phosphate buffered saline
PBST	Phosphate buffered saline with tween
PCR	Polymerase chain reaction
PD	Proportionate distance
PEG	Polyethylene glycol
pfu	Plaque forming unit
pH	Concentration of hydrogen ion in a solution
pI	Isoelectric point
IPTG	Isopropyl-ß-D-1-thiogalactopyranoside
pM	Picomolar
PMFS	Phenylmethanesulfonyl fluoride solution
PolioV	Poliovirus
PT	Proline threonine
qPCR	Quantitative polymerase chain reaction
qRT-PCR	Quantitative reverse transcriptase polymerase chain reaction
Rif	Rifampicin
RO	Reverse osmosis
rpm	Revolutions per minute
RT	Room temperature
RV	Rotavirus
S. aureus	*Staphylococcus aureus*
SDS-PAGE	Sodium dodecyl sulfate polyacrylamide gel electrophoresis
sdAb	Single domain antibody
Sec	Second
Ser	Serine
SEM	Scanning electron microscopy
SFM	Serum free medium
SP	Structural protein
ssRNA	Single stranded ribonucleic acid
TB	Terrific broth
TCID	Tissue culture infectious dose
TEM	Transmission electron microscopy
TEMED	Tetramethylethylenediamine
TFF	Tangential flow filtration
Thr	Threonine
RT-PCR	Reverse transcriptase polymerase chain reaction
TSP	Total soluble protein
UF	Ultrafiltration
VCF	Volumetric concentration factor
VFF	Vortex flow filtration
V_H	Variable heavy domain
V_HH	Camelid single domain antibody fragments
V_L	Variable light domain

NSP	Non structural protein
6x-His	Hexa-histidine

1 LITERATURE REVIEW

This review will examine the key strengths and limitations of enteric virus (EV) detection from aquatic environments, including: concentration methods and current solutions to enhance detection. Regarding enhancements to concentration and detection, application of recombinant antibody engineering will be discussed.

1.1 Enteric Viruses in Water Environment

Globally, diarrheal disease is one of the most common causes of illness and death annually in early childhood (World Health Organization, 2017). Most cases (between 6 to 22%) of acute and watery diarrhea (or acute gastrointestinal illness, AGI) are caused by EVs, particularly norovirus (NoroV) (de Roda Husman et al., 2007; Borchardt et al., 2012; Ganesh and Lin, 2013 & Health Canada, 2017).

Enteric viruses are classified into several families, including: *Adenoviridae, Astroviridiae, Caliciviridae, Picornaviridae, Polyomaviridae* and *Reoviridae,* that are based on differences in morphological, physical and chemical characteristics. They are shed in high concentrations in feces (10^5 to 10^{11} viral particles per gram) and vomit of infected hosts that may or may not exhibit symptoms (Salim et al., 1990; Blacklow and Greenberg, 1991; Wyn-Jones and Sellwood, 2001 & Ganesh and Lin, 2013). Consequently, viruses can contaminate water sources through various routes such as wastewater treatment plant effluent, disposal of sanitary sewage or sludge on land, leaking sanitary sewers, septic system effluents and infiltration of surface water into groundwater aquifers (Powell et al., 2003; Borchardt et al., 2004 & Bradbury et al., 2013). Numerous studies have indicated the presence of EVs in treated sewage, recreational

waters (e.g., pool), urban rivers, groundwater, drinking water and shellfish harvested from contaminated waters (Krikelis et al, 1985; Dewailly et al., 1986; Cecuk et al., 1993; Muscillo et al., 1994; Le Guyader et al., 1995; Patti et al., 1996; Lipp and Rose, 1997; Jiang et al., 2001 & Lee et al., 2002). Viruses enter the environment and impact susceptible hosts most frequently by the fecal-oral route (e.g., ingestion or drinking of contaminated food or water) and less frequently through respiratory droplets and contact (Taylor et al., 1995; Wyn-Jones and Sellwood, 2001; Griffin et al., 2003 & Widdowson et al., 2005). Infectious doses of EVs are considered low, ranging between 1 to 100 infection units of virus (CDCP, 2002; Lindesmith et al., 2003 & Leon and Moe, 2006). For instance, 2 to fewer than 18 NoroV particles are required to cause infection (Teunis et al., 2008). As a result, EVs can eventually become common water pollutants and public health issues (Haas et al., 1993; Fong and Lipp, 2005, Arraj et al., 2008; Okoh et al., 2010 & La Rosa et al., 2012). Human EVs associated with waterborne transmission are illustrated in Table 1.1, outlining common characteristics and diseases they cause.

The cellular and molecular structures of EVs play critical roles toward viral stability and infectivity. The absence of a lipid envelope surrounding the virus particles, results in high stability of the virus under a wide range of environmental conditions (Girones et al., 2010). Naked viruses have viral capsids, which are comprised of proteins, resistant to disinfectants and solvents. For instance, EVs in the water environment are resistant to many water treatment processes such as chlorination and are able to withstand pH ranging from 3 to 10 at low temperature (Kocwa-Haluch, 2001; Jiang et al., 2001; Fujioka and Yoneyama, 2002; Thurston-Enriquez et al., 2003 & Girones et al., 2010). For example, rotavirus (RV) and poliovirus (PolioV) have been shown to be more stable at 4

Table 1.1. Features of common human enteric viruses associated with waterborne transmission.

Family	Common Virus	Nucleic Acid	Diameter (nm)	Genome Size (bp)	Isoelectric Point	Diseases Caused	References
Adenoviridae	Adenoviruses	dsDNA	80 - 100	35,000	2.6 - 4.5	Respiratory disease, pneumonias, conjunctivitis, cystitis, gastroenteritis	Jiang, 2006
Astroviridae	Astroviruses	ssRNA	28 - 33	6,000 - 8,000	_	Gastroenteritis, diarrhea, vomiting	Schwab, 2007; Lee and Kurtz, 1982 & Finkbeiner et al., 2008
Caliciviridae	Noroviruses SRS	ssRNA	35 - 39	7,300 - 7,700	5 - 6	Gastroenteritis, nausea	Schwab, 2007 & Patel et al., 2009
Picornaviridae	Hepatitis A	ssRNA	27	7,500	2.8	Hepatitis	Pinto and Saiz, 2007
	Enterovirus e.g., Poliovirus and Coxsackievirus		30	7,000 - 8,500	4 - 6.4	Gastroenteritis, paralysis, meningitis, respiratory disease, hand-foot-mouth disease and diabetic,	Hovi et al., 2007
Polyomaviridae	Polyomaviruses	dsDNA	40 - 55	5,000	_	Kidney nephritis, respiratory and merkel cell carcinoma	Bofill-Mas et al., 2006 & Hamza et al., 2009
Reoviridae	Rotaviruses	dsRNA	70 - 80	11,000 - 25,000	8	Gastroenteritis, dehydration	Schwab, 2007 & Greenberg and Estes, 2009

Note: nm, nanometer; bp, base pair; ssRNA, single strand ribonucleic acid; dsRNA, double strand ribonucleic acid; dsDNA, double strand deoxyribonucleic acid.

°C while several types of enteroviruses (EnteroV) have been found to be most stable at -20 to 1°C (Moe, 1982 & Hurst, 1988). Thus, certain EVs, such as astrovirus (AstroV), RV, adenovirus (AdenoV) and NoroV, are capable of surviving in the environment for long periods, up to 120 days in freshwater and sewage, 130 days in seawater, up to 168 days in tap water and up to 3 years in groundwater (Melnick et al., 1980; USEPA, 1992; Jaing et al., 2001 & Health Canada, 2017).

In the environment, the number and diversity of viruses are highly variable based on many factors such as the hygienic level of the population, the prevalence of infection in distinct geographical regions and seasonal distributions. For example, in France, Le Guyader et al. (2000) reported that over a 3-year study the detection of various EVs such as EnteroV, RV and AstroV in shellfish samples occurred mostly during winter time. Also, in Japan, NoroV were detected in raw sewage throughout a year-long period with a peak in the winter (Haramoto et al., 2006). Similarly, in Canada, Pang et al. (2019) reported detection of a wide range of EVs including RV, AdenoV, AstroV, NoroV, EnteroV, sapovirus and JC virus from 6 major rivers in Alberta with RV being the most common. The group also demonstrated that NoroV, AstroV, AdenoV, sapovirus and JC virus peaked during winter months (November to March). Although little is known about detection of EVs from water sources in South America, the presence of hepatitis E-3 was reported for the first time in river and sewage sources in the central region of Argentina (Pisano et al., 2018).

Potential factors that may contribute to virus concentration and survival in water environments include sources of the water, seasonality, pH, temperature, salts and organic matter (Lodder et al., 2015 & Regnery et al., 2017). The survival of human EVs

in different environments and under various conditions (e.g., temperature, surface, pH) was reviewed in Rzeżutka and Cook (2004). The group reviewed published work on the robust survival of EVs on fomites, in waters, soil and foods. They also highlighted the lack of information particularly for water environments. The group suggested the interpretation of common features, such as number of infectious virus used in a sample, sampling times and statistical analysis of the results, to facilitate the acquisition of comparable findings for all virus types studied.

1.1.1 Challenges in Enteric Viruses Analysis

Detection and monitoring of EVs in water environments (e.g. recreational waters) is challenging for a number of reasons including: (1) their small physical size and stability, (2) viruses are diluted to a range that cannot be directly detected by current methods and (3) the concentration range of EVs in water environments varies and is not reported for many EVs. (Harwood et al., 2005; Rose et al., 2005; Eftim et al., 2017 & Gerba et al., 2017). Therefore, analysis of viruses in water environments has evolved to enhance the concentration and detection steps (Sections 1.1.1.1 and 1.1.1.2).

1.1.1.1 Concentration Step

The principle of virus concentration is based on early studies that investigated the adsorption of virus to graded collodion membranes according to virion particle size (Elford, 1931 & Ver et al., 1968). Since the 1950s, various techniques such as ion-exchange resins (Logrippo and Berger, 1952 & Kelly, 1953), flocculation (Chang et al., 1958) and filtration-elution were developed to isolate and aid in detecting viruses from

water environments. These techniques indicated the efficiency of virus recovery is influenced by many factors such as concentration method, water source (e.g., surface and ground waters), volume of the sample and the targeted virus (Cashdollar and Wymer, 2013; Pang et al., 2019 & Sinclair et al., 2019). A good concentration method should be technically simple, fast, inexpensive, able to recover viruses in a small concentrated volume (~10 to 20 ml), adequate for a wide range of viruses, be repeatable (within a laboratory) and be reproducible (between laboratories) (Wyn-Jones and Sellwood, 2001 & Fong and Lipp, 2005). However, there is currently no concentration method that can fulfill all these criteria.

Generally, concentration of viruses from water samples is performed in 2 steps. During the primary concentration step, viruses in the initial water sample are collected by adsorption onto a suitable solid surface by charge interaction or size and subsequently eluted into a smaller volume (100 to 500 ml) with a suitable buffer at a specific pH. Determining the initial volume that is required for EVs monitoring depends on the source water. Sampling volumes of 1 L for untreated wastewater are recommended (concentrated about a 10-fold). Larger volumes of 10 L for natural surface water sources (e.g., recreational and river water, concentrated about 20- to 2000-fold) and 100 to 1,000s L for drinking and ground water (concentrated about a 10- to 1000-fold) are usually collected (Wyn-Jones and Sellwood, 2001; McQuaig and Noble, 2011; Ikner et al., 2012; Gebra et al., 2018 & Haramoto et al., 2018). In the secondary step, the eluted virus from the primary concentration is concentrated further using acid flocculation or polyethylene glycol (PEG) precipitation followed by low speed centrifugation to result in a final volume between 1 to 20 ml in a neutral buffer (e.g., sodium phosphate ($NaPO_4$) or Tris-buffered

saline). The concentrated virus can be used immediately for analysis or stored at low temperature (e.g., -80 to -20ºC) (Wyn-Jones and Sellwood, 2001; Fong and Lipp, 2005; Cashdollar and Wymer, 2013 & Kunze et al., 2015). Concentrating the sample into a smaller volume results in concentration of matrix components as well, but allows removal of some factors of the matrix inhibitors (e.g., microorganisms such as mold, algae) that may interfere with the detection assay thus enabling a high level of detection specificity and sensitivity (Fong and Lipp, 2005; Hamza et al., 2011; Knight et al., 2013 & Haramoto et al., 2018).

Although many reviews have been published on the concentrating methods of EVs from different water sources (Clarke and Chang, 1959; Wyn-Jones and Sellwood, 2001; Fong and Lipp, 2005; Ikner et al., 2012; Cashdollar and Wymer, 2013 & Haramoto et al., 2018), selection of a suitable method is mainly based on the type of water sample and the target virus. The principles of each method along with applicable fields, advantages and disadvantages are summarized in Table 1.2. This review discusses concentrating EVs in water samples by adsorption and elution using membrane filters and potential matrix effects on virus adsorption and detection.

1.1.1.1.1 Membrane Filter Methods

To recover EVs from water samples, currently, 2 methods of filtration have widely been used for primary concentration step: (1) filtration by adsorption based on electro-charged filter media and (2) filtration by size (ultrafiltration e.g., capillaries, hollow fibers). Enteric viruses vary in their retention characteristics as the nature of their capsid proteins can be affected by the virus size (see Table 1.1). The net negative charge, hydrophobicity

Table 1.2. Comparison of common methods used for the concentrating of enteric viruses in water samples.

Methods	Principles	Applications	Advantages	Disadvantages	References
Ultracentrifugation	Relies on weight to separate particles.	-	Fractional of diverse virus types	Effective for small volumes, costly, requiring specialized equipment, may concentrate inhibitors	Cliver and Yeatman, 1965; Hill et al., 1971 & Fumian et al., 2010
Precipitation PEG/NaCl	Addition of PEG to a sample elute at sufficient concentration results in precipitation of the virus and other proteins.	Sewage Salt and fresh water	Simple, inexpensive, quantitative, effective for collecting several samples inexpensive, does not require specific equipment and applied to many viruses and different samples.	Time consuming, effective for small volumes, not field deployable, require pre-filtration	Chowdhary and Dhole, 2008
PEG/ dextran					Etsano et al., 2016 & Adeniji and Adewumi, 2017
Organic flocculation Ammonium sulfate	Addition of flocculants results in destabilization of particles and colloidal (agglomerate)	Surface water			
Adsorption/Elution HBGAs-magnetic	Can be coated with antibodies or other molecule (e.g., ligands) to bind the virus then separate it magnetically.	Norovirus in surface water and wastewater	Simple, fast and specific	Antibody/antigen may be too specific to group or strain, not field deployable, costly,	Cannon and Vinjé, 2008
Immuno-magnetic		Surface water			El-Galil et al., 2005
Cotton gauze pads	-	Wastewater, Sewage and seawater	Simple, effective and inexpensive for large volumes	Poor adsorption of viruses, not quantitative	Tambini et al., 1993
Microporous glass	-	-	Effective for large volumes	Not quantitative	World Health Organization, 2003
Filtration - Electropositive membrane filters	Relies on charge of the viral capsid proteins	Surface and tap waters	Reusable, effective for large volumes, no preconditioning of the sample is required	Clog easily in turbid water, costly	See Table 1.3 for more details
- Electronegative membrane filters		Surface and tap waters and sewage	Effective for large volumes	Requires preconditioning of the sample, costly	See Table 1.4 for more details
- Ultrafilters	Relies on size	Surface, drinking, and ground waters	Economical, no manipulation of the sample is required	Limited to the volume	See Table 1.5 for more details

Note: HBGAs, histo-blood group antigens.

and isoelectric point of the viral capsid are believed to be important in the attachment of viruses to a surface (Ikner et al., 2012). Adsorbing the virus to a suitable surface by charge interaction and subsequent elution of the virus by a pH-adjusted solution has been well researched.

A wide range of elution buffers including skimmed milk (pH 9), beef extract (pH 9.5), glycine/sodium hydroxide (glycine/NaOH) (pH ranges between 9.5 to 11.5) and phosphate buffers have showed successful recovery of viruses after being eluted from the electro-charged filters (Ikner et al., 2012 & Wyn-Jones and Sellwood, 2001). These buffers are capable of disturbing the electrostatic interactions between the viruses (electronegative) and the charged filter (electropositive and electronegative). Adsorption of viruses with an electropositive filter relies on the natural net negative charge of the virus surface, hence no pre-adjustment of water pH is required (Lipp et al., 2001). The adsorption of the virus is promoted by low pH and high ionic strength (Gerba, 1984a).

Several electropositive charged filters have been used for recovery of EVs in different water sources. Common electropositive filters employed in several studies with their recovery rate for EVs in waters are presented in Table 1.3. The recovery rate of the virus varies among EVs and water types. For example, recovery rates of ~72% and ~87 to 100% were demonstrated for PolioV in drinking and river water sources, respectively (Vilaginès et al., 1997 & Cashdollar and Dahling, 2006). The advantages of most electropositive filters include availability at relatively low cost (US $ 150 to 180 per filter), ease of use, effective for large volumes (20 to 100 L) with high filtration rate (up to 20 L/min) and no clogging in most cases (Cashdollar and Dahling, 2006 & Karim et al., 2009). However, they may be clogged and have low recovery rates (e.g., ~44 to 75% for PolioV

Table 1.3. Comparison of common electropositive-charged filters used for concentrating enteric viruses in water samples.

Filter	Isolated Virus	Recovery	References	Remark
1MDS Zetapor Virosorb (Cuno, Meriden, CT, USA)	Echovirus 1 in tap water	33%	Hill et al., 2009	Reusable, costly, effective for large volumes in turbid waters before occurrence of clogging, does not require preconditioning.
	Poliovirus seeded in river water	95%	Dahling, 2002	
	Poliovirus seeded into 100 L of river water	36%	Karim et al., 2009	
	Poliovirus seeded into 100 L of tap water	67%		
N66 Posidyne	Poliovirus in river water	87-100%	Cashdollar and Dahling, 2006	Economical, no cross-contamination between uses, available in cartridge and self-contained formats, Effective for large volumes, does not require preconditioning. However, clog easily in more turbid waters.
NanoCream® (Argonide, Sanford, FL, USA)	Coxsackievirus B5 seeded in tap water	27%	Karim et al., 2009	
	Echovirus 7 seeded in tap water	32%		
	Poliovirus seeded in tap water	54-84%		
	Adenoviruses in sea water	<3%	Gibbons et al., 2010	
	Noroviruses in seawater	>96%		
	Poliovirus 1 in 20 L spiked tap water	66%	Ikner et al., 2011	
	Echovirus 2 in 20 L spiked tap water	84%		
	Adenovirus 2 in 20 L spiked tap water	14%		
ViroCap	Poliovirus in deionized water	37%	Bennett et al., 2010	Economical, does not require preconditioning, simple to use, field-deployable, limited to volume and turbid waters.
	Poliovirus in seawater	44%		
Glass Wool	Poliovirus in drinking water	72%	Vilaginès et al., 1997	Economical, field-deployable, simple to use. However, clogged with turbid water and may cause inter-laboratory variation.
	Poliovirus in seawater	75%		
	Poliovirus in tap water	98%	Lambertini et al., 2008	
	Adenovirus 41 in tap water	28%		
	Norovirus GII in tap water	30%		

in sea water) when used for viruses in marine or high turbidity waters (Cashdollar and Dahling, 2006 & Bennett et al., 2010). This may be explained by the poor adsorption of viruses to the membrane filters in the presence of salt and alkalinity of seawater (Fong and Lipp, 2005 & Cashdollar and Wymer, 2013).

Adsorption of viruses to electronegative filters, on the other hand, relies on the manipulation of the water sample to result in viral particles with a net positive surface charge to adsorb on the membrane filter. Manipulation of the water can be achieved by adjusting salt concentration (addition of magnesium "Mg^{2+}" or aluminum chloride "$AlCl_3$") (Wallis and Melnick, 1967a-c; Sobsey, 1995 & Wyn-Jones and Sellwood, 2001) and pH to an acidic condition (pH 3.5) (Sobsey et al., 1973 & Wyn-Jones and Sellwood, 2001). Adding salts to a water sample promotes hydrophobic interactions and interferes with electrostatic interactions between the virus and the filters. Salts may effect virus adsorption directly by altering the charge of the filter or indirectly by (1) decreasing the pH of the sample and/or (2) forming insoluble precipitates (e.g., flocs or complexes, which result from the salt interacting with the organic material) that adsorb viruses and consequently trapped by the the filters (Lukasik et al., 2000). Negatively-charged filters have been used in cellulose nitrate and epoxy resin-bound glass-fibre tubes for recovery of EVs from different water sources. The cellulose filters were employed commonly for concentration of viruses from effluent, recreational and service waters in addition to diluted raw sewage and sludge samples (Wyn-Jones and Sellwood, 2001). The epoxy resin-bound glass-fibre tubes were employed for concentration of viruses from tap water (Jakubowski et al., 1974), river water (Morris and Waite, 1980) and other water sources (USEPA 1984, cited in Wyn-Jones and Sellwood, 2001). Common electronegative filters

employed in several studies with their recovery rate for EVs in waters are presented in Table 1.4. Although virus recoveries from negatively-charged filters are similar to those from positively-charged filters, negatively-charged filters showed higher recoveries (10 times) from seawater (Katayama et al., 2002). Generally, virus recovery rates vary with negatively-charged filter media (60% to 100%) depending on the virus and the water type (Table 1.4) (Wyn-Jones and Sellwood, 2001). The main disadvantages of using negatively-charged filters are difficulties with conditioning large volumes of water (e.g., require time and effort to transfer samples from the field to the lab for pH-adjustment and filtration process) and potential variability in charge of the filter surface that may affect the data (Fong and Lipp, 2005 & Cashdollar and Wymer, 2013).

In contrast to electro-charged filters, ultrafiltration is an alternative development for concentrating viruses from large volumes of water (ranging from 1 to 200 L) (Griffin et al., 2003 & Francy et al., 2013). The method relies on the molecular size of the virus rather than its charge and is independent of pH thus an elution step is not required. Ultrafiltration involves passing the water under pressure through a cylindrical filter with pore sizes that retain viruses (large molecular weight substances) in the retentate, whereas water and low molecular weight substances pass into the filtrate. Currently, 4 types of pressure-driven membranes are used in drinking water treatment. They are classified based on the type of targeted removal, operating pressure and pore size or molecular weight cut-off (MWCO) into low-pressure and high-pressure membranes. The types of low-pressure membranes include microfiltration (MF, 0.05 to 5 μm pore sizes) and ultrafiltration (UF, 0.005 to 0.05 μm pore sizes) and are usually used for particle/pathogen removal (Health Canada, 2017). The types of high-pressure membrane include nanofiltration (NF) and re-

Table 1.4. Comparison of common electronegative-charged filters used for concentrating enteric viruses in water samples.

Filter	Sample	Isolated Virus	Recovery	References	Remark
Millipore membrane filter (cellulose nitrate)	Surface water	Enterovirus	60%	Block and Schwartzbrod, 1989	Available at moderate cost (but more expensive than electropositive charged filters) in wide selection pore sizes and assorted adsorbent materials, applicable to adsorb viruses from different water sources, pre-adjustment with salt or acid is essential for virus adsorption. However, this may result in precipitate formation and filter clogging, and inactivation of the virus due to acidic condition, weak with higher water turbidity and often difficult to elute viruses. Generally, not field deployable.
Millipore HA coated with AL ions	40 ml MilliQ	Poliovirus	99% with 1mM NaOH (pH 10.8)	Haramoto et al., 2004	
	0.5 - 1 L Tap water		>80%		
	10 L MilliQ		>80% from		
Type-HA (Nihon Millipore, Tokyo, Japan)	2 L Seawater	Poliovirus	94% and 95% eluted with BE* and NaOH, respectively	Katayama et al., 2002	
	2 L Pure water	Poliovirus	83% and 95% eluted with BE* and NaOH, respectively		
Cox-disk filter (fiberglass asbestos epoxy)	Tap water with thiosulfate solution	Poliovirus	42-57%	Jakubowski et al., 1974	
Balston filter tube (fiber glass epoxy)	5 L Lakes, tap water and seawater	Poliovirus 1, coxsackievirus A9 Coxsackievirus B1 and echovirus	97%	Guttman-Bass and Nasser, 1984	
	3 L Wastewater		63 - 75%		
Filtrate-pleated cartridge filter (epoxy-fiberglass)	100-gal seawater	Poliovirus	~50%	Payment et al., 1976	
Fiber glass depth filter (wound)	River water	Enteric viruses	77.4%	Payment et al., 1988	
		Coliphages	65%		
Column (glass powder)	20 L tap water	Hepatitis A	100%	Gajardo et al., 1991	
	Freshwater		80%		
	Seawater		75%		
	sewage		61%		

Note: BE is beef extract elution buffer of pH 9.5, NaOH is sodium hydroxide buffer at 10 (mM) of pH 10.5-10.8.

verse osmosis (RO) and are usually used for the removal of organics and inorganics (Health Canada, 2017). Common pore size of a flow pattern used in ultrafiltration ranges between 30 to 100 kDa, although membranes with 10 kDa were used to concentrate viruses from large volumes (typically ~50 L into 20 ml) (Wyn-Jones and Sellwood, 2001 & Cashdollar and Wymer, 2013). Ultrafiltration can be done in a single pass using vortex flow filtration (VFF) with no need for pre-filtration of the sample or multiple circulations using tangential flow filtration (TFF) that requires pre-filtration of the sample (Fong and Lipp, 2005). Ultrafiltration techniques have also shown high recovery rates for multiple viruses in different water sources (average of ~70 % for Bacteriophage T1 from spiked groundwater with VFF and TFF) (Olszewski et al., 2005). Common ultrafilters with recovery rates for EVs from different water sources are presented in Table 1.5. However, ultrafiltration is less time and cost-effective than adsorption-elution methods (Jiang et al., 2001; Wyn-Jones and Sellwood, 2001; Fong and Lipp, 2005 & Cashdollar and Wymer, 2013).

1.1.1.1.2 Limitations of Membrane Filter Methods

Although each concentration method described previously is advantageous to a certain extent, no single method can be completely effective for concentrating or preventing the loss of all viruses. These difficulties have been attributed to 3 main issues: (1) the effect of the water matrix on binding viruses to the filter materials, (2) the co-elution of virus and potential inhibitors that can impact detection methods and (3) the requirement for multiple steps to concentrate the viruses from the water and elute from the filter. Maximizing virus recovery at the same time as minimizing virus loss due to the concentra-

Table 1.5. Comparison of common ultrafilter membranes used for the concentrating of enteric viruses in water samples based on size.

Filter	Used in	Samples	Isolated Virus	Recovery	References	Remarks
Hollow-filter	Primary step	Drinking water	Murine norovirus	42% for triplicate analysis	Gibson and Schwab, 2011	Economical, multi-pathogen concentration filter, no manipulation is needed and showed higher recovery rate in comparison to electro-charged filter. However, it is limited volumes of sample, not easily field deployable, may clogged with turbid water and limited data are available.
		Surface water	Murine norovirus	74% for single replicate sample		
		Spiked surface water (100 L)	Poliovirus 1	56%	Olszewski et al., 2005	
			Bacteriophage T1	70%		
			Bacteriophages PP7	86%		
		Spiked groundwater (100 L)	Poliovirus 1	82%		
			Bacteriophage T1	70%		
			Bacteriophages PP7	57%		
Tangential flow filter	Primary step	Spiked surface water (100 L)	Poliovirus 1	69%	Olszewski et al., 2005	
			Bacteriophage T1	123%		
			Bacteriophages PP7	104%		
		Spiked groundwater (100 L)	Poliovirus 1	95%		
			Bacteriophage T1	74%		
			Bacteriophages PP7	71%		
Centriprep YM-50 filter	Secondary step	MilliQ water	Poliovirus	74%	Haramoto et al., 2004	

tion procedure is a vast challenge, especially with low concentrations of the viruses present in large volumes of the sample (i.e., primary concentration step).

When considering adsorption of viruses to a surface (e.g., filters or beads), it is essential to consider the water's quality (e.g., macro and microorganisms, pH, organic matter), the volume of the sample and the type of filter being used. Water matrices are highly variable with respect to their physical, chemical, and biological factors (Boyd, 2015). Theoretically, everything present in the sample will be simultaneously concentrated in addition to the viruses. Virus adsorption to a surface is a reversible process that is basically governed by several energy contributions (electrostatic, van der Waals attractive forces and hydrophobic interactions) (Gerba, 1984a). In the adsorption step, the pH plays a significant role as the isoelectric point of EVs varies and therefore the pH level of the water plays a significant role in adsorption of the viruses (Metcalf et al., 1995 & Pang, 2009). Generally, pH above neutral tends to inhibit adsorption. In a study on the adsorption of EVs and other viruses from spiked drinking water, the authors found that the recovery rates were 4 times higher at a pH of 6 than 7.5 (Lambertini et al., 2008). Because EVs tend to be electronegative at near-neutral pH, they easily attach to positively-charged surfaces. However, consideration must be given to varying isoelectric points of different viruses and adjusting the pH to virus types and the waters they are being removed from (in the case of using electronegative filters). Besides pH, dissolved organic matter (classified in 4 groups: humic, fulvic, humin and ulmin acids) negatively impacts viral adsorption to filter materials (Gjessing et al., 1999). In a study conducted to measure the role of colloids in virus transport in groundwater, the authors conducted studies where 2 m long columns were packed with heterogeneous gravel aquifer media

and several factors measured with respect to viral adherence (Walshe et al., 2010). Using a bacteriophage as a model virus and kaolinite as a colloid, the authors reported where kaolinite was absent, the phage travelled faster (less adherence to the gravel) and the reverse was true when kaolinite was present. Similarly, decreasing the pH or increasing the ionic strength resulted in increased phage attachment, probably because of the isoelectric point of the phage. Lastly, when the authors increased the concentration of dissolved organic matter in the water, the phage travelled faster through the columns. In another study, it was found that viruses (e.g., PolioV with isoelectric point of 6.6) adsorbed to negatively- and positively-charged silica at pH below and above their isoelectric points, respectively (Gerba, 1984b). This mechanism can be beneficial in understanding virus transport in aquatic environments and in developing methods to concentrate viruses. Overall, optimal pH, organic matter and salt conditions that encourage maximum adsorption of the virus to a surface will vary among viruses in different sources (due to charge differences). Mechanisms involved in the adsorption of viruses to a solid particle was extensively reviewed in Gerba (1984b); with respect to the surface, these adsorption factors are similar.

Once viruses adsorb to a surface, they are subsequently eluted from the surface with alkaline buffers (Section 1.1.1.1.1) capable of disrupting virus-surface interactions (e.g., organic and inorganic solutions of varying pH levels) since high concentrations of cations tend to enhance virus retention (Metcalf et al., 1995). The recovery of viruses following adsorption and elution steps differs when using different filtration systems (Tables 1.3 to 1.5). Also, the recovery rate of viruses for first elution is usually higher than second elution (e.g., 39 ± 4 vs. 28 ± 6 and 25 ± 20 vs. 11 ± 4 using 1MDS electropositively-

charged filter from 100 L tap and river water, respectively) depending on the filter, water type and volume filtered (Karim et al., 2009). In general, membrane systems have higher viral recovery rates (reported after secondary concentration step) (up to 100%, see Tables 1.3 and 1.4) as compared to virus recovery associated with ultrafiltration system (up to 74%, see Table 1.5) (Huang et al., 2000; Kittigul et al., 2001; Albinana-Gimenez et al., 2009; Karim et al., 2009; Li et al., 2010 & Ikner et al., 2012). Despite the high recovery levels, the elution efficiency of viruses from all filtration systems remains highly variable (Ikner et al., 2012).

Furthermore, analytical procedures for estimating the concentration of the virus in water sample involve: primary concentration (filtration), elution, secondary concentration (e.g., flocculation) steps. Each step of this process requires time and effort and is known to cause loss of target viruses (Petterson et al., 2015). Despite these failings, the subsequent detection step can utilize methods such as cell culture to estimate infectious virus particle and/or quantitative polymerase chain reaction amplification (qPCR) to estimate infectious and non-infectious virus particles.

1.1.1.2 Detection Step

Detection of viruses in a sample requires sufficient concentration of the virus. A wide range of detection techniques have been developed since 1950s for the detection of viruses in various environments (Table 1.6). Cell culture and qPCR techniques have become the principal detection methods of EVs in water environments (Table 1.7) (Griffin et al., 2001). These techniques are used as standard methods by different agencies such as United States Environmental Protection Agency (USEPA), Health Canada and the On-

Table 1.6. Comparison of common methods used for the analysis and detection of enteric viruses in different environments. Cell culture- and molecular-based methods are common detection methods for enteric viruses in water samples.

Method	Pros	Cons
Electron Microscopy (EM)	Allows a rapid screen, provide direct visualization of virus particles, can differentiate empty capsid shells from intact particles, qualitative, and can be quantitative when combined with fluorescence.	Requires access to expensive instrument (EM), requires training, labor-intensive for routine detection, can not differentiate viruses based on their morphology, detection limit (ranges between 10^6 - 10^7 virus particles) can be lowered when combined with fluorescently-labelled antibodies, not suitable with water samples.
Cell culture Methods (CC) - Plaque assay - Tissue culture infectious dose (TCID 50%)	Quantitative, qualitative, determine infectivity	Virus may not be able to complete cycle of infection and may lack of the outer capsid, risk of contamination, not distinguish between primitive isolate and the adaptive virus, lack of a proper virus concentration for cultural detection, labor-intensive, timely, some virus do not grow in cell culture, relatively expensive
Molecular Methods - Gel electrophoreses	Rapid, qualitative	Interfere with inhibitors, primers not sensitive and not specific, time consuming
- Reverse transcript polymerase chain reaction (RT-PCR)	Rapid, sensitive and specific in compare to CC	Qualitative, interfere with inhibitors, does not determine infectivity
- Quantitative PCR (qPCR)	Quantitative, less contaminated, saves time	Qualitative, expensive and specific equipment, less sensitive that Nested-PCR
- Multiplex-PCR	Detect several target in a single reaction, save time and cost	Qualitative, not sensitive for all targets, non specific amplification and does not determine infectivity
- Nested-PCR	Increased sensitivity to PCR, confirmation step	Risk of contamination
- Integrated cell culture/polymerase chain reaction (ICC-PCR)	Detects all viruses, provides results in short time comparing to cell culture, determine infectious and non infectious viruses.	Less risk of contamination, more costly, interfere with inhibitors
- Nucleic acid sequence-based amplification (NASBA)	Provide result in less time and effort compared to CC	Qualitative, expensive, subjected to generate false data
Immunological Methods - Enzyme linked immunosorbent assay (ELISA)	Simple, do not require a skilled technician or pre-treatment, can be field-portable, may be quantitative and/or qualitative, rapid (strips)	Antibody can be moderately or non-selective to the target and be predispose to interference to sample matrix, time consuming and fail to determine infectivity. Cost depend on antibody, magnetic beads and special equipment (e.g., plate reader and magnetic separation device)
- Immuno-magnetic beads	Simple, do not require a skilled technician or pre-treatment, can be field-portable	

tario Ministry of the Environment, Conservation and Parks. The cell culture technique relies on whether the target virus can replicate in a cell line (USEPA, 1996). Since viruses are obligate intracellular parasites, they must be provided with susceptible host cells (e.g., whole organism, organ or cell) to complete their life cycles. The choice of an appropriate culture system is limited to some extent and depends on the aims of the study (e.g., isolation of virus, structural studies, biochemistry of multiplication and cytopathic effects (CPE)) and the availability of an acceptable host cell line. This is a basic and standard approach to confirm the presence of infectious EVs in water. Molecular techniques, on the other hand, rely on detecting specific genetic sequences in viral nucleic acids. Several PCR technologies such as quantitative reverse transcriptase PCR (qRT-PCR), multiplex-PCR and integrated cell culture-PCR (ICC-PCR; only used with culturable virus) have been utilized to detect a wide range of EVs in different water sources (Reynolds et al., 1997 & Fong et al., 2005). In general, PCR-based methods are rapid, less laborious, quantitative, highly specific and sensitive. They can also be automated to process large numbers of samples (32 to 48 samples per plate) as compared to cell culture (1 sample per flask). However, none of the PCR methods can distinguish between infectious and non-infectious virus particles whereas cell culture can only determine infectious virus particles (Griffin et al., 2001; Fong and Lipp, 2005; Girones et al., 2010; Hamza et al., 2011 & Knight et al., 2013).

1.1.1.2.1 Limitations of Detection Methods

Several limitations are associated with virus detection by cell culture and qPCR. These include, but are not limited to, (1) the presence of co-elution of materials (inhibitors)

in the concentrated sample, (2) the volume of the sample being analyzed and (3) time required to quantify the virus concentration in the sample.

Virus-matrix-surface interactions play key roles in determining the robustness of downstream processes (e.g., recovery rate/sensitivity of detection). Detection methods are therefore subjected to inhibition by whatever is present in the concentrate volume (e.g., salts or chemicals in the elution buffer and co-elution materials off the filter). These co-eluted materials may be co-extracted when virus nucleic acids are collected and affect their purity. They can also interfere with the amplification of the nucleic acids and cause false negative results in qPCR (Gibson and Schwab, 2010).

Another important consideration with detection methods is the volume of the sample and the specificity of the detection method. A few microliters (µl) of the concentrated sample (~10 to 20 ml) are used in detection step (e.g., 10 µl of virus nucleic acid is required for qPCR). Also, the concentration step is not specific to a target, as everything in the sample can bind to the filter, whereas qPCR is specific to a target. In this regard, it is important to determine the lower detection limit of the assay for the virus. For example, if virus is present in the water at low concentration, the virus count in the sample may be under the lower detection limit of the qPCR assay.

Recoveries of some EVs (AdenoV, EnteroV, NoroV, PolioV and RV) using cell culture- and PCR-based methods after concentrating the virus from previous studies was summarized in Kunze et al., (2015) (Table 1.7). Although cell culture and qPCR are less likely to cause degradation of viral nucleic acid, they lack specificity. It is possible that inactivated viruses be recovered and their nucleic acid be amplified and detected by qPCR. An enzymatic amplification of specific viral genomic nucleic acid sequences sequ-

Table 1.7. Published enteric virus recovery rates estimated by cell culture- and PCR-based methods after concentrating the viruses from water sources by adsorption and elution methods (modified from Kunze et al., 2015).

Water Source	Initial Volume (L)	PCM	SCM	VCF	Detected Viruses	Detection Method	Recovery (%)	References
River	20	Nanocream	Flocculation with $FeCl_3$	-	Rotavirus, adenovirus, norovirus	PCR	87 44 36	Pang et al., 2019
Ground	1500 - 1900	Nanocream (EPF)	Flocculation	~10^4	Poliovirus	PCR	20	Cashdollar et al., 2013
					Norovirus	Cell culture	30	
Ground	1500	1MDS (EPF)	Flocculation (acidification, PEG)	~10^5	Enterovirus, adenovirus, rotavirus, norovirus	PCR	ND	Borchardt et al., 2004
Well	1500	Glass wool	Flocculation	~10^5	Poliovirus	PCR	56	Lambertini et al., 2008
					Adenovirus		28	
Well	2010	1MDS (EPF)	Celite	~10^4	Norovirus	PCR	ND	Parshionikar et al., 2003
River	600	UF (ENF)	UF	~10^3-10^4	Enterovirus	PCR	ND	Rutjes et al., 2005
Tap	100 - 532	HA filter (ENF)	2.HA	~10^4	Norovirus	PCR	ND	Haramoto et al., 2004
			3.CeUF	~10^5				
Tap	1000	Membrane with $AlCl_3$	Membrane with $Al(OH)_3$	~10^4	Poliovirus	Cell culture	70	Farrah et al., 1978
Tap	1900	Cellulose filter	Membrane filter	~10^5	Poliovirus	Cell culture	92	Wallis et al., 1972
Tap, sea, sewage	19 - 1000	Fiberglass depth filter	Flocculation	~10^2	Poliovirus	Cell culture	50	Gebra et al., 1978

Note: PCM, primary concentration method; SCM, secondary concentration method; VCF, volumetric concentration factor, EPF, electropositive charged filter; ENF, electronegative charged filter. ND, not determined.

ences by PCR followed by detection of the amplified nucleic acid by hybridization has increased the specificity and sensitivity of detection. The main concern with this approach is the interference with nucleic acids from the virus and the polymerase enzymes by inhibitory agents in the sample (Hamza et al., 2011 & Knight et al., 2013). In cell culture, on the other hand, additional analysis may be required to identify the infectious virus.

An additional consideration with detection methods is the length of time to obtain an acceptable result. For example, cell culture-based methods could require days to weeks for infection to become apparent. While qPCR requires about 6 to 8 hours (h) for virus extraction and qPCR (or qRT-PCR) analysis.

1.1.2 Recommendations for Analysis of Enteric Viruses in Waters

Since humans are constantly threatened by risk of viral gastroenteritis associated with consumption of contaminated water, researchers continue to develop novel methods to balance 4 key areas (specificity, sensitivity, cost and time). An antibody is one bio-recognition molecule that can specifically bind to its target (e.g., antigen). This feature of the antibody makes it an ideal capturing and detection tool in immunoassays. Developments in the field of antibody engineering leads to the core of many researchers' interest in the development of antibody-based technologies that can rapidly and specifically detect targets. Although most of these technologies have been developed to detect targets (e.g., bacterial pathogens) in other environment than water, their use in water environment to concentrate a virus in water environments with regard to the 4 key characteristics mentioned above is also possible.

1.2 Antibody Engineering Technology

1.2.1 Conventional Antibodies

Antibodies, also known as immunoglobulins (Igs), are large Y-shaped protein molecules (i.e., glycoproteins) generated by the vertebrate immune system in response to antigens from external objects or pathogens. Antibodies can exist conventionally according to their heavy chain (H_C) types and subunit structure in different classes or isotypes known as IgA, IgD, IgE, IgG and IgM. These major isotypes vary in their size, locations, functions, biological properties, and capability to detect a specific target. The IgG is the most important and abundant antibody of all the Ig classes in vertebrates reaching ~80% of total Igs in circulation with a molecular weight of about 150 to 160 kDa (Maynard and Georgiou, 2000; Kuby, 2007; Deffar et al., 2009 & Hassanzadeh-Ghassabeh., et al., 2013). Antibodies (IgG type) consist of 4 polypeptide chains possessing binding sites that are complementary to specific structural features of the antigen(s) they recognize (Figure 1.1). These chains include 2 large heavy polypeptide chains (H_C ~450 to 550 amino acids of approximately 55 to 70 kDa) combined with 2 small light polypeptide chains (L_C ~211 to 250 amino acids of approximately 25 kDa) via disulfide bonds and numerous non-covalent interactions (Kuby, 2007). Both H_C and L_C are composed of structural domains, known as antibody domains or regions, that are classified based on their size and function into variable (IgV) and constant (IgC) domains. The paired N-terminal variable domains, known as antigen-binding fragments (F_{ab}), of H_C and L_C represent the arm of the antibody and are responsible for binding to the antigen. The constant region, known as fragment crystallizable (F_C), represents the tail (C-terminal) of an antibody that binds to various cell

receptors and complement proteins. These domains (IgV and IgC) are able to rotate and bend with the aid of the hinge region (Figure 1.1).

The H_{Cs} are identical to one another and each one consists of a single variable heavy domain (V_H) comprised of approximately 110 amino acids (~13 to 15 kDa) plus 3 constant domains (C_{H1}, C_{H2}, C_{H3}). The L_{Cs} are also identical; however, each chain consists of a single variable light domain (V_L) plus a single constant domain (C_L). The variability of the variable domain among diverse conventional antibodies is mostly confined to 6 complementarity-determining regions (CDRs) in V_H and V_L (Figure 1.1). Although the CDRs are hypervariable and form loops contributing to the antigen binding site at the N-terminus of each F_{ab}, the CDR_3 loop exhibits great variability in amino acid sequencing and confirmation. Also, the CDRs in each variable domain confers high affinity for a specific target and are separated by 4 conserved framework regions (FRs), which form the core structure of the Ig domain (Harmsen and Haard, 2007).

The large size of the full-length IgG antibody (~150 kDa) leads to practical disadvantages. The full-length IgG with high affinity (nanomolar “nM”) is often preferred format for therapeutic applications. However, it has weak tissue penetration (e.g., inaccessible to concave binding sites) and long half-life in blood (up to 21 days) that may cause poor contrast in imaging applications and toxicity (i.e., not freely eliminated through the kidney) (Chames et al., 2009). It also contains several disulfide bonds that must form for stable folding and post-translation modifications (glycosylation) that requires eukaryotic machinery (e.g., mammalian and/or plant system) to be produced in an active form (i.e., slow production at high cost) (Giritch et al., 2006 & Graumann and Premstalle, 2006). On the other hand, full-length IgG has also been used as an analytical tool in diff-

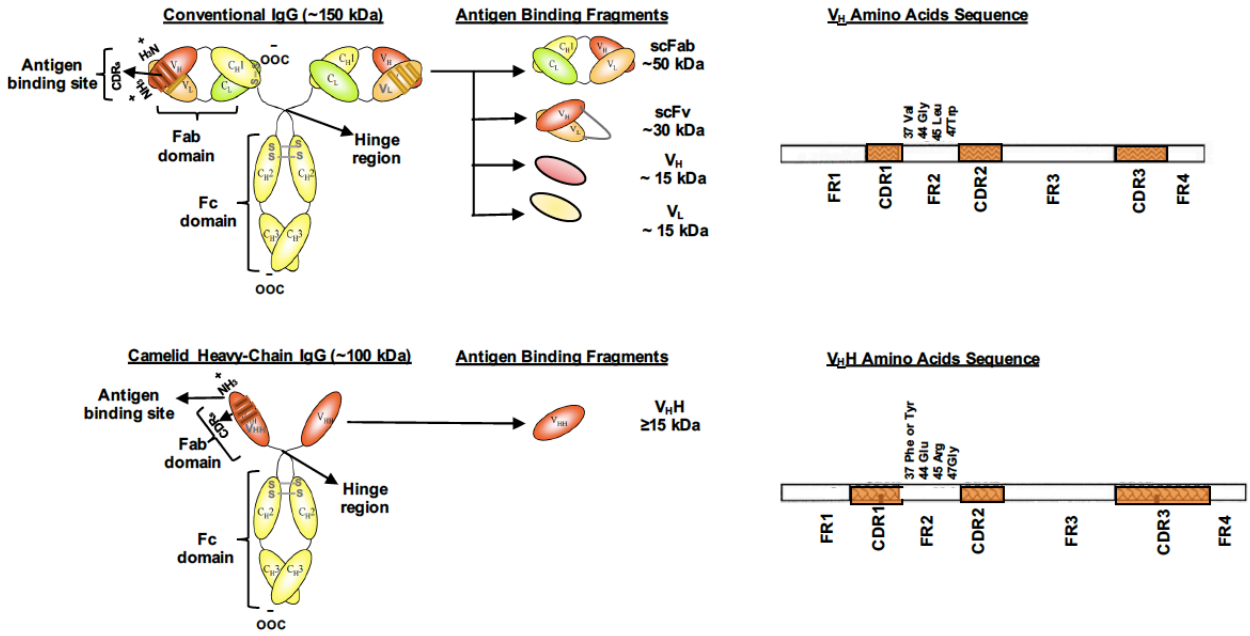

Figure 1.1. Schematically representation of the structure of conventional and camelid heavy-chain antibodies with possible antigen binding fragments and amino acid sequences of the V_H in the conventional IgG and the V_HH in the camelid heavy chain IgG. Variable domains derived from the antibody heavy (V_H) and light (V_L) chains are shaded in red and orange, respectively. Constant domains derived from the antibody heavy (C_H) and light (C_L) chains are shaded in yellow and green, respectively. Note the absence of the light chain and the C_{H1} domain in camelid heavy-chain antibody. Both types of the antibody formats provide various antigen binding fragments by progressive subtraction of constant domains. The amino acid sequences of the V_H and V_HH domains presents the mutation in the FRs. The position of the CDRs in between FRs is indicated in orange, however, there are more variations at the 4 positions for V_HH (e.g., position 37 could be Phe or Tyr). The CDR_1 and CDR_3 of the V_H is shorter than in the V_HH gene. FR, framework region; CDRs, complementarity determining regions (Modified from Harmsen and Haard, 2007 & Gene, 2012).

erent immunoassays such as Western blot, enzyme-linked immunosorbent assay (ELISA), immuno-fluorescence and immuno-sensor to capture specific targets in different environments (e.g., medical, food and water) (see Section 1.2.2.2 for more details on applications) (Garaicoechea et al., 2008; Park et al., 2008 & Yang et al., 2011). Several temperature-dependent studies were conducted to determine the stability of full-length antibody using its both domains (F_{ab} and F_C). These studies reported different melting temperatures for the F_{ab} (70°C and 61°C) (Zav'yalov and Tishchenko, 1991 & Vermeer et al., 2000) and the F_C (66 to 82°C and 71°C) (Tishchenko et al., 1998 & Vermeer et al., 2000) fragments. These findings suggested that the difference in the melting temperatures of both antibody domains is mainly based on the stability of the F_{ab} fragments, which is affected by the amino acids sequence of the variable domains. In addition, it was found that full-length IgG remains stable at temperature (37°C for several hours) and neutral pH while its binding reactivity gradually decreases as the pH changes to ≤ 4 and ≥ 10 (Otani et al., 1991; Shimizu et al., 1993 & Chen and Chang, 1998). Another study by Domínguez et al. (2001) demonstrated that the activity of full-length IgG did not change after incubation at low temperature (4°C) and low pH (4.5) for 24 h.

1.2.2 Camelid Heavy Chain Antibodies

At the end of the 1980s, Dr. Raymond Hamers (Vrije Universiteit Brussel, Brussels, Belgium) discovered that members within the *Camelidae* family (e.g., *camels*, *llamas, dromedaries, alpacas* and *vicugna sp*) produce, in addition to the conventional IgG, a unique type of conventional IgG devoid of light chains (L_C) in their sera termed heavy-chain antibodies (H_CAbs), resulting in the formation of a single-domain antibody fragment

(sdAb) (Figure 1.1) (Vu et al., 1997; Deffar et al., 2009; Fu et al., 2013 & Muyldermans, 2013). The sdAb is known as a nanobody (Nb) or abbreviated V_HH in the H_CAbs of camelids. The terms V_HH and Nb are often used interchangeably to refer to recombinant single variable domain antibody fragments (Hassanzadeh-Ghassabeh et al., 2013).

A specific repertoire of antibody genes is responsible to form these H_CAbs in B-lymphocytes; however, these repertoire genes are different from those responsible for forming conventional antibodies (De Genst et al., 2006 & Nguyen et al., 1998). Although variable domains in camelids lack the L_C and the C_{H1} present in conventional IgG antibody, they differ in their amino acid sequences and architecture. The H_CAbs in camelids comprise a single variable domain (V_HH antigen binding fragment) with size of about 4.2 nanometer (nm) in length and 2.5 nm in diameter linked to a pair of constant domains (C_{H2} and C_{H3}) via an extended hinge region.

Similar to conventional IgG, the variable domain in the H_CAbs varies in the sera of different camelids. This variability as well as the high specificity and affinity in the H_CAbs are mostly confined to a total of 3 flexible antigen binding loops (or CDRs). The CDRs display a greater structural repertoire than those observed for conventional V_H, with CDR_1 and CDR_3 loops being more extended, facilitating and increasing the paratope surface area available for antigen binding (Figure 1.1) (Muyldermans, 2001; Deffer et al., 2009 & Muyldermans, 2013). Also, the V_HH can access a unique antigen binding site (in comparison to the F_{ab} fragment of the IgG), such as enzyme active sites, which usually bind a groove or cavity at the V_H-V_L interface via the long CDR_3 domain (Muyldermans 2001; Harmsen and Haard, 2007; Fu et al., 2013 & Muyldermans, 2013).

The sdAbs fragments possess unique features that have drawn considerable interest from biotechnology and biomedical fields in comparison to conventional antibodies and other antibody fragments. The sdAbs are the smallest antibody fragments (12 to 15 kDa) with high affinity (nM and picomolar “pM” range) and specificity (e.g., more efficient capture of targets) as well as low inherent toxicity. The small size of V_HHs enable them to rapidly penetrate the membrane of a specific target cell and recognize even novel and inaccessible epitopes (e.g., concave surfaces) (Spinelli et al., 2000; Muyldermans, 2013; Deffer et al., 2009; Hassanzadeh-Ghassabeh et al., 2013 & Fu et al., 2013). They also have short half-lives in blood (<1.2 h) that results in their rapid filtration by the kidney, which might limit their usage in therapeutic applications (Chames et al., 2009 & Vincke and Muyldermans, 2012). Compared to other antibody fragments, V_HHs are soluble and highly aggregation resistant (Deffer et al., 2009 & Harmsen and Haard, 2007). This feature is attributed to the inter-CDR disulfide bond between cysteine (Cys) residues in the CDR_1 and CDR_3 loops (Figure 1.1) (Govaert et al., 2012). Additionally, V_HHs are highly stable and capable of functioning under several harsh conditions including high temperature (90 to 100°C) (Goldman et al., 2006 & Harmsen and Haard, 2007), long incubation time (~168 to 200 h) at 37°C (Deffer et al., 2009), extreme pH (e.g., acidic environment of the stomach), and denaturation conditions (Ewert et al., 2002 & Deffer et al., 2009). Furthermore, V_HHs produce high expression yields in various expression systems at economical cost and ease of efficacy engineering (e.g., for higher affinity, higher stability). In *E. coli*, the expression yield accounted up to 10 mg/L of purified periplamic extract and 60 to 200 mg/L in cytoplasmic protein accumulation (Deffer et al., 2009 & De Meyer et al., 2014). Also, total soluble protein (TSP) of 3.4% of V_HH

accumulation was obtained from transgenic tobacco leaves (Ismaili et al., 2007), while a level of <1% was reported in *Arabidopsis thaliana* (*A. thaliana*) leaves (Winiechayakul et al., 2009) and seeds (De Buek et al., 2013). For all these distinctive features, V_HHs have been broadly preferred for various applications including: research (e.g., structural studies), biotechnology (e.g., analytical tools, “biosensors”) and biomedical (e.g., vaccination) (Section 1.2.2.2).

1.2.3 Applications of Recombinant Antibody Technology

The reduced size, improved solubility and higher stability of mAb fragments using recombinant antibody technology are of special interest for basic research, medical and biotechnological applications. The mAbs are useful for defined specificity in distinguishing between morphologically similar lesions (adenocarcinoma vs mesothelioma) and in identifying specific receptors on cell surface (Nelson et al., 2000). Several recombinant mAb fragments have been developed with affinities against EVs, including AdenoV, NoroV and RV, with application in vitro for their antiviral activity and for detection such as ELISA (Table 1.8). For example, Aiyegbo et al. (2013) showed the ability of dimeric IgG or IgA and single chain F_{ab} mAb fragment against a common RV-capsid protein (VP_6) to inhibit RV replication inside epithelial cells at an early stage of infection. Another study by Maffey et al. (2016) reported a significant reduction of intestinal infection with RV when neonatal mice were treated with 200 µg V_HH mAb fragments that were also targeting RV-VP_6.

Recombinant antibody fragments have also been used for developing several types of biosensors such as optical, surface plasmon resonance and immuno-sensors. A

Table 1.8. Various published monoclonal recombinant antibodies against enteric viruses targeting extracellular protein (Modified from Wu et al., 2017).

ID	Antibody's Type	Origin	Targeted Antigen	Targeted Virus	Potency in Vitro/affinity	Virus Neutralization	Applications	References
anti-RV-25 H_C	F_{ab}	Hybridoma	VP_6	Rotavirus group A	-	-	Kinetic, structural and functional studies	Kallewaard et al., 2008
anti-RV-25 L_C					-	-		
anti-RV-26 H_C	IgG or IgA & F_{ab}	Hybridoma			0.045 nM	-		Kallewaard et al., 2008& Aiyegbo et al., 2013
anti-RV-26 L_C						-		
2KD1 & 3B2	Monovalent V_HH	Llama			IC_{80}: 0.2-3.91 µg/ml (13-67 nM)	Yes	Vaccine, library, ELISA, neutralization assay	Garaicoechea et al., 2008; Vega et al., 2013 & Maffey et al., 2016
	Bivalent V_HH				IC_{80}: >3.91 µg/ml			Garaicoechea et al., 2008
2B10	Monovalent V_HH	Llama	Rhesus-monkey rotavirus serotype G3		IC_{50}: <1 µg/ml	Yes	ELISA, neutralization assay	van der Vaart et al., 2006
Norovirus P domain of VLP	V_HH	Alpaca	GII.10 VLP	Norovirus		Particle disassembly	Neutralization assay	Koromyslova and Hansman, 2015
Poliovirus receptor-binding site	V_HH	Dromedary	Type 1 Sabin strain	Poliovirus type 1	IC_{50}: 0.007-0.69 µM IC_{90}: 0.017-1.77 µM	Yes	Neutralization assay	Thys et al., 2010; Schotte et al., 2014 & Strauss et al., 2016
1C11	IgG_{2a}	Hybridoma	Human adenovirus 40-hexon	Adenovirus 40	-	Yes	Neutralization assay	Herrmann et al., 1987
9B9	IgG_{2a}			Adenovirus 41	-	Yes	Neutralization assay	
9D4	IgG_1		Human adenovirus 40 & 41-hexons	Adenovirus group C types 2, 5, 6	-	No	-	
5D8/2C2	IgG	Hybridoma	Polypeptide VII	Adenovirus 40 & 41	-	No	-	Singh-Naz and Naz, 1986
2H6/1E11				Adenovirus 41	-		-	

biosensor is defined by the International Union of Pure and Applied Chemists (IUPAC) as an analytical device that uses a biological recognition element retained in direct spatial contact with transduction system for the analysis and the detection of biomaterial samples. Several surfaces such as gold, cellulose, steel, and magnetic beads have been used to immobilize antibodies with particular orientations (i.e., accessibility to bind a target via the antigen-binding sites of the antibody). Immobilization approaches range from small molecule to whole-cell diagnostics or detection (Gunneriusson et al., 1996 & Stahl et al., 1997) and can be achieved by physical or chemical adsorption, biochemical coupling or with bioactive pigments. The physical immobilization relies on van der Waals forces and the electrostatic interaction between biosensor material (e.g., antibody) and adsorbent (i.e., surface). Although this method was found to be weak and reversible, it is also efficient and robust. In the chemical immobilization; however, the recognition molecule (e.g., antibody) adheres to the surface via covalent bonds with little side effect. In the biochemical coupling, a bio-conjugate can naturally bind its associated matrix (e.g., cellulose binding module “CBM” binds to cellulose matrix) with exceptionally high affinity, low desorption rate and irreversibility. Finally, the bioactive pigments refer to the covalent coupling of the recognition molecule to colloid/carrier particles that can be printed, coated or even added during the process of paper rank (Lei et al., 2006; Pelton, 2009 & Kong and Hu, 2012).

In this regard, biosensors are capable of converting the binding of an antigen to its respective antibody into a signal, which is produced typically within ~10 to 90 minutes (min) (Zeng et al., 2012 & Zhao et al., 2014). During the bio-sensing process, non-specific binding of other molecules (e.g., proteins) with the surface containing adsorbed antibody

may occur. One simple approach to eliminate non-specific binding is to maximize the available antigen-binding sites of the antibody with other proteins (e.g., casein) (Larsson et al., 2013). Most of these biosensors have been successfully developed to primarily detect bacterial foodborne pathogens, such as *E. coli O157:H7, Staphylococcus aureus, Salmonella and Listeria monocytogenes* and different microbial toxins such as staphylococcal enterotoxins and mycotoxins. Different types of biosensor-based foodborne pathogen with their detection limit and processing time are reviewed in Zhao et al. (2014). However, sometimes mAb fragments selected for specific detection fail to function properly upon immobilization on a surface. The loss of antibody biological activity in biosensors may be attributed to unpredictable conformation changes of the antibody on surfaces, unwanted reactivities mediated by the F_C region of the full-length antibody or un-complementary orientation of the antibody fragments (Saerens et al., 2008). One potential approach to obtain oriented immobilization of an antibody on a surface is to fuse an antibody fragment with proteins such as a cellulose binding module (CBM) using recombinant CBM-fusion technology.

1.3 Recombinant CBM-Fusion Technology

Cellulose binding modules were originally known as cellulose binding domains (CBDs), and were linked to carbohydrate-active enzymes. The CBM allowed binding to cellulose, enhancing the hydrolytic activity of the carbohydrate active enzymes against their insoluble substrate (Oliveira et al., 2015). The CBMs were first isolated and characterized in the fungus *Trichoderma reesei* (*T. reesei*) (Van Tilbeurgh et al., 1986) and the bacterium *Cellulomonas fimi* (*C. fimi*) (Gilkes et al., 1988). In addition to cellulose, CBMs

are linked to a range of degradative enzymes active against diverse plant cell wall materials such as xylan, chitin, maltose and starch. Based on amino acid sequence similarities, 71 CBM families have been identified with a range of 30 to 200 amino acids (McLean et al., 2000; Shoseyov et al., 2006 & Oliveira et al., 2015). In addition, CBM families are further classified based on their binding specificity and three-dimensional (3D) structures into 3 types (McLean et al., 2000; Shoseyov et al., 2006 & Oliveira et al., 2015). Type A is the surface-binding CBM site that has a flat hydrophobic surface comprised of aromatic residues. This type of CBM binds to insoluble crystalline cellulose and chitin and has low or no affinity for soluble carbohydrates (Boraston et al., 2004). Type B is described as having a groove glycan-chain-binding site that has several sub-sites able to interact with a single glycan chain (i.e., high affinity to glycan). Type C possesses a small sugar binding site (lectin-like CBMs) that recognizes terminal (exo-type) glycans such as mono-, di- and tri-saccharides (Boraston et al., 2004; Shoseyov et al., 2006 & Oliveira et al., 2015). For the scope of this review, CBMs are discussed in term of their possible use in immobilization of antibody fragments on a cellulose surface for the purpose of capturing and detecting a specific target in various environments.

1.3.1 Applications of CBM-Fusion Technology

Recombinant CBM-fusion proteins have several properties that make them potentially useful in various fields of biotechnology. These include properties of the CBM itself, such as: present in a wide range of forms and sizes, chemically inert, independently folding units, enhance protein expression via secretion, high-capacity purification tags, relative low production cost, low affinity for non-specific protein binding and pharmaceutically safe

(Levy and Shoseyov, 2002). Many studies have affirmed the feasibility of linking the CBM with various molecules such as enzymes or antibodies (Shoseyov et al., 1999; Nahálka and Gemeiner, 2006; Shoseyov et al., 2006 & Hussack et al., 2009). These fusion proteins have been successfully expressed in bacterial and yeast systems at a relatively low cost (Oliveira et al., 2015). Consequently, CBM-fusion proteins have been used in a broad range of applications. In an early study, Shoseyov et al. (1999) investigated the effect of different values of pH and concentrations of salt (NaCl) on the binding ability of a fusion protein consisting of CBM and protein A (CBM-A) to cellulose beads. The group demonstrated an increase in the fusion protein binding to cellulose (up to 70 mg/g cellulose) at low pH values (2 to 3.5) and high salt concentration (0.5 to 1 M) after incubation for 1 h at 37ºC with occasional mixing. Several studies also have demonstrated the use of recombinant CBMs in industrial setting to enhance the mechanical and physical properties of paper fibers e.g., water drainage (Von der Osten et al., 2000; Berry et al., 2001 & Pala et al., 2001), in molecular biology (e.g., large-scale production and purification of recombinant proteins) and as immobilization tools of cells or recombinant fused proteins (Linder et al., 1998; Shpigel et al., 2000; Shani and Shoseyov, 2001; Fuglsang and Tsuchiya, 2001; Xu et al., 2002; Maurice et al., 2003 & Hussack et al., 2009).

The use of CBMs as immobilization tools of recombinant proteins present many advantages in biotechnology e.g., bioremediation of toxic metals and biosensor development for the detection of pathogens. The efficacy of CBMs as immobilization tools relies on 3 basic properties: (1) they are usually independently folding units, (2) the attachment matrices (e.g. cellulose) are abundant and inexpensive and have excellent

chemical and physical properties and (3) the CBM binding specificities can be controlled via changing the distinctive orientation of the aromatic side chains that interact with the cellulose surface (Simpson et al., 2000; Shoseyov et al., 2006; & Arola and Linder, 2016).

The CBMs have been useful immobilization tool of recombinant fusion protein for the rapid removal of the pesticide atrazine and toxic trace metals from water (Xu et al., 2002 & Levy and Shoseyov, 2002). For example, a CBM and synthetic phytochelatin (EC20) fusion protein was successfully developed by Xu et al. (2002) to specifically remove cadmium (Cd^{+2}) in solution. The group demonstrated the efficient removal of Cd^{+2} with consistent ratio of ~10 Cd^{+2} per immobilized CBM-EC20 in a single step onto various cellulose matrixes for 3 cycles. The results indicated that the high affinity of the fusion protein (CBM-EC20) retained the functionality of the CBM (e.g., binding to cellulose) and EC20 (e.g., metal-binding).

Several studies have also developed fusion proteins incorporating a CBM and an antibody binding domain to provide an adaptor molecule for separation and detection of a target on a cellulose surface. Craig et al. (2007) successfully immobilized a fusion protein containing a CBM and protein LG on cellulose hollow fiber membrane to separate KG1a cells from a high-density culture. The group reported complete binding of KG1a cells (96±2.5%) or KG1a cells labeled with anti-CD34 (mouse IgG_{2a} mAbs) (91±4.3%) on fibers coated with fusion protein CBM-LG and a very low level (0.1±0.7%) of non-specific cell binding for unlabeled KG1a cells. In an other study, Hussack et al. (2009) produced several bispecific pentameric sdAb fused with CBMs engineered for expression in *E. coli* and *P. pastor*is for simultaneous immobilization on cellulose paper and detection of the human bacterial pathogen *S. aureus*. The group reported the fusion protein, at 150 nM,

was specifically capable of binding *S. aureus* in solution and on the filter paper with a detection limit of 10^5 cfu/ml. The group also reported binding of the sdAb only at 18.7 nM to *S. aureus* in solution while no binding was seen on the paper. This results suggested that fusion protein containing CBM and sdAb was able to retain the binding ability of sdAb to *S. aureus* while fusion protein excluding CBM may have some detrimental effect on the activity of sdAb. The outcome from these studies suggested that integrating the use of recombinant antibody and CBM-fusion technologies could also provide an avenue to develop a concentration methodology that will specifically capture and may visually detect viruses in water environment on a cellulose matrix as possible future outcome.

2 RATIONALE, GOAL, HYPOTHESES AND OBJECTIVES

2.1 Rational of the Research

The challenge in directly detecting EVs in water sources is that their concentration is below the detection limit of current methods, such as PCR and cell culture. Usually, environmental water samples are collected in large volumes (up to 1,000s L) and concentrated into smaller volumes (about 10 to 20 mls final volume) through primary and secondary steps before being analyzed for their virus content. Advances in filtration (e.g., electro-charged filters and ultrafiltration), cell culture- and molecular-based methods have provided many opportunities for improved concentration and detection of EVs in the water environment. However, there remain various challenges at each stage (e.g., sampling/filtration, concentration and detection) of viral analysis in the water environment. In addition to the potential loss of virus during the primary concentration step, other components present in the water (e.g., biological and chemical factors, such as organic matter, salts and metal ions) tend to be concentrated and can negatively affect downstream analysis. As a result, and despite improvements in detection sensitivity, these assays require extensive sample cleanup and biomolecule purification before analysis.

This research aimed to develop an antibody-based capture system that can increase the recovery of EVs from water as compared to standard techniques during initial concentration step and enhance their detection in the downstream process. In this regard, RV was used as a model system in this proof-of-principle project for several reasons. First, RV is a well studied EV. Second, it can be easily propagated in the lab using cell culture methods. Third, we have access to different human and bovine RV strains. Fourth,

it is safe to work with. Finally, to our knowledge, among all EVs, this is the only virus that has different mAb fragments produced against its main capsid protein VP_6 (Table 1.8).

Monoclonal sdAb fragments (2KD1 and 3B2) (Garaicoechea et al., 2008; Vega et al., 2013 & Maffey et al., 2016) and F_{ab} fragment (Aiyegbo et al., 2013) against a common RV-capsid protein (VP_6) were selected. They have previously showed high binding ability to different strains of the virus in ELISA and neutralization assays (reduced infection). Due to the unique features of sdAbs, these fragments were selected to be produced in *E. coil* and subsequently immobilized on a cellulose filter using recombinant technologies discussed previously (Sections 1.2 and 1.3). Also, recombinant antibody technology was used to generate a full-length IgG against RV in plant system. Both sdAb and full-length IgG were immobilized on magnetic bead surfaces. Each of these approaches is expected to provide a good test for developing a bioactive paper and immuno-magnetic beads, as rapid and economical concentration methods, and examining matrix effects (water quality) on RV binding to the antibody fragments. Ultimately, having multiple V_HHs to different EVs (e.g. AdenoV, NoroV and RV) would be the goal. This chapter presents RV in related points to this research and discusses the goal, hypotheses and the objectives of this research project.

2.1.1 Rotavirus

Historically, RVs were first isolated in the epithelial cells of the small intestines of children with acute gastroenteritis (Bishop et al., 1973). The virus was described by Bishop and colleagues in 1973 as a complete particle of 70 to 100 nm in diameter having a wheel-like appearance with a smooth surface and displaying short spokes when viewed by

electron microscopy (EM) of negatively stained fecal extracts (Ward, 2008; Johne et al., 2011 & Jain et al., 2014). The name RV is derived from the Latin word *rota*, which means wheel. Tissue culture was used to isolate and cultivate RV in vitro; however, the cultivation of RV was only successful after trypsin treatment (Babiuk et al., 1977). Globally, RV is estimated to contribute to 100 million episodes of diarrhea each year, causing 2 million hospitalizations and about 450,000 deaths in children less than 5 years of age (Kawai et al., 2012). In 1988, the use of cryo-electron microscopy provided a detailed description of the structural and functional relationships (e.g., cell entry and antibody interactions), while the use of x-ray crystallography has provided more information on the atomic structures of several structural and nonstructural proteins (SP and NSP) in addition to enhancing our understanding of the 3-D structure of the RV (Dormitzer et al., 2004).

2.1.1.1 Structure

Rotaviruses are non-enveloped viruses consist of a genome of 11 segments of double stranded ribonucleic acid (dsRNA) with a total molecular weight of 18,550 base pair (bp) that ranges in length from 667 to 3,302 bp (Ward, 2008 & Jain et al., 2014). These segments encode a variety of structural (VP_1-VP_4 and VP_6-VP_7; known as viral proteins “VP”) and non-structural proteins (NSP_1-NSP_6; exist only in infected cells), which in turn form a rigid icosahedral protein capsid that protects the viral genetic information as it passes among infected cells. Each gene of the 11 segments encodes a protein responsible for a specific function during the viral life cycle except gene 11, which encodes 2 nonstructural proteins (NSP_5 and NSP_6) (Table 2.1). The icosahedral capsid (Figure 2.1) is composed of a core containing 12 vertices, 20 faces and 30 edges and co-

Table 2.1. Rotavirus proteins characterization (modified from Ward, 2008).

Segment	Protein	Size (bp)	Type	Location	Function
1	VP_1	3302	SP	Core	RNA binding and transcriptase
2	VP_2	2687	SP	Inner layer	Immunogenic and serum antibodies to VP2 are good indicators of previous infection
3	VP_3	2591	SP	Core	Encode proteins required for RNA transcription and correct viral structure
4	VP_4	2362	SP	Out layer	Viral adsorption and penetration into epithelial cells
5	NSP_1	1611	NSP		Facilitate viral replication and thus increase the efficiency of virus formation
6	VP_6	1356	SP	Middle layer	Encode proteins required for RNA transcription and correct viral structure
7	NSP_3	1104	NSP		RNA binding and translational control
8	NSP_2	1062	NSP		Facilitate viral replication and thus increase the efficiency of virus formation
9	VP_7	1059	SP	Out layer	Viral adsorption and penetration into epithelial cells
10	NSP_4	751	NSP		The first described viral enterotoxin
11	NSP_5 NSP_6	667	NSP		Facilitate viral replication and thus increase the efficiency of virus formation

Note: SP, structural protein. NSP, non structural protein.

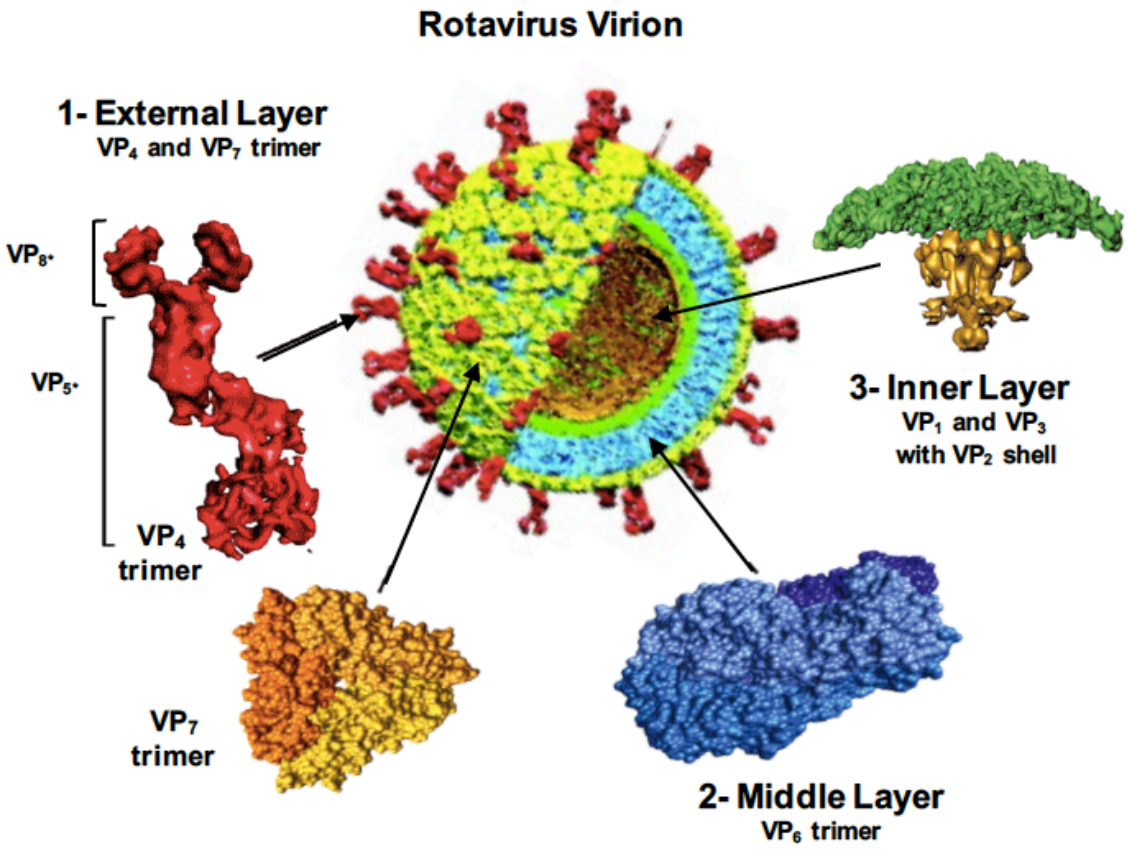

Figure 2.1. Structure of rotavirus virion. The virus consists of three layers. External layers consist of VP_7 and VP_4 (VP_{8*} and VP_{5*}). A middle layer consists of VP_6. An inner layer consists of VP_2 shell with VP_1 and VP_3 (Modified from https://talk.ictvonline.org/ictv-reports/ictv_9th_report/dsrna-viruses-2011/w/dsrna_viruses/190/reoviridae-figures).

ntains 11 dsRNA segments that are surrounded by 3 concentric protein layers (Prasad et al., 1988; Yeager et al., 1990; Prasad et al., 1996 & Estes et al., 2001). An inner layer is formed by 120 copies of VP_2 enclosing 12 copies each of 2 enzymes (the viral transcriptase VP_1 dependent RNA polymerase, the guanyl-transferase VP_3) and the viral dsRNA segments (Valenzeula et al., 1991; Liu et al., 1992 & Chen et al., 1999). A middle layer is formed by 780 copies of a single protein VP_6 that represents half of the virion mass (45 kDa in size). The middle layer is surrounded by an external layer comprised of 120 copies of hemagglutinin spike protein VP_4 (encoded by gene segment 4 and is about 88 kDa in size; protease sensitive) embedded into 870 copies of glycoprotein VP_7 (encoded by gene segment 9 and is about 37 kDa in size). The VP_4 and VP_7 proteins have high genetic variability and are considered critical to vaccine development as they elicit neutralizing antibodies that are believed to be important for protection (Burke and Desselberger, 1996; Ward, 2008; Collin et al., 2010; Han et al., 2010 & Jain et al., 2014).

2.1.1.2 Classification

Based on sequence identities of VP_6 (serological cross-reactivity and genetic variability), RVs have been assigned by the International Committee on Taxonomy of Viruses (ICTV) to nine antigenic groups, RV A to H and J (Burke and Desselberger, 1996; Matthijnssens et al., 2008; Matthijnssens et al., 2012; Jain et al., 2014; Mihalov-Kovács et al., 2015 & Bányai et al., 2017). These groups are distinguishable by electro-pherotype based on the profile of the RNA segments on polyacrylamide gel. Furthermore, the antigenic relationships of two structural viral proteins in the outer layer VP_4 and VP_7 are used to distinguish strains within a group.

Currently, only groups A, B, C and H have emerged as major etiologic agents of acute gastroenteritis in humans and animals. The highest universal rate of morbidity and mortality is largely attributed to group A RVs (Burke and Desselberger, 1996; Leung et al., 2005; Jain et al., 2014 & Afchangi et al., 2019). RV groups D, E, F and G are only reported in animals (Ball, 2005 & Matthijnssens et al., 2010). Within RV group A, several subgroups are differentiated (SG I, SG II, SG I + II, SG non-I, SG non-II) according to the presence of several distinct epitopes of VP_6 that may or may not react with mAbs targeting VP_6 (Greenberg et al., 1983; Gómara et al., 2002; Johne et al., 2011 & Afchangi et al., 2019).

2.1.1.3 Diversity and Prevalence

The epidemiological data from different geographical locations suggests significant diversity of RV genotypes, which are monitored by surveillance systems in different countries (e.g., World Health Organization). These systems are used to confirm the trends in RV activity, estimate the distribution and the burden of the RV in gastroenteritis as well as evaluate the impact of vaccination.

Several combinations of G and P types have been independently identified in human and animals as these structural proteins are coded by different RNA segments (Burke and Desselberger, 1996 & Jain et al., 2014). Currently, G1 P[8], G2 P[4], G3 P[8], G4 P[8]) and G9 P[8]) of h-RV genotypes are predominant worldwide accounting for 74% of RV infections (Bányai et al., 2012). However, genotype G1 P[8] is the most prevalent combination representing 47%, 44%, 43% and 33% in Western Pacific, Kingdom of Saudi

Arabia, United States and Europe, respectively (Tcheremenskaia et al., 2007; Kheyami et al., 2008 & Jain et al., 2014).

A number of uncommon genotypes have also been reported across the world. Uncommon combinations such as G5 associated with P[8] were found in Brazil, G8 with P[6] or P[4] were found in Malawi, G2 with P[4] was found in Saudi Arabia, G2 with P[6], G3 with P[6], G12 with P[8] or P[6] and G9 with P[6] were predominant in African and South-East Asian regions (Tcheremenskaia et al., 2007; Kheyami et al., 2008; Cunliffe et al., 2009 & Jain et al., 2014). Despite the diversity in P and G types, the VP_6 capsid protein is a constant that can be targeted to detect a diverse range of hRV geno/sero-types.

2.1.1.4 Biology of RV-VP_6

Protein VP_6 is a structural protein on the surface of the immature inner capsid particle representing 51% of the virion mass. It has 90% amino acid homology among all members within the same group (Tang et al., 1997 & Colomina et al., 1998). Protein VP_6 from RV group A comprises 397 amino acids with a molecular weight of about 45 kDa and is encoded by segment 6 of the RV genome (Petitpas et al., 1998). In addition to its ability to specifically interact with itself, it has the ability to interact with all other structural proteins of the virion (VP_2, VP_4 and VP_7) at different positions of its two domains B and H (Figure 2.2). Domain B contains a bundle of 8 alpha-helices that are formed by amino acids 1-150 and 335-397 at the N- and the C-terminus, respectively. Domain H folds into a ß-sheet and is formed by amino acids 151-334 (Mathieu et al., 2001 & Desselberger, 2014).

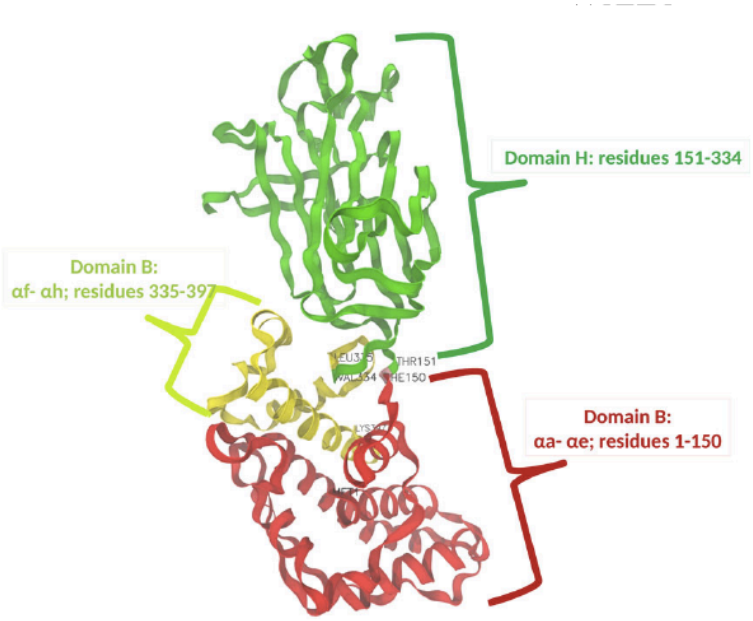

Figure 2.2. Structure of VP_6. The VP_6 consists of two domain B and H. Domain B is formed by α-helices (red) started from amino acids 1-150 and αf-αh (yellow) started from 335-397. Domain H (green) folds into a ß-sheets and is inserted between amino acids151-334 (Copied from Afchangi et al., 2019).

Protein VP_6 acts as a physical adaptor between 2 distinct biological functions of the virus, i.e. cell entry and packaging of genomic RNA. It plays several roles in the viral replication cycle as it is an essential component for the virus to be transcriptionally active. When the RV enters the cell, its outer layer proteins, VP_4 and VP_7, are removed before replication, thus creating double-layered particles (DLP) with a surface consisting of VP_6. This may indicate the reason behind antibody development targeting VP_6 instead of other viral proteins (e.g., VP_4 or VP_7) in infected mice (Ward and McNeal, 2010). Although VP_6 is not the viral transcriptase, the integrity of these DLP is required for transcription. Also, VP_6 binds to an encoded glycoprotein receptor (NSP_4), which facilitates the budding of an immature capsid into the endoplasmic reticulum where final maturation and assembly of the virus takes place (Hsu et al., 1997).

Furthermore, VP_6 is the target antigen in most immuno-diagnostic tests for group A RV detection as it is highly conserved and immunogenic (Estes and Cohen, 1989). A protective immune response was induced in RV-infected mice when they administrated with RV-VP_6 regardless of the RV A strain (Esteban et al., 2013a) or forms of VP_6 (e.g., trimers, spherical single-layered, dl2/6-VLPs) (Li et al., 2014). Several laboratories have developed antibodies against RV-VP_6 as potential RV vaccine candidates (Table 1.8). Although antibodies directed against this protein do not have neutralizing activity in vitro, a few studies reported the contrary. Llama single domain antibodies (V_HH) were indicated to neutralize a broad range of RV A strains in vitro independently of G and P types and demonstrated a partial protection in RV-infected neonatal mouse and pig (van der Vaart et al., 2006; Garaicoechea et al., 2008; Aladin et al., 2012; Gomez-Sebastian et al., 2012 & Vega et al., 2013). These laboratories demonstrated that the smaller size of the V_HH

molecule, compared to conventional antibodies, seems to play an important role in protecting the animals and suggested that V_HHs should be further investigated as an appropriate treatment for gastroenteritis. Although VP_6 has been widely used as a vaccine target, it may be useful for other purposes such as diagnostic and detection assays. This highlights the fact that there is a crucial need to also investigate the V_HH as a specific and sensitive detection tool for pathogens in the environment, particularly when they are present at low concentrations (e.g., EVs in water sources).

2.2 Goal of the Research

The use of recombinant antibody and CBM-fusion technologies opens the possibility of engineering and developing a stable recombinant fusion protein with high affinity to its target, whether an environmental pollutant, pathogenic microorganism or a toxin (Harmsen and Haard, 2007 & Hussack et al., 2009). The V_HH possesses certain bio-recognition features such as their small size, stability and ability to refold following physical and/or chemical denaturation. These features were important considerations for their choice in bioactive paper development (van der Linden et al., 1999; Goldman et al., 2006 & Wang et al., 2012). The overall goal of this research was to develop and evaluate an antibody-based capture technology for the direct isolation of EVs from environmental water samples. This technology may be further developed, in the future, to a biosensor. Such biosensor technology would be usable in diverse locations of the world to target different strains of a group (based on common protein e.g., VP_6).

One approach for an antibody-based capture technology is to develop an immunoassay to capture RV A strains by constructing a CBM2a protein linked to V_HH at

either the N- or the C-terminus. Two published monomeric sdAbs, V_HHs, (2KD1 and 3B2) specific to a common capsid protein in RV group A (VP_6) were selected. The fusion protein (e.g., CBM2a-V_HH and the V_HH-CBM2a) will attach on cellulose filter paper through CBM2a whereas the RV A strains will bind on the paper through the V_HH, which specifically recognizes RV-VP_6 capsid protein. This will be accomplished by fusing V_HH antibodies against non-overlapping epitopes on the VP_6 virus capsid to the CBM2a and immobilizing the V_HH on the cellulose filter paper. The CBM2a will be linked to V_HH at each terminus: (1) the N-terminus where the binding site to an antigen is anticipated to be located and (2) the C-terminus which is located away from the binding site (Kuby, 2007). Two common linkers: a proline threonine linker with a sequence of $([PT]_3T)_{3x}S$ (Gilkes et al., 1991 & Shen et al., 1991) and glysine-serine with a sequence of $([Gly]_{4x}$-$Ser)_{nx}$ (Hudson and kortt, 1999 & Ahmad et al., 2012) will be used for linking the V_HHs to CBM2a and tested for better functionality.

Another approach is to develop an immunoassay to detect RV A strains by using magnetic beads conjugated to V_HH and full-length IgG antibodies against RV-VP_6 protein. In this sense, magnetic beads can be coated with antibodies (e.g., full-length IgG and sdAb) that efficiently bind viral particles. Subsequently, bead-virus complexes can be magnetically separated from the sample and washed to yield concentrated and purified viral particles (Myrmel et al., 2000; Mattison and Bidawid, 2009 & Toldrà et al., 2018). It is believed that several parameters influence viral binding to beads including physical characteristics of the virus (e.g., isoelectric point and size), properties of the bead (hydrophobicity and specificity of the coated molecule) and characteristics of the chemical (e.g., pH and turbidity) and physical (e.g., temperature) properties of the sample (Toldrà

et al., 2018). Numerous studies have employed the use of immuno-magnetic separation as a secondary concentration step, following primary concentration using adsorption-elution/flocculation procedure, to achieve sensitive detection of different EVs such as EnteroV, RV, human adenoviruses (hAdenoV) and NoroV from spiked environmental water samples (Jothikumar et al. 1998; Myrmel et al. 2000; El-Galil et al., 2005 & Hwang et al., 2007). Immuno-magnetic beads have the advantage of being target specific and easily separated from the sample, which eliminates upstream processing steps and saves time (Papafragkou et al., 2008). However, the cost of magnetic beads can be higher than other methods, depending on the reagents coupled to the beads. The purpose of this approach in this PhD thesis is to compare (1) the effectiveness of full-length IgG vs. V_HH using a common surface in capturing the virus and (2) the binding ability of antibody-coupled beads vs. bioactive filter paper (i.e., antibody-cellulose filter paper) to capture the virus in a primary step. The immuno-magnetic beads (e.g., IgG-coupled- and V_HH-coupled-magnetic beads) will attach specifically to the virus in the sample through the capture of the antibodies, which specifically recognize RV-VP_6 capsid protein. After several wash steps the virus can be eluted and concentration of the virus can be estimated by qPCR.

The retention of the virus in both approaches will be analyzed by various techniques including ELISA, Western blot and qPCR. Ultimately, the technology will be tested using spiked environmental water samples (e.g., tap and river waters) to examine matrix effects on virus binding to the antibody-cellulose filter paper or beads coated with RV specific antibodies. The successful development of an antibody-based technology for

the capturing of EVs will provide a critical tool for monitoring of a critical group of pathogens to inform water treatment and safety in rapid and cost-effective manner.

2.3 Hypotheses of the Research

2.1.2 Cellulose Filter-V_HH Capture Technology

Fusion proteins produced with V_HH, targeting VP_6-capsid protein on RV, at N-terminus will bind the virus more effectively than fusion proteins produced with V_HH at C-terminus. Also, the developed cellulose filter with V_HH-CBM2a (i.e., antibody-cellulose filter) capturing system will enhance the recovery of RV and be more specific to capture RV from water sources as compared to cellulose filter with CBM2a only.

2.1.3 Immuno-Magnetic Bead Capture Technology

The magnetic-beads coupled with full-length IgG 26 and V_HH will equally and specifically capture RV from water sources in a primary step.

2.4 Objectives of the Research

- To engineer the CBM2a-V_HH and the V_HH-CBM2a fusion proteins for expression in *E. coil HB2151*.
- To engineer full-length IgG 26 recombinant antibody against RV-VP_6 capsid protein for expression in plant.
- To functionally characterize the fusion proteins with respect to specificity and sensitivity for human and bovine RV A strains (e.g., validating V_HH-virus binding).

- To immobilize the V_HH-CBM2a fusion proteins on a cellulose filter paper and characterize their ability to capture RV strains A from different water types with respect to specificity, sensitivity and matrix effects.

- To immobilize the V_HHs and the IgG 26 on magnetic beads and characterize their ability to capture RV strains A from different water types with respect to specificity, sensitivity and matrix effects.

3 MATERIALS AND METHODS

All buffers, transfer equipment, and glassware were sterilized with either an autoclave at 101.3 kilopascals (kPa) and 121 Celsius (°C) for 20 min or filtered through 0.22 µm syringe filter prior to use to minimize the contamination of samples, unless otherwise specified. Millipore-Q (MQ) grade water (Millipore, Bedford, MA) was used in media and buffers preparation. Recipes for all stocks, media and buffers used in this work are present in Appendix 1.

All work during bacterial cell culturing, plating, transformation as well as protein expression was done in a laminar flow hood (Labculture® Reliant™ Class II Type A2 Biosafety Cabinet, Model: 1385, Esco Technologies, Inc., USA), unless stated, to minimize the risk of contamination. Cell culture for virus work was conducted in a class II biological safety cabinet (BSC II; certified as NSF-49 Safety Standard). A PCR preparation hood (Model #P-036-02, C.B.S. Scientific Co., California, USA) was used for RT-PCR samples preparation. All materials used for bacterial examination were sterilized afterward at 101.3 kPa and 121°C for 20 min. All materials used for virological examination were sterilized afterward with EZTest® Biological Indicators for Steam Sterilization (*Geobacillus stearothermophilus*; MesaLabs, Bozeman, USA) according to manufacture's instructions at 101.3 kPa and 121°C for 60 min to prevent release of infectious viruses from the materials and to ensure of a proper sterilization.

Nucleotide sequence alignment for genes of interest was analyzed using the nucleotide blast tool on the National Center for Biotechnology Information (NCBI) website (https://blast.ncbi.nlm.nih.gov/Blast.cgi?PAGE_TYPE=BlastSearch). Oligonucleotide primers and probes used in this work were analyzed using the 'Oligo Analyzer' tool on the

Integrated DNA Technologies (IDT) web page (http://www.idtdna.com/analyzer/Applications/OligoAnalyzer/) using default settings. Primers for gene cloning and sequencing were synthesized by Laboratory services (University of Guelph, Guelph, ON, CA). Optimized synthetic DNA sequences for V_HHs (with or without CBM2a) and RV-VP_6 gene fragment were subcloned into a pITKan bacterial expression vector while optimized DNA sequences for RV-IgG 26 was subcloned into pPFC0205 plant expression vector by GeneWiz (New Jersey, USA). The synthetic gene constructs were provided as lyophilized plasmids at 4 Microgram (µg).

3.1 Gene Constructs of Recombinant RV-Single Domain Antibodies

In the following sections, the procedures for preparing the gene constructs and cloning of the different recombinant antibodies against RV group A strains and the recombinant RV-VP_6 are described.

3.1.1 Preparation of V_HH-His DNA Constructs

Two V_HHs against the major inner capsid structural protein (VP_6) of RV group A were previously developed by Garaicoechea et al. (2008). These V_HHs named "2KD1 and 3B2" are monomeric fragments with molecular weights of about 13.45 and 14.24 kDa, respectively. These V_HHs were derived from an immune V_HH phage display llama library.

The nucleic acid sequences encoding the sdAbs 2KD1 and 3B2 were retrieved from the GenBank with accession numbers: JC036616 and JC036618, respectively. The FRs and the CDRs of each V_HH were determined (Figure 3.1). Both genes were codon optimized for expression in *E. coli* and synthesized, individually, to contain 5' NcoI and 3'

(A) 2KD1 (pI/MW: 6.02/16048.55)

MADVQLQASGGGFVQPGDSLSLSCAASGGTFSSYSIGWFRQGPGKEREFVATISSSDSPWYGEP
AKGRFTVARVNAKNTAYLHLNRLKPEDTATYYCAAGSVQHMANENEYVYWGQGTQVTVSSAAA*H*
*HHHHH*GAA**EQKLISEEDLN**GAA*

(B) 3B2 (pI/MW: 5.80/16147.83)

MADVQLQASGGGLAQAGDSLTLSCAASGRTFSGYVVGWFRQAPGAEREFVGAIRWSEDSTWYGD
SMKGRILISRNNIKNTVNLQMFNLKPEDTAVYVCAAGAGDIVTTETSYNYWGRGTQVTVSSAAA
*HHHHHH*GAA**EQKLISEEDLN**GAA*

Figure 3.1. Framework (FR) and complementarity determining regions (CDR) in the amino acids sequence of (A) 2KD1 and (B) 3B2 in the pITKan expression vector. The CDRs are underlined while FRs regions are not underlined. The C-terminal 6x-His and c-Myc tags are represented in *italics* and bold, respectively. Star represent a stop codon. The synthetic 2KD1 and 3B2 gene constructs encode 122 and 123 amino acids, respectfully, were inserted in pITKan by an N-terminal NcoI and a C-terminal NotI restriction enzymes.

NotI restriction endonuclease sites for insertion into the expression vector pITKan. This vector is a phagemid (pHage3.2) vector derived from M13 and was modified in Dr. J. Christopher Hall's lab to bear a selectable marker for kanamycin (Kan) resistance hence known as pITKan (Figure 3.2). The molecular size of pIT modified vector is 4,453 base pair (bp) that bears an N-terminal pelB leader sequence directing nascent protein to the periplasm and a T7-Lac operator system which provides strong robust expression. It also contains a C-terminal hexa-histidine (6x-His) tag followed by c-Myc tag. These tags facilitate detection and purification of the protein of interest. The c-Myc tag is followed by an amber stop codon which permits the expression of the foreign gene as a fusion with only the c-Myc tag in a non-suppressor host strain *E. coli HB2151*.

The expected molecule sizes of 2KD1 and 3B2 are about 382 and 385 bp for the inserted regions that encode 122 and 123 amino acids respectively. These constructs (Figure 3.3 A) were aimed to be used as positive controls to evaluate rotavirus binding to the V_HHs.

3.1.2 Preparation of HA-CBM2a-$([PT]_3T)_{3x}$S-V_HH-His DNA Construct

Native CBM2a (GenBank with accession number AAA56792), from the enzyme xylanase 10 A found in the soil bacterium *C. fimi* was utilized for this research (Figure 3.4 A). In the current study, the sequence of 2KD1 and 3B2 gene fragments were further modified by fusing them to a native CBM2a (13.05 kDa, 108 amino acids at the 5` end (N-terminal) via a proline-threonine linker ($([PT]_3T)_{3x}$S, 2.09 kDa consisting of 21 amino acids). The synthetic gene constructs (Figure 3.4 B-C) contained an N-terminal hemagglutinin (HA-

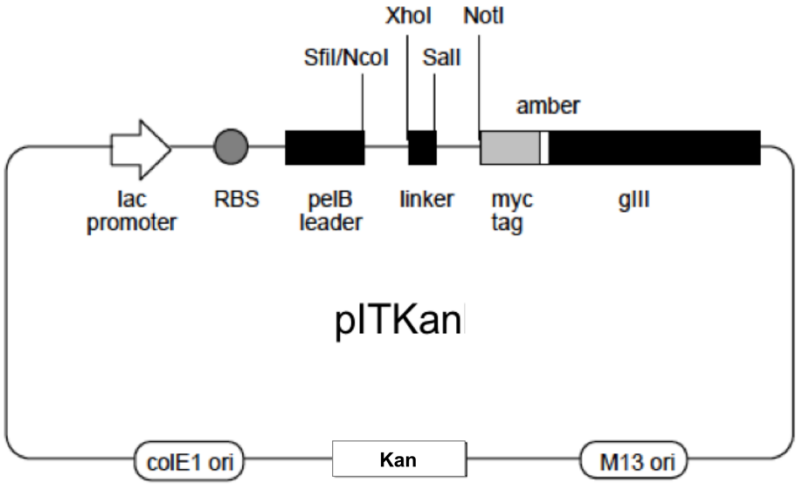

Figure 3.2. Schematic representation of the expression vector pITKan. The main features of the vector include the pelB leader secretion sequence upstream of the multi-cloning site, 6x-His and c-Myc epitope tags before an amber stop codon, a lac promotor, colE1 ori, M13 origin of replication, and Kan antibiotic resistance gene as a selectable marker. The molecular size of pITKan is 4,453 bp.

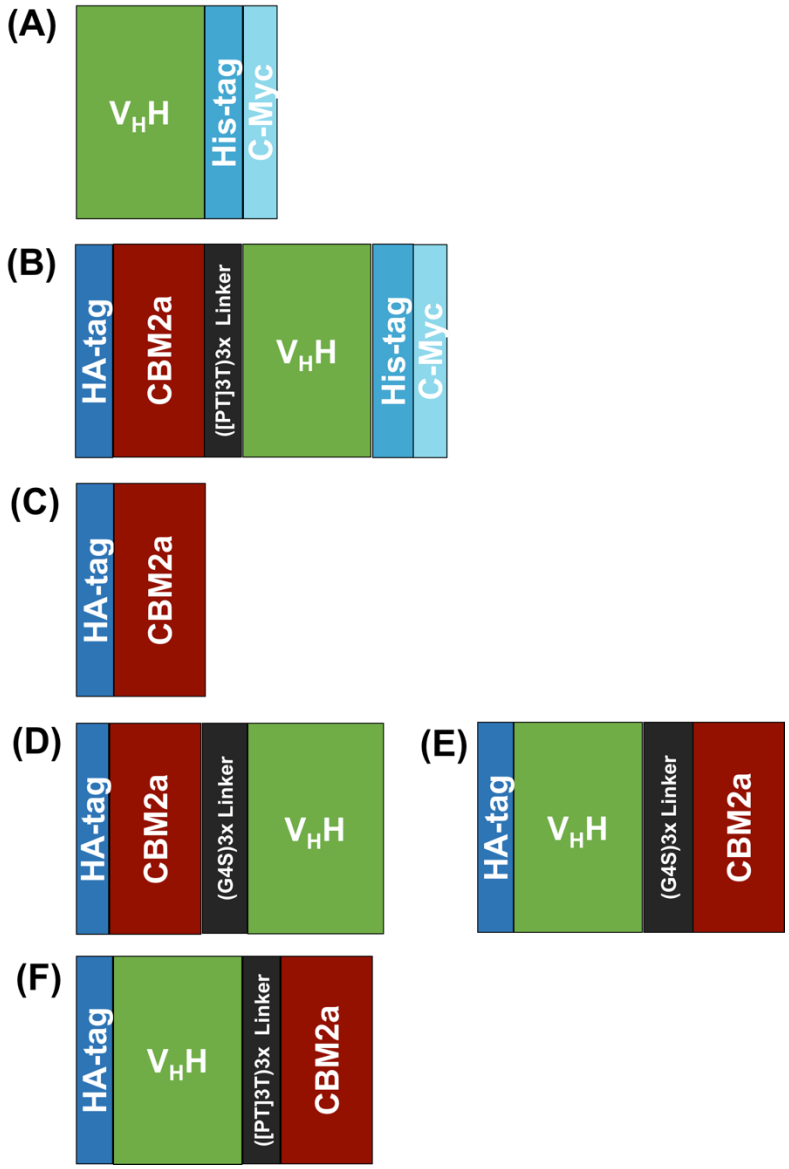

Figure 3.3. Schematic representation of V_HH gene constructs in pIT2Kan plasmid used for protein expression in *E. coli*. (A) V_HH alone (2KD1 or 3B2 single domain antibodies, total size of 382 and 385 bp, respectively; (B) Cellulose binding model (CBM2a; 357 bp) fused at N-terminus of V_HH (2KD1 or 3B2) with a flexible proline/threonine linker ($([PT]_3T)_{3x}S$; 63 bp), total size of 802 and 805 bp. All molecules tagged to 6x His-tag followed by c-Myc at the C-terminus and will be used for the detection of RV (A) and test immobilization on a cellulose filter paper; (C) CBM2a, was immobilized on a cellulose filter paper and used as a control; (D-E) CBM2a fused at N- and C-terminals to 2KD1 with a flexible glycine/serine $(G4S)_{3x}$ linker, total size of 787bp. (F) CBM2a fused at C-terminal to 2KD1 with a $([PT]_3T)_{3x}S$ linker, total size of 805 bp. All molecules (C-F) contain a stop codon before NotI restriction site at the C-terminal to prevent expression of 6x His-tag at protein level, was used for immobilization the 2KD1 on a cellulose filter paper.

- **(A) Native CBM2a (pI/MW: 7.82/10922.90)**

SGPAGCQVLWGVNQWNTGFTANVTVKNTSSAPVDGWTLTFSFPSGQQVTQAWSSTVTQSGSAVT
VRNAPWNGSIPAGGTAQFGFNGSHTGTNAAPTAFSLNGTPCTVG

- **(B) HA-CBM2a-([PT]$_3$T)$_{3x}$S-2KD1-His (pI/MW: 5.95/30557.35)**

MAYPYDVPDYAAASGPAGCQVLWGVNQWNTGFTANVTVKNTSSAPVDGWTLTFSFPSGQQVTQA
WSSTVTQSGSAVTVRNAPWNGSIPAGGTAQFGFNGSHTGTNAAPTAFSLNGTPCTVGPTPTPTT
PTPTPTTPTPTPTSDVQLQASGGGFVQPGDSLSLSCAASGGTFSSYSIGWFRQGPGKEREFVAT
ISSSDSPWYGEPAKGRFTVARVNAKNTAYLHLNRLKPEDTATYYCAAGSVQHMANENEYVYWGQ
GTQVTVSSAAA*HHHHHH*GAA**EQKLISEEDLN**GAA*

- **(C) HA-CBM2a-([PT]$_3$T)$_{3x}$S-3B2-His (pI/MW: 5.74/30656.63)**

MAYPYDVPDYAAASGPAGCQVLWGVNQWNTGFTANVTVKNTSSAPVDGWTLTFSFPSGQQVTQA
WSSTVTQSGSAVTVRNAPWNGSIPAGGTAQFGFNGSHTGTNAAPTAFSLNGTPCTVGPTPTPTT
PTPTPTTPTPTPTSDVQLQASGGGLAQAGDSLTLSCAASGRTFSGYVVGWFRQAPGAEREFVGA
IRWSEDSTWYGDSMKGRILISRNNIKNTVNLQMFNLKPEDTAVYVCAAGAGDIVTTETSYNYWG
RGTQVTVSSAAA*HHHHHH*GAA**EQKLISEEDLN**GAA*

- **(D) HA-CBM2a (pI/MW: 5.89/17961.60)**

MAYPYDVPDYAAASGPAGCQVLWGVNQWNTGFTANVTVKNTSSAPVDGWTLTFSFPSGQQVTQA
WSSTVTQSGSAVTVRNAPWNGSIPAGGTAQFGFNGSHTGTNAAPTAFSLNGTPCTVG*PTPTPT
TPTPTPTTPTPTPTS*AAA*HHHHHH*GAA**EQKLISEEDLN**GAA*

Figure 3.4. Amino acid sequences of native family 2a carbohydrate binding models (CBM2a) from the enzyme xylanase 10A found in *Cellulomonas fimi*. (A) Native CBM2a (also known as Cex or Xyn 10A CBM2a) with 5 N-glycosylation sites (N-X-T/S, where X is any amino acid) are underlined (Xu et al., 1995). (B) The amino acid sequence of the native CBM2a expressed in this study fused to 2KD1 with ([PT]3T)$_{3x}$S C-terminal linker (underlined). (C) The amino acid sequence of the native CBM2a expressed in this study fused to 3B2 with ([PT]3T)$_{3x}$S C-terminal linker (underlined). (D) The amino acid sequence of the native CBM2a expressed in this study with a stop codon (*) before the 6x-His tag. The C-terminal 6x-His and c-Myc tags are represented in italics and bold, respectively. Note: the HA-tag is included at the N- terminus (underlined).

tag; 1.10 kDa, 9 amino acids) and C-terminal 6x-His and c-MYC peptide tags optimized for expression in *E. coli*. Similar to 2KD1 and 3B2, the constructs were synthesized by GeneWiz to contain 5' NcoI and 3' NotI restriction endonuclease sites, giving pITKan HA-CBM2a-$([PT]_3T)_{3x}$S-2KD1-His and pITKan HA-CBM2a-$([PT]_3T)_{3x}$S-3B2-His. The expected molecular sizes were about 802 and 805 bp for the inserted regions encoding 262 and 265 amino acids for HA-CBM2a-$([PT]_3T)_{3x}$S-2KD1-His and HA-CBM2a-$([PT]_3T)_{3x}$S-3B2-His, respectively (Figure 3.4). The constructs were considered as treatments for testing their binding to the virus.

3.1.3 Preparation of HA-CBM2a DNA Constructs

The HA-CBM2a DNA was prepared in the lab from the HA-CBM2a-$([PT]_3T)_{3x}$S-2KD1-His DNA and aimed to be used as a negative control for virus detection. Primer set was designed to include a stop codon before the linker region in the HA-CBM2a-$([PT]_3T)_{3x}$S-2KD1-His DNA followed by NotI at the C-terminal giving the HA-CBM2a DNA, which excludes the 6x-His tag (Figure 3.4 D). The removal of the His tag was needed to avoid cross-reactivity in Western blot and ELISA when an anti-histidine antibody was being used for detection. The expected molecular size of the plasmid was about 376 bp for the inserted region that encode 119 amino acids plus a stop codon for HA-CBM2a.

To construct the expression plasmid pITKan HA-CBM2a, PCR (total volume of 200 µl) was carried out to generate amplicons containing the HA-CBM2a gene sequences. The HA-CBM2a-$([PT]_3T)_{3x}$S-2KD1-His plasmid was used as template DNA to amplify the HA-CBM2a using the forward primer (5' CGGCCATGGCCTATCCATATGATGTTCC 3')

and the reverse primer (5' ATGTGCGGCCGC**TTA**GCCGACCGTGCAGGGCGTGC 3'); restriction sites and stop codon in the primer set are underlined and in bold, respectively.

The PCR conditions used are discussed in Section 3.4.1. The PCR products (expected band size was 376 bp in length) were purified with the Gene JET PCR purification kit (Cat. #K0702, Thermo Fisher Scientific, Burlington, ON, CA) according to manufacturer's instructions. Centrifugation was repeated to elute the DNA and concentration was determined by NanoDrop spectrophotometer (Model 2000 C, Thermo Fisher Scientific, Burlington, ON, CA).

The purified PCR products were then cloned into the linearized pGEM®-T easy cloning vector (Cat. #A3600, Promega, Madison, WI, USA) using 2x rapid ligation buffer and T4 DNA ligase (Cat. #M0202, New England BioLabs® Inc., Whitby, ON, CA) to create the plasmid pGEM®-T-HA-CBM2a. The pGEM®-T vector is approximately 3,000 bp that bears a selectable marker for ampicillin (Amp) resistance (100 µg/ml).

The ligation reaction was performed according to the manufacturer's instruction with a molar ratio of the insert to vector DNA calculated to be 3:1. To achieve the maximum number of transformants, the ligation reaction was performed overnight at 4°C. Next, the ligation reaction was centrifuged briefly at room temperature (RT) and 3-5 µl of the reaction was transformed into 22 µl *NEB 5-alpha* chemically competent *E. coli* cells (C2988, New England BioLabs® Inc., Whitby, ON, CA) by heat-shock (see Section 3.3.1 for protocol). Next, 100 µl of the recovered cells were spread on selective Luria-Bertani Miller (LB; Cat. #BP1426-2 Fisher BioReagents®, Fisher Scientific, NJ, USA) agar plates (Petri dishes; 100 mm x 15 mm, Fisherbrand®, USA) containing 100 µg/ml Amp (Cat. #AMP201, Bioshop®, Burlington, ON, CA), 0.5 mM Isopropyl-ß-D-1-

thiogalactopyranoside (IPTG; Cat. #IPT002, Bioshop, Burlington, ON, CA), and 80 µg/ml X-Gal (Cat. #V394A, Promega, Madison, WI, USA) and incubated overnight at 37ºC in an inverted position. Blue/white colour screening of the resulting colonies was used to indicate successful cloning of the insert into the pGEM®-T vector, observed as white colonies. To confirm positive clones, a colony PCR (see Section 3.4.1 for protocol) using cloning specific primers was performed on several white clones with the expectation of observing a band at 376 bp on a 1% agarose gel. Once the insert was confirmed by colony PCR, one clone was randomly selected for DNA extraction (Section 3.4.2) and tested via plasmid digestion (Section 3.4.3) and sequencing using vector specific primers (Section 3.4.4).

pGEM®-T-HA-CBM2a clones with 100% DNA sequence match to the predicted CBM2a nucleotide sequence were used to transfer the HA-CBM2a fragment into the pITKan expression vector. The pGEM®-T-HA-CBM2a plasmid DNA was digested with NcoI (Cat. #R0193S, 1000 units, New England BioLabs® Inc., Whitby, ON, CA) and NotI (Cat. #R0189S, 500 units, New England BioLabs® Inc., Whitby, ON, CA) restriction enzymes (Section 3.4.3). The digested DNA was purified from 1% 1x TAE agarose gel with the Gene JET gel extraction kit (Cat. #K0692, Thermo Fisher Scientific, Burlington, ON, CA) according to manufacturer's instructions. The concentration and purity of extracted DNA was determined by NanoDrop spectrophotometer.

Simultaneously, the pITKan vector was also digested with NcoI and NotI restriction enzymes and treated in the same manner as the CBM2a fragment. The digested HA-CBM2a fragment was cloned into the NcoI and NotI sites of the pITKan expression vector using T4 DNA ligase to create the plasmid pITKan HA-CBM2a. The ligation reaction with

a molar ratio of 5:1 (insert: vector) DNA was performed overnight at 16°C as described by the manufacturer. Next. 3-5 µl of the ligation reaction was transformed into freshly prepared electro-competent *HB2151 E. coli* (Cat. #BU-00036-VIAL, Nordic BioSite, Wayne, PA, USA) using a MicroPulser™ electro-porator (Section 3.3.2). This strain of *E. coli* is a non-amber-suppressor host that recognizes the amber stop codon between the cloned gene and the gene III fragment. Next, 100 µl of the recovered cells were spread on selective LB agar plates containing 50 µg/ml Kan (Cat. #201.10, Bioshop®, Burlington, ON, CA) and incubated overnight at 37ºC in an inverted position. Putative transformants were initially confirmed by colony PCR using vector specific primer set, with expected size of 578 bp. The DNA was further analyzed as indicated in Sections 3.4.

3.1.4 Preparation of HA-CBM2a-Linker-2KD1 DNA Constructs at C- & N-Terminals

Similar to HA-CBM2a, to prevent cross-reactivity with the 6x-His tag on 2KD1 and VP_6 recombinant proteins, the nucleotide sequence of the 2KD1 fused to CBM2a was designed to include a stop codon before the C-terminal NotI in the pITKan expression vector to exclude expression of the His-tag during expression of the fusion protein. The CBM2a was designed to be fused to either N-terminal or C-terminal via two types of flexible linkers: $([PT]_3T)_{3x}S$ and/or $(G4S)_3$ giving HA-2KD1-$([PT]_3T)_{3x}S$-CBM2a, HA-2KD1-$(G4S)_{3x}$-CBM2a and HA-CBM2a-$(G4S)_{3x}$-2KD1 (Figure 3.3 D-E). The constructs were codon optimized for expression in *E. coli* to contain 5' NcoI and 3' NotI restriction endonuclease sites into the expression vector pITKan and synthesized by GeneWiz. The length of the insert with $([PT]_3T)_{3x}S$ and $(G4S)_{3x}$ linkers are about 805 and 787 bp that encode 263 and 257 amino acids, respectively (Figure 3.5).

- **(A) HA-2KD1-($[PT]_3T)_{3x}$S-CBM2a (pI/MW: 5.95/31055.96)**

MAYPYDVPDYADVQLQASGGGFVQPGDSLSLSCAASGGTFSSYSIGWFRQGPGKEREFVATISS
SDSPWYGEPAKGRFTVARVNAKNTAYLHLNRLKPEDTATYYCAAGSVQHMANENEYVYWGQGTQ
VTVSSPTPTPTTPTPTPTTPTPTPTSAASGPAGCQVLWGVNQWNTGFTANVTVKNTSSAPVDGW
TLTFSFPSGQQVTQAWSSTVTQSGSAVTVRNAPWNGSIPAGGTAQFGFNGSHTGTNAAPTAFSL
NGTPCTVG*AAA*HHHHHH*GAA**EQKLISEEDLN**GAA*

- **(B) HA-2KD1-$(G_4S)_{3x}$-CBM2a (pI/MW: 5.95/29928.53)**

MAYPYDVPDYADVQLQASGGGFVQPGDSLSLSCAASGGTFSSYSIGWFRQGPGKEREFVATISS
SDSPWYGEPAKGRFTVARVNAKNTAYLHLNRLKPEDTATYYCAAGSVQHMANENEYVYWGQGTQ
VTVSSGGGGSGGGGSGGGGSAASGPAGCQVLWGVNQWNTGFTANVTVKNTSSAPVDGWTLTFSF
PSGQQVTQAWSSTVTQSGSAVTVRNAPWNGSIPAGGTAQFGFNGSHTGTNAAPTAFSLNGTPCT
VG*AAA*HHHHHH*GAA**EQKLISEEDLN**GAA*

- **(C) HA-CBM2a-$(G_4S)_{3x}$-2KD1 (pI/MW: 5.95/29928.53)**

MAYPYDVPDYAAASGPAGCQVLWGVNQWNTGFTANVTVKNTSSAPVDGWTLTFSFPSGQQVTQA
WSSTVTQSGSAVTVRNAPWNGSIPAGGTAQFGFNGSHTGTNAAPTAFSLNGTPCTVGGGGGSGG
GGSGGGGSDVQLQASGGGFVQPGDSLSLSCAASGGTFSSYSIGWFRQGPGKEREFVATISSSDS
PWYGEPAKGRFTVARVNAKNTAYLHLNRLKPEDTATYYCAAGSVQHMANENEYVYWGQGTQVTV
SS*AAA*HHHHHH*GAA**EQKLISEEDLN**GAA*

Figure 3.5. Amino acid sequences of modified 2KD1, expressed in this study, fused in two orintations via different linkers to native family 2a catrbohydrate binding models (CBM2a) from the enzyme xylanase 10A found in the bacteria *Cellulomonas fimi*. (A) The amino acid sequence of the native CBM2a fused to N-terminal 2KD1 with $([PT]_3T)_{3x}$S C-terminal linker (underlined). (B) The amino acid sequence of the native CBM2a fused to N-terminal 2KD1 with $(G_4S)_{3x}$ C-terminal linker (underlined). (C) The amino acid sequence of the native CBM2a fused to C-terminal 2KD1 with $(G_4S)_{3x}$ N-terminal linker (underlined). The C-terminal 6x-His and c-Myc tags are represnted in *italics* and bold, respectively. Note: a stop codon (*) was added before the 6x-His tag and the HA-tag is included at the N- terminus (underlined.)

3.1.5 Preparation of Recombinant RV-IgG 26 DNA Construct for Expression in Planta

Human VP_6-specific mAb RV-VP_6-26 was previously developed from a single B cell (Weitkamp et al., 2003). In the current study, the coding sequences for the RV-VP_6-26 heavy (accession number, AF452996) and light (accession number, AF453157) domains were fused to the signal sequence from the basic chitinase gene of *Arabidopsis thaliana* (*A. thaliana*) (GenBank accession: AY054628) for secretion into the apoplast and the sequence of the constant region to construct a full-length IgG 26. The H_V and L_V of RV-VP_6-26 genes (Figure 3.6) were codon optimized for expression in *Nicotiana benthamiana* (*N. benthamiana*) (Figure 3.7). The codon usage table of *N. benthamiana* was found at http://www.kazusa.or.jp/codon/cgi-bin/showcodon.cgi?species=4100. Amino acid translation to nucleotide sequence was done using the online analyzing tool on http://www.attotron.com/cybertory/analysis/trans.htm. Sequence clean up was done using the online analyzing tool on https://pga.mgh.harvard.edu/web_apps/web_map/start.

For expression as a full-length IgG 26, construction of VP_6-26 H_V (1,448 bp) and VP_6-26 L_V (712 bp) fragments were inserted between the 5' SacI and 3' BamHI sites resulting in pPFC0205 (11,110 bp) plant expression plasmid (Figure 3.8), known as RV-IgG 26. The pPFC0205 plasmid vector was kindly provided by PlantForm Corporation (Guelph, ON, CA) and DNA nucleotide sequences were synthesized by GeneWiz. The structure of the expression cassette is shown in Figure 3.9. The expression cassette carries fragments containing a doubled enhancer 35S promoter, 5′UTR of the *Cauliflower*

(A) Anti-VP_6-26 H_V

❖ (A1) Original Amino Acids Sequences of Anti-VP_6-H_V (pI/MW: 5.36/14693.40)

VQLVESGAEVKKPGASVKVSCKASGYSFTSYYVHWVREAPGEGLEWMGMINPSDGSTYYAQRFQ
PRVTMTRDTSTTTVFMEMSGLRSEDTAVYYCARGVVGATNEIDFWGQGTTVTVSSAGTKGPV

❖ (A2) Original Nucleotides Sequences of Anti-VP_6- 26 H_V

gagctcaaaaGAGGTTCAGTTGGTTGAGTCTGGCGCCGAAGTAAAGAAGCCCGGTGCTTCAGTT
AAAGTGTCATGTAAGGCAAGCGGATATTCATTCACATCTTATTACGTACATTGGGTAAGAGAGG
CACCTGGGGAGGGCCTGGAATGGATGGGAATGATCAATCCATCTGACGGGTCTACATACTACGC
ACAACGTTTTCAACCAAGGGTTACAATGACACGTGATACAAGCACTACAACGGTCTTCATGGAG
ATGTCTGGTTTGCGTTCAGAGGATACCGCAGTTTATTACTGTGCTAGAGGTGTAGTCGGTGCTA
CTAATGAGATCGACTTCTGGGGACAGGGTACTACCGTTACTGTCAGCTCTGCAGGCACTAAGGG
CCCTGTTggatcc

➢ (B) Anti-VP_6-26 L_V

❖ (B1) Original Amino Acids Sequences of Anti-VP_6-26 L_V (pI/MW: 9.07/14422.07)

VLATAAAAPAMADIRLTQSPSSLSASVGDRVTITCRASQSISNYLNWYQKKPGQAPKLLIYAAT
SLQSGVPSRFSGSGSGTDFTLTISSVQPEDFATYYCQKTLRTWTFGQGTK

❖ (B2) Original Nucleotides Sequences of Anti-VP_6-26 L_V

gagctcaaaaGTGTTGGCAACAGCTGCAGCTGCCCCTGCTATGGCAGAGACTACCCTGACTCAA
AGCCCTGCTACACTGAGCGTATCCCCTGGGGAAAGGGCAACACTGTCCTGTCGTGCCAGTCAGA
GCGTGTCTTCTAACTTGGCCTGGTATCAGCAGAAGCCAGGTCAGGCCCCTAGGCTTTTAATTTA
TGGTGCTAGTACAAGAGCTACTGGTATTCCAGCCAGATTTAGTGGTTCAGGTAGTGGGACTGAG
TTTACCCTTACCATTTCTAGTCTTCAGTCCGAGGATTTTGCCGTTTATTACTGTCAGCAATACA
ACAATTGGCCACGTACCTTCGGGCAAGGGACCAAAGTTGATATAAAGAGAACGGTCGCTTCCAG
TAGAGAAggatcc

Figure 3.6. Amino acid and nucleotide sequences of anti-VP_6 heavy varible (H_V) (A) and anti-VP_6 light variable (L_V) (B) domains expressed in this study as full RV-IgG 26. (A1) Original amino acids sequence of anti-VP_6-26 H_V (127 amino acids). (A2) Original nucleotides sequence of anti-VP_6-26 H_V (397 bp). (B1) Original amino acids sequence of anti-VP_6-26 L_V (127 amino acids). (B2) Original nucleotides sequence of anti-VP_6-26 L_V (397 bp). Anti-VP_6-26 H_V and anti-VP_6-26 L_V sequences are capitalized. SacI & BamHI restriction enzyme sites are highlighted in green. Underlined regions represent CDR_1, CDR_2 and CDR_3, respectively.

➢ (A) Optimized Nucleotides Sequence of Anti-VP_6-26 H_C

gaattctcgagtctgcaggccaacATGGTGGAGCACGACACTCTCGTCTACTCCAAGAATATCAAAGATACAGTCTC
AGAAGACCAAAGGGCTATTGAGACTTTTCAACAAAGGGTAATATCGGGAAACCTCCTCGGATTCCATTGCCCAGCTA
TCTGTCACTTCATCAAAAGGACAGTAGAAAAGGAAGGTGGCACCTACAAATGCCATCATTGCGATAAAGGAAAGGCT
ATCGTTCAAGATGCCTCTGCCGACAGTGGTCCCAAAGATGGACCCCCACCCACGAGGAGCATCGTGGAAAAAGAAGA
CGTTCCAACCACGTCTTCAAAGCAAGTGGATTGATGTGAACATGGTGGAGCACGACACTCTCGTCTACTCCAAGAAT
ATCAAAGATACAGTCTCAGAAGACCAAAGGGCTATTGAGACTTTTCAACAAAGGGTAATATCGGGAAACCTCCTCGG
ATTCCATTGCCCAGCTATCTGTCACTTCATCAAAAGGACAGTAGAAAAGGAAGGTGGCACCTACAAATGCCATCATT
GCGATAAAGGAAAGGCTATCGTTCAAGATGCCTCTGCCGACAGTGGTCCCAAAGATGGACCCCCACCCACGAGGAGC
ATCGTGGAAAAAGAAGACGTTCCAACCACGTCTTCAAAGCAAGTGGATTGATGTGATATCTCCACTGACGTAAGGGA
TGACGCACAATCCCACTATCCTTCGCAAGACCCTTCCTCTATATAAGGAAGTTCATTTCATTTGGAGAGGACACGCT
GAAATCACCAGTCTCTCTCTACAAATCTATCTCTgagctcCAACAATG**GCTAAAACAAATCTTTTCTTGTTTTTAAT**
CTTTTCTCTTCTCTTGTCCCTTTCATCCGCTGAAGTTCAATTAGTTGAAAGCGGAGCAGAGGTAAAAAAGCCTGGCG
CCAGCGTTAAAGTCTCTTGTAAGGCCTCCGGTTATAGCTTCACTAGTTACTACGTTCATTGGGTTAGAGAAGCTCCT
GGCGAGGGGCTCGAGTGGATGGGAATGATCAATCCTTCTGACGGTTCCACATATTACGCACAACGATTTCAGCCAAG
GGTTACTATGACTAGGGATACTTCAACAACTACCGTTTTTATGGAAATGAGCGGTTTGAGATCTGAGGACACAGCTG
TGTATTATTGTGCACGTGGAGTGGTAGGGGCTACCAACGAAATTGATTTCTGGGGTCAAGGGACTACCGTGACTGTG
TCCTCTGCTGGCACAAAGGGTCCTAGCGTGTTTCCATTGGCACCAAGTTCTAAGTCAACCAGTGGCGGGACCGCTGC
ACTTGGATGCCTGGTAAAGGACTACTTTCCTGAGCCTGTTACTGTCTCATGGAACTCCGGTGCTCTTACAAGCGGTG
TTCATACCTTCCCAGCCGTCCTCCAATCTAGTGGATTATATTCTCTCTCAAGTGTCGTGACTGTACCATCTTCCTCT
TTGGGAACCCAGACATACATCTGTAATGTGAACCACAAGCCTAGCAATACCAAGGTGGATAAGAAAGTTGAACCAAA
ATCATGCGATAAAACTCACACATGCCCTCCATGCCCTGCTCCTGAATTGCTGGGTGGACCTTCTGTTTTTTTGTTTC
CACCAAAACCAAAAGACACTTTGATGATTAGTAGAACACCAGAAGTGACATGTGTAGTTGTCGACGTCTCTCATGAA
GATCCTGAGGTTAAGTTCAATTGGTACGTTGATGGAGTAGAGGTGCACAACGCTAAGACTAAACCTCGTGAAGAGCA
GTATAATTCTACATACAGGGTTGTGTCTGTTCTTACTGTACTTCATCAGGATTGGCTTAATGGCAAAGAATATAAAT
GCAAGGTTTCAAATAAAGCACTGCCTGCCCCTATTGAAAAGACTATATCTAAGGCTAAAGGACAGCCTCGGGAACCT
CAAGTTTATACACTTCCTCCATCTAGAGAGGAAATGACAAAGAACCAAGTGTCTCTGACATGTTTGGTTAAGGGGTT
TTATCCATCAGACATTGCTGTCGAGTGGGAAAGTAATGGTCAGCCAGAAAACAATTATAAAACAACTCCTCCTGTTT
TAGATAGTGATGGTTCTTTCTTTTTGTACTCTAAGTTAACTGTCGATAAATCTAGATGGCAACAGGGAAACGTGTTC
AGTTGTTCTGTTATGCATGAGGCTCTCCATAACCACTATACTCAAAAGTCACTGTCTTTGTCACCTGGATGAggatc
cggaTCGATAATGAAATGTAAGAGATATCATATATAAATAATAAATTGTCGTTTCATATTTGCAATCTTTTTTTTAC
AAACCTTTAATTAATTGTATGTATGACATTTTCTTCTTGTTATATTAGGGGGAAATAATGTTAAATAAAAGTACAAA
ATAAACTACAGTACATCGTACTGAATAAATTACCTAGCCAAAAAGTACACCTTTCCATATACTTCCTACATGAAGGC
ATTTTCAACATTTTCAAATAAGGAATGCTACAACCGCATAATAACATCCACAAATTTTTTTATAAAATAACATGTCA
GACAGTGATTGAAAGATTTTATTATAGTTTCGTTATCTTGGGCCCCAAGCTTATGAtc*gaattc*

➢ (B) Optimized Nucleotides Sequence of Anti-VP_6-26 L_C

gagctccaacaATG**GCTAAGACCAATTTATTCCTTTTCTTGATCTTCTCATTGCTTTTGAGCCTCTCTAGCGCT**GAT
ATTCGTCTTACACAATCTCCAAGTAGCCTTAGTGCTTCTGTAGGAGATAGAGTTACTATCACATGTCGGGCTTCACA
GTCAATATCAAACTATTTGAATTGGTATCAGAAGAAGCCTGGACAAGCTCCAAAGCTCTTGATTTACGCAGCCACAA
GCCTGCAAAGTGGTGTGCCTTCTAGATTTTCTGGTTCTGGTTCCGGGACAGACTTCACCTTAACTATCTCCTCTGTT
CAGCCAGAAGATTTTGCAACCTACTATTGCCAAAAGACATTGAGGACTTGGACTTTCGGACAGGGCACTAAAGTCGA
GATTAAACGAACTGTTGCAGCTCCTTCAGTATTCATATTTCCACCATCAGATGAACAACTTAAGAGTGGCACAGCTT
CTGTGGTTTGTCTCTTGAACAATTTTTATCCACGTGAAGCAAAAGTGCAATGGAAGGTAGATAACGCCCTTCAGTCA
GGTAATAGTCAGGAATCTGTGACTGAGCAAGATTCTAAGGATAGCACATACTCTCTTTCCAGCACTTTGACATTGAG
CAAAGCTGACTACGAGAAACATAAAGTTTATGCTTGCGAAGTTACTCATCAAGGGCTGTCTTCACCAGTCACAAAGT
CTTTTAATAGAGGGGAATGTTGAggatccgga

Figure 3.7. Optimized nucleotides sequence of (A) Anti-VP_6-26 H_C (1,433 bp) and (B) Anti-VP_6-26 L_C (725 bp) in pPFC0205 for expression in *N. benthamiana*. The nucleotides sequence before the SacI site in anti-VP_6-26 H_C represents a part of the 35S promoter sequence from the vector. Restriction enzyme sites EcoI represented in italic, SacI highlighted in green, BamHI highlighted in yellow. Start and stop codons highlighted in red. Arabidopsis basic chitinase signal peptide represented in bold. Constant regions are included after the nucleotide sequence of the H_C and the L_C (underlined). Constant region in the H_C sequence includes hange and F_C regions.

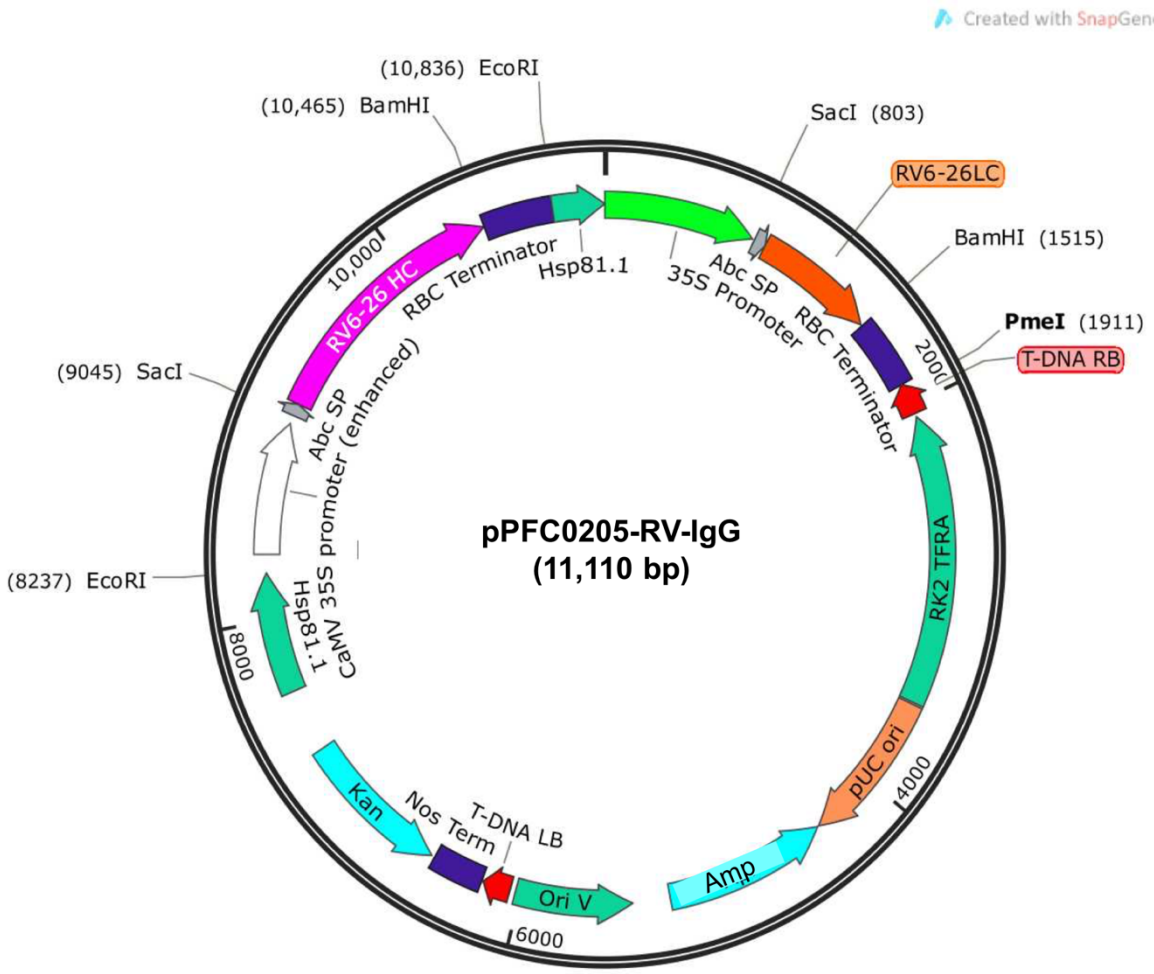

Figure 3.8. Schematic representation of RV-IgG 26 gene construct in pPFC0205 expression vector. The coding sequences for the RV-VP_6-26 heavy chain (RV-VP_6-26 H_c) and light chain (RV-VP_6-26 L_C) were fused to the signal sequence from the basic chitinase gene of *A. thaliana* for secretion into the apoplast. The H_C (in pink, 1,433 bp) and L_C (in orange, 725 bp) of RV-VP_6 were codon optimized for expression in *N. benthamiana* and were inserted between the 5' SacI and 3' BamHI sites giving plasmid pPFC0205-RV-IgG 26 (11,110 bp). Image was created with Snapgene™ 1.1.3. software package.

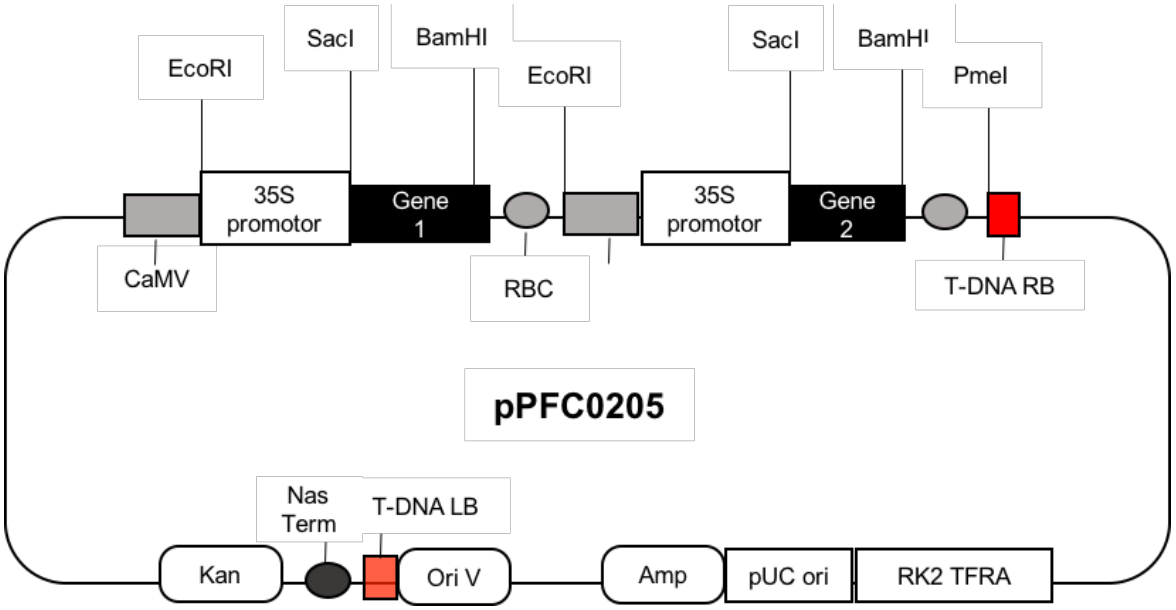

Figure 3.9. Schematic representation of the plant expression vector pPFC0205. The main features of the vector include a doubled enhancer 35S promoter and 5′UTR of Cauliflower mosaic virus (CaMV), 3′ UTR and terminator sequences from RBC gene of RubiCo gene. The vector contains ampicillin (Amp) and kanamycin (Kan) antibiotic resistance genes as selectable markers in *Agrobacterium*.

mosaic virus (RubiCo), 3′ UTR and terminator sequences from RBC gene of *CamV*. The vector also contains Kan and Amp resistance genes as selectable markers. For DNA digestion to confirm the size of the insert, SacI-HF (Cat. #R3156S, 2,000 units, New England BioLabs® Ltd. Whitby, ON, CA) and BamHI-HF (Cat. #R31365S, 10,000 units, New England BioLabs® Ltd. Whitby, ON, CA) restriction enzymes were used (Section 3.4.3).

3.1.6 Recombinant RV-Capsid Protein VP_6

The nucleotide sequence encoding human RV Group A capsid protein VP_6 was retrieved from the GenBank with accession number ACR22820. The RV-VP_6 gene was codon optimized for expression in *E. coli* and synthesized by GeneWiz. The expected molecular size is 1,201 bp for the inserted region that encodes 397 amino acids and restriction sites (Figure 3.10). This construct was used as the backbone for the construction of all RV-VP_6 plasmids to be transformed into *E. coli*. Appropriate restriction sites (5' NcoI and 3' NotI) flanking the VP_6 gene were incorporated into the expression vector pITKan to enable directional sub-cloning into the relevant shuttle vectors pET-22b$^{(+)}$ and pET-SUMO.

The pET-22b$^{(+)}$ vector (Cat. #69744-3, Novagen®, COUNTARY) was kindly provided by Dr. George Harauz (University of Guelph, Chemistry department). The vector has a molecular mass of 5,493 bp that bears an Amp resistant gene, an N-terminal pelB leader sequence directing nascent protein to the periplasm and a T7-Lac I operator system which provides a strong robust expression. It also contains a C-terminal 6x-His tag. The small ubiquitin related-modifier (SUMO) vector was kindly provided by Dr. Joseph S. Lam (University of Guelph, Molecular and Cellular Biology Department, ON,

➢ (A) Amino Acids for RV-VP$_6$ A (pI/MW: 5.90/47557.98)

MEVLYSLSKTLKDARDKIVEGTLYSNVSDLIQQFNQMIVTMNGNDFQTGGIGNLPVRNWTFDFG
LLGTTLLNLDANYVENARTIIEYFIDFIDNVCMDEMARESQRNGVAPQSEALRKLAGIKFKRNF
DNSSEYIENWNLQNRRQRTGFVFHKPNIFPYSASFTLNRSQPMHDNLMGTMWLNAGSEIQVAGF
DYSCAINAPANIQQFEHIVQLRRALTTATITLLPDAERFSFPRVINSADGATTWFFNPVILRPN
NVEVEFLLNGQIINTYQARFGTIIARNFDAIRLLFQLMRPPNMTPAVNALFPQAQPFQHHATVG
LTLRIESAVCESVLADANETLLANVTAVRQEYAIPVGPVFPPGMNWTELITNYSPSREDNLQRV
FTVASIRSMLIKAAA*HHHHHH*GAA**EQKLISEEDLN**GAA*

➢ (B) Optimized Nucleotides Sequence for RV-VP$_6$ A

CCATGGAGGTTCTGTACAGTCTGAGCAAGACCCTGAAGGATGCACGCGACAAGATCGTTGAAGG
CACCCTGTACAGCAATGTTAGCGACCTGATTCAGCAGTTCAATCAAATGATTGTGACCATGAAT
GGTAACGACTTTCAGACCGGCGGTATCGGCAACCTGCCTGTTCGCAATTGGACCTTCGATTTCG
GCCTGCTGGGCACCACCCTGCTGAACCTGGATGCCAACTACGTTGAGAACGCCCGCACAATCAT
CGAGTACTTCATCGACTTCATCGACAATGTGTGCATGGATGAGATGGCCCGCGAGAGCCAGCGT
AATGGTGTTGCCCCTCAAAGCGAAGCCTTACGCAAGCTGGCCGGCATCAAGTTCAAGCGTATCA
ATTTTGACAACAGCAGCGAGTACATCGAGAACTGGAACCTGCAAAATCGCCGCCAGCGTACCGG
CTTTGTGTTCCACAAACCGAACATTTTCCCGTATAGTGCCAGCTTCACCCTGAATCGCAGCCAG
CCGATGCATGACAACCTGATGGGCACCATGTGGCTGAACGCAGGTAGCGAGATCCAGGTTGCCG
GCTTCGATTACAGCTGTGCAATTAACGCCCCGGCCAACATCCAGCAATTCGAGCACATCGTGCA
GTTACGCCGCGCCTTAACAACAGCCACCATCACCCTGCTGCCTGATGCCGAACGTTTTAGCTTC
CCGCGCGTGATCAATAGCGCCGACGGTGCCACCACCTGGTTTTTCAACCCTGTGATCCTGCGTC
CGAACAACGTGGAAGTGGAGTTCCTGCTGAACGGCCAGATCATCAACACCTACCAGGCACGCTT
CGGTACCATCATCGCCCGTAACTTCGACGCCATCCGCCTGCTGTTTCAGCTGATGCGTCCGCCG
AACATGACCCCGGCAGTGAATGCCTTATTCCCGCAAGCCCAGCCTTTCCAACACCACGCCACCG
TGGGCTTAACCTTACGCATCGAGAGCGCAGTGTGCGAAAGCGTGCTGGCCGACGCCAATGAGAC
CCTGCTGGCCAACGTTACAGCCGTGCGTCAGGAATACGCCATTCCTGTTGGCCCGGTGTTCCCG
CCGGGTATGAACTGGACCGAGCTGATCACCAACTACAGCCCGAGCCGCGAGGATAACCTGCAAC
GCGTGTTTACCGTGGCCAGTATTCGTAGCATGCTGATCAAAGCGGCCGC

Figure 3.10. Amino acid and nucleotides sequences of capsid protein VP$_6$ from human rotavirus (hRV-VP6) group A (RV-VP$_6$). (A) The amino acid sequence of the RV-VP6 group A (underlined). (B) The optomized nucelotides sequence of the RV-VP6 for expression in *E. coli*. The C-terminal 6x-His and c-Myc tags are represnted in *italics* and bold, respectively. Note: restriction endonuclease sites (5' NcoI and 3' NotI sites) for cloning into pITKan vector are indicated (highlighted in green).

CA). The pET-SUMO vector (Cat. #1001K, Life Sensors Inc., PA, USA) has a molecular size of 5,628 bp that bears a Kan resistance gene, a T7 promotor system and an N-terminal 6x-His tag that enhances expression and facilitates protein purification and detection. The 6x-His tag followed by a SUMO tag that also enhances the expression and solubility of a target protein as well as decrease proteolytic degradation.

The plasmid pITKan/VP_6 (20 ng/µl) was transformed into freshly electro-competent *E. coli* HB2151 cells by electroporation (Section 3.3.2) and positive transformants were initially identified by colony PCR (Section 3.4.1) using vector specific primers, with expected length of 1,403 bp. Further analyses were done as indicated in Section 3.4.

To construct the expression plasmid pET-22b$^{(+)}$/VP_6 and pET-SUMO/VP_6, two PCR reactions were carried out to generate amplicons containing the VP_6 gene sequence using the plasmid pITKan/VP_6 DNA as a template. The forward primer (5' ATCCATGGAGGTTCTGTACAGTCTGA 3') and the reverse primer (5' GTGCGGCCGCTTTGATCAGCATGCTACG 3') were used to amplify the VP_6 for pET-22b$^{(+)}$ vector, with expected size of 1,205 bp in length. The forward primer (SUMO-VP_6/F: 5' GATTGGTCTCGAGGTATGGAGGTTCTGTACAGTCTGAGC 3') and the reverse primer (SUMO-VP_6/R: 5' ATTCGGTCTCTCTAGATTATTTGATCAGCATGCTACGAATACTG 3') were used to amplify the VP_6 for the pET-SUMO vector, with an expected band at 1,225 bp when run on a 1% agarose gel. The PCR conditions are presented in Section 3.4.1. The purified PCR product (detailed in Section 3.2.1.3) for pET22b$^{(+)}$ was digested with NotI and NcoI restriction enzymes while BsaI-HF (Cat. #R35355, 1,000 units, New England BioLabs® Ltd. Whitby, ON, CA) restriction enzyme was used with purified PCR product for pET-

SUMO. Once the fragment of VP_6 visualized under the UV light, DNA band was excised and re-purified. Concentration and purity of extracted DNA were estimated via NanoDrop spectrophotometer.

Simultaneously, the pET-22b$^{(+)}$ and pET-SUMO vectors were digested with corresponding restriction enzymes and purified from 1% 1x TAE-agarose gel as detailed previously in Section 3.2.1.3. However, to reduce the background of non-recombinants due to self-ligation of the vector, the pET-SUMO was dephosphorylated using a calf intestine alkaline phosphatase (Cat. #M0290S, New England BioLabs® Inc., Whitby, ON, CA), incubated at 37ºC for 30 min before purification. Each digested PCR fragment of VP_6 "insert" was cloned into the expression vector using T4 DNA ligase to create the plasmids pET-22b$^{(+)}$/VP_6 and pET-SUMP/VP_6. The ligation reactions were performed as per manufacturer's instructions with a molar ratio of the insert to vector DNA of 3:1.

Next, 3-5 µl of each ligation reaction was transformed into freshly prepared *E. coli* chemically competent cells (Section 3.3). Putative transformants were initially confirmed by colony PCR using the same primer sets used to amplify VP_6 for pET-22b$^{(+)}$ while the forward primer (SUMO-VP_6/F: 5' GATTGGTCTCGAGGTATGGAGGTTCTGTACAGTCTGAGC 3') and the reverse primer (SUMO-REV: 5' GCAGCCGGATCTCAGTGG 3') were used to confirm correct sequence of VP_6 into pET-SUMO, with expected bands at 1,446 bp in length. Further analyses were done as indicated in Sections 3.4.

3.2 Transformation

The pGEM®-T, and pET-SUMO plasmids, upon ligation, were individually introduced into chemically cloning competent *DH5α E. coli* cells (Cat. #60602-1, Biosearch™ Technologies Lucigen, Middleton, WI, USA) by heat shock with Amp (100 µg/ml) and Kan (50 µg/ml) selections, respectively (Section 3.3.1). The 10 beta chemically cloning competent cell (Cat. #C30191, New England BioLabs® Inc., Whitby, ON, CA) was used with pET-22b$^{(+)}$ plasmid by heat shock and under Amp selection. These cloning cells were used for plasmid maintenance purpose. For protein expression purpose, all pITKan plasmids were individually introduced into *E. coli HB2151* (Nordic BioSite Inc, Wayne, PA, USA) electro-competent cells by electroporation with Kan selection (Section 3.3.2), while chemically competent *E. coli BL21* (*DE3*) (original stock from C2527H, New England BioLabs® Inc., Whitby, ON, CA) strain was used with pET22b$^{(+)}$ and pET-SUMO plasmids with a suitable antibiotic selection. The *E. coli BL21* strain is deficient in lon and ompT proteases.

The RV-IgG 26 plasmid was first introduced into chemically competent *E. coli NEB 5-alpha* cells by heat shock with carbenicillin (Carb, 50 µg/ml) selection. Once correct size and sequence were confirmed, the plasmid was electro-porated into electro-competent *Agrobacterium tumefaciens* (*A. tumefaciens*) AT564 cells (Provided by PlantForm Corporation, Guelph, ON, CA). The cells were allowed to recover in LB at 28ºC and 180 rpm for 2 h before plated on LB agar with Carb selection. A glycerol stock of a single *A. tumefaciens* colony was made from an overnight culture with Carb and Rifampicin (Rif) selections and stored at -80ºC (Section 3.3.2).

3.2.1 Preparation of Chemically Competent Cells and Heat-Shock Protocol

Following ligation, the constructs were transformed into chemically competent cells. The competent cells were prepared by inoculating 5 ml of LB with a single colony and incubated at 37°C with vigorous agitation at 180 rpm (Model SK-757 L, Amerex Instruments, Inc., USA) for overnight. The overnight culture was used to inoculate 100 ml of a sterile LB broth medium contained in a 0.5-L baffled flask and incubated at 37°C with vigorous agitation (220 rpm) until the optical densities (OD) reached 0.4-0.5. Optical densities of bacterial cultures were measured at a wave length of 600 (OD_{600}) by a spectrophotometry (Ultrospec 3100 pro UV/Visible spectrophotometer, Amersham Biosciences, Biochrom Ltd. Cambridge, England). The culture was then divided into sterile, ice-cold 50-ml falcon tubes and incubated on ice for 10 min. The cells were recovered by centrifugation at 2,700 x g for 10 min at 4°C. The cell pellets were gently re-suspended in 30 ml of ice-cold 80 mM magnesium chloride ($MgCl_2$) and 20 mM calcium chloride ($CaCl_2$) before centrifuging, as described previously. Finally, the pellets were suspended in 2 ml of ice-cold 0.1 mM $CaCl_2$, aliquoted in 50 µl volumes, flash frozen in a liquid nitrogen and immediately stored at -80°C until further use. For transformation, 1-5 µl containing about 100 ng of the ligation mix was added to 50 µl of thawed cells. The DNA mixture was incubated on ice for 30 min, heat-shocked at 42°C for 30 second (sec) and incubated on ice for 5 min. To allow the cells to recover, 950 µl of SOC (Cat. #B9020S; New England, BioLabs® Ltd., Whitby, ON, CA) outgrowth medium was pipetted into the mixture and incubated while shaking for 1 h at 37°C and 250 rpm. The mixture (50 to 100 µl) was diluted (indicate dilutions made), plated onto selective LB agar plates and incubated in an inverted position overnight at 37°C. Bacterial transformants were

analyzed as described in Section 3.4. Transformation efficiency was calculated as in the following equation:

$$\mathrm{TE}\ (\frac{\mathrm{cfu}}{\mathrm{ng}}\mathrm{DNA}) = \frac{\text{average of bacterial colonies (cfu)}}{\text{dilution of the inoculum (ng)}} \qquad \text{Equ. 3.1}$$

where *TE* is the transformation efficiency calculated to be about 15 x 10^6 cfu/ng DNA.

3.2.2 Preparation of Electro-Competent Cells and Electroporation Protocol

Isolated plasmids (DNA) at 20 ng/µl were transformed into *E. coli HB2151* electro-competent cells by electroporation. The competent cells were prepared by inoculating 5 ml of a sterile LB broth medium with a single colony. The culture was incubated at 37°C overnight with shaking at 180 rpm. The next day, 500 ml of LB contained within a 2-L baffled flask was inoculated with 5 ml of the overnight culture and incubated at 37°C with shaking at 180 rpm until the optical density (OD, measured at A_{600}) reached 0.6. The culture was then centrifuged at 4,000 x g and 4°C (Beckman J2-21 centrifuge, USA) for 15 min. The cell pellets were washed three times by gently suspending them in 500, 250 and 20 ml ice-cold 10% glycerol (G-7893, Sigma® Chemical Co., USA) before centrifuging each time at 4,000 x g and 4°C. Finally, the pellets were suspended in 1 ml ice-cold 10% glycerol, aliquoted in 50 µl volumes, flashed frozen in liquid nitrogen and immediately stored at -80°C until further use. The cells (50 µl) were transformed with 2 µl of DNA to test its efficiency. In this method, 1-2 µl of DNA was transferred to a micro-centrifuge tube containing 25 µl of *E. coli*. This mixture was incubated on the ice for 2 min followed by pipetting 25 µl of cell-DNA mixture into a pre-chilled Gene Pulser Cuvette® (Cat. #1652089, 0.1 cm gap cuvette, Bio-Rad Laboratories, CA). The cuvette was then pulsed in Bio-Rad Gene Pulser Xcell™ (Model GPX, Bio-Rad, USA) at 1,800 volts. To allow

recovery of the cells and expression of antibiotic resistance, the cells were immediately mixed with 225 µl of SOC outgrowth medium and incubated for 1 h at 37°C with vigorous shaking at 250 rpm. The transformation mixture (100 µl) was spread on selective LB agar plates containing appropriate antibiotic for selection. The plates were incubated for 18 h at 37°C in an inverted position. Bacterial transformants were analyzed as described previously (Section 3.3.1).

3.3 Plasmid DNA Analysis

Upon identification of positive transformants by colony PCR, only one clone of each plasmid was randomly selected for plasmid extraction and analyzed by restriction enzymatic digestion. Correct band patterns following agarose gel electrophoresis verified the presence of target gene in desired plasmids. Clones that were found to contain the gene were subjected to DNA sequencing.

3.3.1 Polymerase Chain Reaction Amplification

The resulting constructs were confirmed by PCR amplification from colony or total genomic DNA extraction using vector/gene specific primer sets. The PCR reaction mixture contained 8.3 µl Go Taq® Hot Start Green Master Mix 2x (Lot. #0000155474, Promega, Madison, USA), 0.33 µl of the vector specific forward and reverse primers at concentration of 10 µM/µl (Table 3.1), 0.6 µl of 500-2000 ng of DNA template and filled up to 16.5 µl with nuclease-free water. For colony PCR, single colony from the titer plates were touched with a P10 pipette tip and then swirled in the PCR tubes. The DNA template was replaced with nuclease-free water and treated in the same manner as a negative co-

Table 3.1. Oligonucleotide primers and PCR product information for sequence confirmation of positive colonies.

Target Gene	Primers [10μM/μl] Sequence 3'-5'	Product Size (bp)
pGEM-HA-CBM2a	Forward, T7 promotor: : TAATACGACTCACTATAGGG Reverse, SP6 long promotor: ATTTAGGTGACACTATAGAAT	504
pITKan/2KD1-His	Forward, LMB3: CAGGAAACAGCTATGAC Reverse, pHEN: CTGAATGGGGCCGCATAGACT	584
pITKan/3B2-His		587
pITKan/HA-CBM2a-$([PT]_3T)_3$xS-2KD1-His		1004
pITKan/HA-CBM2a-$([PT]_3T)_3$xS-3B2-His		1007
pITKan/HA-2KD1-$([PT]_3T)_3$xS-2KD1		1004
pITKan/HA-CBM2a-$(G_4S)_{3x}$-2KD1		986
pITKan/HA-2KD1-$(G_4S)_{3x}$-CBM2a		986
pITKan/VP_6		1403
pITKan/HA-CBM2a	Forward, LMB3: CAGGAAACAGCTATGAC Reverse Reverse, pHEN-2: CTATGCGGCCCATTCA'	578
pET22b$^{(+)}$/VP_6	Forward, T7 promotor: TAATACGACTCACTATAGGG Reverse, T7 terminator GCTAGTTATTGCTCAGCGG	1448
pETSUMO/VP_6	Forward: ACCACTCCTTTAAGAAGGC Reverse: GCAGCCGGATCTCAGTGG	1446

ntrol. The PCR reaction took place in 0.2 ml reaction tubes at a Bio-Rad Thermal System (C1000™ Thermal cycler, Bio-Rad, Hercules, CA, USA) with the following program parameters: an initial DNA denaturation at 94°C for 2 min followed by 40 cycles of 30 sec at 94°C for denaturation, 30 sec for primer annealing, 1:20 min at 72°C for elongation, and a final elongation at 72°C for 10 min followed by holding at 4°C. To confirm that the PCR reaction was successful, 3 µl of the PCR product was separated along with 1 Kb DNA ladder (Cat. #SM0311, Thermo Fisher Scientific, Burlington, ON, Canada) on 1% agarose gel in 1x TAE buffer containing 10 µg SYBR® Safe DNA gel stain (Ref. #S33102, Invitrogen™, Life Technologies, Carlsbad, CA, USA) at 80 volts for 30-45 min. The gel was visualized and pictured under universal hood (II Bio-Rad Laboratories Inc., USA) using Bio-Rad Quantity One® 1-D Analysis for Windows version 4.2.1 software package. Clones that were found to contain the gene were subjected to DNA sequencing.

3.3.2 DNA Extraction

A single clone was grown in 5 ml of LB broth medium contained within 50-ml falcon tube supplemented with 50 µg/ml of a suitable antibiotic and incubated at 37°C for maximum of 16 h. After centrifuging the 5 ml at 12,000 rpm for 3 min at RT (IEC MicroCL 17 centrifuge, Cat. #75002451, Thermo Electron Corporation, Germany), cell pellets were lysed and plasmid DNA was eluted using a Gene JET Plasmid Miniprep kit (Cat. #K0503, Thermo Fisher Scientific, Burlington, ON, CA). The concentration and purity of extracted DNA from each clone was determined using a NanoDrop spectrophotometer. The pure plasmid DNA was kept at -20°C for additional methodical investigation.

Also, after 16 h of incubation, glycerol stocks (25 %) of each overnight culture were prepared by mixing 1:1 ml (v:v) of culture and 50% glycerol and stored at -80°C.

3.3.3 Restriction Digestion

The purified plasmid DNA from the clones was digested with appropriate restriction enzymes to ensure insertion of the correct insert. In this method, plasmid DNA was linearized in the following reaction: 1µg of purified plasmid DNA, 2 µl of corresponding reaction buffer, 1 µl of 10 µM of each restriction enzyme. The reaction was diluted to a final volume of 20 µl with MQ-grade water and then incubated in a water bath (VWR™ international, USA) at 37°C for 2-4 h to allow for digestion. Un linearized reaction was treated in a same manner and considered as a negative control. Both linearized and non-linearized reactions [mixed with 4 µl 6x loading dye solution] and 1 Kb DNA ladder were loaded on a 1% 1x TAE-agarose gel containing SYBR® Safe DNA gel stain to visualize the bands. The gel was then submerged into a 1x TA EDTA buffer and allowed to run at 90 volts for 30-45 min. The separated DNA bands were visualized and imaged using a universal hood.

3.3.4 Plasmid DNA Sequencing

Plasmid DNA from positive colonies harboring the gene of interest as confirmed by colony PCR and restriction digest, was sequenced to confirm inserts contained the appropriate gene sequence. The plasmid DNAs (10 µl at 100 ng/µl) were sent along with vector primer sets (10 µl at µM/µl) presented in Table 3.1 to the Guelph Molecular Supercenter (Guelph, ON, CA) for sequencing. The data was analyzed using Snapgene™ 1.1.3. software package and alignment tool on NCIB's website. Permanent stocks of clones with correct sequences were prepared in 25% glycerol for long term storage at -80°C.

3.4 Proteins Expression and Extraction

Protein parameters such as theoretical molecular weight, amino acid composition, molar extinction coefficient (ε), and isoelectric point (pi) were obtained using the ProtParam tool on the ExPASy server. All recombinant proteins expressed in *E. coli* were subjected to short and long expression protocols to determine the best outcome. All cultures were centrifuged at 4°C for protein extraction using a Sorvall® RC-5B refrigerated super-speed centrifuge (SS-34 rotor). Although 2 expression protocols were conducted to express RV-antibody in *E. coli*, the short expression protocol was preferred. About 15 ml of each culture was collected before induction of protein expression and was treated in the same manner representing a non-induced negative control.

3.4.1 Recombinant RV-V_HH Antibodies

For the short expression protocol, 5 ml of LB broth supplemented with 50 µg/ml Kan was inoculated with a loopful of culture from a freezer stock and grown for overnight at 37°C and 180 rpm. The entire overnight culture was added to 500 ml of LB broth in a 2-L baffled flask supplemented with 50 µg/ml Kan. The culture was incubated in a shaker-incubator at 37°C and 220 rpm. Once the OD_{600} reached 0.6-0.8, IPTG (0.5 mM final concentration) was added to induce protein expression. The culture was incubated at 24°C and 180 rpm for 18 h.

For the long expression protocol, 30 ml of 2xTY media in a 125-ml baffled flask supplemented with 50 µg/ml Kan was inoculated with a loopful of culture from a freezer stock and incubated at 37°C and 180 rpm. After 16 h of incubation, the entire starter culture was added to 1 L of M9 minimal salts medium (Cat. #DF0485170, Thermo Fisher,

Mississauga, ON, CA) in 4-L baffled flask supplemented with 50 µg/ml Kan, 1 mM $MgCl_2$, 0.1 mM $CaCl_2$, 0.5 µg/ml vitamin B1, 0.2 % Glucose and 0.4 % Casamino acids. The culture was incubated at 25°C and 180 rpm for 36 h. To induce periplasmic protein expression, 0.1 mM IPTG (final concentration) and 100 ml of 10x Terrific Broth (TB) nutrient were added to the culture and incubated at 25°C with shaking at 180 rpm for 60 h.

To extract the periplasmic protein “from both protocols”, a sucrose shock protocol was used. The cultures were harvested by centrifugation at 5,000 rpm for 20 min at 4°C. The supernatant was discarded and the cell pellets were re-suspended in 150 ml of ice-cold wash solution (10 mM Tris pH 8 and 0.5 M NaCl) and centrifuged at 10,000 rpm and 4°C for 10 min. The supernatant was discarded and the pellets were collected and re-suspended in 50 ml of ice-cold sucrose solution (10 mM Tris pH 8, 1 mM EDTA and 25% sucrose) then centrifuged at 10,000 rpm and and 4°C for 25 min. The supernatant was discarded and the pellets were chilled on ice for 20 min and re-suspended in 50 ml ice cold shock solution (10 mM Tris pH 8 and 0.5 mM $MgCl_2$) before centrifuging at 1,000 rpm for 25 min. Finally, the supernatant (containing the periplasmic protein) was filtered through a 0.22 µm filter (Millipore, Nepean, ON, CA) and dialyzed using an appropriate MWCO dialysis tubing (Spectrum Medical Industries, INC., Los Angeles, CA, USA). For those recombinant proteins containing a His-tag, they were dialyzed against immobilized metal ion affinity chromatography (IMAC) buffer A (20 mM phosphate, 0.5 M NaCl and 10 mM imidazole of pH 7.4) at 4°C for overnight. For V_HHs linked to CBM2a without 6x-His tag, the recombinant fusion proteins were extracted and TSP was dialyzed into phosphate buffer solution (1x PBS) pH 7.4 at 4°C overnight. These fusion proteins did not need to

be purified by FPLC, as they could be isolated by binding to cellulose and were used directly as TSP in detecting assays All dialyzed proteins were aliquoted and stored at -80°C until needed. Insoluble proteins found in inclusion bodies were not processed further. Ten µl of each supernatant, known as total soluble protein (TSP), was examined by sodium dodecyl sulfate polyacrylamide gel electrophoresis (SDS-PAGE) and Western blotting (Section 3.6.1) to verify the expression of the target protein.

3.4.2 Agroinfiltration of RV-IgG 26 and Protein Expression

The expression of recombinant RV-IgG 26 against RV-VP_6 capsid protein in *N. benthamiana* was performed using a transient viral-based expression system (Giritch et al., 2006). For RV-IgG 26 expression, *A. tumefaciens* containing pPFC0205 (RV-IgG 26 DNA) and *Agrobacterium* containing p19 (provided by PlantForm Corporation) were used to co-infiltrate *N. benthamiana* plants. *Agrobacterium* p19 acted as a plant anti-silencer to boost antibody RV-IgG 26 antibody production. The agroinfiltration procedure was done with support from PlantForm Corporation using greenhouse facilities and the Dixon Lab (University of Guelph, Guelph, ON, CA).

To perform expression, 2 L *A. tumefaciens* culture (in a 4-L flask) was grown overnight at 28 °C and 180 rpm in LB media supplemented with Carb and Rif (50 µg/ml for both). Similarly, *Agrobacterium* p19 culture was grown overnight at 28 °C and 180 rpm in LB supplemented with Kan and Rif (50 µg/ml for both). Dense overnight cultures (up to OD_{600}= 2.5) were adjusted to an OD_{600} of 0.2 in Agro-infiltration buffer (AIB) containing 10 mM 2-4-morpholino-ethanesulfonic acid (MES), 10 mM magnesium sulfate ($MgSO_4$)

pH 5.5 to create an *Agrobacterium* infiltration cocktail (AIC) for plant treatment (Giritch et al., 2006).

Plant were prepared by planting *N. benthamiana* seeds (KDFX, lot. #17-7-26-9-3, made by PlantForm Corporation) in soil-filled pots (Sunshine Mix L4A, Sun Gro Horticulture). The pots (48 pots, 3.5 square inch pots) were grown in a greenhouse under 50% humidity, 86 μmol/m^{-2}s photon light intensity and 16 h day/night cycle at 23ºC. The plants were watered daily with tap water (pH 8) for 6 weeks. To transiently express the antiVP_6-IgG, *N. benthamiana* plants were submerged in a beaker containing the AIC and placed in a vacuum chamber. A vacuum was applied for 2 min with pressure ranging from 0.5 to 0.9 bar and then slowly released (Marillonnet et al., 2005 and Garabagi et al., 2012). Shortly after treatment, the plants were placed back in the greenhouse and watered daily for a week prior to harvest. When harvesting infiltrated plants, newly emerged leaves were discarded and the infiltrated leaves were separated from the stems and biomass was measured before storing at -80°C until further processing.

To extract RV-IgG 26, frozen biomass was homogenized and approximately 200 g of leaf tissue was mixed with 3 volumes of extraction buffer (50 mM trisodium phosphate (Na_3PO_4), 1 M NaCl, 10 mM EDTA, 40 mM ascorbic acid, pH 7.4). Samples were disrupted in a 500-ml centrifuge bottle (2 bottles each contains about 300 ml) containing two stainless steel ball bearings for 5 min using a TissueLyser (Qiagen, Toronto, ON, CA) to prepare a crude protein extract. The biomass extract was filtered using 2 layers of Miracloth (Calbiochem CN biosciences, inc., La Jolla, CA, USA) into a 1-L flask. The filtrate was transferred into centrifuge bottles and centrifuged at 10,000 rpm for 30 min at 4°C. The supernatant was transferred into new centrifuge bottles and centrifuged under the

same conditions. The supernatant (crude plant extract) was filtered using a Nalgene™ rapid-flow™ sterile disposable bottle top filter units with 0.45 µm PES membrane (Cat. #165-0045, Thermo Fisher Scientific™, CA) and used for protein A purification.

3.4.3 Recombinant RV-VP_6 Protein Expression

For the rapid expression protocol, a single bacterial colony containing the VP_6-recombinant plasmid was used to inoculate 5 ml of LB broth supplemented with a suitable antibiotic. The cultures were grown in a shaker-incubator for overnight at 37°C and 180 rpm. Subsequently, 2.5 ml of each overnight culture was added to 250 ml LB broth in a 1-L baffled flask supplemented with a suitable antibiotic and grown in a shaker-incubator at 37°C and 220 rpm. Once the OD_{600} reached approximately 0.7, IPTG was added (1 mM final concentration). The cultures were grown for an additional 3 h under the same conditions.

For the long expression protocol, overnight cultures of each plasmid were grown as described above. Each culture was added to 500 ml LB broth in 2-L baffled flasks supplemented with a suitable antibiotic and grown at the same conditions. Once the OD_{600} reached approximately 0.7, IPTG was added to final concentrations of 0.5 mM (for cultures with pITKan/VP_6 and pET-22b$^{(+)}$/VP_6) and 0.25 mM (for culture with pET-SUMO/VP_6). The cultures were grown an additional 12 h at 24ºC and 180 rpm (Bugli et al., 2014).

Regardless of the expression protocol, the cells were harvested by centrifugation at 5,000 rpm and 4°C for 20 min and pellets were frozen at -20ºC until needed. To extract the periplasmic protein, cell pellets were lysed using a lysozyme total cell lysis protocol

as follows. The frozen pellets were thawed and resuspended in 20 ml of ice-cold lysis buffer (IMAC buffer A, 300 mM NaCl, 20 mM K-phosphate buffer pH 7.8, 0.05% triton X114 (Cat. #9036-19-5, Sigma-Aldrich®, St. Louis, MO, USA), 2 mM dithiothreitol (DTT; Cat. #3483-12-3, Sigma-Aldrich®, St. Louis, MO, USA), 5% glycerol, 10 mM imidazole). Protease inhibitor, phenylmethanesulfonyl fluoride solution, (PMSF; Cat. #93482-50ML-F, Sigma Life Science, St. Louis, MO, USA) was then added to a final concentration of 1 M and mixed. The cells were lysed by addition of 1 mg/ml lysozyme (Ref. #1083705900, Sigma Life Science, St. Louis, MO, USA) and incubating at RT for an hour. Next, the homogenates were sonicated (Model D100, Fisher Scientific, CA) 6 times for 30 sec, with 60 sec interval between each sonication on ice before a final centrifugation step at 14,000 rpm and 4ºC for 25 min. The resulting supernatant (TSP) was filtered through a 0.22 µm membrane filter and immediately used for purification by IMAC.

3.4.3.1 Recombinant SUMO-Protease Protein Expression

A single colony of *E. coli Rosetta* transformed with plasmid pET-Ulp1 containing SUMO-protease gene (provided with protocols for expression and purification by Dr. Anthony Clarke's lab, University of Guelph, Molecular and Cellular Biology Department, ON, CA) was grown in 5 ml LB medium with Kan (50 µg/ml) overnight at 37ºC and 180 rpm. The overnight culture was subsequently used to inoculate 1 L of SuperBroth in a 4-L baffled flask and grown at 37ºC with shaking at 180 rpm until an OD_{600} of 0.8 to 0.9 was reached. At that point, IPTG was added at a final concentration of 1mM and the culture incubated a further 3 h at 37ºC with shaking at 180 rpm to induce SUMO-protease expression. The culture was then pelleted by centrifugation at 5,000 rpm for 20 min at

4ºC and pellet was frozen until needed. The frozen pellet was suspended in a lysis buffer (IMAC buffer A: 20 mM Tris pH 8.0, 350 mM NaCl, 1 mM DTT) and lysed using sonication. Unbroken cells were cleared by centrifugation at 25,000 x g for 20 min at 4ºC. The cleared lysate containing TSP was filtered through a 0.22 µm syringe filter prior to purification step.

3.5 Protein Purification

3.5.1 Soluble Proteins with 6x-His Tag

Upon expression, the periplasmic extracts for all 6x-His tag recombinant fusion proteins were purified by IMAC using 5 ml HisTrap™ Chelating HP IMAC columns (17-5248-01, GE Healthcare, Piscataway, NJ, USA) using an ÄKTA™-Purifier 900 FPLC system using Unicorn™ version 4.00 software (Amersham pharmacia biotech, Piscataway, NJ, USA). Briefly, a 5 ml HisTrap™ column was charged and equilibrated according to manufacturer's instruction with IMAC washing buffer A before loading the extracted filtered protein at a flow rate of 3 ml per minute (50 ml maximum). The column was then washed with IMAC buffer A and buffer B (contains 50 mM imidazole). For VP_6 purification, the column was washed with 200 ml of 25 mM imidazole followed by 130 ml of 50 mM imidazole in the IMAC buffer A. All buffers used in the RV VP_6 capsid protein purification included the use of Triton X-114 at a final concentration of 0.05% to reduce endotoxins during histidine fusion-protein purification. A gradual increase in imidazole concentration to 500 mM in the above buffers was used for elution of the antibodies, while 300 mM imidazole and 250 mM imidazole were used to elute SUMO-VP_6 and SUMO-protease, respectfully. Eluted fractions of 1 ml each were collected and analyzed by SDS-PAGE

and Western blotting (Section 3.7.1) to confirm the purity and the size of each fraction. Upon confirmation of fractions containing pure fusion proteins, those with high concentration were pooled and dialyzed using appropriate dialysis tubing size and buffer at 4°C overnight. The antibodies were dialyzed into 1x PBS, VP_6 was dialyzed into a cleavage buffer (20 mM Tris HCl, 150 mM NaCl, 1 mM DTT pH 7.5) and SUMO-protease was dialyzed into 20 mM Tris pH 8, 200 mM NaCl, 1 mM DTT and 5% glycerol. Pure proteins were concentrated using polyethylene glycol (PEG 35,000, Cat. #1546660, Sigma-Aldrich®, St. Louis, MO, USA) to 1mg/ml before being aliquoted and stored at -80°C.

3.5.1.1 Cleavage of SUMO-VP_6

Following purification of SUMO-VP_6 and SUMO-protease by IMAC, the SUMO-VP_6 was combined with SUMO-protease (3 ml of VP_6 at ~1.5 mg/ml with 500 µl of protease at ~2 mg/ml) at 30°C for 2 - 6 h. The SUMO-protease is a highly active cysteinyl protease that recognizes the 3D structure of the ubiquitin-related-modifier protein (SUMO), and the conserved C-terminal sequence (Gly-Gly; cleavage site). Therefore, it can be utilized for efficient removal of the 6x-His tag in the protein of interest (RV-VP_6). Upon confirmation of protein cleavage by SDS-PAGE, the cleaved sample was then loaded onto a charged nickel (Ni^{+2}) column (HisTrap™ Chelating HP IMAC columns). Most of the VP_6 without His tag was eluted in the flow through (unbound) fractions, and the rest was recovered by washing the resin with IMAC washing buffer A. Purified protein was checked by SDS-PAGE and Western blotting using RV-IgG 26 antibody. The VP_6 protein (~45 kDA) was

dialyzed 1x PBS overnight at 4ºC before being aliquoted and stored at -80°C for further analysis.

3.5.2 Soluble RV-IgG 26

The RV-IgG 26 protein was purified using ÄKTA™-Purifier 900 FPLC system. The crude plant extract (~600 ml) was applied to a protein-A resin MabSelect™ (17-5199-03; GE Healthcare, Bio-Sciences AB, Uppsala, Sweden) equilibrated with 50 mM sodium phosphate, pH 7.4 and 1 M NaCl at a flow rate 0.7 ml/min. The column was washed with about 100 ml equilibrated buffer to remove unbound protein. The antibody was eluted with 100 mM sodium acetate, pH 3 and 200 mM arginine and neutralized with 1 M Tris-HCl, pH 8. The eluates were pooled (final volume, 20.6 ml, pH 7) and dialyzed against 1x PBS buffer at 4°C before being stored at -80°C.

3.6 Soluble Protein Characterization

3.6.1 Gel Electrophoresis and Western Blotting

To confirm expression and purification of the proteins, SDS-PAGE and Western blotting were conducted. For SDS-PAGE, all protein samples were prepared in 8 µl of 5 x reducing solution (see Appendix 1 for solution composition) and boiled at 100°C for 10 min. The RV-IgG 26 samples were also prepared in 8 µl of 5 x non-reducing buffer (see Appendix 1 for solution composition) to indicate variations in molecular size between the treatments. For each sample a total volume 40 µl was loaded into each well of the SDS-PAGE gel. A molecular weight protein standard was included in each gel (Precision plus protein™ dual color standard; Cat. #161-0374, Bio-Rad, Mississauga, ON, CA). Gels were run at 70 V

through 6% stacking gel then increasing the voltage at 125 V through the 12% resolving gel using 1x running buffer until the dye left the glass plate. This was followed by either gel staining with Coomassie brilliant blue (SIGMA, St. Louis, MO, USA) or transferring to an Immobilon™-P polyvinylidene fluoride (PVDF, Cat. #162-0177, Bio-Rad Laboratories, Inc., Hercules, CA) transfer membrane for Western blotting.

In Coomassie staining (see Appendix 1 for dye composition), gels were stained at RT for 60 min with continuous rocking on a shaker (Model 260350 Rocker II, Boekel Scientific, USA), rinsed twice with MQ-water, then de-stained overnight in de-staining buffer (see Appendix 1 for buffer composition). Finally, gels were dried using gel drying solution, placed on the DryEase gel drying frame (N12387, Invitrogen™ Life Technologies, USA) between 2 pieces of cellophane. Coomassie staining confirmed the expression and the purity of the proteins.

For Western blotting, proteins were transferred to PVDF membrane for 60 min at 100 V and 4°C. On a shaker at RT, membranes were then blocked with 4% skim milk (Cat. #DF0032173, BD-Difco™, Thermo Fisher, CA) diluted in PBST wash buffer (0.5% Tween-20 (Cat. #BP 337-100; in PBS pH 7.3) for 60 min. Next, membranes containing proteins were probed for 60 mins at RT on a shaker with different antibodies (see Table 3.2 for antibodies used in this test). Next, membranes were washed 4x with PBST for 10 min each time before detecting proteins with 10 ml of corresponding substrate for 10 min. A nitro-blue tetrazolium 5-bromo-4-chloro-3-indolyl-phosphate (AP) substrate (Prod # 34042, 1-Step™ NBT/BCIP, Thermo Scientific, Rockford, IL, USA) was used to detect antibodies conjugated to AP while 3,3',5,5'-Tetramethyl Benzidine substrate solution (Prod. # 34018, 1-Step™ TMB-Blotting, Thermo Scientific, Rockford, IL, USA) was used

Table 3.2. Secondary antibodies used in Western blot for the detection of rotavirus and RV-VP6 on PVDF membrane.

Protein on PVDF Membrane	Secondary Antibody	Supplier
- RV-V_HH-His tag - RV-V_HH-CBM2a-His tag	Monoclonal anti-polyhistidine-alkaline phosphatase (AP) antibody produced in mouse, diluted at 1:5,000 in skim milk	Cat. #A5588-0.5 µl, Sigma-Aldrich®, St. Louis, MO, USA
- RV-V_HH-CBM2a (excluded of His tag)	Monoclonal anti-HA tag conjugated horseradish peroxidase (HRP) produced in mouse, diluted 1:5,000 in skim milk	Cat. #ab173826, abcam
- RV-IgG 26	A mix of AP conjugated anti-human kappa light chain and anti-human IgG (γ-chain specific) conjugated to AP, both produced in goat, diluted at 1:10,000 in 4% skim milk	L_C; Cat. #A3813, Sigma-Aldrich®, St. Louis, MO, USA Cat. #A3187, Sigma-Aldrich®, St. Louis, MO, USA

to detect antibody conjugated to HRP. Once bands appeared on the membranes, the colorimetric reaction was stopped with water and the membranes were allowed to air dry on a Kimwipe.

3.6.2 Protein Concentration

Bradford colorimetric assay was used to estimate the concentration of TSP of proteins with CBM2a and pure proteins. An albumin standard (Cat. #PI23209, Thermo Scientific, Rockford, IL, USA) was prepared in 5 dilutions (0.05, 0.125, 0.250, 0.375 and 0.5 mg/ml) used to make a standard curve. The 1x PBS buffer was used as a blank sample. Ten µl of each protein (sample and standard) was added in triplicate within the wells of a 96-wellplate (Ref. #9018, Corning Incorporated, NY, USA). Next, 200 µl of Bradford dye (Cat. #5000006, Bio-Rad, Hercules, CA, USA) freshly prepared at 1:5 v/v was added to each well. The plate was incubated at RT for 5 min before reading at 595 nm using a microplate reader (Model 680, Bio-Rad, Hercules, CA, USA). Microplate Manager® software (version 5.2.1 Build 106, Bio-Rad Laboratories, Inc.) was used to calculate the correlation coefficient of the linear curve fit and the concentration (mg/ml) of the TSP for each sample. The pure protein was aliquoted and stored at -80°C.

3.7 Production of Virus Strains

3.7.1 Cell Lines Propagation

An African Green monkey kidney epithelial cell line (AGMK- MA104; ATCC® CRL-2378.1™, Manassas, USA) was used to grow and characterize RV group A strains (Arnold et al., 2009). Frozen stock of cell line MA104 (1 ml at about $2x10^6$ cells/ml) was

grown in a 25 cm^2 flask (Ref. #353109, Falcon® A Corning Brand) containing minimal essential medium with Earle's salts (MEM; Cat. #10-010-CM, Corning®, USA) supplemented with 10% fetal bovine serum (FBS; Cat. #SH30396.03HI, GE Healthcare Life Sciences, CA), 0.075% sodium bicarbonate (HCO_3) (Cat. #25080094, Gibco™, CA) and 1% penicillin-streptomycin solution (CAS: 113-98-4, HyClone™ Laboratories, Utah, USA). The flask (total volume of 6 ml per flask) was incubated at 37°C, in a humidified 5% carbon dioxide (CO_2) environment (Model: 3110, Thermo Fisher Scientific, USA). The MA104 cells were sub-cultured regularly, to either two 25 cm^2 or one 75 cm^2 (Ref. #353136, Falcon® A Corning Brand) tissue culture flask(s), two times a week.

The human embryonic kidney 293 (HEK-293) cell line was used to grow and characterize human adenovirus (hAdenoV) while BV2 cell line was used to propagate murine norovirus (mNV) (Brown, 1990 & Cox et al., 2009). The same procedure as described for MA104 was followed to generate the cell cultures of HEK-293 and BV2. The hAdenoV stock was obtained from Dr. Martha Brown (University of Toronto) while BV2 cell line and mNV stock were obtained from Health Canada (Bureau of Microbial Hazards) and served as negative controls for the RV-mAbs. The propagation and titration of mNV were kindly done by Jamie Goltz (4^{th} year undergrad student) according to a protocol provided by Health Canada.

Stocks of the cells were prepared by taking 95-100% confluent cell monolayers, washing 3x with 1x PBS, trypsinizing, neutralizing with growth medium and counting the cells using a hemocytometer (Freshney, 2010). Cells were centrifuged to remove cell debris at 1,000 rpm and 4°C for 10 min using an Eppendorf AG centrifuge 5810 R (Hamburg, Germany). The supernatant was discarded and the pellets were re-suspended

in new growth medium at a final concentration of $2x10^6$ cells/ml. The cells (900 µl) were transferred to a sterile 2-ml cryogenic storage vial followed by addition of 100 µl of dimethyl sulfoxide (DMSO). Tubes were placed in -20°C for 20 min then moved to -80°C for overnight before storing in liquid nitrogen.

Rotavirus human strain Wa and bovine (bRV) strains B223 and C486 were used representing different subgroups and serotypes from different species of RV group A. The hRV strain Wa (G1 for VP7; Rotavirus A ATCC® VR-2018™) was purchased from the American Type Culture Collection (ATCC, Manassas, USA). The bRV strains B223 and C486 were kindly provided at $1.8x10^6$ pfu/ml and $2.2x10^6$ pfu/ml, respectfully, by Dr. Volker Gerdts from Vaccine and Infectious Disease Organization International Vaccine Center (VIDO-IVC) at Saskatchewan University (Saskatchewan, CA). Prior to infecting the MA104 cells, 1 ml of RV stock (described above) was activated by incubating with 1 µg/ml Trypsin-EDTA (Ref. #15400-054, Gibco™) at 37°C, in a humidified 5% CO_2 environment for 30-45 min. The activated virus was then diluted 1:3 v/v with serum free medium (SFM) and added to a 75 cm^2 culture flask with an approximately 95-100% confluent cell monolayer, which had been rinsed 2 times with 1x PBS. The flask was visualized by light microscopy (Model DMi1 inverted microscope, Leica Microsystems CMS GmbH) to ensure the monolayer was intact following virus adsorption. The flask was then incubated at 37°C, in a humidified 5% CO_2 environment with slow continuous rocking (every 15 min by hand) for 1 - 1.5 h to ensure equal coverage of the monolayer with the inoculum and allow for virus adsorption. Following infection, SFM was added to a final volume of 15 ml. The flask was then incubated as indicated previously and checked daily

for CPE of the cell monolayer that includes change in cell morphology (e.g., refractile, rounding, detaching and sloughing) and lysis (24-72 h). A similar procedure was followed with hAdenoV and mNV with their corresponding cell lines.

3.7.2 Viruses Harvesting

The viruses were harvested from the flasks after the cell monolayers were about 80 to 90% lyzed. To harvest RV, cells were dislodging by hitting the side of the flask. The cell lysate containing the virus was pooled from 4-5 flasks into a sterile falcon tube and the virus was clarified by centrifugation at 2,300 rpm and 4°C for 20 min to pellet the cell debris. The supernatant was then transferred to a sterile 1-ml cryogenic storage vial and stored at -80°C until being used for titration and other biological assays. To harvest hAdenoV and mNV, once the monolayers were 80-90% lysed, the flasks were subjected to five cycles of freeze-thawed before centrifugation at which point the process was the same as for RV. The viruses were then stored at -80°C.

3.7.3 Quantification of Viruses

Quantification of the RV was determined by different methods such as plaque assay, tissue culture infection dose (TCID 50%) and qPCR. The titer of hAdenoV was determined by qPCR while plaque assay was used to titer mNV.

3.7.3.1 Plaque Assay

About 2 - 3 days prior to infection for titration, MA104 cells were seeded at a density of 125,000 cells/well in Costar® 6-well tissue culture plates (Cat. #353046, Corning

Incorporated, NY, USA). The plates (three plates/virus) were incubated at 37°C in a humidified 5% CO_2 environment. Once the monolayers were approximately 90 to 100% confluent, the cells were infected. The virus was activated as described above (Section 4.8.2) and serial 10-fold dilutions (up to 10^{-8}) of the activated virus were made in SFM. The growth medium was removed from the MA104 cells and the monolayers were gently rinsed two times with SFM before being infected with 350 µL/well of each virus dilution. The plates were placed at 37°C in a humidified 5% CO_2 environment for 1.5 h with rocking every 15 min. The liquid was then carefully removed and the wells were rinsed once with SFM. For RV strains, the wells were overlaid with 2 ml of a single overlay media (3 media were tested separately): (1) SFM supplemented with 0.8% agarose, (2) MEM supplemented with 4% sephadex G-75, 200 mM glutamine and 2.5% pancreatin or (3) SFM supplemented with 1% methyl cellulose. For mNV, the wells were overlaid only with 2 ml of SFM supplemented with 1% methyl cellulose. The plates were placed back at 37°C in a humidified 5% CO_2 environment and monitored for plaque development after 5 days of infection. The overlay media were aspirated and each well was stained at RT with 500 µL of 0.1% crystal violet in 20% ethanol for 25 to 60 min. Next, the stain solution was aspirated and wells were washed 3 times with MQ H_2O then allowed to air dry. Finally, plaques were counted and viral titer was calculated using the following equation:

$$\frac{\text{pfu}}{\text{ml}} = \#\ \text{of plaques x}\ \frac{\text{dilution of the virus}}{\text{volume of the virus}} \qquad \text{Equ. 3.2}$$

where *pfu* is plaque forming unit.

3.7.3.2 Tissue Culture Infective Dose (TCID) 50%

This method was used only with RV strains. Costar® 96-well tissue culture plates (Ref. #3628, Corning Incorporated, NY, USA) were seeded with 100 µl of MA104 ($2x10^6$ cells/ml) in complete media with MEM per well. The plates were incubated at 37 °C in a humidified 5% CO_2 environment for 48 h. The medium was then discarded and monolayers were washed 2x with SFM. In separate sterile 96 well microtiter plates serial 10-fold dilutions of each virus (up to 10^{-8}) were performed (10^{-1} dilution: 22.5 µl virus stock in 202.5 µl SFM with MEM). Using a multichannel pipet, 200 µl of each virus dilution was transferred into wells containing the cell monolayers. Columns 1 and 2 were used as uninfected control treatments containing 200 µl of complete media and SFM, respectively. After incubating the plates for 5 days at 37°C in a humidified 5% CO_2 environment, the number of CPE positive and negative wells was recorded. The TCID 50% titer was calculated using Excel software and titration of the virus was converted to pfu/ml using the Reed-Muench method as in the following equations (Equ. 3.3 to Equ. 3.6):

$$\mathrm{PD} = \frac{(\%\ \text{at dilution next above } 50\%) - 50\%}{(\%\ \text{next above } 50\%) - (\%\ \text{next below } 50\%)} \qquad \text{Equ. 3.3}$$

where *PD* is the proportionate distance between the two dilutions nearest the 50% death.

$$50\%\ \mathrm{EPD} = (-\log_{10} \text{of next dilution above } 50\% + \mathrm{PD})\ \mathrm{x}\ (\text{dilution factor}) \qquad \text{Equ. 3.4}$$

where *50% EPD* is the end point dilution of the lowest concentration at which there is no infection.

$$\mathrm{TCID}\ 50/\mathrm{mL} = (50\ \%\ \mathrm{EPD})/(\text{viral innoculum in ml}) \qquad \text{Equ. 3.5}$$

where TCID 50, *Tissue Culture Infectious Dose*, is the dose that gives rise to CPE in 50% of inoculated cultures.

$$\mathrm{pfu/ml} = (\mathrm{TCID}\ 50/\mathrm{ml})/(\mathrm{C}) \qquad \text{Equ. 3.6}$$

where *pfu, plaque forming unit,* is the number of infective particles within one ml of the sample and is based on the assumption that each plaque formed is representative of one infective virus particle. The *C* is a constant of 0.69, referring to the theoretical ratio between TCID 50% and pfu.

3.7.3.3 Quantitative PCR

Quantitative PCR was used to titer RV strains and hAdenoV. The qPCR for RV was conducted in two steps including cDNA synthesis and DNA amplification. All primers and probes used for virus analysis by qPCR were ordered from Integrated DNA Technologies, Inc. (IDT®) and Applied Biosystems® (Life technologies™), respectively, and were provided at a concentration of 100 mM.

RNA extraction for RV strains: 140 µl of each RV cell culture supernatant was used to extract total viral nucleic acid (dsRNA) using the QIAamp® Viral RNA Mini kit (Cat. #52904, QIAgen Canada, ON, CA) according to the manufacturer's instructions. Each 140 µl sample was vortexed for 15 sec with 560 µl of AVL lysis buffer (without carrier RNA) and incubate at RT for 10 min. 560 µl 96% ethanol was added and vortexed for 15 sec. The mixture was applied to the QIAamp column (maximum of 630 µL per cycle) and centrifuged at 8,000 rpm for 1 min. The column was then washed with 500 µl of AW1 and centrifuged at 8,000 rpm for 1 min. Additional wash with 500 µl of AW2 buffer was performed and column was centrifuged at 14,000 rpm for 3 min. The spin column was then placed into a new micro centrifuge tube and centrifuged at 14,000 rpm for 1 min before adding 60 µl of AVE elution buffer to the spin column. The column was left for 1 min at RT before being centrifuged at 8,000 rpm for 1 min at RT. The samples (RNA) was

immediately placed on ice and used for cDNA synthesis. The cDNA was stored at -20C until used in qPCR.

DNA extraction for hAdenoV, total viral nucleic acid (dsDNA) were extracted using the Allprep® Power Viral® DNA/RNA kit (Cat. #28000, QIAgen Canada, ON, CA). According to the manufacturer's instructions, 200 µl of virus supernatant was mixed with 600 µl of pre warmed PM1 solution and incubated at RT for 5 min. A 150 µl of IRS solution was added and vortexed before incubating the mixture at 4ºC for additional 5 min. After centrifuging the tube at 13,000 x g for 1 min, 700 µl of the supernatant was transferred to a clean 2 ml collection tube. 600 µl each of PM3 and PM4 solutions were added to the supernatant and vortexed. The mixture was applied to the spin column (maximum of 625 µl per cycle) and centrifuged at 13,000 x g for 1 min. After discarding flow through, 600 µl of PM5 solution was loaded on the column and centrifuged for 1 min. 600 µl of PM4 solution was loaded on the column and centrifuged for 1 min. The column was centrifuged for additional 2 min to dry the membrane. The spin column was then placed into a new micro centrifuge tube and a 50 µl of RNase-free water was added to the spin column. The column was left for 1 min at RT before centrifuging at 13,000 x g for 1 min at RT to complete the nucleic acid elution. The DNA was stored at -20C until used in qPCR.

The concentration and purity of all extracted nucleic acids (RNA or DNA) was determined using a NanoDrop spectrophotometer.

Prior to qPCR, the RNA extracts were converted to cDNA using the iScript™ cDNA Synthesis kit (Cat. #170-8891, Bio-Rad Laboratories, Hercules, CA, USA), according to the manufacturer. Each 20 µl reaction contained 4 µl of 5x iScript™reaction mix (containing oligo (dT) and random primers), 1 µl of iScript™ reverse transcriptase, and

15 µl RNA extract. The assay was carried out in a C1000™ thermal cycler (Bio-Rad, Hercules, CA, USA), a priming step at 25˚C for 5 min was followed by incubation at 46˚C for 20 min; reverse transcriptase inactivation at 95˚C for 1 min and finally the reaction was held at 4˚C. The cDNA samples were stored at −20˚C until analyzed by qPCR. The purified dsDNA from samples with hAdenoV were used directly in qPCR.

The C1000™ thermal cycler CFX96™ Real-Time detection system (Bio-Rad, Hercules, CA, USA) with Bio-Rad CFX maestro (version 4.1.2434.0124 for Mac, ©2017 Bio-Rad Laboratories) was used for the qPCR assays. Each sample was assayed in duplicate (technical replicates) and each assay had a total volume of 25 µl. The sequences of qPCR forward primer (5' TCCGACCCACGATGTAACCA 3') and reverse primer (5' GACGGCCAGCGTAAAGCG 3') with probe (5' ACAGGTCACAGCGACT 3') were used to target the hexon structure gene species F (type 41) for hAdenoV while forward primer (5' CATCTACACATGACCCTCTATG 3') and reverse primer (5' AAATGGCTATAGGGGCG 3') with probe (5' AATAGTTAAAAGCTAACACTGTC 3') were used to target to target the non-structural protein 3 (NSP3) for RV strains. These primer sets and probes were modified (shorter in size) from Lee et al. (2016). The RV primer set was used in the study by Lee et al. (2016) to detect only hRV strain Wa although the set in this study was tested with bRV stains based on the 84% identity in the nucleotide sequence of hRV (accession number: DQ146697) and bRV (accession number: JN626230) (Figure 3.11). For each primer/probe combination, a qPCR master mix was prepared using 12.5 µl of SsoAdvanced™ Universal Probes Supermix (Cat. #172-5284, Bio-Rad Laboratories), 0.075 µl of each primer (final concentration of 300 nM), 0.05 µl probe (final concentration of 200 nM) and 2.3 µl MQ-grad water. The 25 µl reactions, all

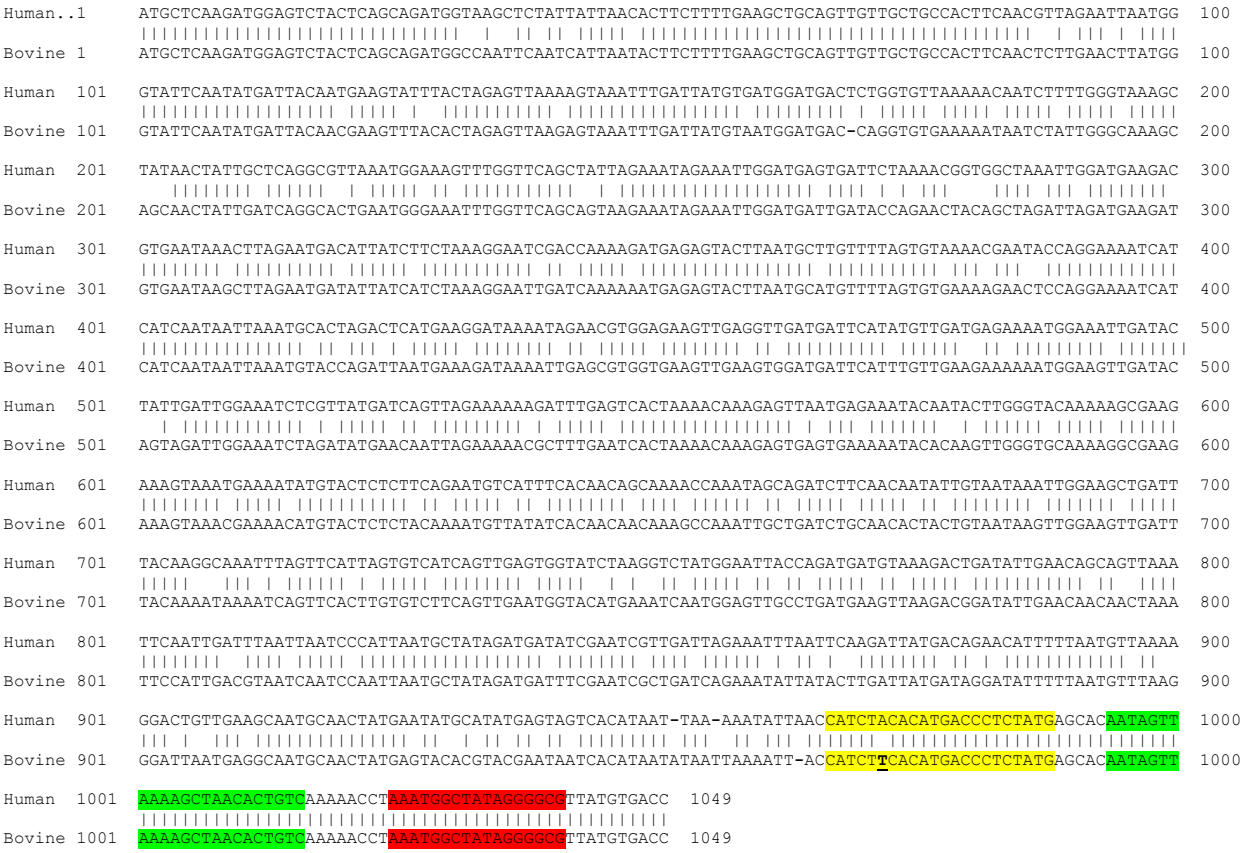

Figure 3.11. Complete sequence alignment for non-structural protein NSP3 gene (1049 bp) from human and bovine rotavirus group A strains. The nucleotide sequences are 84% identical with 0% gaps. Forward primer highlighted in yellow. Reverse primer highlighted in red. Probe highlighted in green. Note that within the primers and probe binding region (from 901 to 1049 bp), there is only one mismatched nucleotide associated with the forward primer (A vs T, bold) and that it did not impact detection of the bRV strains using this primer/probe set.

containing 15 µl of master mix and 10 µl of the cDNA/DNA template, were aliquoted into Hard-Shell® PCR plates 96-well, thin-wall (Cat. #HSP9601, Bio-Rad Laboratories) and qPCR parameters were: one cycle at 95◦C for 2 min and 40 cycles of 95°C for 15 sec and 60°C for 30 sec. Blank (no template control, MQ-grad water) and positive controls (standard plasmids) were (10 µl in a final volume of 25 µl per well) included with each run. A plasmid standard curve, for each target, was run in duplicate on all plates and the threshold was automatically set by the system software. Standard plasmids for the NSP3 and hexon genes were prepared as described in Lee et al. (2016). Briefly, transformed *E. coli* cells (with either the NSP3 or hexon plasmid standard) were grown in 5 ml of LB broth with 100 µg/ml Amp, plasmid was extracted (Section 3.3.2) and concentration was determined at 260 nm using a Nanodrop spectrophotometer. The DNA concentration was used to determine plasmid copy number at http://scienceprimer.com/copy-number-calculator-for-realtime-pcr website using Equ.3.7.

$$\mathrm{CN/\mu l} = \frac{\text{ng of DNA} * 6.022\text{x}10^{23}}{\text{length in bp} * 1\text{x}10^{9}\,\frac{\text{ng}}{\text{g}} * 660\,\frac{\text{g}}{\text{mole}}\,\text{of bp}} \qquad \text{Equ. 3.7}$$

where *CN* is plasmid copy number in µl, *ng* is concentration of DNA and $6.022x10^{23}$ (atom/mole) is Avogadro constant.

The standard curves were prepared from 10-fold dilutions of plasmid stocks from 1x10 to $1x10^{7}$ copies of plasmid per well and assayed in duplicate. The qPCR products were run on a 1% 1x TAE-agarose gel to confirm the size of the amplicons. Performance of the RT-qPCR assay had been previously validated in Lee et al. (2016) in terms of absolute quantification capacity, specificity of target virus detection and absence of competition effect. Acceptability criteria used to assess each qPCR assay was based upon efficiency and R^2 values associated with the standard curve (Bustin et al., 2009).

Efficiency (*E*) of qPCR was calculated from the slope of the standard quantification curve while precision of qPCR quantification was estimated from the R^2 value of the standard quantification curve using test for significance of a regression line.

3.8 Functional Analysis of Antibodies

3.8.1 Confirmation of RV-mAbs Binding

Western blot and SDS-PAGE assays were conducted to test the specificity and sensitivity of different RV- mAbs, produced in this study. Gels containing hAdenoV and mNV as negative controls, RV-VP_6 as a positive control, and serial 10-fold dilutions (2 dilutions) of RV bovine (bRV-B223 and bRV-C486) and human (hRV-Wa) strains were transferred to PVDF membranes and membranes were then blocked with 4% SM at RT for 1 h (see Section 3.7.1 for details). Subsequently, membranes were probed with 2 µg/ml of pure RV-mAbs (2KD1, 3B2 and RV-IgG 26) or 5 µg/ml of TSP of fusion protein with CBM2a and His tag (HA-CBM2a-2KD1-His, HA-CBM2a-3B2-His and HA-CBM2a), produced in this study, for 1 h at RT. Membranes were then washed 3 times with 1x PBST, and incubated with a secondary antibody (either anti-His conjugated to AP or anti HA conjugated to HRP, depending which protein is present on the membrane and/or primary antibody that was used) at RT for 1h. After a final set of 4 washes with 1x PBST, membranes were developed with an AP or HRP substrate corresponding to secondary antibody used. Once bands were visualized (~20 min), membrane development was stopped with MQ-water and allowed to air dry. One corresponding SDS-PAGE was stained with Coomassie blue to observe all bands that would have been present on the blot (described in 3.7.1).

3.8.2 Enzyme-Linked Immunosorbent Assay

Indirect and sandwich ELISA were performed to test and compare the binding of the different RV-V_HH and RV-IgG 26 mAbs with different antigens. Recombinant RV-VP_6 protein and different EVs (hAdenoV and mNV) were included in the assay to serve as antigens for positive and negative controls, respectively. The RV-VP_6 and RV- antibodies were diluted in 1x PBS only when used to coat a Costar® EIA/RIA 96-well microtiter plates (Ref. #9018, high-binding, Corning Incorporated, Corning, NY, USA) and in 4% skim milk prepared in 1x PBST when it used as an antigen or as a detecting antibody. The viruses were diluted in SFM. The 1x PBS and the SFM without antigen were used as background blanks for the RV-VP_6 and the viruses, respectively. Optimization steps were conducted to determine desired concentration of the RV-VP_6 and RV-mAbs (produced in this study) needed for detection purposes.

For indirect ELISA, triplicate wells on a Costar® EIA/RIA 96-well microtiter plates (technical replicates) were coated with 100 µl 10-dilutions of the virus or VP_6. The plates were covered and sealed to prevent evaporation and incubated either overnight at 4°C or at 37°C for 1.5 h. The plates were then blocked with 200 µl 4% SM/well at 37°C for 2 h followed by five washes with 200 µl 1x PBST per wash/well. Rotavirus mAbs (100 µl at 100 ng/well) were added to the wells and plates were incubated 37°C for 2 h. After washing five times, 100 µl of secondary conjugated-HRP antibody (see Table 3.3 for different secondary antibodies used in this test) was added and the plates were incubated under the same conditions. After washing 5 times with 1x PBST, 100 µl of 1-Step™ Turbo TMB-ELISA (Ref. #34022, Pierce Biotechnology, Rockford, IL, USA) substrate was added and allowed to develop in the dark at RT for 20 min. To stop the colour development, 100

Table 3.3. Primary and Secondary antibodies used in ELISA for the detection of rotavirus antigen present in a sample.

Primary Antibody	Secondary Antibody	Supplier
- RV-V_HH-His tag - RV-V_HH-CBM2a-His tag	Rabbit polyclonal to 6x-His tag antibody conjugated to HRP (Penta anti histidine-HRP), diluted at 1:5,000 in skim milk	Cat. #ab1187, abcam
- RV-V_HH-CBM2a (excluded of His tag)	Monoclonal anti-HA tag conjugated horseradish peroxidase (HRP) produced in mouse, diluted 1:5,000 in skim milk	Cat. #ab173826, abcam
- RV-IgG 26	Antihuman IgG heavy and light chains conjugated to HRP, diluted at 1:10,000 in skim milk	Cat. #ab6759, abcam

µl 1 M sulfuric acid (H_2SO_4) per well was added. The color development was measured at 450 nm using a microplate reader. Binding of each RV-mAbs to the antigen (RV-VP_6 or the virus) was calculated by averaging the reading of 3 wells and subtracting it from the average of 3 corresponding blank wells.

For sandwich ELISA, the plate was coated with 100 µl RV-mAbs (produced in this study) and incubated either at 4°C overnight or at 37°C for 1.5 h. Subsequently, wells were blocked with 200 µl of 4% skim milk and plates were incubated at 37°C for 2h. After 5 times washing with 200 µl 1x PBST, 100 µl of the virus or the RV-VP_6 (0.6 µg/well) were added to the appropriate wells and incubated at 37º C for 1 h. Similar to the steps described above for the indirect ELISA, the wells were washed thoroughly, followed by application and incubation with the primary RV-mAbs, and then application and incubation with the secondary antibody (conjugated-HRP). The plates were incubated at 37ºC for 1 h each time and washed after each antibody application. The plates were then allowed to develop for 20 min after the addition of 1-Step™ Turbo TMB-ELISA substrate and the reaction was stopped by the addition of 1 M H_2SO_4 before reading at 450 nm. The binding of RV-mAbs to the antigen (virus and RV-VP_6) was calculated as mentioned above.

3.9 Antibody Capture Technology Development

3.9.1 Cellulose Filter Paper Capture System

3.9.1.1 Binding RV on RV-mAb Coated Cellulose Filter Paper

To confirm the HA-CBM2a protein specifically binds to cellulose, an ELISA was performed on cellulose paper filters. Briefly, circular discs (0.5" diameter) were prepared from Whatman cellulose filter paper grade 5 with 2.5 µm particle retention (GE

Healthcare, Piscataway, NJ, USA) using a standard hole-punch. Based on prior preliminary ELISA results, HA-CBM2a-$(G_4S)_{3x}$-2KD1 was selected for further analysis. The discs were placed in a syringe filtration system (Swinnex® filter holder, Cat. #SX 0001300, EMD Millipore, Billerica, MA) and 20 µl of HA-CBM2a and HA-CBM2a-$(G_4S)_{3x}$-2KD1, at 0.2 µg, were added to discs as negative and positive controls, respectively. After incubation for 30 min at RT, the discs were blocked with 300 µl of 4% SM in PBS-T for 30 min, then washed 3x with 900 µl of PBS-T before the addition of 100 µl of each RV strain (10^3 virus particles/µl). After 30 min, the virus was discarded and discs were washed 3x with 900 µl of PBS-T, probed with 100 µl of RV-IgG diluted in PBS-T (1 µg/ml) followed by 100 µl antihuman-HRP for 30 min each. After washing, discs were developed with 100 µl HRP substrate for 30 min. The solutions were then transferred to a 96-well plate and reaction was stopped with 100 µl of 1M sulfuric acid (H_2SO_4) before reading at 450 nm.

3.9.1.2 Removal of RV by RV-mAb Coated Cellulose Filter Paper

The assay was conducted to examine the ability of the bioactive paper (produced in this study) to capture RV from spiked water samples. Cellulose filter discs were prepared as described above (Section 3.9.1.1). The h-RV and the h-AdenoV were spiked individually and in combination in the presence of different water environments, all tests were performed in triplicate. The viruses were spiked individually at 10^3 and 10^4 CN/µl for h-RV and h-AdenoV, respectively. Mixtures of (1) both viruses at 10^3 CN/µl each and (2) h-AdenoV at 10^4 CN/µl with h-RV at 10^3 CN/µl were evaluated. Tests were conducted in SFM solution, tap water and river water. Tap water was obtained from the laboratory and river samples were collected by the end of March in 1-L amber glass bottles from Speed

River in Guelph, Ontario, Canada. Water quality parameters including, temperature, pH and turbidity were determined for each water type tested (tap and river waters). A pH meter (Mettler Toledo SevenCompact™ pH meter S210, Millipore Sigma-Aldrich, CA) was used to determine pH of the water samples while a turbidimeter (2100Q portable turbidimeter, HACH, CA) was used to measure water turbidity.

For each spiking experiment a cellulose disc was placed in a syringe filtration system and treated with CBM2a or RV-2KD1-$(G_4S)_{3x}$-CBM2a as described previously (Section 3.9.1.1). After blocking and washing the filter, a volume of 1 ml sample (virus in SFM or water) was passed through at a flow rate of 1 ml per min. Discs were washed with 4 ml of filtered tap water to remove non-specifically bound viruses. Influent (un inoculated and spiked samples), flow through and wash were collected separately in clean tubes while discs were frozen at -80°C until being analyzed by RT-PCR. Total viral nucleic acids were extracted using the QIAamp® MinElute® Virus spin kit (Cat. #57704, QIAgen Canada, ON, CA) according to the manufacturer's instructions. Briefly, 25 µl of QIAGEN protease-AVE and 200 µl of AL buffer (without carrier RNA) were added to each 200 µl sample. For filters, 200 µl of 0.9% NaCl solution was added to the filter along with same volumes of the protease and the AL buffer. The samples were vortexed for 15 sec and incubate at 56°C for 15 min. 250 µl 96% ethanol was then added and vortexed for 15 sec. The mixture was incubated for 5 min at RT before being applied to a QIAamp column and centrifuged at 8,000 rpm for 1 min. The column was then washed once with 500 µl of AW1, AW2 and 96% ethanol. The column was centrifuged after each wash at same conditions. The spin column was then placed into a new micro centrifuge tube and centrifuged at 14,000 rpm for 3 min. The empty column was incubated at 56ºC for 3 min

to allow complete drying. The spin column was then placed into a new micro centrifuge tube and 45 µl AVE buffer was added to the spin column. Finally, column was left for 1 min at RT before being centrifuged at 14,000 rpm for 1 min at RT to complete the nucleic acid elution.

Viral RNA was converted to cDNA and qPCR was conducted in duplicate with water (negative control) and standard quantification plasmids (positive control) targeting NSP3 and hexon genes for hRV and hAdenoV, respectively, as described previously (Section 3.7.3.3). Concentration of the viruses from the samples and estimation of virus removal (Equ. 3.8) were calculated.

$$\text{Removal}\ (\%) = \frac{(\text{IF}-\text{FT})}{\text{IF}} \text{x}\ 100 \qquad \text{Equ. 3.8}$$

where *IF* is influent concentration of virus (copy number/ml) and *FT* is the concentration of virus (copy number/ml) in the flow through.

3.9.2 Immuno-Magnetic Capture System

3.9.2.1 Magnetic Beads-Antibody Conjugation

Dynabeads® M-270 Epoxy (Cat. #14311D, novex®, Life technologies™) were conjugated with RV-IgG 26 or RV-2KD1, according to the manufacturer's instructions. The antibody-coupled beads were stored at 4ºC until further analysis.

To ensure conjugation of the beads with the antibody, an SDS-PAGE gel was conducted. The RV-IgG 26 and RV-2KD1 antibody-coupled beads (100 µl at 10 mg/ml) and control beads were each incubated with 1 mg/ml of RV-VP_6 (SUMO/VP_6) at RT on a shaker for 1 h. Subsequently, the supernatants (containing unbound-VP_6) were removed and beads were washed 3 times with 500 µl 1x PBS. The samples of RV-VP_6,

supernatants, washes (32 µl + 8 µl dye) and beads (suspended in 32 µl 1x PBS + 8 µl dye) were boiled for 10 min at 95ºC and were run on SDS-PAGE under reducing conditions.

3.9.2.2 Removal of RV by RV-mAbs Coated Magnetic Beads

The assay was conducted to examine the ability of the immune-magnetic beads (produced in this study with either RV-2KD1 or RV-IgG 26) to capture RV from spiked water samples. Conjugated beads and free-conjugated beads at 2 µg/ml were incubated with RV in SFM (at low, medium and high concentrations) and also in river water spiked with lower concentration of hRV (10^3 virus particles/µl) and highest concentration of hAdenoV (10^4 virus particles/µl) for 1 h at RT on a shaker. The virus was then extracted from the flow through and the beads (beads were washed 3 times with water) and quantified by qPCR as described in Section 3.9.1.2. Concentration of the viruses from the samples and estimation of virus removal were also calculated as described in Section 3.9.1.2.

3.10 Electron Microscopy Analysis

The virus particle and virus binding on cellulose and beads were visualized by using transmission electron microscopy (TEM) and scanning electron microscopy (SEM), respectively, at the Molecular and Cellular Imaging Facility (The University of Guelph Advanced Analysis Centre, Guelph, ON, CA).

3.10.1 Transmission Electron Microscopy

A drop of the virus (5 µl of bRV-B223 at 10^4 CN/µl, was the only strain available with known quantification by the time of the test) was applied to the surface of a filter paper and allowed to air dry for 5 min. A formvar-coated grid was then floated onto the filter (where the drop was placed) for a minute. The grid was immediately transferred and floated on a drop of 1% aqueous uranyl acetate. The grid was allowed to air dry for a few minutes before insertion into the microscope column (FEI Tecnai G2 F20, 200 kv field emission TEM). The sample was screened and images of the virus were taken.

3.10.2 Scanning Electron Microscopy

Both filter paper and immuno-magnetic bead capture systems were analyzed by SEM to visualize the capture of RV (spiked at 10^4 CN/ µl in SFM). The filter paper and antibody-coupled beads were prepared and exposed to RV as described previously (Sections 3.9.1 and 3.9.2). The filter paper discs with or without RV were washed 3 times with 1x PBS and placed on carbon discs. For the beads, antibody-coupled and control beads were suspended in 15 µl 1x PBS after washing 5 times in 1x PBS. To prepare samples for SEM, 5 µl of a bead sample was spread on the surface of a carbon disc and allowed to air dry. The discs were then sputtered coating with gold and visualized by SEM (FEI Quanta FEG 250 SEM). The SEM images were analyzed by ImageJ (64-bit version of Java for Microsoft® Windows® 10 software).

3.11 Statistical Data Analysis

Statistical data analysis was done using SAS® System for Microsoft® Windows® version 9.0 software. Significant differences among means of 3 replicates was accepted when P values were ≤0.05.

3.11.1 Data from ELISA

Graphical work for ELISA was prepared using SigmaPlot® version 11 software packages. Data are means and standard error of 3 technical replicates. All standards (controls) and samples were replicated 3 times (technical replicates, n=3). Blank is the absorbance value obtained with all components of the assay excluding the antigen, i.e. no RV-VP_6 or virus. Factorial analyses of variance (ANOVA) with a further Tukey test (when the group sizes were different) were performed for the evaluation of the sample means. The tests were performed for the evaluation of the means between (1) the binding of different antibody concentration to the viruses (e.g., 200 vs. 100 vs. 10 ng/well), (2) the different samples within same antibody (e.g., bRV-B223 vs. bRV-C486 vs. hRV-Wa at same dilution of the virus detected with the same concentration of an antibody) and (3) each treatment separately among all RV-mAbs (e.g., detection of the virus at same dilution by RV-2KD1 vs. RV-3B2 vs. RV-IgG 26 at same concentration of the antibodies).

3.11.2 Data from qPCR

Graphical work for qPCR standard curves was prepared using Microsoft® Excel for Mac version 15.18 software. Data are means and standard deviation of 3 biological replicates. All standards (positive controls, spiked) and samples were replicated 3 times (biological

replicates, n=3) for virus extraction. Each biological replicate was evaluated in duplicate for qPCR analysis (technical replicates, n=2). In qPCR, positive controls were the plasmid standards that contained the target gene sequence, while no template controls, i.e. samples lacking the target genetic sequence, were used as negative controls. The *t*-test was performed for the evaluation of the means between (1) the removal of RV via cellulose filter treated with RV-HA-2KD1-$(G_4S)_{3x}$-CBM2a and cellulose filter treated with HA-CBM2a within same treatment (e.g., hRV only and hRV in completion with hAdenoV), (2) the specific removal from different treatment (e.g., hRV vs. hRV in completion with hAdenoV) and the removal from different sources (e.g., tap vs. river, tap vs. SFM and river vs. SFM).

4 RESULTS

Concentrating virus from an environmental water sample, which is necessary due to their low concentration, is an important step toward detection. The main goal of this study was to develop a novel concentrating method utilizing recombinant antibody technology to rapidly capture EVs in source waters. Bovine and human strains of RV group A were used as model targets in this study for specific monomeric antibody fragments (e.g., V_HHs, L_C and H_C) against RV group A capsid protein VP_6 that were previously developed and published (Weitkamp et al., 2003 & Garaicoechea et al., 2008). Other strains from EVs group, including hAdenoV and mNV, were used as negative controls through out the study.

To develop a bioactive filter (i.e., antibody-cellulose filter) to directly capture RV in water samples, previously developed V_HHs (2KD1 and 3B2; Garaicoechea et al., 2008) were fused to a CBM2a for the attachment on cellulose filter paper. Hypothetically, linkage of V_HHs to a CBM2a domain should not affect the functionality of the V_HHs to bind RV as CBM2a is used to immobilize the V_HHs on a cellulose surface. The plasmid constructs, V_HHs with or without CBM2a, were cloned into *E. coli HB2151* for expression and purification by IMAC. Eventually, all RV-mAbs were characterized for their specificity and sensitivity to bind to their specific RV A antigen (RV-VP_6 fragment and the whole virus). Different assays, such as, SDS-PAGE, Western blot, ELISA, RT-qPCR and EM were assessed for these investigations.

4.1 Cloning and Transformation of Expression Cassettes

A number of constructs (RV-V_HHs, RV-CBM2a-V_HH, RV-V_HH-CBM2a, RV-IgG 26 and RV-VP_6) were prepared for protein expression. The results of cloning and transformation of these constructs in bacteria are presented in Appendix 2.

4.2 Protein Expression and Purification

Results of protein expression and purification experiments for recombinant proteins (RV-V_HHs, RV-CBM2a-V_HH and RV-V_HH-CBM2a expressed into *E. coli HB2151*, RV-IgG 26 expression in *N. benthamiana*, and RV-VP_6 from pET-SUMO expressed in *E. coli BL21 (DE3))* are presented in this section. Production of RV-VP_6 from pITKan in *E. coli HB2151* and pET22b$^{(+)}$ in *E. coli BL21 (DE3)* are presented in Appendix 3.

4.2.1 Recombinant RV-V_HHs

The RV-V_HHs with or without CBM2a were expressed in *E. coli HB2151* using rapid and long expression protocols. For rapid protein expression, the cultures were induced overnight (IPTG, 0.5 mM final concentration) at 24^{o}C. For the long protein expression, cultures were induced for 60 h (IPTG, 0.1 mM final concentration) at 24^{o}C. The mass of the cell pellet was estimated to be 10.62 g/L and 23.45 g/L for 2KD1, while the mass was estimated to be 11.8 g/L and 24.65 g/L for 3B2 for the rapid and long protein expression protocols, respectively.

For isolation of all recombinant proteins, total soluble proteins were extracted from the periplasm of *E. coli HB2151* by sucrose shock protocol. Both 2KD1 and 3B2 V_HHs not linked to CBM2a were purified using IMAC Ni^{+2}-charged resin via FPLC. Fractions were

eluted over a gradual increase in imidazole concentration to 500 mM (see Figure 4.1 A and 4.2 A for protein purification from rapid expression protocol and Appendices 3.1 A and 3.2 A for purification from long expression protocol). SDS-PAGE analysis of the purified products indicated the V_HHs were of high purity (Figures 4.1 B and 4.2 B and Appendices 3.1 B and 3.2 B). Western blot confirmed the expected sizes of 2KD1 and 3B2 which are 16.04 and 16.14 kDa, respectively (Figure 4.3). The protein concentrations of pure 2KD1 and 3B2 resulting from the rapid expression protocol were 15 and 9 mg protein/L, respectively, estimated at A_{280} using a Nanodrop. Concentrations of purified 2KD1 and 3B2 were about 4 times higher when the long expression protocol was used resulting in 62 and 39 mg protein/L, respectively. The rapid protocol was selected for future protein expression and purification because (1) the purities of the isolated proteins were similar for both expression protocols, (2) the concentration of the pure protein resulting from the rapid protocol was sufficient for the required tests in this work (e.g., ELISA) and (3) of the shortened length of time and limited access to facilities (e.g., large incubator).

4.2.2 Recombinant RV-CBM2a with and without V_HHs

For V_HHs linked to CBM2a, fusion proteins were expressed in *E. coli HB2151*. Each culture was induced using the rapid expression protocol and total soluble proteins retrieved by sucrose shock protocol. The bacterial masses of HA-CBM2a-$([PT]_3T)_{3x}$S-2KD1-His, HA-CBM2a-$([PT]_3T)_{3x}$S-3B2-His, HA-2KD1-$([PT]_3T)_{3x}$S-CBM2a, HA-CBM2a-$(G_4S)_{3x}$-2KD1 and HA-2KD1-$(G_4S)_{3x}$-CBM2a were estimated to be 12.5, 9.5, 10.4, 11.92 and 12.32 g/L, respectively. The bacterial mass of HA-CBM2a was estimated to be 12.68

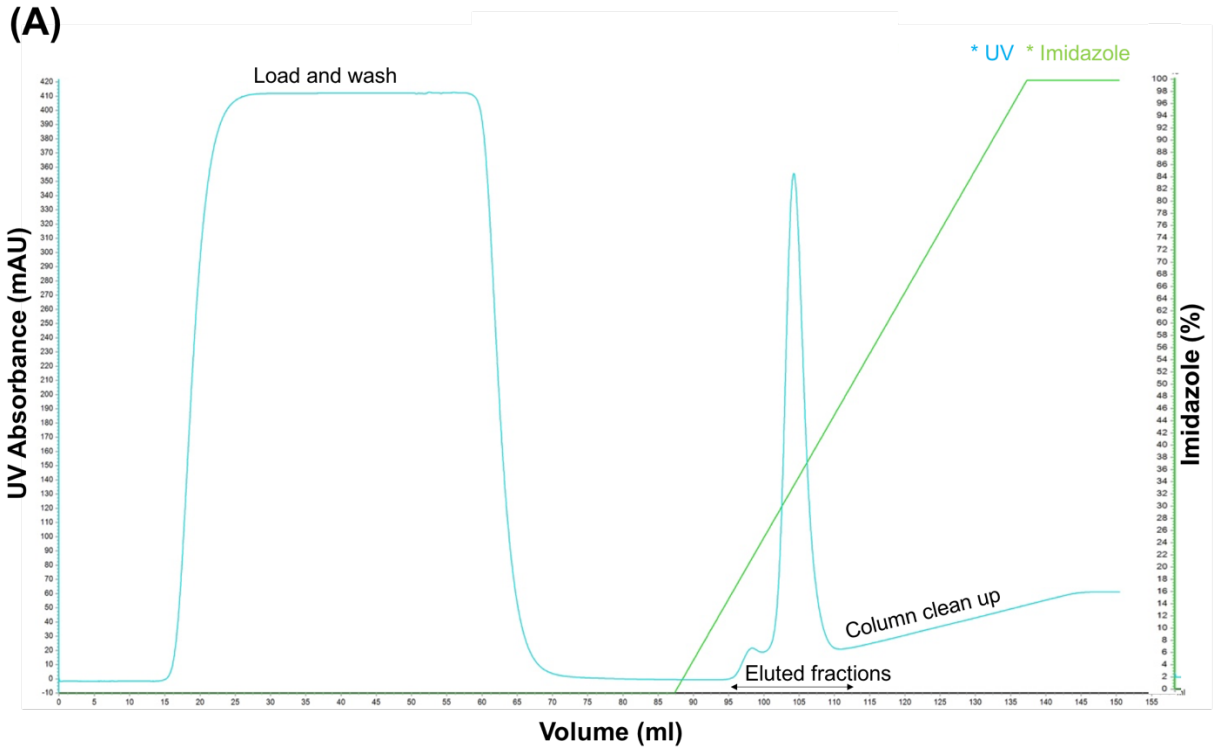

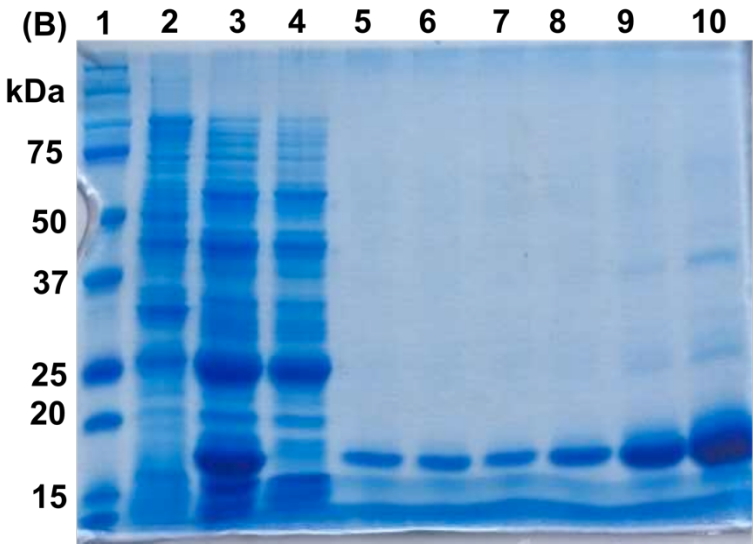

Figure 4.1. Affinity 6x-His tag chromatography purification profile of RV-2KD1 expressed with rapid protocol (*E. coli HB2151*; pITKan/2KD1) culture induced with 0.5 mM IPTG at 24^0C for 16 h). The periplasmic protein was extracted via sucrose shock protocol and applied to Ni^2-resin. After column washing, 2KD1 was eluted over 500 mM imidazole in 1 ml fractions. (A) Elution chromatographic profile illustrating the absorbance at 280 nm (blue line) and collection of eluted fractions (green line). (B) A 12% SDS-PAGE gel indicating expression and purification of RV-2KD1 (observed at about 16.04 kDa). Lane 1: protein standard. Lane 2: Total soluble protein (TSP) from un-induced *E. coli HB2151* (pITKan/2KD1) culture. Lane 3: TSP from induced *E. coli HB2151* (pITKan/2KD1) culture, Lane 4: column wash. Lanes 5-10: eluted fractions of RV-2KD1.

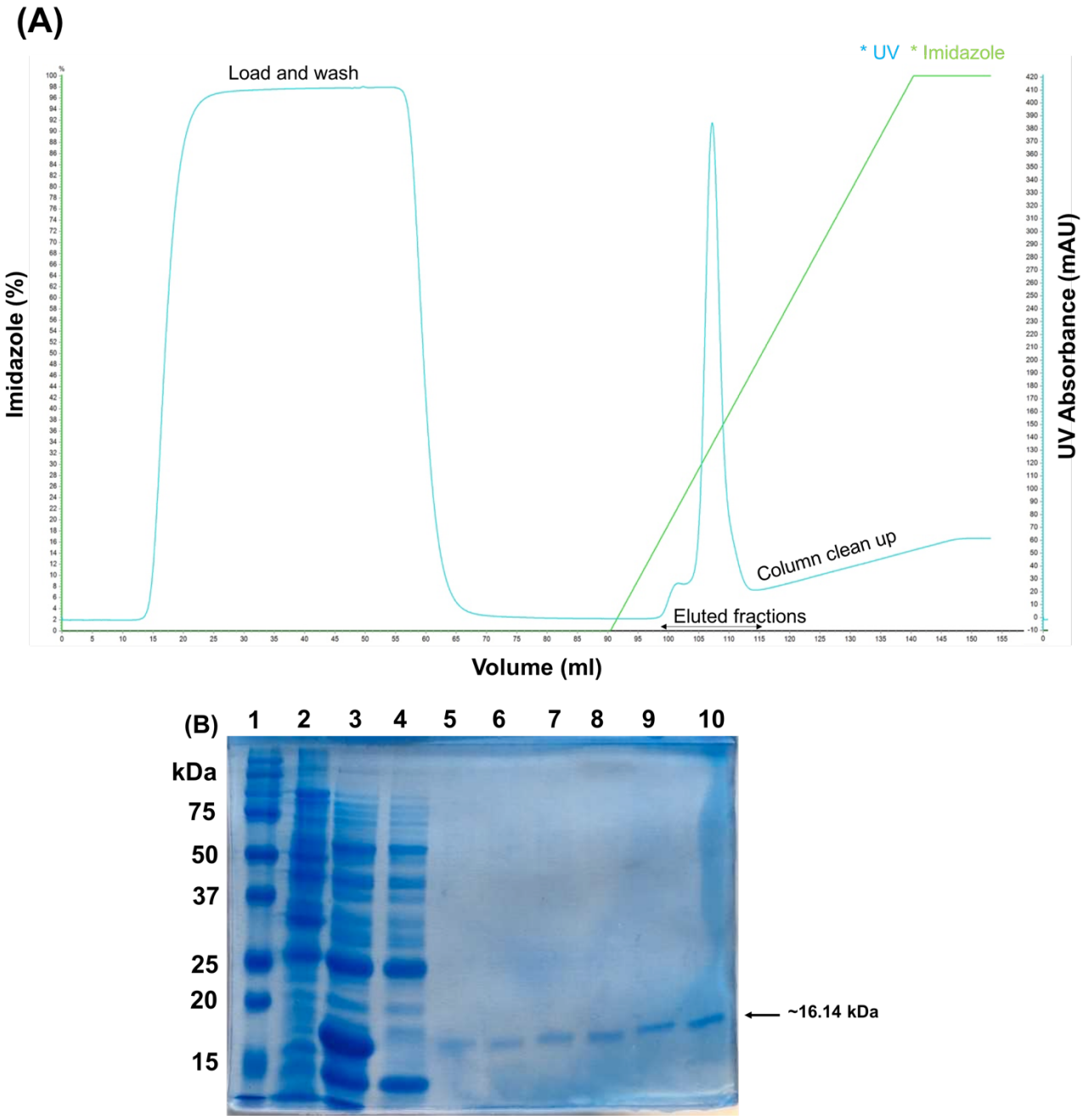

Figure 4.2. Affinity 6x-His tag chromatography purification profile of RV-3B2 expressed with rapid protocol (*E. coli HB2151*; pITKan/3B2) culture induced with 0.5 mM IPTG at 24^0C for 16 h). The periplasmic protein was extracted via sucrose shock protocol and applied to Ni^{+2}-resin. After column washing, 3B2 was eluted over 500 mM imidazole in 1 ml fractions. (A) Elution chromatographic profile illustrating the absorbance at 280 nm (blue line) and collection of eluted fractions (green line). (B) A 12% SDS-PAGE gel indicating expression and purification of RV-3B2 (observed at about 16.14 kDa). Lane 1: protein standard. Lane 2: Total soluble protein (TSP) from un-induced *E. coli HB2151* (pITKan/3B2) culture. Lane 3: TSP from induced *E. coli HB2151* (pITKan/3B2) culture, Lane 4: column wash. Lanes 5-10: eluted fractions of RV-3B2.

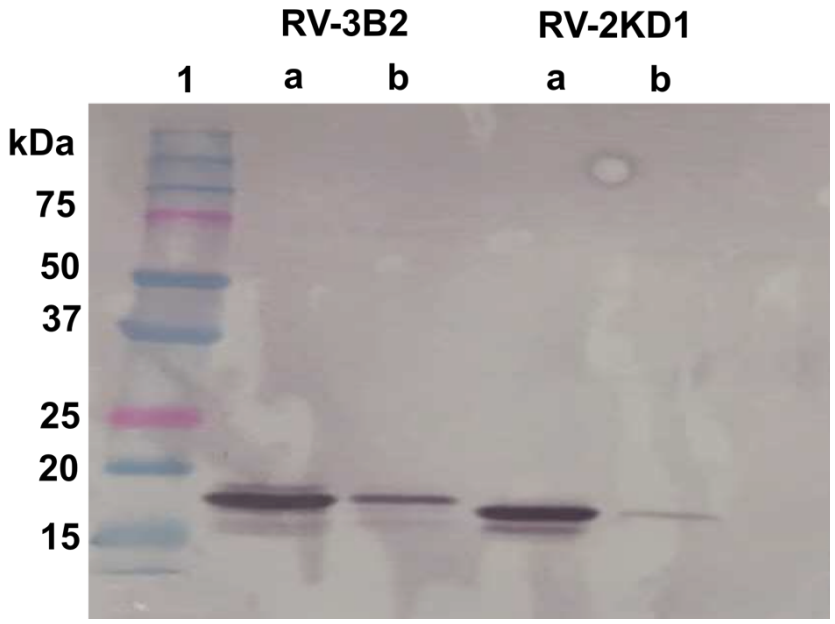

Figure 4.3. Western blot analysis of expressed and purified RV-3B2 and RV-2KD1 as presented in Figures 4.1 and 4.2. Total soluble proteins (TSP) and pooled purified proteins (diluted to 1:5) were run on 12% SDS-PAGE gel before transferring to PVDF membrane and probed with a polyclonal anti-His antibody conjugated to alkaline phosphate. Lane 1: protein standard. Lanes labeled "a" represent TSP of RV-V_HH. Lanes labeled "b" represent pooled purified RV-V_HH.

g/L. The molecular weight for these fusion proteins and level of expression were analyzed by SDS-PAGE and Western blot (Figure 4.4). The sizes of HA-CBM2a-$([PT]_3T)_{3x}$S-2KD1-His and HA-CBM2a-$([PT]_3T)_{3x}$S-3B2-His were 30.5 and 30.65 kDa, respectively, matching the expected sizes.

Furthermore, removal of the His-tag from HA-CBM2a-$([PT]_3T)_{3x}$S-2KD1-His did not affect the expression of the fusion proteins (V_HHs linked to CBM2a without His tag and CBM2a only) in *E. coli* (Figure 4.5). The appearance of the bands on Western blot occurred at the expected size for each fusion protein: 17.9 kDa for HA-CBM2a, 29.9 kDa for HA-CBM2a-$(G_4S)_{3x}$-2KD1 and HA-2KD1-$(G_4S)_{3x}$-CBM2a, and 31 kDa for HA-2KD1-$([PT]_3T)_{3x}$S-CBM2a. Although the bands appeared faint on the Western blot (Figure 4.5 B), which was developed with HRP substrate, the bands corresponded to correct size of all recombinant proteins. The TSP concentration of each recombinant antibody was estimated by Bradford assay and the V_HH-CBM2a fusion proteins ranged between 23.5-46.8 mg/L and 50 mg/L for CBM2a.

4.2.3 Recombinant RV-IgG 26

The RV-IgG 26 was expressed in *N. benthamiana*, following whole-plant vacuum infiltration of recombinant *Agrobacterium* suspensions, for seven days. The biomass of the harvested leaves from 48 plants was estimated to weigh 728 g.

Following extraction and purification of RV-IgG 26 by FPLC (Figure 4.6), its concentration was estimated to be 57.46 mg from 200 g leaves mass. Purity of RV-IgG 26 was determined by SDS-PAGE and immunoblotting under reducing and non-reducing conditions (Figure 4.7). Under reducing condition, 2 bands were observed on the gel and

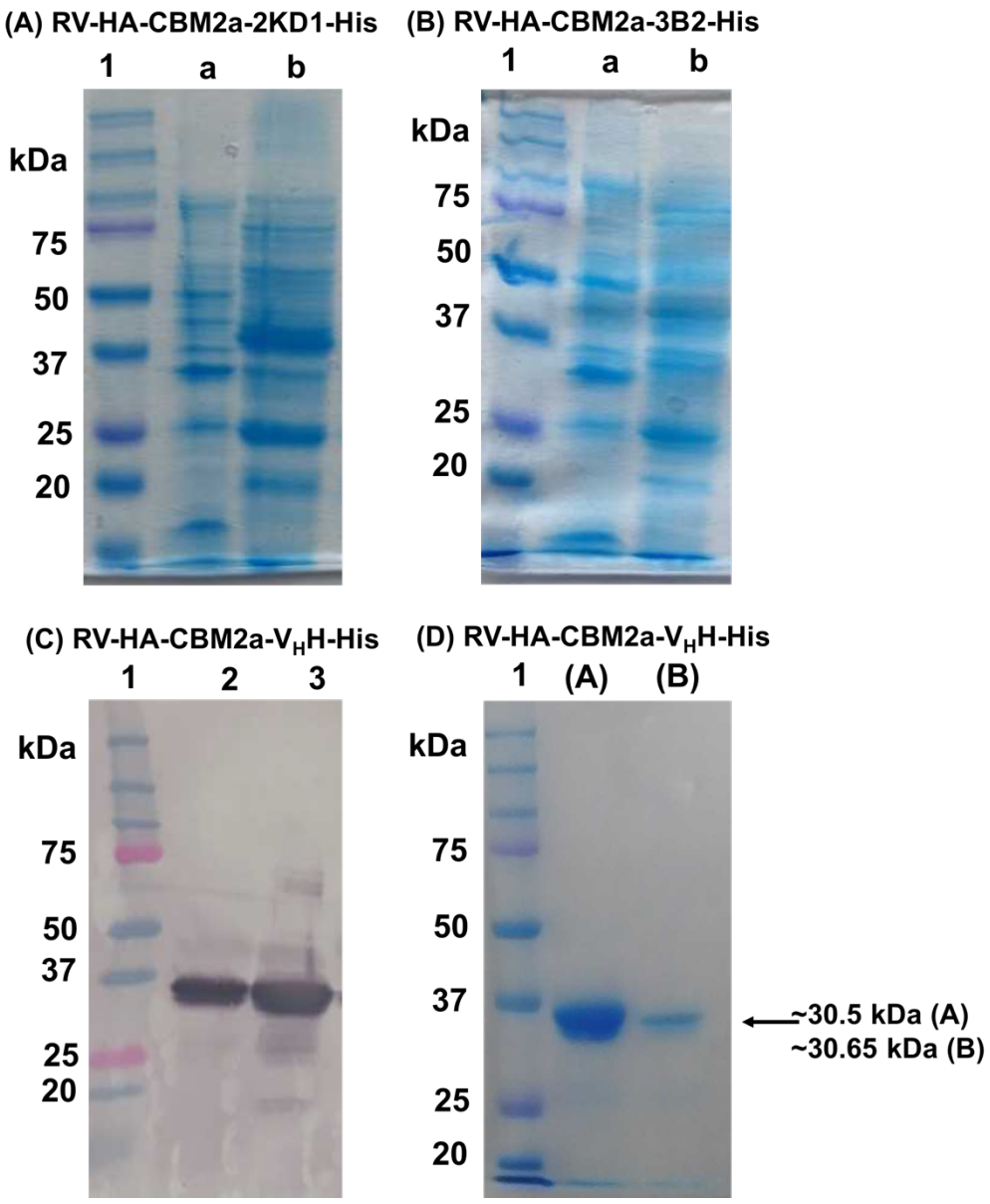

Figure 4.4. Fusion protein expression and purification of RV-V_HHs linked to HA-CBM2a at N-terminal and His-tag at C-terminal. (A) A 12% SDS-PAGE gels for RV-HA-CBM2a-$([PT]_3T)_{3x}$S-2KD1-His (30.5 kDa). (B) A 12% SDS-PAGE gel for RV-HA-CBM2a-$([PT]_3T)_{3x}$S-3B2-His (30.65 kDa). The fusion proteins were expressed using the rapid expression protocol and TSP released via sucrose shock protocol. Lanes labeled "a" represent TSP from un-induced cultures. Lanes labeled "b" represent TSP from induced cultures. (C) Western blot of total soluble protein (TSP) from induced cultures (diluted at 1:3) indicating the detection of RV-HA-CBM2a-$([PT]_3T)_{3x}$S-2KD1-His (Lane 2) and RV-HA-CBM2a-$([PT]_3T)_{3x}$S-3B2-His (Lane 3) on PVDF membrane by a polyclonal anti-His antibody conjugated to alkaline phosphate (AP). (D) A 12% SDS-PAGE gel indicating purification of fusion proteins by IMA. Lane labeled "A" represent pure RV-HA-CBM2a-$([PT]_3T)_{3x}$S-2KD1-His. Lane labelled "B" represent pure RV-HA-CBM2a-$([PT]_3T)_{3x}$S-3B2-His. Lane 1: Protein standard. Arrow refers to the expected molecular size of fusion proteins.

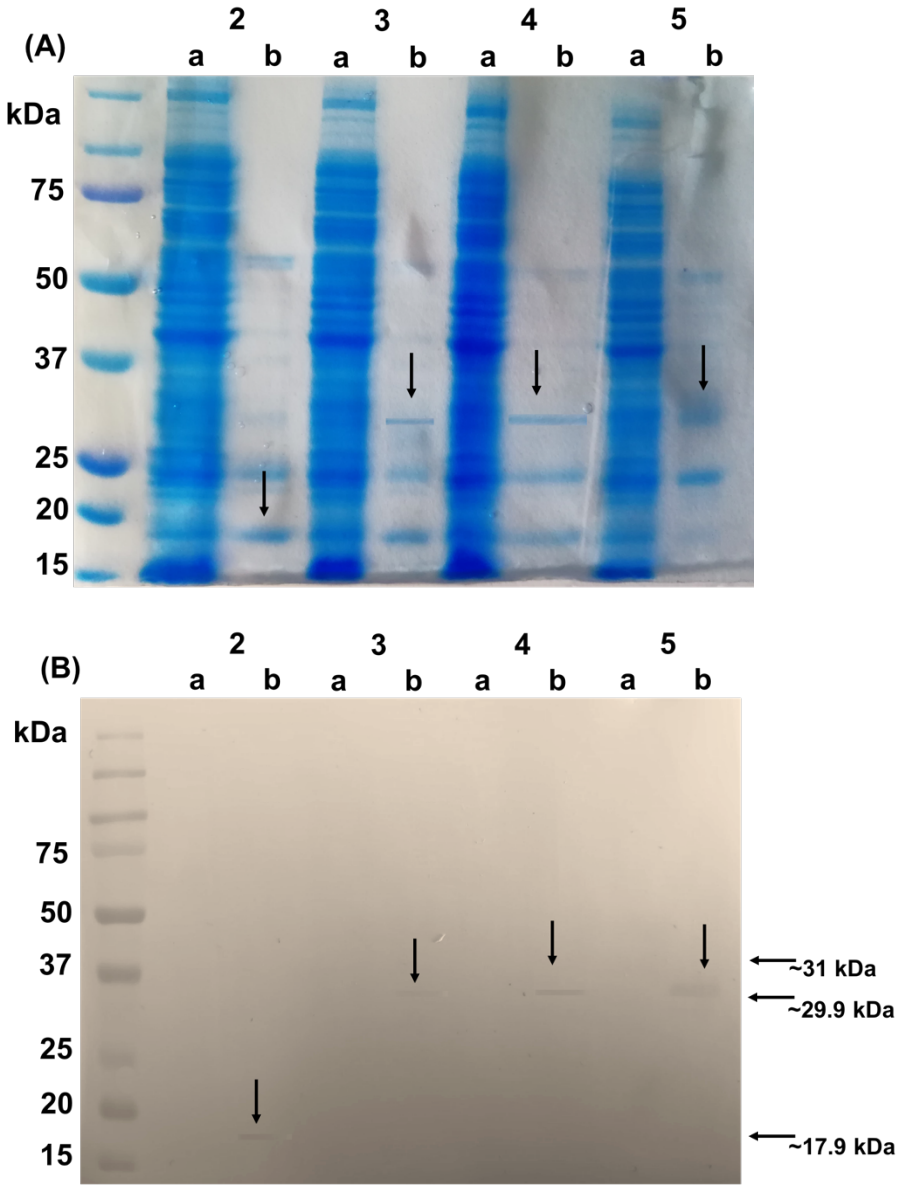

Figure 4.5. Fusion protein expression of RV-V_HHs linked to HA-CBM2a at N- and C-terminal on 12% SDS-PAGE gels (A) and Western blot (B) of TSP from induced cultures (10 µl of TSP was loaded in each well) indicating the detection of RV-HA-CBM2a (labelled "2", ~17.9 kDa), HA-CBM2a-$(G_4S)_{3x}$-2KD1 (labelled "3", 29.9 kDa), HA-2KD1-$(G_4S)_{3x}$-CBM2a (labelled "4", 29.9 kDa) and HA-2KD1-$([PT]_3T)_{3x}$S-CBM2a (labelled "5", 31 kDa) on PVDF membrane by a polyclonal anti-His antibody conjugated to horseradish peroxidase (HRP). Lane 1: Protein standard. The fusion proteins were expressed using the rapid expression protocol and total soluble proteins (TSP) released via sucrose shock protocol. Lane 1: protein standard. Lanes labeled "a" represent TSP from un-induced cultures. Lanes labeled "b" represent TSP from induced cultures. Arrows indicate expected size of fusion proteins.

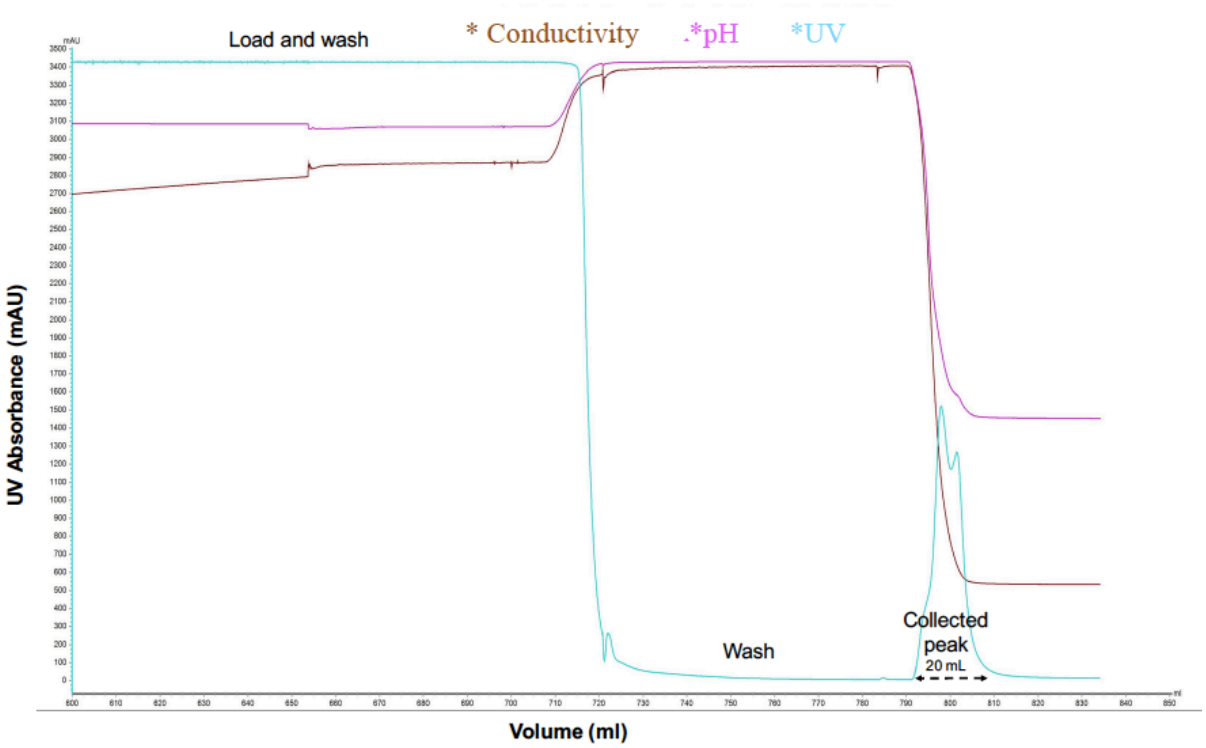

Figure 4.6. Protein A affinity chromatography purification profile of RV-IgG 26. Elution chromatographic profile illustrating loading, washing and elution of RV-IgG 26 on a pre charged 5-ml protein A (MabSelect) column (UV, blue line). The loading and washing were conducted in 20 mM phosphate buffer pH 7.4, and elution in 100 mM sodium acetate pH 3 and 200 mM arginine-HCL. The eluted protein was collected in a 20 mL volume (collected peak) neutralized with 1 M Tris-HCL pH 8.5 and dialyzed overnight at 4°C against 1x PBS. Pink and brown lines indicating the stability of pH and conductivity, respectively, during washing step and the decrease of both during fraction collection.

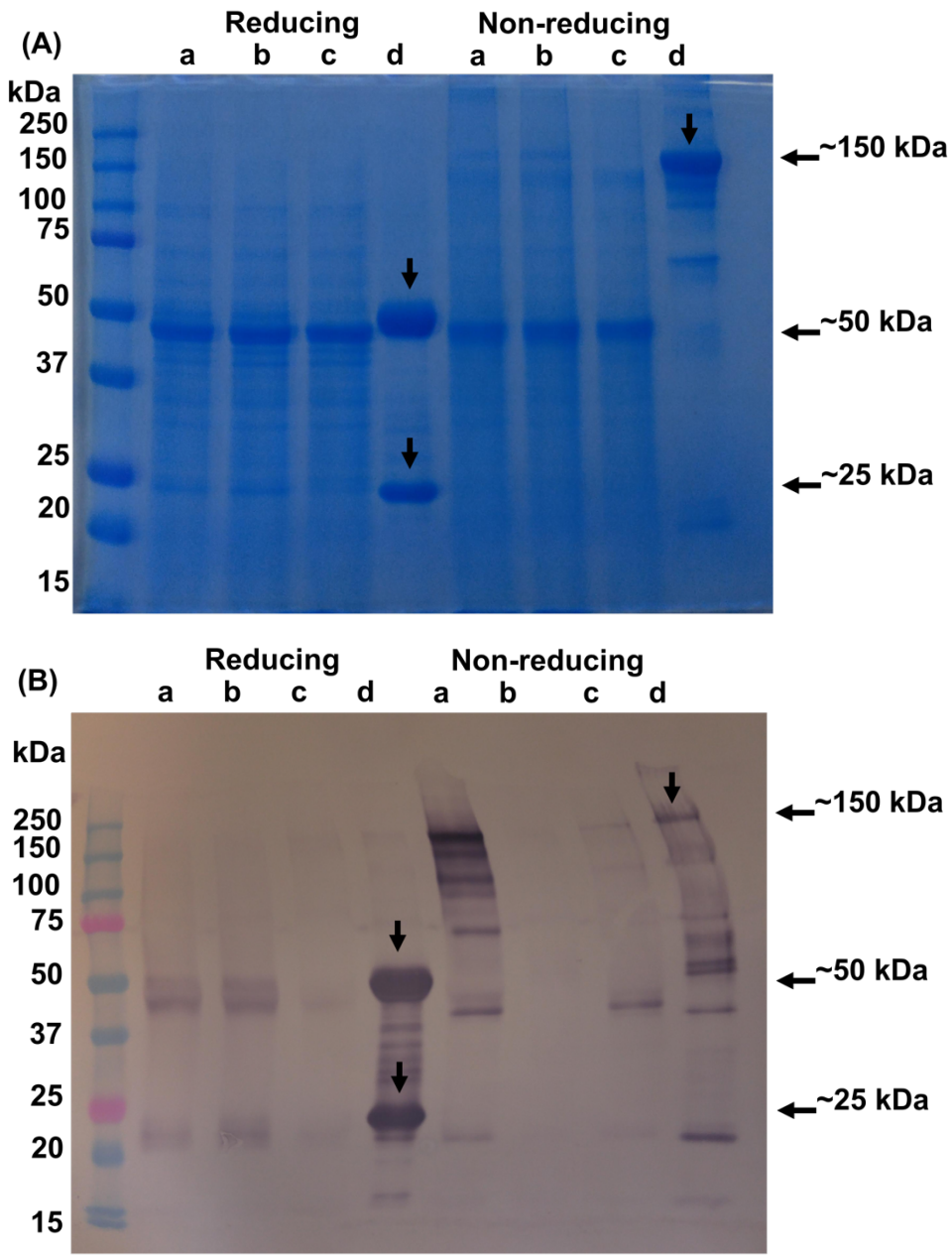

Figure 4.7. Qualitative analysis of RV-IgG 26 expression in *N. benthamiana* under reducing and non-reducing conditions. (A) Coomassie stained 12% SDS-PAGE analysis of RV-IgG expression; (B) Immunoblot analysis of RV-IgG 26 expression. The immunoblot was probed with a mixture of anti-human gamma and kappa probes. Under reducing condition, the molecular weights of the RV-IgG 26 H_C and RV-IgG 26 L_C are ~50 and ~25 kDa, respectively while RV-IgG 26 is 150 kDa under non-reducing condition. Lane 1: protein standard. Lanes labeled "a" represent total soluble protein (TSP). Lanes labeled "b" represent retention of RV-IgG 26 on the purification column (i. e., flow through). Lanes labeled "c" represent wash. Lanes labeled "d" represent eluted RV-IgG 26.

the immunoblot membrane at ~50 and ~25 kDa representing the size of RV-IgG 26 H_C and RV-IgG 26 L_C, respectively. Under non-reducing condition, the gel and the immunoblot membrane showed a band at 150 kDa representing the molecular weight of full-length RV-IgG 26 (Figure 4.7).

4.2.4 Recombinant RV-VP_6

The purpose of producing RV-VP_6 in this study was to use it as a positive control in future experiments. However, since all V_HHs in the current study were His-tagged and to prevent cross-reactivity with anti-His antibody in ELISA experiments, it was crucial to produce a soluble RV-VP_6 without 6x-His tag. The RV-VP_6 capsid protein sequence was optimized for *E. coli* and cloned in 3 different bacterial expression vectors. Since the pET-SUMO/VP_6 construct produced high yields of soluble RV-VP_6, similar to those of the pITKan nor pETb22$^{(+)}$ expression constructs (Appendix 4), however, it is possible to remove the His tag from this recombinant protein unlike the others. As a result, large scale expression and purification of RV-VP_6 were continued with this construct only.

The soluble protein was extracted from 1-L *E. coli BL21 (D3)* induced culture with 0.25 mM IPTG by lysozyme as mentioned previously. The soluble cell lysate (30 ml) was loaded into a pre charged 5 ml of an Ni^{+2}-NTA column. The fusion SUMO/VP_6 was eluted with 300 mM imidazole after extensive column wash (Figure 4.8 A). The purity and size of eluted fractions (1 ml each) were analyzed by SDS-PAGE gel stained with Coomassie blue (Figure 4.8 B). Concentration of SUMO-VP_6 pure fractions were estimated by A_{280} to range from 1.85-3.07 mg/ml.

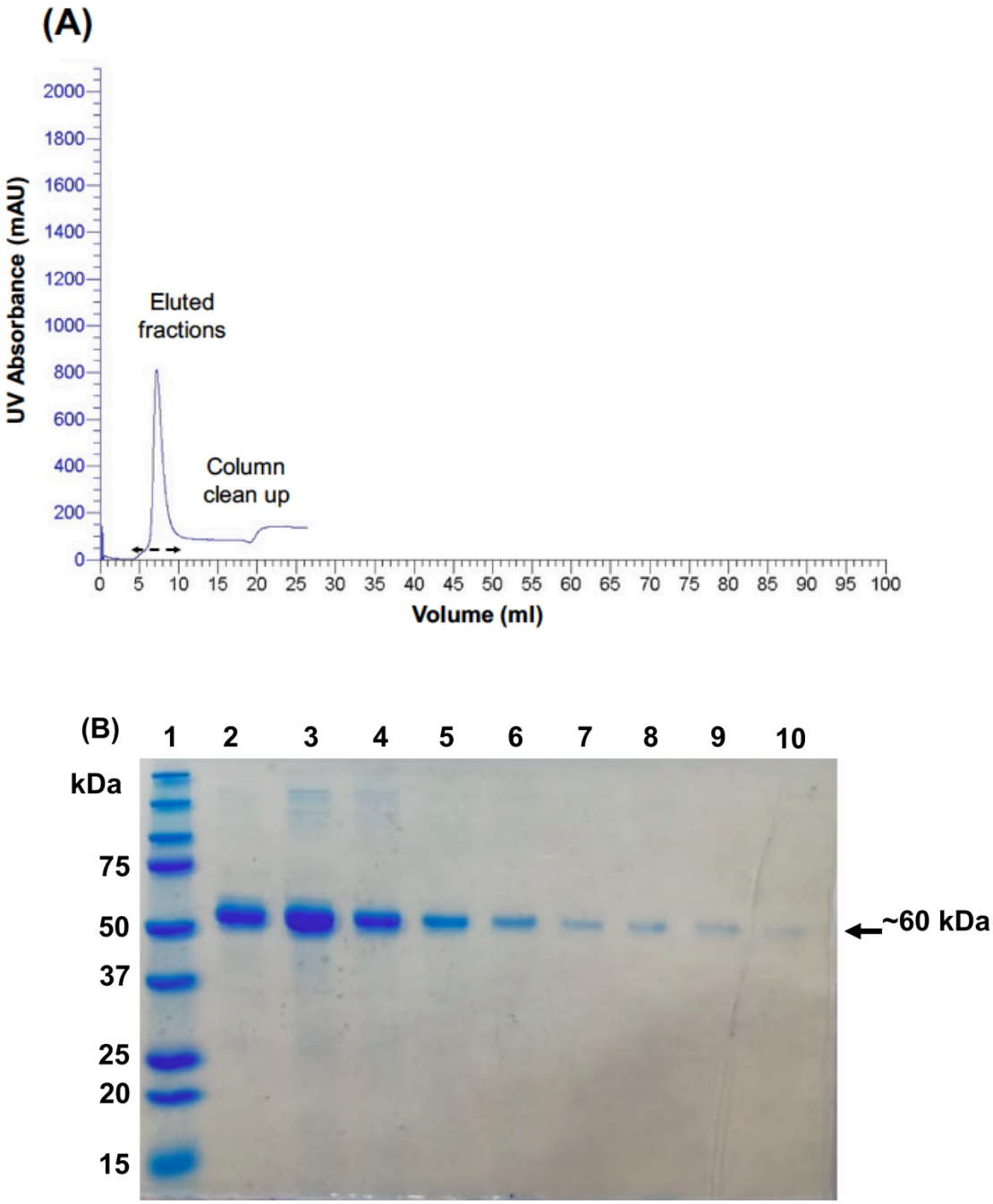

Figure 4.8. Affinity 6x-His tag chromatography purification profile of RV-SUMO/VP$_6$. (A) Elution chromatographic profile for RV-SUMO/VP$_6$ (blue line) showing showing fractions collected (3-10 mL) with a 300 mM imidazole. (B) A 12% SDS-PAGE gel run under reducing condition indicating expression and purity of RV-SUMO/VP6 (4 µl loaded) at a molecular weight of about 60 kDa. The fusion protein was expressed in LB medium and induced with 0.25 mM IPTG at 24^{0}C for 16 h. The periplasmic protein was extracted via lysozyme protocol and further purified via IMAC. Lane 1: protein standard. Lanes 2-10: eluted fractions of RV-SUMO/VP$_6$.

To remove the VP_6 target protein from its SUMO tag partner, pure SUMO-VP_6 was incubated with SUMO-protease (see Appendix 4 for expression and purification of recombinant enzyme SUMO-protease) at 30°C for up to 6 h and collecting a test sample every 2 h. The reaction mixture was analyzed by SDS-PAGE (Figure 4.9 A), which showed approximately 90% cleavage of SUMO-VP_6 in 2 h. This was demonstrated by the disappearance of the 60 kDa fusion protein and the appearance of 3 new bands corresponding to the expected molecular weights of SUMO-protease-His fusion tag (25 kDa), SUMO-protease (15 kDa) and RV-VP_6 (45 kDa). To obtain RV-VP_6 only without His tag, the cleaved reaction mixture was reapplied to the Ni^{+2}-affinity column to recover the untagged RV-VP_6 product in the flow through, as its unable to bind to Ni^{+2}-NTA resin (Figure 4.9 B). Immunoblot analyses were conducted using the RV-IgG 26 antibody for detection, produced in this study, as a primary antibody followed by a human antibody as a secondary antibody detection to recognize RV-VP_6 cleaved protein (Figure 4.9 C). Pure RV-VP_6 was stored at 4°C up to 3 days before adjusted to 1 mg/ml and being stored at -80°C. The RV-VP_6 was not found to form any precipitate after the 3 days storage, as indicated by lack of a pellet after high speed centrifugation.

4.3 Virus Propagation and Quantification

4.3.1 Infectivity in Cell Types

The cell lines used in this study were MA104 to propagate all RV strains, HEK-293 to propagate hAdenoV and BV2 to propagate mNV. Propagation of the virus was judged by visualization by light microscopy (Figure 4.10). Generally, CPE began to appear as an initial rounding of cells with indistinct outlines, followed by aggregation or accumulation of

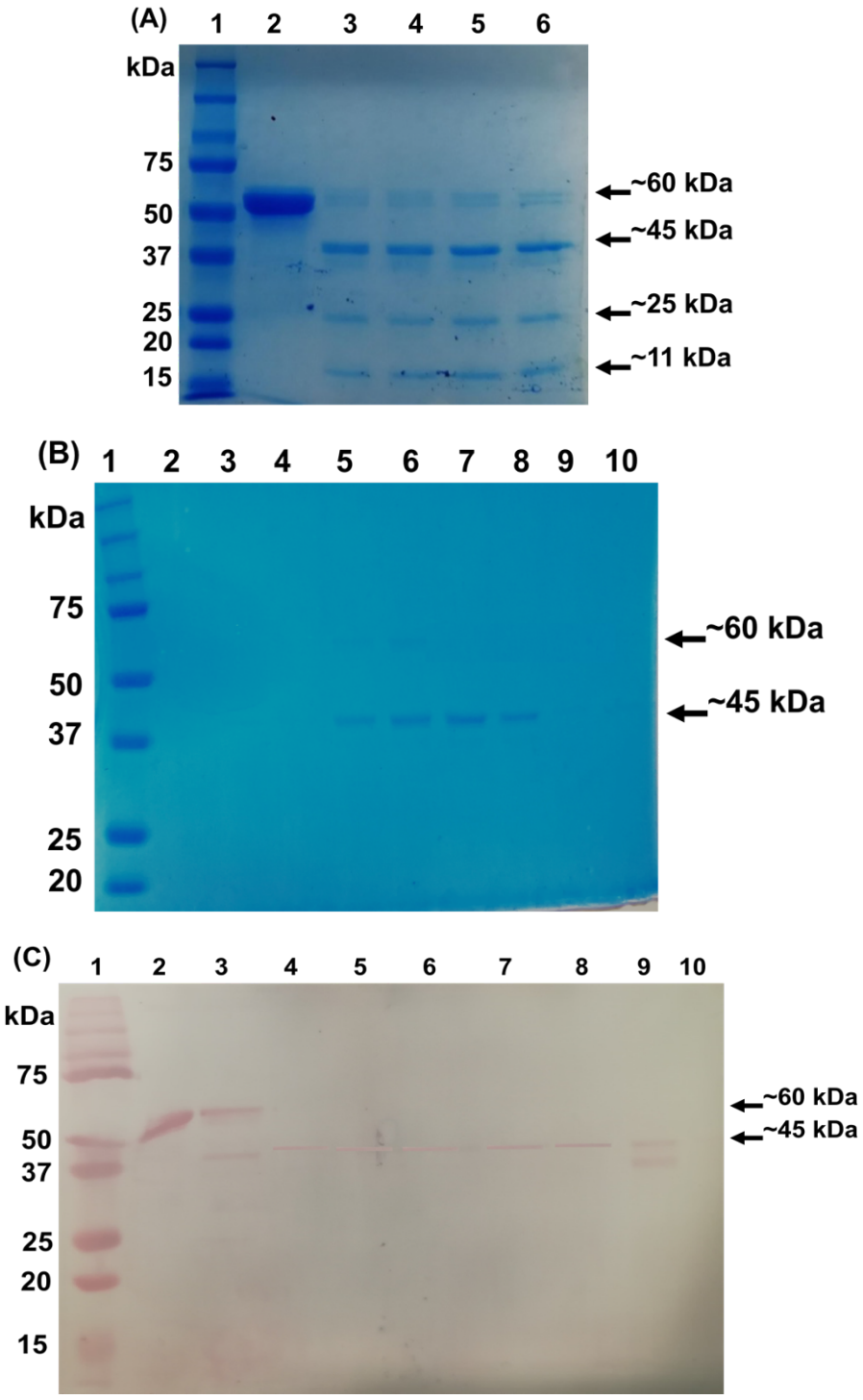

Figure 4.9. Proteolytic cleavage of SUMO-VP_6 with SUMO-protease. (A) Sodium dodecyl sulfate polyacrylamide gel electrophoresis (SDS-PAGE) stained with Coomassie blue with purified SUMO-VP_6 before (lane labeled "2") and after (lane labeled "3-6") digestion by SUMO-protease. Digested protein mixture (SUMO-VP_6 and SUMO-protease reaction) was passed through a Ni^{+2}-resin column and flow through was collected (lanes labeled "2-10") then analyzed by (B) SDS-PAGE stained with Coomassie blue and (C) Western blot. Lane 1: protein standard. Lane 2: purified SUMO-VP_6. Lane 3: cleaved SUMO-VP_6 digestion with SUMO-protease. Lanes 4-10: RV-VP_6 after protease digestion detected via RV-IgG 26.

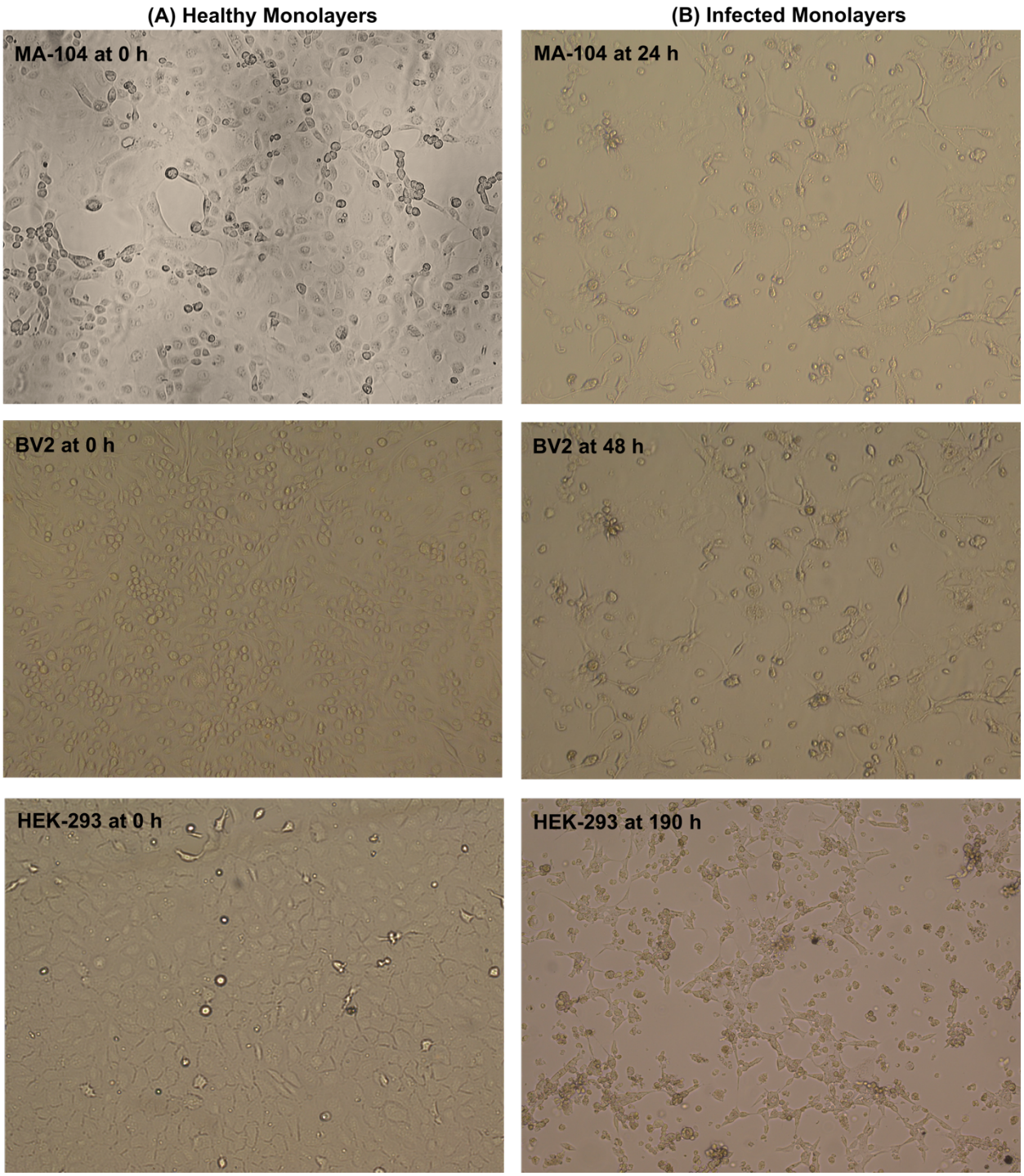

Figure 4.10. Visualization of cytopathic effects by enteric viruses in cell lines. (A) Confluent monolayers of MA104, VB2 cells and HEK-293 cells pre-infection with their corresponding virus (control). (B) Cell monolayers post-infection showing CPE for MA-104 infected with h-RV (after 24 h), BV2 infected with mNV (after 48 h) and HEK-293 infected with hAdenoV (after 190 h). CPE observed as rounding and destruction of cells; many cells have detached while other cells are spindle shaped indicting infection.

dead cells. Some of the cells assumed spindle shapes with one end attached to the glass surface while other end floated in the medium. The MA104 cell monolayers were lyzed after 48-72 h post infection with h-RV, while BV2 and HEK293 infection with mNV and hAdenoV, respectively, showed clear CPE at 48 h and 190 h of post-infection.

4.3.2 Quantification of the Virus

In this study, RV strains were quantified via 3 methods including a plaque assay, TCID 50% and qPCR. The hAdenoV was quantified via qPCR and plaque assay was used to quantify mNV. Since RV and hAdenoV were consistently used to quantify viruses in further tests, quantification of those viruses by qPCR was selected (see Appendix 5 for quantification of RV and mNV by other tests). Virus enumerated by TCID 50% and plaque assay will be presented as number of plaque forming units (pfu) while those enumerated using qPCR will be presented as copy number (CN) or virus particle.

4.3.2.1 Quantification by qPCR

The primer/probe set used in this study to detect all strains of RV A was previously designed to target NPS3 gene of hRV A strain only (Lee et al., 2016). In this study, 2 bovine RV A strains (bRV-B223 and bRV-C486) were also detectable by the same primer/probe set. This was expected from investigation of complete nucleotide sequences (1049 bp) for group AhRV (Accession number: X81436.1) and bRV (Accession number: JN626230.1) NPS3 genes. The sequence alignment results showed 84% match in the whole sequence between these strains (Figure 3.9). However, the nucleotide sequence in the targeted region (75 bp) was identical except for one nucleotide located at the

beginning of the forward primer binding region (A in hRV vs. T in bRV), which did not impact detection of the bRV strains in qPCR using this primer/probe set.

From qPCR assay for hAdenoV and RV A based on genes quantification, standard curves were produced (Figure 4.11). Analysis of qPCR standard curves revealed an inverse linear relationship with R^2 valued of 0.99 for both targets and slope valued of -3.54 and -3.29 for hAdenoV and hRV, respectively, when the Ct values were plotted versus the logarithm of the 10-fold dilutions (i.e., target gene copy numbers). Efficiency values were 91.62% and 101.09% for hAdenoV and hRV, respectively. Although these data presented in this work were generated from a single run, they were repeated twice and were in acceptable ranges (i.e., averages (n=2) were R^2 of 0.99 ± 0.001 and 0.99 ± 0.004, slope of -3.51 ± 0.04 and -3.24 ± 0.07 and efficiency of 92.7 ± 1.5% and 103.44 ± 3.3% for hAdenoV and hRV, respectively). The operating data from each qPCR assay were within acceptable ranges as outlined in the MIQE standards (Bustin et al., 2009).

Melt-curve analysis indicated a single peak for each amplicon. Additionally, products from qPCR were also analyzed by gel electrophoresis and each PCR product was observed at their expected sizes (112 bp for hAdenoV and 75 bp for hRV). Concentrations of the RV stocks were estimated to be 1.58×10^6, 3.39×10^7 and 1.09×10^7 virus particles/ml for bRV-B223, bRV-C468 and hRV, respectively, while concentration of hAdenoV estimated to be 1.09×10^9 virus particles/ml (these concentrations are averages of 2 technical replicates).

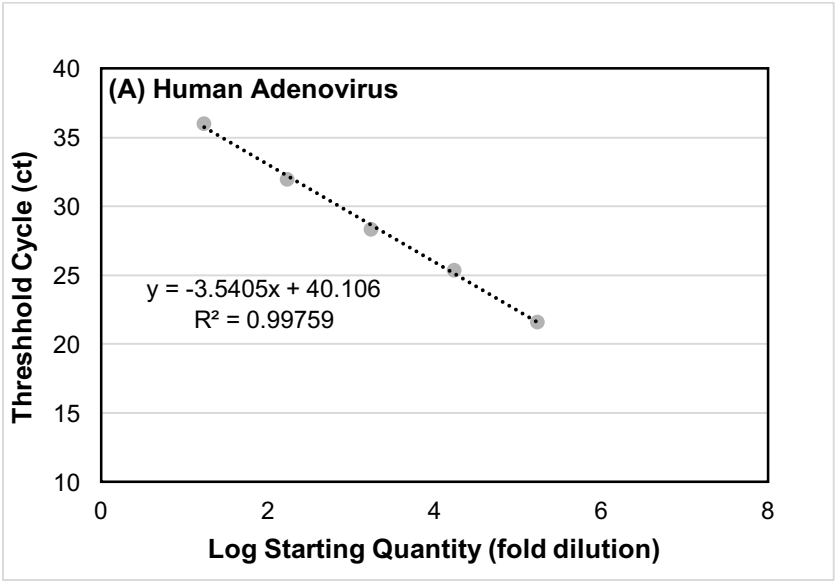

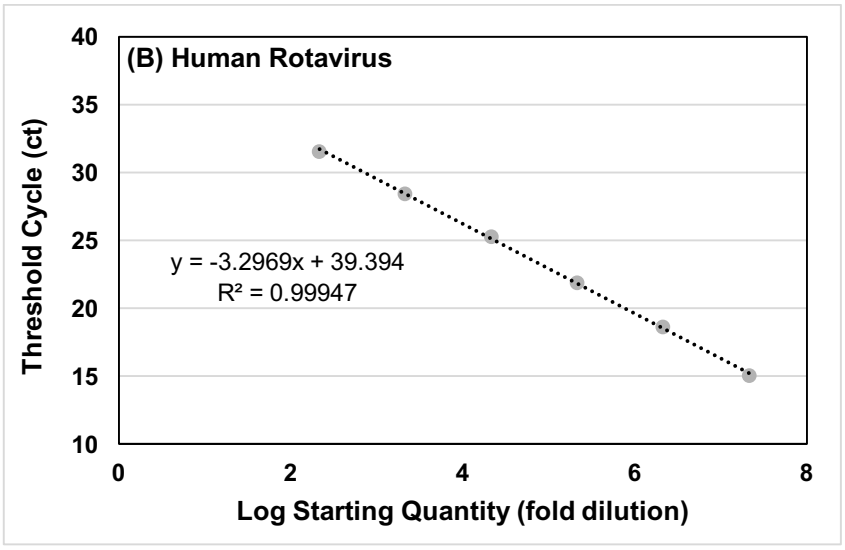

Figure 4.11. Standard quantification curves of qPCR assays for (A) human adenovirus type 41 and (B) human rotavirus group A. Standard quantification plasmids were diluted by 10-fold series and quantified by a primer and probe set specific for a single virus gene. Data on the graphs are readings from 2 technical replicates.

4.4 Functionality of RV-Antibodies

4.4.1 Detection by Western Blot

To gain insight into whether (1) the RV-VP_6-specific antibodies recognized RV group A strains based on VP_6 and (2) fusion of V_HHs to CBM2a affect their binding functionality to RV, Western blotting using RV-mAbs as primary antibodies was performed. Briefly, protein extracts of bRV-B223 (1.5×10^4 and 1.5×10^3 virus particles/well) bRV-C486 (3.39×10^4 and 3.39×10^3 virus particles/well) and hRV-Wa (1.09×10^4 and 1.09×10^3 virus particles/well) along with hAdenoV (1.09×10^6 virus particles/well), mNV (1.5×10^6 pfu/well) and recombinant RV-VP_6 (2 µg/well) were run on 12% SDS-PAGE gel under reducing conditions. One gel was stained with Coomassie blue dye as a reference (Figure 4.12 A) while others were transferred to PVDF membranes (Figure 4.12 B-G) and probed with His-tagged-RV-V_HHs, His-tagged-RV-HA-CBM2a-V_HHs, RV-IgG 26 and HA-CBM2a and binding was detected with anti His-AP, anti-mouse IgG-AP and anti HA-HRP secondary probes, respectively. Western blot analyses indicated that all RV-VP_6 mAbs specifically detected the 3 RV group A strains at concentrations of about 10^4 virus particles/well and RV-VP_6 protein (Figure 4.12 B-F). None of the strains at 10^3 virus particles/well were observed on SDS-PAGE or detected on Western blot. Western blot analysis also confirmed that fusion of V_HH to CBM2a did not affect the binding ability of the V_HHs to their target. The native CBM2a recombinant protein was not able to detect any of the EVs or RV-VP_6 on Western blot as was expected (Figure 4.12 G). Both of hAdenoV and mNV (at concentrations about 100-fold higher than those tested for the RV strains) were used as negative controls and were not detected by any RV-mAbs.

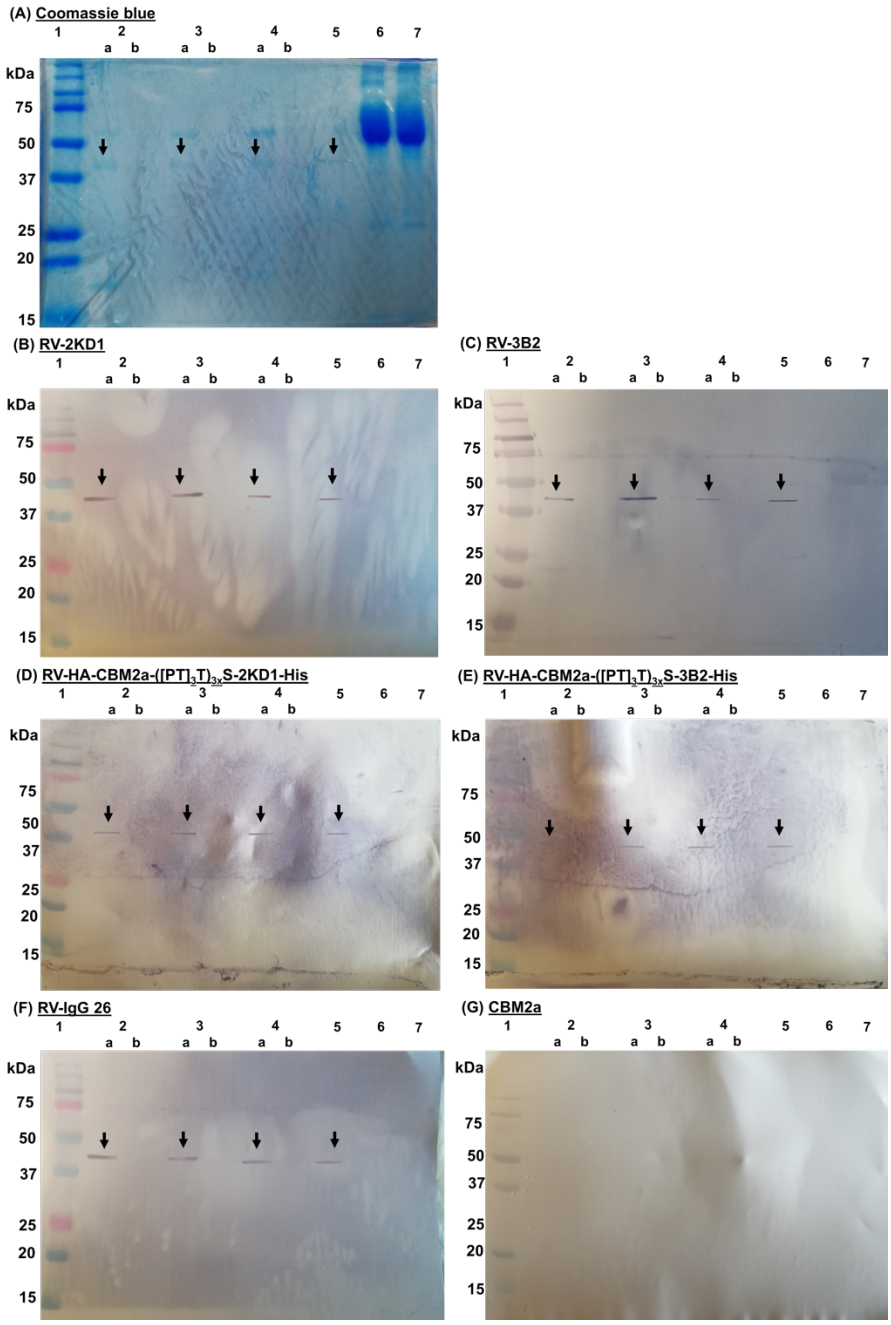

Figure 4.12. Detection of different rotavirus strains on Western blot using V_HHs with and without CBM-V_HHs and full-length IgG 26. The RVs were loaded on wells of SDS-PAGE in 2 dilutions (10^4 and 10^3 virus particles/well) for both bovine (bRV) (lanes labelled "2" represent bRV-B223 and lines labelled "3" represent bRV-C486) and human (lanes labelled "4") strains. The RV-VP_6 at 2 µg/well (lanes labelled "5") was used as a positive control. Human adenovirus (lanes labelled "6") and murine norovirus both at 10^6 pfu/well (lanes labelled "7") were used as negative controls. One gel stained with Coomassie blue (A) and others were transferred to PVDF membranes for Western blot analysis (B-G). Fusion proteins at 2 µg/ml of pure proteins (B-C and F) and at 5 µg/ml of total soluble protein (D-E and G) were used as a primary antibody to detect RVs, anti-his antibody (B-D), anti-human (F) and anti-HA (G) were used as a secondary antibodies. Lane 1: protein standard. Lanes labelled "a" represent higher dilution of the virus. Lanes labelled "b" represent lower dilution of the virus. Arrows refer to VP_6 RV group A protein (~45 kDa).

4.4.2 Detection by ELISA

ELISA in different experimental designs was used to test (1) RV-V_HHs binding to RV group A strains, (2) effect of CBM2a on binding of RV-V_HHs to RV strains, (3) RV-IgG 26 binding to RV and (4) impact of fusing CBM2a with different peptide linkers connected to the N- or C-terminal of the RV-V_HHs. For all statistical analyses and graphs, blank samples have been left out as they were already subtracted from the absorbance values of wells contain samples.

4.4.2.1 Indirect ELISA

For these tests, the viruses were adsorbed to the surface of the wells in an ELISA plate. In a two-step detection process, RV-primary antibodies (RV-IgG 26 and RV-2KD1) were used to bind to the target followed by application of an enzyme conjugated secondary antibody for detection. Various concentrations of purified RV-VP_6 immobilized on the ELISA plate could be detected by different concentrations of RV-IgG 26 (at 100 and 10 ng/well) and RV-2KD1 (at 500 and 200 ng/well) (Figure 4.13 A). However, no signal was obtained when the virus was immobilized on the plate (Figure 4.13 B). This suggested that the viruses were washed off and were not able to be immobilized on the type of ELISA plate used, as a result a sandwich ELISA was evaluated.

4.4.2.2 Sandwich ELISA

In this test, RV-2KD1 and RV-IgG 26 were interchangeably used as capture and detection antibodies for RV, as they were expected to bind to non-overlapping regions on

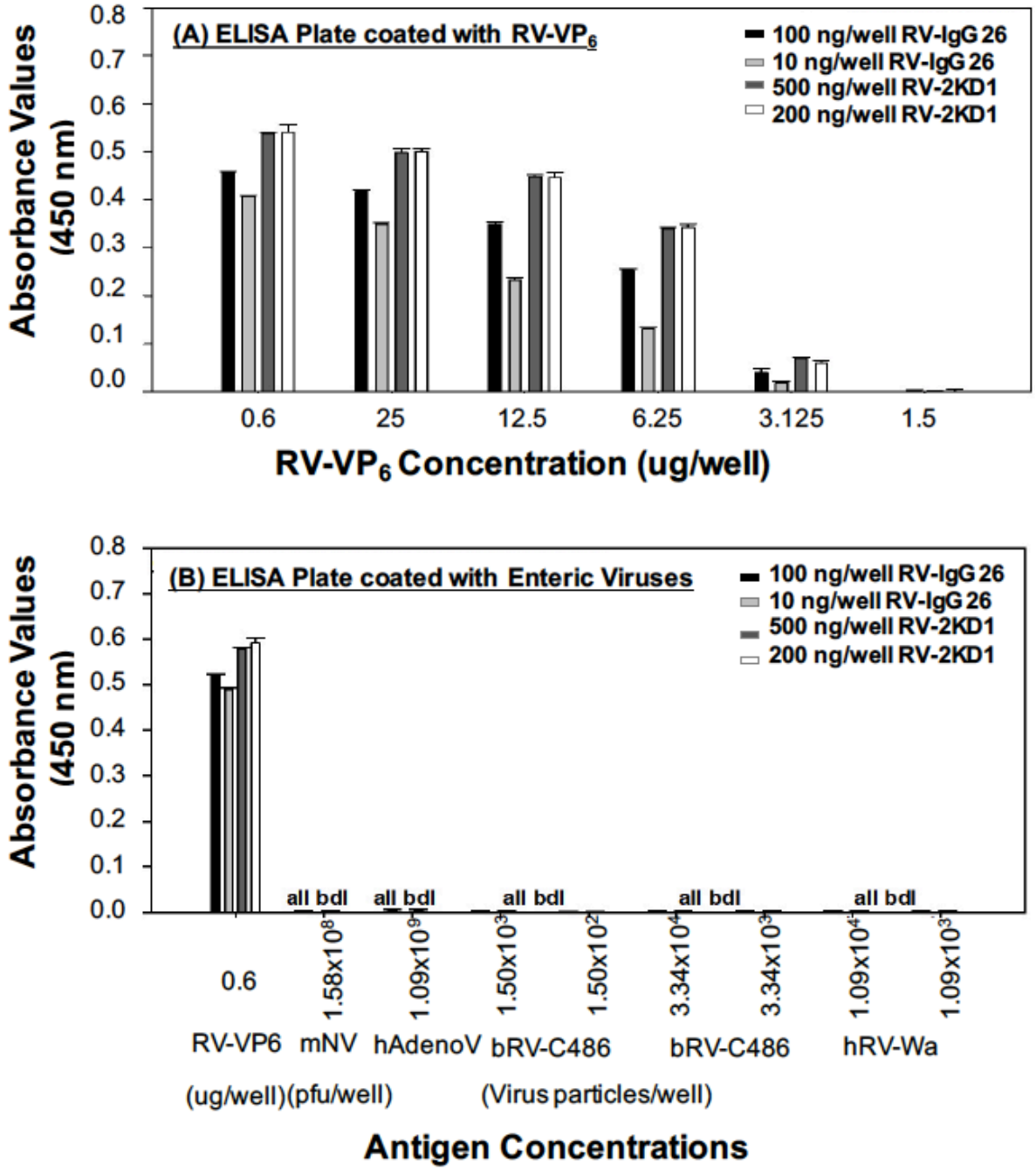

Figure 4.13. Characterization of rotavirus monoclonal antibodies binding specificity and sensitivity to rotavirus in indirect ELISA. (A) ELISA plate was coated with 2-fold dilution of purified VP_6 (µg/well). (B) ELISA plate was coated with 10-fold dilution of different enteric virus strains and RV-VP_6 (µg/well). The RV-IgG 26 (100 and 10 ng/well) and RV-2KD1 (500 and 200 ng/well) were used as a primary detection antibody. Anti-human conjugated to HRP and anti-his conjugated to HRP were used as a secondary detection antibody, respectively. The RV-VP_6 was used as a positive control whereas murine norovirus (mNV) and human adenoviruses (hAdenoV) where used as negative controls. Data are means and standard error of 3 technical replicates. bRV: bovine rotavirus. hRV: human rotavirus. bdl: below detection limit.

the RV surface. Both approaches showed the ability of immobilizing the virus on the ELISA plate and for determining the binding specificity and sensitivity of the RV-mAbs to RV group A strains (Figures 4.14 and 4.15).

For these initial ELISA tests, detection of RV by the RV-IgG 26 and the RV-V_HHs (lacking the CBM) were evaluated. For the first experiments, the ELISA plate was coated with RV-2KD1 at 100 ng/well. The wells were then exposed to RV-VP_6 or different EVs. Subsequently, RV-IgG 26 at 100 ng/well was used for detection. Only wells containing RV-VP_6 and different concentrations of RV strains were successfully detected by RV-IgG 26 (Figure 4.14). Positive signals were also obtained when RV-IgG 26 was used to coat the ELISA plate and RV-V_HH-His (e.g., RV-2KD1 or RV-3B2) used for detection (Figure 4.15). Univariate analyses indicated that the RV-2KD1 more strongly bound the virus than RV-3B2 at concentrations of 100 and 10 ng/well (Figure 4.15). When an ANOVA was run to compare differences in the detection across RV-2KD1 and RV-3B2 concentrations, no statistical difference between both antibodies at the 200 ng/well was observed ($P>0.56$). However, the absorbance values for RV-2KD1 were significantly higher in detecting RV than the RV-3B2 at concentrations of 100 ($P<0.02$) and 10 ($P<0.0001$) ng mAb/well. The mean of absorbances detected at each antigen concentration by a specific concentration of RV-mAbs were compared by Tukey test for unequal variance, as ANOVA was significant ($P<0.0001$ for RV-2KD1 at each concentration and for RV-3B2 at concentration of 100 ng/well (and 200 ng/well only with RV-VP_6 vs. RV strains)). There was no binding detected when 3B2 was used at a concentration of 10 ng mAb/well (Figure 4.15 B). Both data sets showed that all RV strains were equal in term of sensitivity as they were detectable to a lower concentration of 10^2 viruses (Figure 4.15). Overall these data indica-

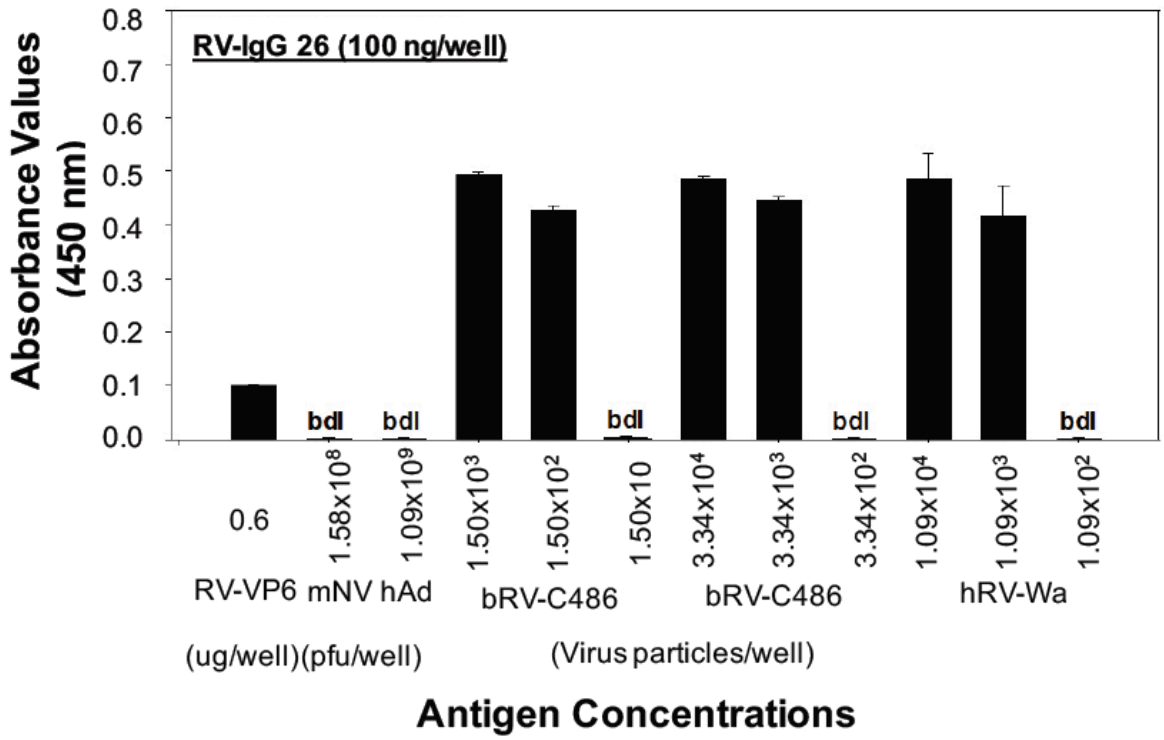

Figure 4.14. Characterization of rotavirus monoclonal antibodies binding specificity and sensitivity to rotavirus in sandwich ELISA. The ELISA plate was coated with RV-2KD1 (100 ng/well) and different strains of enteric viruses and RV-VP_6 then were detected with RV-IgG 26 (100 ng/well) and anti-human conjugated to HRP. The RV-VP_6 was used as a positive control whereas murine norovirus (mNV) and human adenoviruses (hAdenoV) where used as negative controls. Data are means and standard error of 3 technical replicates. bRV: bovine rotavirus. hRV: human rotavirus. bdl: below detection limit.

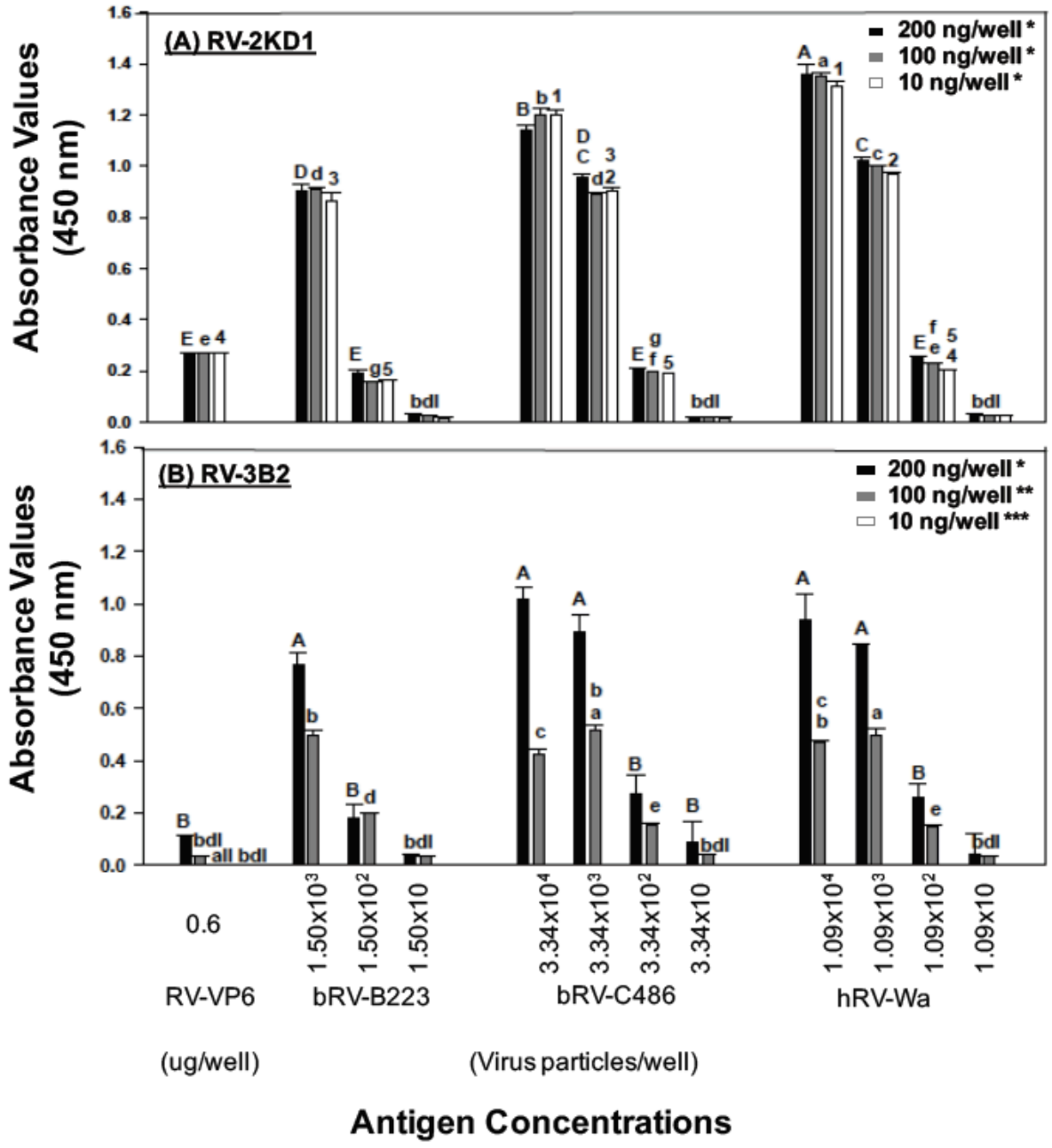

Figure 4.15. Characterization of RV-V_HHs binding specificity and sensitivity to rotavirus in sandwich ELISA. The plate was coated with RV-IgG 26 (100 ng/well) and different strains of enteric viruses and RV-VP_6 (0.6 µg/well) were detected in two steps by 200 and 100 ng/well of RV- 2KD1 (A) and RV-3B2 (B) and anti-his conjugated to HRP. The RV-VP_6 was used as a positive control whereas murine norovirus (mNV) and human adenoviruses (hAdenoV) where used as negative controls. Data are means and standard error of 3 technical replicates. bRV: bovine rotavirus. hRV: human rotavirus. bdl: below detection limit. Capital letters represent statistical difference among different antigen sources detected by 200 ng/well of antibody. Small letters represent statistical difference among different antigen sources detected by 100 ng/well of antibody. Numbers represent statistical difference among different antigen sources detected by 10 ng/well of antibody.

te that although RV-2KD1 was better in detecting different strains of RV and RV-VP_6 than RV-3B2, there was no statistical difference between them at concentrations of 200 ng/well whereas a significant defence was observed at lower concentrations (100 and 10 ng/well).

Detection of RV-VP_6 and whole virus by the RV-V_HHs linked to CBM2a was also evaluated to determine the binding ability of the fusion proteins to the antigen in ELISA. Positive signals were obtained when RV-IgG 26 was used to coat the ELISA plate and RV-CBM2a-V_HHs-His (e.g., RV-HA-CBM2a-$([PT]_3T)_{3x}$S-2KD1-His or RV-HA-CBM2a-$([PT]_3T)_{3x}$S-3B2-His) were used (as TSP) to specifically detect RV (Figure 4.16). This confirmed that linking the V_HHs to CBM2a with $([PT]_3T)_{3x}$S linker did not affect the functionality of either V_HH. The ANOVA analysis showed that there was no statistical difference for a CBM2a-V_HH when comparing the means among different concentrations (8.5, 5 and 2 µg/well) of RV-CBM2a-2KD1 ($P>0.368$) and of RV-CBM2a-3B2 ($P>0.943$) that were used to detect the virus (Figure 4.16) on a plate coated with RV-IgG 26. Also, no statistical difference was observed between RV-HA-CBM2a-$([PT]_3T)_{3x}$S-2KD1-His and RV-HA-CBM2a-$([PT]_3T)_{3x}$S-3B2-His. Both data sets showed as with data from RV-V_HHs (1) the detection of RV to be similar between bRV-C486 and hRV-WA as compared with bRV-B223 that had lower detection than other strains and (2) equal sensitivity as all strains were detectable to lower concentration of 10^2 (Figure 4.16). Overall these data indicate that linking the V_HHs to CBM2a did not affect the binding ca pacity of the V_HHs.

Furthermore, 2KD1-CBM2a fusion proteins were used as capture antibodies on ELISA plates because it had a higher binding capacity than RV-3B2 to (1) determine the affect of different linkers and N- and C-terminal orientations of 2KD1-CBM2a fusions on

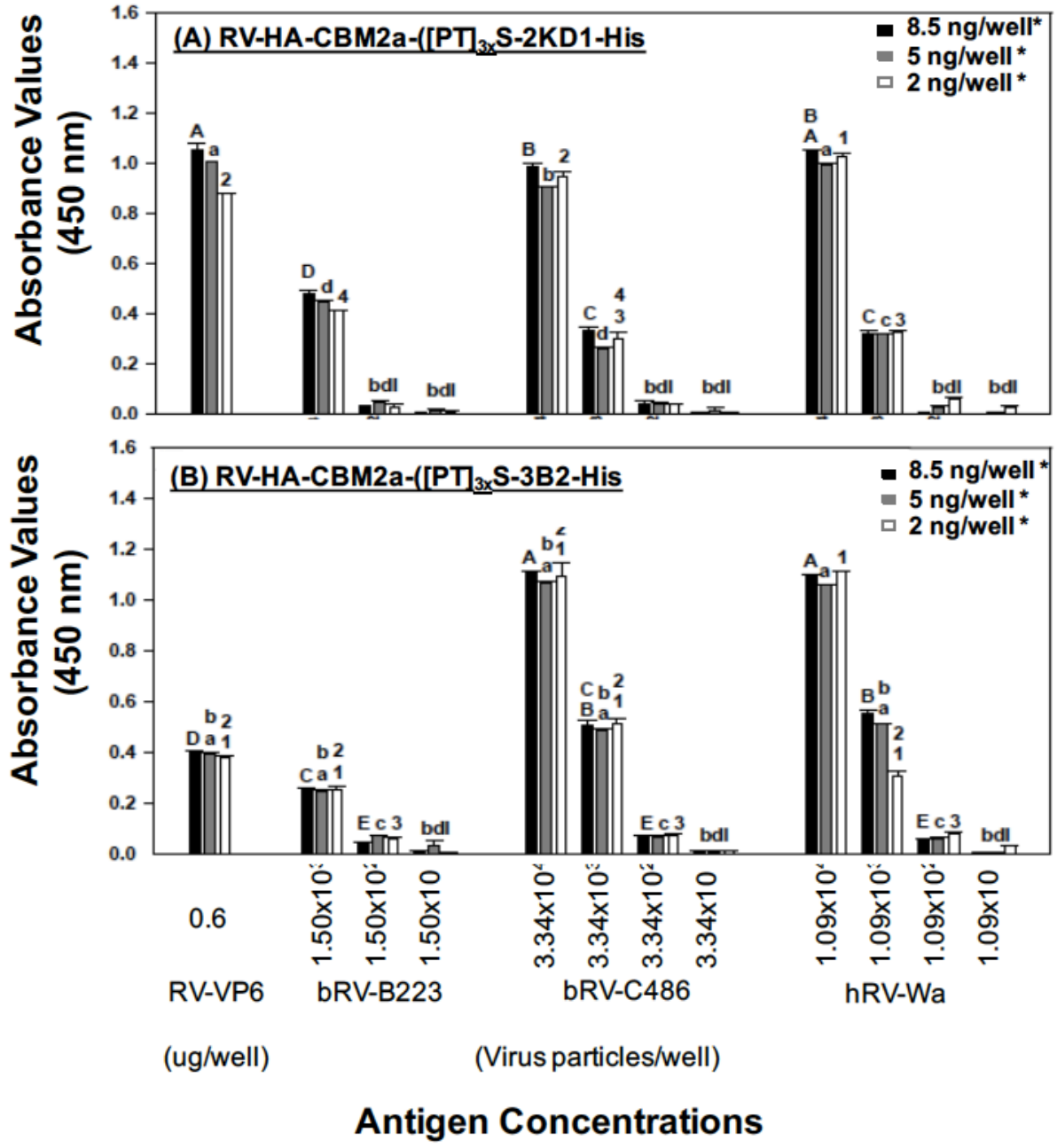

Figure 4.16. Characterization of RV-V_HHs fusion to CBM2a binding specificity and sensitivity to rotavirus in sandwich ELISA. The plate was coated with RV-IgG (100 ng/well) and different strains of enteric viruses and RV-VP_6 (0.6 µg/well) were detected in two steps by 8.5, 5 and 2 µg/well of RV-CBM2a-2KD1 (A) and RV-CBM2a-3B2 (B) and anti-his conjugated to HRP. The RV-VP_6 was used as a positive control whereas murine norovirus (mNV) and human adenoviruses (hAdenoV) where used as negative controls. Data are means and standard error of 3 technical replicates. bRV: bovine rotavirus. hRV: human rotavirus. bdl: below detection limit. Capital letters represent statistical difference among different antigen sources detected by 8.5 µg/well of antibody. Small letters represent statistical difference among different antigen sources detected by 5 µg/well of antibody. Numbers represent statistical difference among different antigen sources detected by 2 µg/well of antibody.

capturing the virus when different RV-mAbs are used for detection and (2) evaluating which RV-mAb has highest detection levels in combination with various RV-2KD1-CBM2a fusion proteins. For these experiments, ELISA plates were coated with 5 µg/well of each fusion protein, and with CBM2a alone as a negative control, followed by exposure to different concentrations of the 3 RV strains. Subsequently, detection by 100 ng/well of either RV-2KD1, RV-3B2 or RV-IgG 26 and appropriate secondary antibody were conducted (Figure 4.17). Positive signals were obtained when RV-2KD1, RV-3B2 and RV-IgG 26 were used to detect different strains of RV regardless of RV-V_HH-fusion protein used to coat the plate, while no signal was obtained on wells treated with CBM2a (Figure 4.17). Analysis by ANOVA showed no statistical difference when different linkers ($([PT]_3T)_{3x}S$ and $(G_4S)_{3x}$) were used, but a statistical difference ($P<0.0001$) was found with orientation of RV-2KD1. Coating the plate with RV-2KD1 linked at its N-terminus to CBM2a resulted in the best capturing of the RV strains, while best detection was obtained with RV-IgG 26. There were significant differences when the plate was coated with RV-HA-CBM2a-$(G_4S)_{3x}$-2KD1 ($P<0.0001$), RV-HA-2KD1-$(G_4S)_{3x}$-CBM2a ($P<0.0002$) and RV-HA-2KD1-$([PT]_3T)_{3x}S$-CBM2a ($P<0.002$) and RV were detected by RV-IgG 26 (Figure 4.17 C) in comparison to RV-2KD1 and RV-3B2 (Figures 4.17 A and B, respectively). These results indicate that RV-2KD1 was not functionally affected when it was linked to CBM2a. Also, detection of the virus was highest when ELISA plates were coated with fusion protein of RV-2KD1 at N-terminal and the detection antibody.

In general, ELISA results demonstrated that RV-mAbs specifically recognized RV-VP_6 and whole RV and RV-2KD1 and RV-IgG 26 (RV-3B2 was not test for this test) did not cross-reacted with mNV and hAdenoV strains. The results also showed that best det-

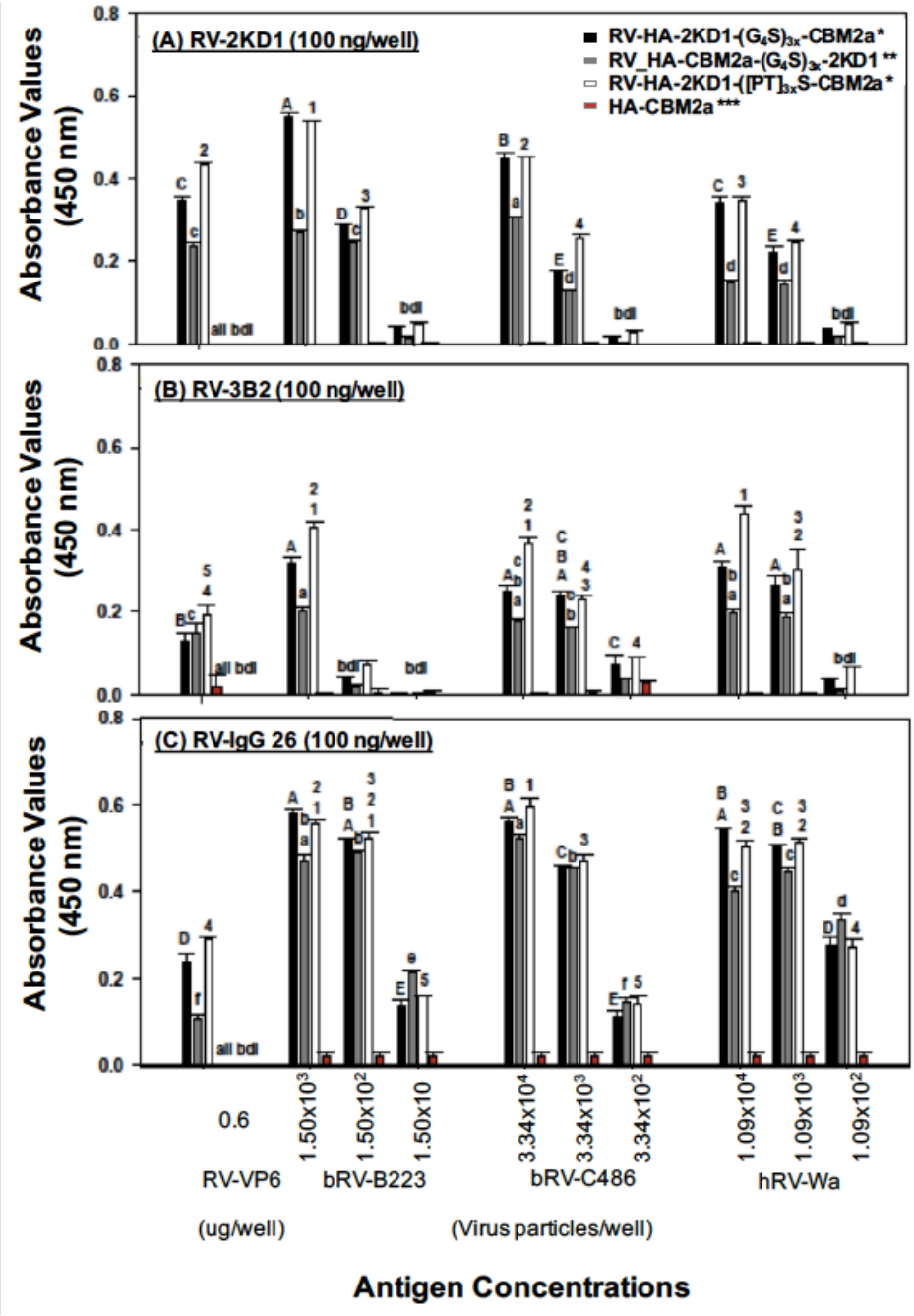

Figure 4.17. Characterization of RV-2KD1-fusion to CBM2a binding specificity and sensitivity to rotavirus in sandwich ELISA. The plate was coated with different fusion proteins (RV-2KD1-CBM2a and RV-CBM2a-2KD1 (5 µg/well) and different strains of enteric viruses and RV-VP_6 (0.6 µg/well) were detected in two steps by 100 ng/well of RV- 2KD1 (A), RV-3B2 (B) and RV-IgG (C) followed by anti-his conjugated to HRP (A-B) or anti-human conjugated-HRP (C). The RV-VP_6 was used as a positive control whereas murine norovirus (mNV) and human adenoviruses (hAdenoV) where used as negative controls. Data are means and standard error of 3 technical replicates. bRV: bovine rotavirus. hRV: human rotavirus. bdl: below detection limit. Capital letters represent statistical difference among different antigen sources immobilized on the plate via HA-2KD1-$(G_4S)_{3x}$-CBM2a. Small letters represent statistical difference among different antigen sources immobilized on the plate via HA-CBM2a-$(G_4S)_{3x}$-2KD1. Numbers represent statistical difference among different antigen sources immobilized on the plate via HA-2KD1-$([PT]_3T)_{3x}$-CBM2a.

ection of different RV strains was obtained by RV-IgG 26 > RV-2KD1 > RV-3B2. Although all RV strains were detectable at lower concentration of 10^2 virus particles/ml, the RV-mAbs have higher binding ability to hRV and bRV-C486 than bRV-B223. However, based on ELISA results presented in Figure 4.17, the RV-HA-2KD1-$(G_4S)_{3x}$-CBM2a RV-mAbs was selected for future testing using a cellulose filter paper (see Section 4.5.1).

4.5 Antibody Capture Technology Development

4.5.1 Cellulose Filter Capture System

To determine whether RV-HA-V_HH-CBM2a is capable of specifically attaching on a cellulose filter for the detection of RV, an ELISA assay was performed on cellulose filter paper. The fusion protein selected for these assays was RV-HA-2KD1-$(G_4S)_{3x}$-CBM2a because fusion protein with CBM2a at the C-terminal (regardless of the linker) detected the viruses in ELISA stronger than fusion protein with CBM2a at the N-terminal. The HA-CBM2a and RV-HA-2KD1-$(G_4S)_{3x}$-CBM2a fusion proteins were incubated on cellulose filter discs (5 and 2 µg of fusion protein per disc, 13 mm diameter disc), blocked for 30 min each, and washed. RV (at 10^4 virus/disc) in SFM was incubated on the discs before detection with RV-IgG 26 followed by anti-human conjugated HRP antibody. No colour development was observed on discs bound with HA-CBM2a (with or without RV) (Figure 4.18 A) or on discs bound with RV-HA-2KD1-$(G_4S)_{3x}$-CBM2a in the absence of RV (Figure 4.18 B, left-side). The RV-HA-2KD1-$(G_4S)_{3x}$-CBM2a was successfully bound to the cellulose filter disc as determined by the development of the blue color on the filter in the presence of RV (Figure 4.18 B, right-side). The disc bound with RV-HA-2KD1-$(G_4S)_{3x}$-CBM2a also produced positive signals with all RV strains (Figure 4.18 C).

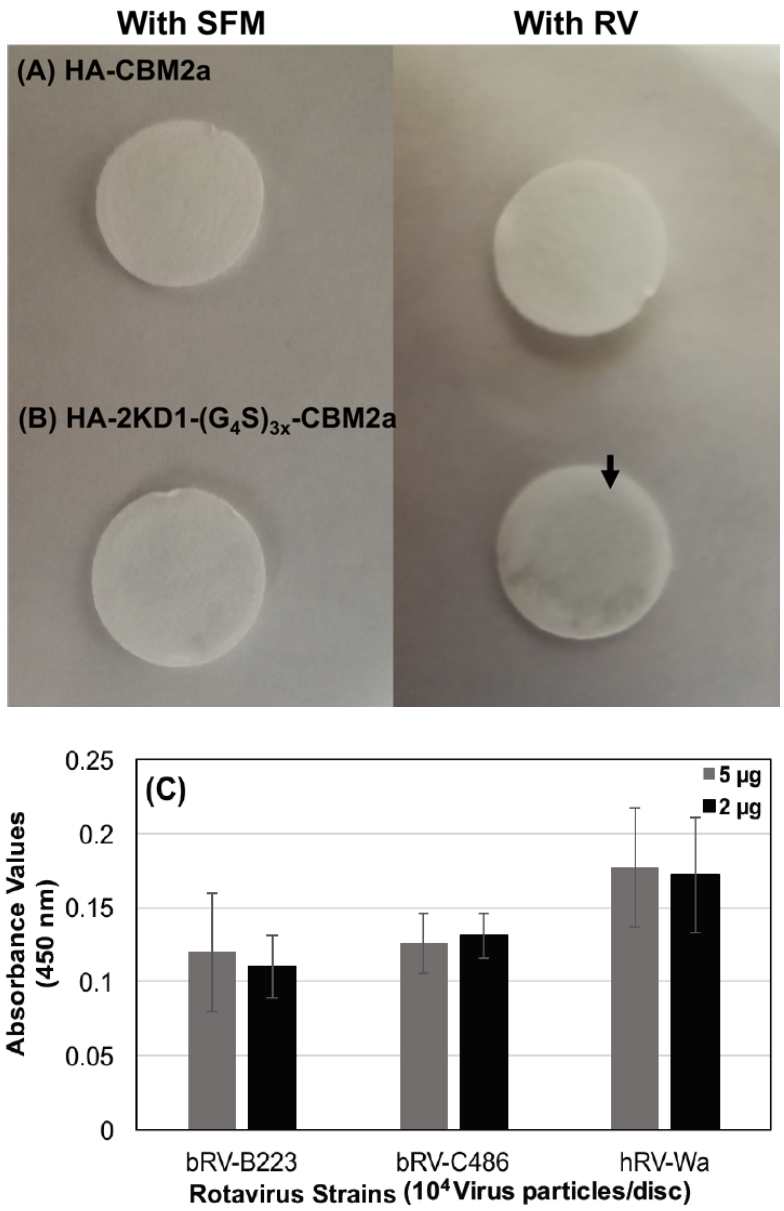

Figure 4.18. Immobilization of HA-CBM2a and RV-HA-2KD1-$(G_4S)_{3x}$-CBM2a on a cellulose disc for the detection of RV strains by sandwich ELISA. After coating the cellulose disc with 5 and 2 µg of HA-CBM2a or RV-HA-2KD1-$(G_4S)_{3x}$-CBM2a for 30 min, the discs were blocked with 4% skim milk for 30 min. After washing, hRV-Wa (100 µl at 10^4 virus particles/disc) and serum free medium (SFM) were incubated for 30 min the washed. The discs were then incubated with a primary RV-IgG 26 (100 µl at 100 ng/disc) followed by a secondary anti-human-HRP antibody, 30 min each. Finally, the discs were developed with ELISA substrate-HRP for 30 min to detect the RV. The HA-CBM2a was used as a control and showed no colour development on the cellulose discs (A) whereas blue colour was developed on the disc (B) representing sucssessful immobolization of RV-HA-2KD1-$(G_4S)_{3x}$-CBM2a on a cellulose disc and detection of the viurs "hRV-Wa" (the image represents colour on the disc coated with 2 µg of fusion protein). (C) Absorbance values on the discs with all RV strains at 10^4 virus particle/disc. Gray bars represent absorbance values from filters coated with 5 µg of fusion protein. Black bars represent absorbance values from filters coated with 2 µg of fusion protein. Data are means and standard error of three technical replicates.

The initial tests showed the RV-HA-2KD1-$(G_4S)_{3x}$-CBM2a fusion protein could be bound to the cellulose filter and detect RV. Both concentrations (5 and 2 µg) of fusion protein showed similar detection values of the virus on the filter paper (when absorbance values were measured (Figure 4.18 C). As a result, the lowest concentration (2 µg) was selected for further tests. The next set of tests were conducted to evaluate the selectivity of the antibody coated paper when multiple viruses (hRV and hAdenoV) are present. Filters were prepared as before, cellulose discs coated with 2 µg of RV-HA-2KD1-$(G_4S)_{3x}$-CBM2a and SFM-spiked with multiple concentrations of hRV and hAdenoV. Spiked samples (1 ml) were filtered through cellulose discs coated with either RV-HA-2KD1-$(G_4S)_{3x}$-CBM2a or HA-CBM2a. The viruses in the influent, flow through (including flow through from the filter wash steps) and bound on the filter paper were extracted and quantified by RT-qPCR.

Initial tests examining hRV or hAdenoV alone indicated that cellulose paper coated with RV-HA-2KD1-$(G_4S)_{3x}$-CBM2a is capable to specifically detect RV (Table 4.1). For samples with hAdenoV alone, there was no significant difference in removing hAdenoV with cellulose-treated RV-HA-2KD1-$(G_4S)_{3x}$-CBM2a (38.46 ± 20.55%) and cellulose-treated HA-CBM2a (23.21 ± 8.94%). This suggested non-specific removal due to virus binding to the filter material. Removal of hRV by cellulose paper coated with RV-HA-2KD1-$(G_4S)_{3x}$-CBM2a or HA-CBM2a was calculated to be 81.75 ± 2.05% and 43.23 ± 10.81%, respectively. These results demonstrate that hRV was removed specifically by 38.52 ± 8.97% via cellulose-treated RV-HA-2KD1-$(G_4S)_{3x}$-CBM2a.

Table 4.1. Removal of enteric viruses from spiked serum free medium (SFM) at different conditions using developed RV-HA-2KD1-$(G_4S)_{3x}$-CBM2a- and HA-CBM2a-cellulose-based filter systems.

Sample Conditions	Analyzed Samples	Detection of Enteric Viruses (virus particle/ml) by Cellulose Filter Paper			
		HA-CBM2a		RV-HA-2KD1-$(G_4S)_{3x}$-CBM2a	
		hRV	hAdenoV	hRV	hAdenoV
hRV alone	Spiked influent	$3.39 \pm 0.07 \times 10^4$	-	$3.39 \times 10^4 \pm 6.87 \times 10^2$	-
	Flow through	$1.92 \times 10^4 \pm 3.34 \times 10^3$	-	$6.17 \times 10^3 \pm 5.80 \times 10^2$	-
	Filter bound	$2.98 \times 10^5 \pm 3.38 \times 10^5$	-	$1.33 \times 10^5 \pm 1.51 \times 10^5$	-
hAdenoV alone	Spiked influent	-	$1.45 \times 10^8 \pm 5.05 \times 10^7$	-	$1.45 \times 10^8 \pm 5.05 \times 10^7$
	Flow through	-	$1.12 \times 10^8 \pm 4.62 \times 10^7$	-	$9.19 \times 10^7 \pm 5.63 \times 10^7$
1:1 ratio of hRV:hAdenoV	Spiked influent	$1.93 \times 10^5 \pm 3.21 \times 10^4$	$2.82 \times 10^5 \pm 9.03 \times 10^4$	$1.93 \times 10^5 \pm 3.21 \times 10^4$	$2.82 \times 10^5 \pm 9.03 \times 10^4$
	Flow through	$1.29 \times 10^5 \pm 5.67 \times 10^4$	$1.84 \times 10^5 \pm 4.07 \times 10^4$	$5.58 \times 10^4 \pm 6.22 \times 10^4$	$1.78 \times 10^5 \pm 3.29 \times 10^4$
1:1000 ratio of hRV:hAdenoV	Spiked influent	$1.17 \times 10^4 \pm 4.19 \times 10^3$	$3.78 \times 10^7 \pm 6.58 \times 10^6$	$1.17 \times 10^4 \pm 4.91 \times 10^3$	$3.78 \times 10^7 \pm 6.58 \times 10^6$
	Flow through	$6.63 \times 10^4 \pm 2.49 \times 10^3$	$1.63 \times 10^7 \pm 6.23 \times 10^6$	$7.21 \times 10^3 \pm 7.21 \times 10^2$	$1.72 \times 10^7 \pm 7.09 \times 10^6$

Note: Data are means and standard deviation of three biological replicated. Each fusion protein was immobilized on a 13 mm diameter cellulose filter disc (2 µg). After blocking the treated filter, 1 ml of spiked sample was filtered through and flow through was collected. The viruses were extracted from spiked, flow through and filter samples (this was done only for hRV alone as a primary test). Quantification of viruses was estimated by qPCR. Filter in this primary test was not washed.

The removal of hRV was then evaluated in the presence of hAdenoV, ratios of 1:1 and 1:1000 of hRV:hAdenoV in SFM were tested (Table 4.1). Removal of hRV in the presence of an equal concentration of hAdenoV was 33.59 ± 28.77% and 67.89 ± 37.26%, whereas hAdenoV was removed by 34.59 ± 14.49% and 33.46 ± 10.05% using cellulose-treated RV-HA-2KD1-$(G_4S)_{3x}$-CBM2a and cellulose-treated HA-CBM2a, respectively. These results demonstrated that hRV was removed specifically by 34.30 ± 30.65% via cellulose-treated RV-HA-2KD1-$(G_4S)_{3x}$-CBM2a filter. In the presence of 1000-fold greater concentration of hAdenoV, removal of hRV was calculated to be 80.40 ± 4.88% and 42.53 ± 9.90% with RV-HA-2KD1-$(G_4S)_{3x}$-CBM2a and HA-CBM2a, respectively. The hAdenoV was removed similarly from both papers (55.56 ± 10.23% with RV-HA-2KD1-$(G_4S)_{3x}$-CBM2a and 57.90 ± 9.27% with HA-CBM2a). These results demonstrated that hRV was removed specifically by about 37.87 ± 13.04% via cellulose-treated RV-HA-2KD1-$(G_4S)_{3x}$-CBM2a filter.

An important aspect to test was the matrix effects of different water types on the ability of the bioactive paper to capture RV. To accomplish this goal, the filtration tests were conducted as indicated previously for SFM spiked with different concentrations of hRV and hAdenoV. For these experiments spiked tap and river waters were used in place of SFM. Each source water (tap and river) sample was characterized with respect to pH, conductivity, turbidity, hRV and hAdenoV quantification. River samples were collected in mid March as RV is expected to peak in the winter months (Le Guyader et al., 2000 & Pang et al., 2019). Tap waters had lower pH (7.65 ± 0.02), conductivity (-32.73 ± 0.20 micro-Siemens per centimeter (µS/cm)) and turbidity (0.58 ± 0.25 nephelometric (NTU)) than the river water (pH 8.32 ± 0.04, -66.50 ± 2.50 µS/cm and 4.44 ± 1.59 NTU). Also, no

virus was detected in tap water source while RV and hAdenoV were detected in river water at concentrations of 99 ± 54 and 92 ± 61 virus/ml, respectively. Both viruses (hRV and hAdenoV) were extracted from influent (spiked), flow through and cellulose filter papers (treated-RV-HA-2KD1-$(G_4S)_{3x}$-CBM2a and treated-HA-CBM2a) for quantification by RT-qPCR.

Results from tests examining samples with hRV alone indicated that the RV-HA-2KD1-$(G_4S)_{3x}$-CBM2a-filter was able to remove RV from tap and river water sources by 64.55 ± 2.68% and 68.06 ± 18.89% whereas HA-CBM2a-filter removed RV by 37.10 ± 23.40% and 41.33 ± 7.54%, respectively (Table 4.2). These results demonstrated that hRV was removed specifically by 27.44 ± 22.93% and 26.72 ± 19.66% from tap and river water sources, respectively, via cellulose-treated RV-HA-2KD1-$(G_4S)_{3x}$-CBM2a filter. Overall, hRV was specifically removed by 38.52 ± 8.97%, 27.44 ± 22.93% and 26.72 ± 19.66% in SFM, tap and river water sources, respectively, when RV is present alone. The specific removal of hRV when in competition with 100 or 1000-fold greater concentration of hAdenoV was 37.87 ± 13.04%, 29.18 ± 2.38% and 32.66 ± 8.74% in SFM, tap and river water sources, respectively.

Results from tests examining samples with RV in the presence of 1:100 ratio of hRV:hAdenoV indicated that the removal of hRV from tap and river sources by RV-HA-2KD1-$(G_4S)_{3x}$-CBM2a-filter were calculated to be 71.36 ± 8.34% and 71.15 ± 12.06%, respectively. Under the same conditions, the HA-CBM2a-filter removed hRV by 42.18 ± 10.28% and 38.48 ± 20.76% from both sources, respectively (Table 4.2). The removal of hAdenoV by RV-HA-2KD1-$(G_4S)_{3x}$-CBM2a-filter was about 39.85 ± 12.96% and 33.14 ± 24.87% from tap and river water, respectively. The hAdenoV was removed similarly from

Table 4.2. Removal of enteric viruses from spiked water samples at different conditions using developed 2KD-cellulose- and CBM2a-based filtration.

Water Type	Sample Conditions	Analyzed Samples	Detection of Enteric Viruses (virus particle/ml) by Cellulose Filter Paper			
			HA-CBM2a		HA-2KD1-$(G_4S)_{3x}$-CBM2a	
			hRV	hAdenoV	hRV	hAdenoV
Tap	hRV alone	Spiked influent	$8.86 \pm 4.26 \times 10^5$	-	$8.86 \times 10^5 \pm 4.26 \times 10^5$	-
		Flow through	$6.24 \times 10^5 \pm 5.28 \times 10^5$	-	$3.15 \times 10^5 \pm 1.59 \times 10^5$	-
		Filter bound	$3.15 \times 10^5 \pm 1.36 \times 10^5$	-	$7.73 \times 10^5 \pm 4.56 \times 10^5$	-
	1:100 ratio of hRV:hAdenoV	Spiked influent	$6.94 \times 10^6 \pm 1.71 \times 10^6$	$2.01 \times 10^8 \pm 2.74 \times 10^7$	$6.94 \times 10^6 \pm 1.71 \times 10^6$	$2.01 \times 10^8 \pm 2.74 \times 10^7$
		Flow through	$4.13 \times 10^6 \pm 1.6 \times 10^5$	$1.28 \times 10^8 \pm 2.02 \times 10^7$	$2.08 \times 10^6 \pm 9.83 \times 10^5$	$1.20 \times 10^8 \pm 2.55 \times 10^7$
		Filter bound	$1.78 \times 10^6 \pm 1.5 \times 10^6$	$2.85 \times 10^6 \pm 7.02 \times 10^5$	$3.08 \times 10^6 \pm 3.9 \times 10^5$	$3.54 \times 10^6 \pm 2.32 \times 10^6$
River	hRV alone	Spiked influent	$1.92 \times 10^5 \pm 1.22 \times 10^5$	-	$1.92 \times 10^5 \pm 1.22 \times 10^5$	-
		Flow through	$1.09 \times 10^5 \pm 6.83 \times 10^4$	-	$4.85 \times 10^4 \pm 3.55 \times 10^4$	-
		Filter bound	$9.05 \times 10^4 \pm 5.8 \times 10^4$	-	$8.1 \times 10^4 \pm 3.82 \times 10^4$	-
	1:100 ratio of hRV:hAdenoV	Spiked influent	$7.75 \times 10^6 \pm 2.21 \times 10^6$	$1.35 \times 10^8 \pm 2.82 \times 10^7$	$7.75 \times 10^6 \pm 2.21 \times 10^6$	$1.35 \times 10^8 \pm 2.82 \times 10^7$
		Flow through	$4.77 \times 10^6 \pm 2.07 \times 10^6$	$8.89 \times 10^7 \pm 1.5 \times 10^7$	$2.23 \times 10^6 \pm 1.11 \times 10^6$	$8.58 \times 10^7 \pm 1.24 \times 10^7$
		Filter bound	$6.94 \times 10^6 \pm 2.74 \times 10^6$	$4.5 \times 10^6 \pm 4.24 \times 10^6$	$4.7 \times 10^6 \pm 1.44 \times 10^6$	$6.07 \times 10^6 \pm 9.07 \times 10^6$

Note: Data are means and standard deviation of three biological replicated. Each fusion protein was immobilized on a 13 mm diameter cellulose filter disc (2µg). After blocking the treated filter, 1 ml of spiked sample was filtered through and flow through was collected. The filters were washed and viruses were extracted from spiked, flow through and filter samples. Quantification of viruses was estimated by qPCR. Water quality of original samples was determined and samples were assessed for their abundance of the viruses. Original water samples were assessed for rotavirus and adenovirus counts. No viruses were detected for tap water source. Rotavirus and adenovirus were detected in river water at concentrations of 99 ± 54 and 92 ± 61 virus/µl, respectively.

both water sources (35.77 ± 13.21% from tap and 33.60 ± 4.93% from river) with HA-CBM2a-filter. These results demonstrated that hRV was removed specifically by 29.18 ± 2.38% and 37.87 ± 13.04% via cellulose-treated RV-HA-2KD1-$(G_4S)_{3x}$-CBM2a filter from tap and river water sources, respectively.

In summary, the cellulose filter paper treated-RV-HA-2KD1-$(G_4S)_{3x}$-CBM2a system, developed in this study, was evaluated for its ability to specifically capture RV under different aquatic environments (SFM, tap and river water sources) and in the presence of single or multiple viruses. The results from cellulose filter paper treated-HA-CBM2a and RV-HA-2KD1-$(G_4S)_{3x}$-CBM2a systems indicated non-specific binding of RV and AdenoV on the filters. The non-specific binding on both cellulose filter papers was assumed to be equal as both contain CBM2a. The results generally indicated about 30.89 ± 6.61% of the RV population was removed when present alone and 33.23 ± 4.37% of the RV population was removed when in competition with hAdenoV (i.e., means of specific removal from all sources). The specific removal of hRV, from different environments indicated that for SFM (38.52 ± 8.97%), tap (27.44 ± 22.93%) and river (26.72 ± 19.22%) waters were not statistically different when RV was the only virus. Similarly, no statistical difference was found for SFM (37.87 ± 13.04%), tap (29.18 ± 2.38%) and river (32.66 ± 8.74%) waters when RV was in competition with hAdenoV. Also, no statistical difference was found between capturing of RV alone or in competition with hAdenoV from all sample sources (SFM: 38.52 ± 8.97% vs 37.87 ± 13.04%, tap: 27.44 ± 22.93% vs 29.18 ± 2.38% and river: 26.72 ± 19.22% vs 32.66 ± 8.74%). In addition, hAdenoV was removed consistently by 57.90 ± 9.27% to 55.56 ± 10.23% in SFM, 35.77 ± 13.21% to 39.85 ± 12.96% and 33.60 ± 4.9% to 33.14 ± 24.78% in tap and

river waters via CBM2a. Overall, these data indicate that the developed cellulose filter paper treated-RV-HA-2KD1-$(G_4S)_{3x}$-CBM2a system was capable to specifically capture RV by about 26.72% to 38.52% when RV was alone and by about 29.18% to 37.87% when RV in competition with other virus regardless of the source of the sample. Additionally, large variability for both tap and river water among the biological replicates was observed which may be originated from non-specific binding.

4.5.2 Immuno-Magnetic Capture System

An alternative application to creating a bioactive filter for selectively capturing EVs from water is to use magnetic beads to immobilized the antibodies and capture viruses. The beads, used in previous studies, were always conjugated to a full-length antibody (e.g., IgG or IgA) and used for secondary concentration and detection of the virus and not for primary concentration purposes (Jothikumar et al. 1998; Myrmel et al. 2000; El-Galil et al., 2005 & Hwang et al., 2007). In this study, however, magnetic beads were coupled with either full-length antibody RV-IgG 26 or sdAb RV-2KD1. These 2 mAbs were compared for their ability to capture RV in a primary concentration step. Following expression and purification of the mAb molecules, RV-IgG 26 and RV-2KD1 were covalently coupled, separately, to magnetic beads to detect RV A strains.

The antibody-coupled beads and control beads (not conjugated to an antibody) at 10 µg /ml were incubated with RV-VP_6 (1 mg/ml) for 60 min on a shaker, washed, and then prepared for SDS-PAGE to investigate the binding of RV-VP_6. The Coomassie blue analysis showed that the RV-mAbs were successfully conjugated on the beads and were able to bind the RV-VP_6 (Figure 4.19). For the RV-IgG 26-coupled beads, 3 bands were

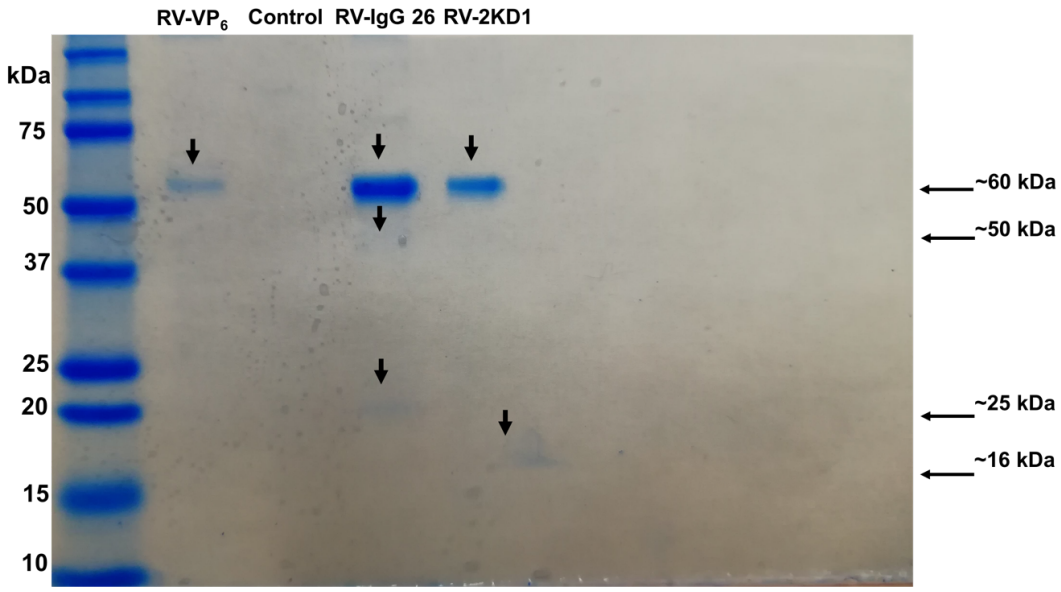

Figure 4.19. Detection of RV-VP_6 on SDS-PAGE using antibody-coupled magentic beads. Magentic beads were conjugated with 10 µg/ml of RV-2KD1 and RV-IgG 26 and incubated with RV-VP_6 (1 mg/ml) for 1 h at room temperature. The antibody-coupled beads were washed and boiled with reducing dye before runing the supernataant on the gel. The gel stained with Coomassie blue. Lane 1: protein standard. Lane 2: RV-VP_6 used as a postive control. Lane 3: antibody-free beads used as a negative control. Lane 4: RV-IgG 26-coupled beads. Lane 5: RV-2KD1-coupled beads. Arrows refer to RV-VP_6 (60 kDa), RV-IgG 26-H_C (50 kDa), RV-IgG 26-L_C (25 kDa) and RV-2KD1 (16 kDa).

observed corresponding to the L_C (~25 kDa), H_C (~50 kDa) and RV-VP_6 (60 kDa). For the RV-2KD1-coupled beads, 2 bands were observed corresponding to RV-2KD1 (~16 kDa) and RV-VP_6 (~60 kDa). No band was observed for antibody-free beads exposed to RV-VP_6.

The initial test showed the RV-mAbs (RV-IgG 26 and RV-2KD1) could be conjugated to magnetic beads and detect the RV-VP_6, suggesting these antibody-coupled beads could be used to remove virus in water samples. The next set of tests were conducted to evaluate the selectively of each antibody-coupled bead when multiple viruses (hRV and hAdenoV) were present. Tests were conducted in SFM-spiked with low and high concentrations of hRV alone using RV-IgG 26 (at 10 µg) only. Spiked samples were incubated with the RV-IgG 26-coupled bead for 60 min. The viruses in the influent, flow through and collected on the magnetic bead were extracted and quantified by RT-qPCR (beads were washed and boiled in 1x PBS for 5 min to release the virus before extraction of the viral nucleic acids).

Results from these tests indicated that magnetic beads conjugated to RV-IgG 26 are capable of detecting RV (Table 4.3). Removal of hRV at low and high concentrations was calculated from flow through to be 55.31 ± 14.15% and 47.64 ± 17.97%, respectively. Binding of the virus on the bead was not calculated as extracting the virus from 1x PBS buffer after heating the beads (suspended in the buffer) resulted in more release of the virus in the buffer.

Table 4.3. Removal of human rotavirus (hRV) using RV-IgG 26-coupled-magnetic beads from spiked serum free medium (SFM) with different concentrations of human rotavirus.

Analyzed Samples	Detection of Enteric Viruses by Magnetic Beads	
	RV-IgG 26-Coupled Beads	
	hRV (virus particle/ml)	Removal (%)
Spiked influent	$1.64 \pm 1.44 \times 10^{4}$	
Flow through	$8.69 \times 10^{3} \pm 9.86 \times 10^{3}$	55.31 ± 14.15
Beads	$2.41 \times 10^{5} \pm 1.34 \times 10^{5}$	
Spiked influent	$1.59 \times 10^{5} \pm 1.06 \times 10^{5}$	
Flow through	$7.11 \times 10^{4} \pm 4.04 \times 10^{4}$	47.64 ± 13.97
Beads	$2.69 \times 10^{7} \pm 2.22 \times 10^{7}$	

Note: Data are means and standard deviation of three biological replicates.

To test the matrix effects of different water sources on the binding of RV by the mAbs-magnetic beads, the incubation test was conducted as indicated previously for spiked SFM. For this experiment, river water samples were spiked with 1:100 ratio of hRV:hAdenoV. Each magnetic-bead bound with RV-IgG 26 or RV-2KD1 and unbound bead “control” (at 2 µg, for comparison to the prior experiments with the antibody-cellulose filter that used the same concentration of antibody) was incubated with 1 ml of the spiked river water sample for 30 and 60 min on a shaker. Quantification of the virus by qPCR in the influent (spiked), the flow through and on the beads.

Results from test indicated that the beads are capable of specifically capturing RV in 30 min, although longer incubation enhance the removal of RV by 21% (Table 4.4). The removal of hRV (after 60 min incubation) from RV-IgG 26- and RV-2KD1-coupled beads in the flow through was about 98.79 ± 0.52% and 97.81 ± 1.43%, respectively. Under the same conditions, the beads alone (no antibodies) removed hRV by 96.93 ± 1.93%. On the other hand, hAdenoV was removed to a similar amount with RV-IgG 26- (31.10 ± 46.36%) and RV-2KD1-coupled beads (31.19 ± 54.95%). The removal of hAdenoV was about 26.71 ± 71.97% for the control beads. These results demonstrated that hRV was specifically removed by 1.85 ± 1.46% and 0.87 ± 0.4% via RV-IgG 26- and RV-2KD1-coupled beads, respectively, from spiked river water.

Overall, there was no statistical difference in removal of RV by RV-IgG 26- and RV-2KD1-coupled beads when in competition with hAdenoV in river water. A high yield of non-specific binding was observed with the beads system and this may be due to insufficient amount of the beads (20 µl) or concentration of the antibody (2 µg) with a large volume of the sample (1 ml). RV-IgG 26-coupled bead was about 2 times as effective in

Table 4.4. Removal of enteric viruses from spiked river water samples at lowest abundance of human rotavirus (hRV) with highest abundance of human adenovirus (hAdenoV) using developed RV-monoclonal antibodies-coupled-magnetic beads.

Analyzed Samples	Detection of Enteric Viruses (virus particle/ml) by Magnetic Beads					
	IgG 26-coupled Beads		2KD1-coupled Beads		Control-coupled Beads	
	hRV	hAdenoV	hRV	hAdenoV	hRV	hAdenoV
Spiked influent	$4.87 \pm 4.22 \times 10^{6}$	$3.51 \times 10^{8} \pm 3.49 \times 10^{8}$	$4.87 \times 10^{6} \pm 4.22 \times 10^{6}$	$3.51 \times 10^{8} \pm 3.491 \times 10^{8}$	$4.87 \times 10^{6} \pm 4.22 \times 10^{6}$	$3.51 \times 10^{8} \pm 3.49 \times 10^{8}$
Flow through (30 min)	$5.67 \times 10^{4} \pm 7.06 \times 10^{3}$	$1.57 \times 10^{8} \pm 3.97 \times 10^{7}$	$6.89 \times 10^{4} \pm 2.47 \times 10^{4}$	$1.51 \times 10^{8} \pm 9.78 \times 10^{6}$	ND	$1.56 \times 10^{8} \pm 1.94 \times 10^{7}$
Flow through (60 min)	$4.48 \times 10^{4} \pm 1.52 \times 10^{4}$	$1.47 \times 10^{8} \pm 4.27 \times 10^{7}$	$6.61 \times 10^{4} \pm 1.25 \times 10^{4}$	$1.32 \times 10^{8} \pm 3.67 \times 10^{7}$	$9.05 \times 10^{5} \pm 1.08 \times 10^{4}$	$1.42 \times 10^{8} \pm 6.98 \times 10^{7}$
Beads	$8.20 \times 10^{4} \pm 2.58 \times 10^{4}$	$5.39 \times 10^{7} \pm 2.17 \times 10^{7}$	$3.17 \times 10^{4} \pm 1.31 \times 10^{4}$	$1.15 \times 10^{7} \pm 5.97 \times 10^{6}$	$2.73 \times 10^{4} \pm 6.09 \times 10^{3}$	$2.96 \times 10^{7} \pm 1.94 \times 10^{7}$

Note: Data are means and standard deviation of three biological replicates. ND, not determined.

removing RV from the water than RV-2KD1-coupled bead, but not significant and this may be due to (1) high affinity of RV-IgG than RV-2KD1 and (2) the small size of the RV-2KD1 "V_HH" allows more antibody immobilization on the beads thus more available binding site to capture the virus. However, capturing the virus using antibody-cellulose filter system was better than antibody-coupled beads system in terms of removal when all were used at same concentration (2 µg). The antibody-coupled beads system may be effective when it is used with higher antibody concentration (e.g., 10 µg).

4.6 Electron Microscopy

TEM was used to examine the morphology of the bRV-B223 strain (Figure 4.20), while SEM of the cellulose filter paper and immuno-magnetic bead surfaces examined the attachment of bRV-B223 in the presence and absence of the RV-mAbs (Figures 4.21 and 4.22).

The TEM of bRV-B223, obtained following propagation in cell culture, showed the typical RV morphology. The single RV particle had a diameter of about 55 nm with a wheel-like appearance with some damage on the upper surface (Figure 4.20).

The SEM images of the cellulose filter paper and immune-magnetic bead surfaces revealed attachment of small circular particles, with a diameter of approximately 50 nm, on the cellulose filter paper treated with RV-HA-2KD1-$(G_4S)_{3x}$-CBM2a (Figure 4.21 C) and on the surface of magnetic bead-coupled with RV-IgG 26 (Figure 4.22 B-C) or RV-2KD1 (Figure 4.22 D-E). The presence of small circular particles suggests the binding of RV to the RV-mAbs bound to the filter paper and magnetic beads. These particles were

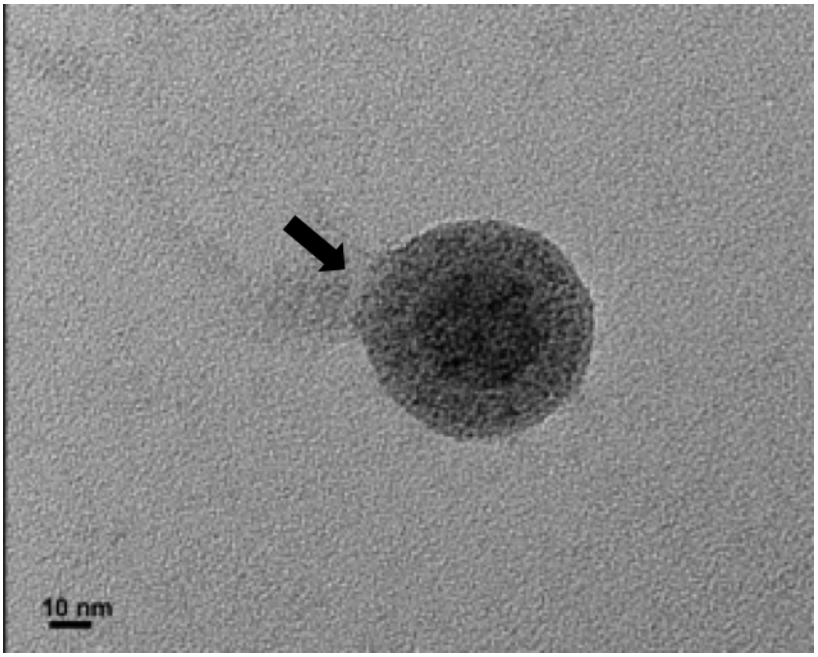

Figure 4.20.Examination of isolated rotavirus (bRV-B223) by transmission electron microscopy shows a typical rotavirus particle. Arrow refers to some damage on the upper surface of the virus particle.

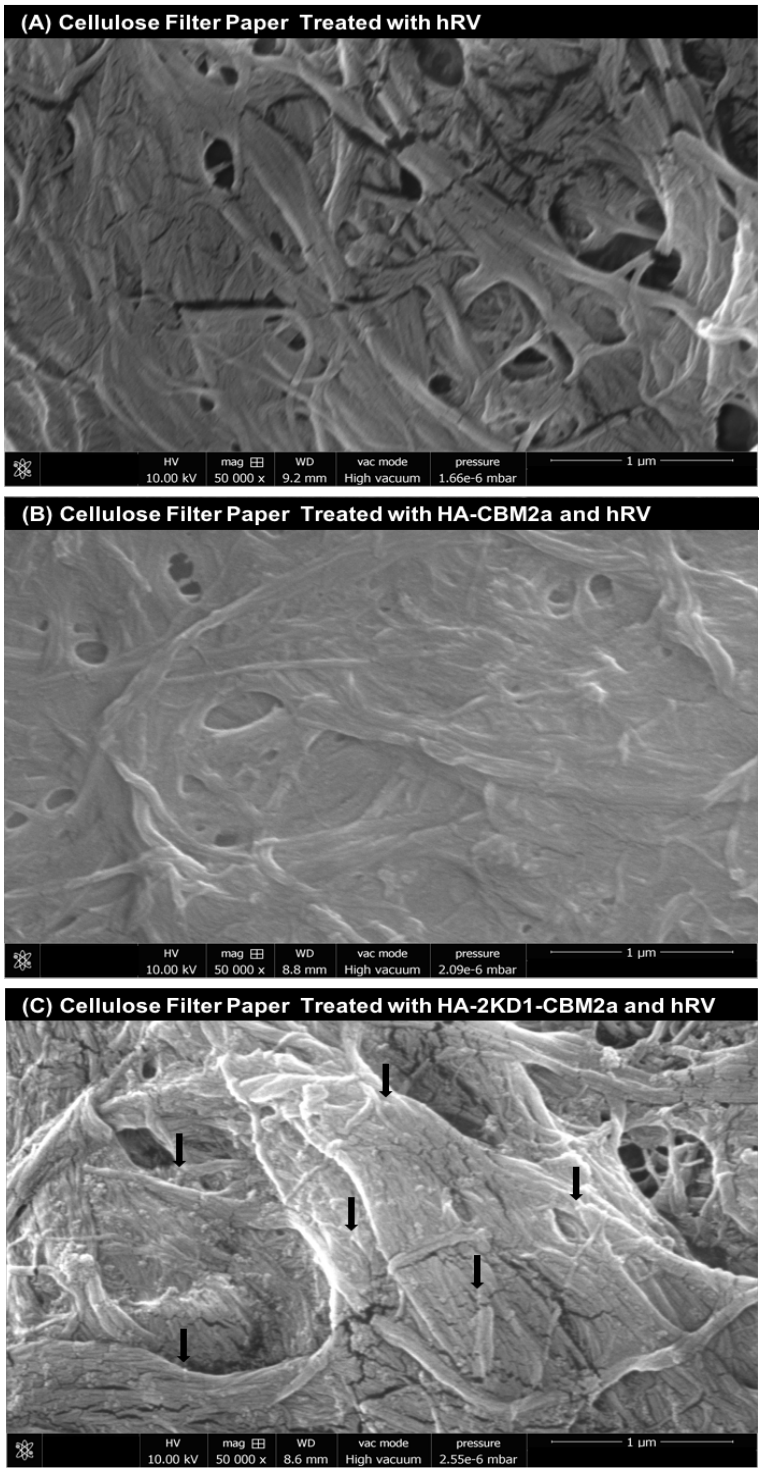

Figure 4.21. Scanning electron microscope micrographs highlighting the attachment of rotavirus on a cellulose filter paper. (A) Cellulose filter paper treated with rotavirus only used as a control indicating the absence of rotavirus particles on the surface of the paper. (B) Cellulose filter paper treated with HA-CMB2a prior filtration of rotavirus indicating absence of rotavirus particles on the surface of the paper. (C) Cellulose filter paper treated with RV-2KD1-CBM2a prior filtration of rotavirus indicating the presence of small particles on the surface of the paper. Arrows refer to particles of about 50 nm in diameter indicating the attachment of the rotavirus on the surface of cellulose filter paper treated with 2KD1. Scale bar is 1 µm.

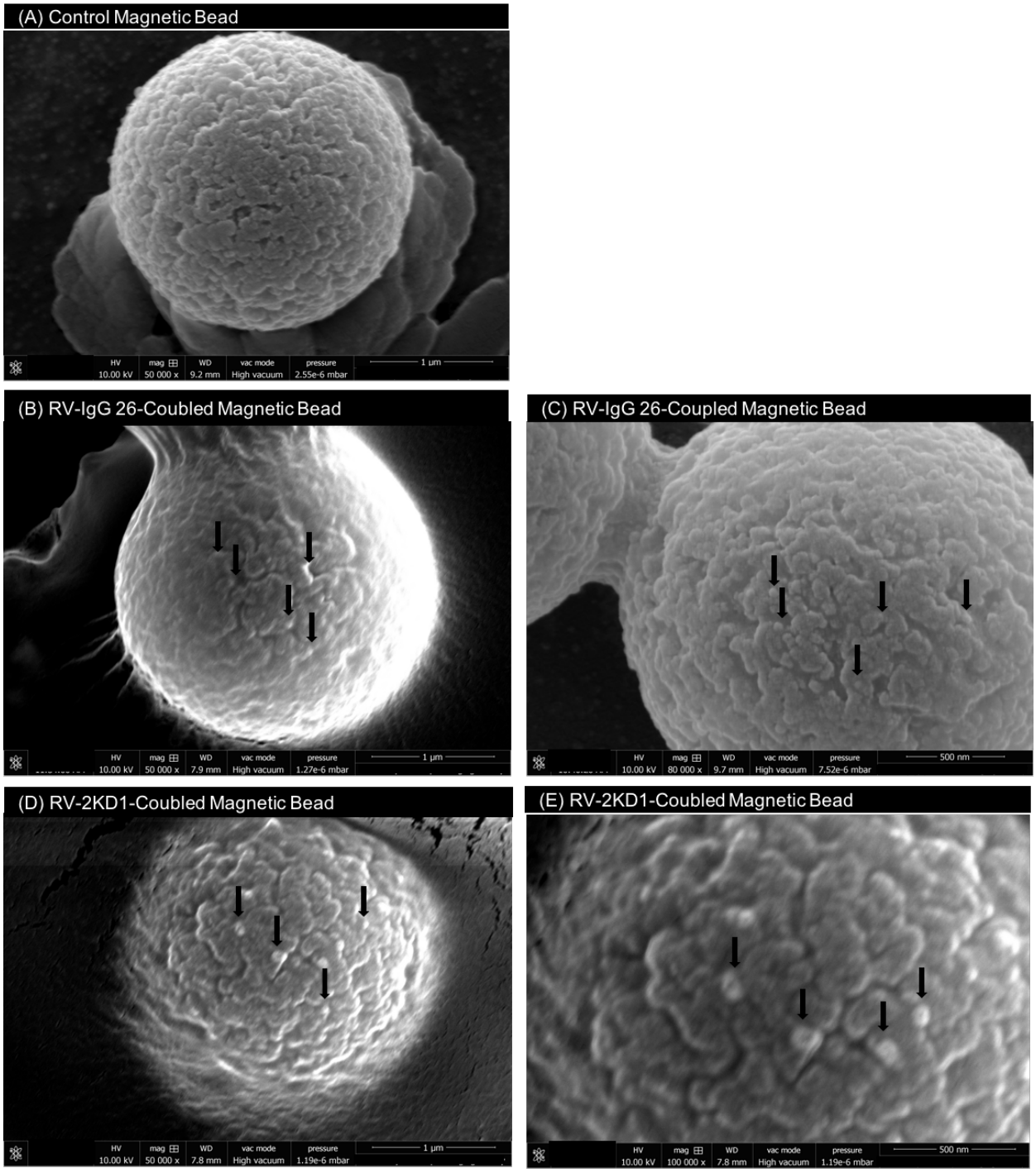

Figure 4.22. Scanning electron microscope micrographs highlighting the dis-attachment of rotavirus on a magnetic bead only (A), bead-coupled RV-IgG 26 (B-C) and bead-couple RV-2KD1 (D-E). Arrows refer to particles of about 50 nm in diameter indicating the attachment of the rotavirus on RV-mAbs-couples' beads. Scale bars are 1µm and 500 nm for left and right images, respectively.

not observed on the surfaces of the cellulose filter paper alone (Figure 4.21 A), bound with the CBM2a alone (Figure 4.21 B), or on the surface of the antibody-free magnetic bead (Figure 4.22 A) after incubation with RV.

5 DISCUSSION

Detection of viruses in water samples occurs in four stages: sampling/filtering, concentration, detection and data interpretation. The concentration stage, which is ordinarily conducted in 2 steps, is a main challenge. Although various methods are available to concentrate viruses from large volumes of water (up to 1,000s L) into a few mls (~10 to 20), filtration-based methods are most commonly performed as a primary step for viral analysis. The binding of the virus to the filter materials, the co-concentration of potential inhibitors (e.g., salts in buffers and organic matter) that can negatively impact detection methods (cell culture and qPCR) and the lengthy, multistep process to concentrate the virus prior to quantification are main challenges encountered with concentrating the virus by filtration. Hence, development of rapid capturing and detection technologies to evaluate EVs in water would benefit this field. Thus, the overall goal of this research was to develop and evaluate an antibody-based capture technology that can increase the recovery of EVs from water sources during initial concentration step and enhance their detection in the downstream process. The goal of this research was to develop and evaluate an antibody-based capture technology for the direct isolation of EVs from environmental water samples by antibody-cellulose filter paper or/and antibody coupled-magnetic beads.

To initiate work on developing a cellulose-based filtration technology for the direct removal of EVs from source water, 2 monoclonal V_HHs (RV-2KD1 and RV-3B2) specific to RV group A were selected for expression in *E. coli*. SDS-PAGE and Western blot analyses showed bands at about 16 kDa for RV-2KD1 and 16.14 kDa for RV-3B2 indicating that recombinant antibodies were successfully expressed in *E. coli*. To detect

RV based on one viral antigen (RV-VP_6), in ELISA, and to develop an antibody-coupled magnetic bead technology, full-length IgG 26 targeting RV-VP_6 was constructed for expression in the leaves of tobacco plant and characterized. Two bands were seen around 25 and 50 kDa under reducing condition on the the SDS-PAGE and the Western blot indicating the successful expression of the $H_{C\ 26}$ and the $L_{C\ 26}$, respectively, whereas a band at about 150 kDa was seen under non-reducing condition indicating production of the full-length IgG 26. These antibodies were selected because the RV group A human and bovine strains used in this proof-of-principle project are, to our knowledge, the only viruses that had different recombinant mAb fragments (e.g., H_C, L_C and V_HH) available for immediate application. In addition, RV-VP_6 is an appropriate target for simultaneous tracking of different RV A strains (e.g., bovine and human), where other targets such as VP_4 and VP_7 have high diversity and, consequently, no conserved sequence to capture a similar range of RV strains. As such, RV-VP_6 can be used to broadly detect subgroups of RV (e.g., bovine and human within group A) that may be present in various samples (e.g., medical, soil, food, water and air). Subsequently, these viruses can be further analyzed by qPCR to identify their geno/sero types based on spike proteins (RV-VP_4 and RV-VP_7) located on the surface of the virus capsid.

In characterizing the binding ability of RV-V_HHs and RV-IgG 26, all antibodies were determined to specifically detect the recombinant VP_6-capsid protein and different RV A strains by Western blot and ELISA. The Western blot analysis showed that all RV-mAbs (RV-2KD1, RV-3B2 and RV-IgG 26) were able to specifically detect the RV-VP_6 and the whole virus at a detection limit of 10^3 virus particle. Also, all RV-mAbs were able to specifically detect RV strains at a detection limit of 10^2 virus particle in ELISA. The RV-

IgG 26 had a higher affinity (0.045 nM) (Kallewaard et al., 2008& Aiyegbo et al., 2013) than the V_HHs (13 to 67 nM) (Garaicoechea et al., 2008; Vega et al., 2013 & Maffey et al., 2016). The ELISA showed that (1) RV-2KD1 was significantly effective in its detection of the RV strains than the RV-3B2 at concentrations of 100 and 10 ng and (2) no binding of hAdenoV and mNV occurred, even at much higher concentrations of virus.

One objective of this research was to immobilize the V_HH on cellulose filter paper and characterize its ability to capture EVs in water samples with respect to specificity and sensitivity. Bacterial CBMs type A (e.g., family 2a 3) have been widely used in various applications in biotechnology (e.g., capture and detection of pathogen). The CBMs can be genetically fused to a protein (e.g., enzyme or antibody) to mediate specific binding to inexpensive cellulose matrices (Ong et al., 1991; Hussack et al., 2009 & Rosa et al., 2014). The fusion protein can be then produced in a bacterial host and immobilized on a cellulose matrix (via CBMs) to bind a specific target (via antibody) if it is correctly folded during protein expression. In this study, the RV-V_HHs were linked with CBM2a at 6x-His tag C-terminal via $([PT]_3T)_{3x}S$ peptide linker and the fusion proteins were functionally characterized. SDS-PAGE and Western blot showed bands of about 30.5 and 30.65 kDa indicating that both RV-HA-CBM2a-$([PT]_3T)_{3x}$S-2KD1-His and RV-HA-CBM2a-$([PT]_3T)_{3x}$S-3B2-His were successfully expressed in *E. coli*. Similar to RV-2KD1 and RV-3B2, fusion proteins with CBM2a were able to specifically detect the VP_6-capsid protein and different RV A strains on Western blot and by ELISA at a detection limit of 10^3 and 10^2 virus particle, respectively. The CBM2a (17 kDa) on its own did not bind the RV-VP_6 or any RV strains on Western blot. The results indicated that the V_HHs were correctly folded during expression and their binding ability to the virus was not impacted by linking

to the CBM. This also suggests that the binding of the virus is due to the V_HHs not the CBM2a.

In developing an antibody-CBM fusion protein for the removal of RV from waters, RV-2KD1 was linked to CBM2a at either the N- or the C-terminus using either the $(G_4S)_{3x}$ or the $([PT]_3T)_{3x}S$ linkers. The constructs were optimized for expression in *E. coli* and characterized. Expression of CBM2a alone was used as a negative control. Bands of about 30 and 31 kDa that refers to the fusion proteins (V_HH-CBM2a and CBM2a-V_HH) in contrast to a band of about 17 kDa representing the CBM2a alone were seen on SDS-PAGE and Western blot indicating the fusion proteins were successfully expressed in *E. coli*.

In characterizing the binding ability of RV-V_HH-CBM and RV-CBM-V_HH fusion proteins, all antibodies specifically captured the VP_6-capsid protein and different RV A strains by ELISA. The testing of different linkers ($(G_4S)_{3x}$ and $([PT]_3T)_{3x}S$) to combine the V_HH (2KD1) to the CBM2a indicated that both designs were able to specifically capture the virus on ELISA plate equally well while CBM2a was not able to capture any of the viruses. This was expected as these linkers are commonly utilized (Gilkes et al., 1991; Shen et al., 1991; Hudson and Kortt, 1999 & Ahmad et al., 2012) and have been reported by previous studies to function with other V_HHs (Hussack et al., 2009 & Wood, 2011). When examining the orientation of the V_HH in the fusion protein, capturing of RV-VP_6 and different RV strains with the RV-2KD1 linked at the N-terminus (RV-HA-2KD1-CBM2a) was significantly higher than the RV-2KD1 linked at the C-terminus (RV-HA-CBM2a-2KD1) when RV-V_HHs were used for detection. However, there was no significant difference in capturing RV-VP_6 and different strains of RV with the different 2KD1-fusion

proteins when RV-IgG 26 was used for detection. One possible explanation is that the activity of RV-HA-CBM2a-2KD1 may be inhibited because the location of the amino acids in the antigen-binding site of the 2KD1 is on the C-terminal side. This may be further confirmed by determining the particular location of epitopes on the RV-VP_6 that are recognized by the RV-2KD1 (Section 6.2). The results, however, suggested that the site of the displayed antibody and other protein fusion (e.g., CBM2a) is important for antibody display without the loss of function.

In addition, the ELISA showed that best detection of the viruses (specially hRV-Wa) was obtained with RV-IgG 26 then RV-2KD1 compared to RV-3B2 which had a lower detection absorbance. This may attribute to the higher affinity of the RV-IgG (0.045 nM) as compare to the affinity of the V_HHs (13 to 67 nM). In previous studies, the V_HHs (2KD1 and 3B2) were produced for therapeutic treatment purposes (RV A-induced diarrhea in neonatal mice) (Garaicoechea et al., 2008; Vega et al., 2013 & Maffey et al., 2016). These studies revealed that a reduction in RV A-induced diarrhea (in 2 days) and less virus counts in the feces of mice were observed when the animal was orally treated with RV-2KD1, RV-3B2 or combination of both before infection (Maffey et al., 2016). However, RV-2KD1 was 3 times more effective at lowering RV shedding in feces and neutralized and bound a wider range of RV A strains including human, bovine and murine more effectively than RV-3B2 (Maffey et al., 2016). The group explained their findings by the higher affinity of the RV-2KD1 than the RV-3B2 and suggested the use of surface plasmon resonance to elucidate the affinity of both V_HHs bind to VP_6. Determination of the exact recognition (binding) sites for the V_HHs on the VP_6 as a quaternary epitope

containing a high density of charged residues was also suggested and it is of our interest too.

The RV-IgG 26, on the other hand, was constructed from H_{C26} and L_{C26} which were previously used by Aiyegbo et al. (2013) in the form of F_{ab}, IgG or dimeric IgA molecule on the in vitro production of mRNA from double-layered particle (DLP, found in the intercellular compartment and is transcriptionally active). It was found that all forms of the antibody were able to inhibit the transcription of mRNA. The group also tested the neutralizing activity of the dimeric IgA form in Caco-2 intestinal monolayers. The test was done by treating the cultures with the antibody for up to 6 h prior to infection with RV then quantifying the virus in the supernatant. The group observed an ~2-fold reduction in the concentration of the virus with IgA in comparison to the control treatment (no IgA). As mentioned previously (Section 2.1.1.4), RV-VP_6 has the ability to interact with proteins in the outer layer (RV-spike proteins, VP_4 and VP_7) and protein in the inner layer (RV-shell, VP_2) at different positions of its B and H domains (Mathieu et al., 2001 & Desselberger, 2014). The T=13 icosahedral symmetry of RV-VP_6 and RV-VP_7 in the intermediate and outer layers identified 132 channels into 3 types based on their location within the architecture of the virus. These are 12 type I channels that have narrow openings and serve as egress points of the viral mRNA during viral transcription, and 60 each of type II and 60 type III channels that have larger openings than other channel types (by Aiyegbo et al., 2013). In this regard, the group was able to determine the binding structure (i.e., pattern or mode of binding) of F_{ab} to DLP using cryo-electron microscopy. The scF_{ab} was capable of binding negatively charged residues on the surface of the type I channel, sterically blocking RNA transcription by the DLP. Furthermore, the group was able to

define the 2 recognition sites on RV-VP_6 using mass spectroscopy (residues 231-260 and 265-292 for site A and B, respectively). These sites were found within the beta-sheet located on the exposed side of VP_6 and partially on the inside of the transcriptional pore.

Taken together, the ELISA results for all RV-mAbs in the current study suggests that RV A strains may be cross-targeting with the conserved nature of the VP_6 within the same group. Therefore, these RV-mAbs could be used to broadly capture subgroups of RV including bovine and human from agricultural sources. However, it is unknown why some mAbs have the ability to neutralize or bind to viruses better than others. This may be explained by the differences of the affinity between antibodies (Maffey et al., 2016). Another contributing factor is likely the differences of the binding patterns to VP_6-capsid protein (i.e., variations in the accessibility of the mAb epitope depending on its position in the channel types).

Another objective of this research was to immobilize the fusion protein (RV-HA-V_HH-CBM2a) onto cellulose filter paper and characterize the ability to capture RV A strains from water samples. Although immobilization of antibodies on a surface to capture a specific target is possible, current approaches to report detection are based on a visible colour (e.g., ELISA in this study with detection limit of 10^2 virus particle), change in colour (e.g., gold nanoparticles) and fluorescence observation (e.g., confocal microscopy) (Pelton, 2009). In the current study, immobilization of the fusion protein (RV-HA-2KD1-$(G_4S)_{3x}$-CBM2a) on the cellulose filter paper was tested by ELISA. The filter papers were coated with 5 and 2 µg of fusion protein and incubated with the RV (10^4 viruses) for 30 min before addition of a primary antibody (RV-IgG 26) followed by a secondary anti-human antibody conjugated to HRP. Colour development was seen in about 30 min on

the cellulose filter papers after the addition of HRP substrate in the presence of the virus. There was no significant difference in colour development when these concentrations of fusion proteins were used on the filter with same concentration of the viruses. However, this developing time would be reduced and colour would be improved on the paper if a more sensitive substrate had been used (e.g., AP substrate is usually used to detect targets on paper support). This assay also needs more optimization steps (e.g., use different concentrations of the fusion protein to coat the papers with the same or different dilutions of the viruses) in order to improve colour development on the filter and evaluate the effect on virus binding on the antibody-cellulose filter. In a study by Hussack et al. (2009), a bispecific pentamer fusion protein was constructed by fusing five CBMs to 5 *S. aureus*-specific human V_HH using VTB domain in both orientations (N- and C-terminals). One of the proteins (N-terminal CBM9 and C-terminal V_HH) was reported to recognize *S. aureus* in a flow through detection assay with a detection limit of 10^4 cfu/ml when impregnated in cellulose filters. The colour on the paper was darker with higher concentration (800 nM) of fusion protein immobilized on the filter than lower concentration (25 nM). The results from this test indicated that fusion proteins (Hussacks et al., 2009 & this study) were able to retain their ability to bind their targets when immobilized on a cellulose surface and detection could occur directly on the filter surface. Overall, the results from this test (in this study) suggest the possibility of creating a bioactive cellulose paper (i.e., antibody-cellulose filter paper) for the concentration and the detection of EVs in aquatic environments.

Furthermore, a preliminary spiked test of the hRV in SFM was conducted to evaluate the capturing ability of the cellulose filter under various conditions. The spiked-

samples (1 ml) with hRV (3.39 ± 0.07 x 10^4 virus particles/ml), hAdenoV (1.45 x 10^8 ± 0.5 x10^8 virus particles/ml) and with hRV in competition with hAdenoV at either 1:1 ratio (10^5:10^5 both) or 1:1000-fold hRV:hAdenoV (10^4 hRV:10^7 hAdenoV) were filtered at a flat rate of 1 ml/min through treated cellulose filters (coated with 2 µg of fusion proteins: RV-HA-2KD1-$(G_4S)_{3x}$-CBM2a-cellulose and HA-CBM2a-cellulose filters) without incubation of the sample. The RV-HA-2KD1-$(G_4S)_{3x}$-CBM2a-cellulose filter was able to remove hRV by 81.75 ± 2.05% whereas the HA-CBM2a filter removed hRV by 43.23 ± 10.8% (specific removal was 38.52 ± 8.97%) in comparison to hAdenoV which was removed by 38.46 ± 20.55% and 23.21 ± 8.94% via RV-HA-2KD1-$(G_4S)_{3x}$-CBM2a- and HA-CBM2a-cellulose filters, respectively, when each virus was present alone. The treated-cellulose filter with RV-HA-2KD1-$(G_4S)_{3x}$-CBM2a, however, was able to specifically remove hRV in the presence of hAdenoV at 1:1 ratio by 34.63 ± 30.65%; hAdenoV was removed by 34.59 ± 14.49% and 33.46 ± 10.05% with RV-HA-2KD1-$(G_4S)_{3x}$-CBM2a- and HA-CBM2a-cellulose filters, respectively. When hRV present at 1-1000-fold hRV:hAdenoV, the treated-filter with RV-HA-2KD1-$(G_4S)_{3x}$-CBM2a removed hRV by 38.52 ± 8.97% while hAdenoV by 55.56 ± 10.23%; hAdenoV was removed by 57.90 ± 9.27% with HA-CBM2a-cellulose filters. Similar results were obtained when hRV spiked tap and river water samples were used to evaluate RV-HA-2KD1-$(G_4S)_{3x}$-CBM2a-cellulose filter. The hRV was specifically removed by 64.55 ± 2.22% and 68.06 ± 18.89% whereas HA-CBM2aa removed RV by 37.10 ± 23. 40% and 41.33 ± 7.5 % (specific removal was 27.44 ± 22.93% and 26.72 ± 19.66%) when tap and river waters, respectively, were spiked with hRV alone. However, hRV was removed by 29.18 ± 2.38% and 32.66 ± 8.74% in tap and river water sources, respectively, spiked with 1-100 fold of hRV:hAdenoV. The removal of

hAdenoV with RV-HA-2KD1-$(G_4S)_{3x}$-CBM2a-cellulose filter (39.85 ± 12.96% for tap and 33.14 ± 24.78 for river waters) was similar to the removal of hRV with HA-CBM2a-filter (35.77 ± 13.21 for tap and 33.60 ± 4.93% for river waters) in all cases, which indicating an ordinary and non-specific removal. In addition, the SEM images confirmed the attachment of the virus only on the surface of RV-HA-2KD1-$(G_4S)_{3x}$-CBM2a-cellulose filter in compare to control filters (un treated-cellulose filter and cellulose filter treated-HA-CBM2a) where no virus attachment was seen on the surface of the filter paper. These data indicated no significant difference in the removal between tap and river waters and consistent specific binding of RV on cellulose filter-treated with RV-HA-2KD1-$(G_4S)_{3x}$-CBM2a in compare to the non-specific binding on cellulose filter-treated with HA-CBM2a. Some potential approaches to minimize non-specific binding in such case include (1) increasing the incubation time in the blocking step to ensure complete blocking of free antibody binding sites; (2) increase the concentration of blocking buffer (might try different buffers), (3) washing the filter after passing the sample through with larger volume of a buffer (e.g., 1x PBST) or water (e.g., in this study the filters were washed with 4 ml of water per 1 ml of the sample) and (4) conjugating the RV-mAbs (e.g., full-length IgG 26) with an enzyme to improve the signal on the bioactive cellulose filter paper for visual detection as only the mAbs that have bound virus will give a signal.

Filtration-based methods have been extensively used for primary concentration of EVs from different water sources using various filter types (Table 1.4 to 1.6). The recovery rates of EVs in collected water volumes (10 to 100 L) varied by filter type and protocol (i.e., second concentration step). Block and Schwartzbord (1989) demonstrated a 60% removal of EnteroV from surface water samples using a Millipore cellulose nitrate

electronegatively-charged filter. In another study by Karim et al. (2009), examined the recovery of 10^5 PolioV in 100 L spiked tap and river waters with NanoCream and 1MDS Zetapor Virosorb electropositive-charged filters. Total recoveries of 51 ± 26% and 67 ± 6% from tap and 38 ± 35% and 36 ± 21% from river samples using NanoCream and 1MDS filters, respectively, were reported. Under the same conditions (e.g., concentration of virus in the sample, water types and the filters), the recovery rate was estimated from 10 L spiked samples. Total recoveries of 277 ± 22% and 44 ± 9% from tap and 65 ± 22% and 30 ± 11% from river samples using NanoCream and 1MDS filters, respectively, were reported. The group indicated no significant difference between both filters for removing PolioV from large volume (100 L) while a significant difference was reported from smaller volume (10 L). Also, 74% removal of mNV from 100 L surface water was obtained using a hollow-filter, ultrafilter membranes (Gibson and Schwab, 2011). Pang et al. (2012) estimated the median recovery in 10 L of tap and river waters spiked with 10^5 pfu NoroV, 10^3 pfu AdenoV and 10^2 pfu Echovirus 30% after filtration (flow rate of 133 to 166 ml/min) with positively-charged NanoCream filters followed by flocculation and elution steps. Medians of 29 ± 15% and 18 ± 3% for NoroV, 21 ± 3% and 19.3% for AdenoV and 42 ± 37% and 87 ± 26% for Echovirus were reported form tap and river waters, respectively. The differences in the recovery rates among these viruses may be due to the differences in the electrostatic interaction of the electro-charged filter with the nucleic acid (DNA or RNA) of the viruses. Another contributing factor to the variation in the recovery rate of the viruses would be the nature of the water sample (i.e., matrix effects e.g., the lack of de-chlorination of the tap water) and the volume of the sample. Although these filters have successfully removed EVs from water samples especially with RNA viruses, they are

associated with difficulties such as cost, clogging and requiring preconditioning (in case of the electronegative charged filter) and are not easily field deployable.

The cellulose filter technology developed in the current study using recombinant antibody and CBM-fusion protein technologies showed specific removal of the virus (mentioned previously) and overcomes difficulties associated with the other filters (e.g., preconditioning). The main challenge associated with this antibody-cellulose filter, as in many antibody-based assays (e.g., ELISA), was the non-specific binding on the cellulose filter. Detection of RV in the flow through may be due to the rate of the filtration (1 ml/min); however, this was the lowest flow rate that could be performed manually with the system (e.g., disc size and volume of the sample). There is no standard flow rate that must be used with filtration-based methods, but a maximum of 11,400 ml/min can be use with 1MDS electropositive filters (Karim et al., 2009). Several studies investigated the effect of flow rate on virus recovery using electropositive filters and indicated no difference between flow rates of 3.8 and 26.4 ml/min/cm^2 (Sobsey et al., 1981), 17, 38 and 63 ml/min/cm^2 and 5,500 and 20,000 ml/min (Karim et al., 2009). In this regard, it is important to mention that previous studies reported removal of multiple EVs after the secondary concentration step with no indication to initial virus abundance or virus recovery with the primary concentration step. In contrast, the RV-HA-2KD1-$(G_4S)_{3x}$-CBM2a-cellulose filter system developed in the current study focused on removing specific virus (RV) with primary concentration step only. The results from using the antibody-cellulose system to remove RV from tap and river water sources highlights its potential usage to enhance detection of RV (due to mAb) in water at the field with less time and effort. This system builds up from cellulose paper and fusion protein, consists of sdAb and CBM, that can be

produced in bacteria in 35 h or plant system in a month (including planting and infiltration steps) and used directly with no need for purification. Also, it is easy to use, does not require preconditioning adjustment (e.g., adjustment of sample pH) and is more fixable filter than electropositive filter (which is commonly used at the filed and does not need preconditioning) as cellulose filters are available in different pore sizes and filter sizes at a lower cost. However, a large scale experiment is needed to test the ability of RV-HA-2KD1-$(G_4S)_{3x}$-CBM2a-cellulose filter system to capture EVs in a very turbid sample without clogging. For this goal, different flow rates to filter large volumes (e.g., 10 to 1000s L) of water through the system, with a larger filter size, may be used in pre-optimization steps. In addition, a second concentration step will give an accurate estimation of the total removal using this antibody-filtration system as compared to other filtration systems.

Another approach for an antibody-based capture system for RV developed during this study was conjugation of the mAbs (V_HH and full-length IgG) to magnetic beads. Immuno-magnetic beads have been used to specifically separate and concentrate EVs from water before detection by qPCR (Mattison and Bidawid, 2009; Ogorzaly et al., 2013 & Toldrà et al., 2018). This approach has been mostly performed in a secondary concentration step, following initial concentration with a filtration-based method, to remove inhibitory substances (Jothikumar et al. 1998; Myrmel et al. 2000; El-Galil et al., 2005 & Hwang et al., 2007). One objective of this research was to conjugate RV-IgG 26 and RV-2KD1 on the surface of magnetic beads and characterize their capability to specifically capture EVs in water samples with respect to specificity. The approach was used in the current study as a primary concentration step.

A preliminary incubation test of recombinant RV-VP6 (1 mg/ml) with the bead (10 mg/ml) was conducted to ensure conjugation of the antibodies to the beads and to evaluate the capturing ability of the antibody-coupled bead to the viral capsid protein (RV-VP_6). SDS-PAGE indicated that antibodies were successfully conjugated to the beads and both types of antibody-coupled beads were able to bind RV-VP_6 in comparison to beads lacking antibodies. The beads conjugated with RV-IgG 26 showed greater binding (thicker band) of RV-VP_6 than those with RV-2KD1. This may be attributed to the high affinity of the RV-IgG 26 (0.045 nM) versus the affinity of the V_HH (13 to 67 nM). The binding of 2KD1-coupled bead to RV-VP_6, on the other hand, may contribute to the small size of the V_HH which allows (1) more immobilization of the V_HH on the surface of the beads, (2) more available free binding sites to capture antigen "i.e., higher binding capacity and avidity" and (3) the V_HH to access difficult site as compared to the full-length IgG.

A preliminary test was conducted with RV spiked in SFM using the RV-IgG 26-coupled beads to evaluate the binding of the virus under different conditions. The antibody-coupled bead (with 10 µg of antibody) was able to specifically detect the virus as a decrease in the virus abundance was observed in the flow through. However, estimation of exact removal of the virus was impossible as the test was not conducted with beads lacking antibodies at this stage. Another problem when using antibody-coupled bead at this stage was the release of the virus RNA by heating the beads (suspended in 1x PBS buffer) before nucleic acid extraction and qPCR estimation. The results from qPCR in this primary test indicated a higher virus abundance on the bead than spiked and flow through (was not heated before nucleic acid extraction) samples. It

is possible that heating may cause more release of the nucleic acids of the virus and greater amplification (more readily breaking open the viral capsid to release the nucleic acids). These problems were resolved in the other objective (matrices affect) by including an antibody free-bead sample and extracting the viruses with a commercial nucleic acids extraction kit without heating.

Another objective for this system was to test the matrix effects of river water on the ability of the antibody-coupled beads to directly and specifically detect RV A strains. Spiked-river water (1 ml) with 1:100-fold of hRV:AdenoV was incubated with 2 µg of antibody-coupled beads (RV-IgG 26-coupled beads and RV-2KD1-coupled beads) and antibody free-beads. The RV-IgG 26-coupled beads were able to specifically bind hRV on the bead by 1.85 ± 1.46% whereas RV-2KD1 bound hRV by 0.87 ± 0.4% after 60 min of incubation. There was no removal of hAdenoV with either antibody-coupled bead or antibody free-bead. Although removal of hRV was twice higher by RV-IgG 26-coupled than RV-2KD1-coupled magnetic bead, there was no statistical difference between both antibodies in detecting the whole virus. Finally, the SEM images confirmed the attachment of the virus on the surface of both RV-IgG 26-coupled and RV-2KD1-couple beads whereas no virus attachment was observed on the antibody free-bead. This system is easy and rapid to perform although it is limited to the volume of the sample, concentration of the antibody on the beads and cost of the test. Increasing the volume of the sample would require adding more beads, which is expensive in compare to the antibody-cellulose filter system.

The use of antibody-based technology to measure the very specific binding capacity between an antibody and its associated target (antigen) continue to grow. In

such technology, antibodies are adsorbed on the surface of a sensor (e.g., plate, paper and/or gold) or covalently coupled via amino and carboxyl groups (Vikholm-Lundin, 2005). Subsequently, blocking, several incubation and washing steps and detection are required to obtain results. The most difficult part of engineering surfaces suitable for bio-sensing is the minimization of other molecules that non-specifically bind to the surface. Non-specific binding may involve hydrogen bonds, ionic and hydrophobic interactions (or a combination of all) and may be affected by various factors such as salts, pH, temperature and agents (Houen, 2019). Various agents such as Tween 20, bovine serum albumin, casein and fat-free milk have been employed in an attempt to prevent non-specific binding and restrict conformational changes of the immobilized antibody on the sensor surface (Jeyachandran et al., 2010). However, neither of these agents was found to provide advantage in terms of preventing non-specifically bound molecules. In this study, both antibody-based systems encounter non-specific binding, which is a common issue with such technologies (e.g., ELISA and biosensors). In this study, non-specific binding was not observed by SEM on the surface of cellulose and/or beads. Perhaps the process to prepare the samples for SEM cause the virus to be released from the bead surface, unless more tightly bounds such as by the antibodies. This suggests that additional optimization could reduce the impact of non-specific binding on detection of EVs with the 2 technologies tested in this study.

In summary, the results from this study indicated that (1) all mAbs produced in this study were able to specifically bind to RV-VP6 capsid protein and whole virus, (2) the V_HHs were not functionally affected by linkage with CBM2a, (3) the detection limit of RV by all mAbs was 10^2 and 10^3 virus particle by Western blot and ELISA, respectively, (4)

there was no difference in detecting the virus when different linkers were used to link the V_HH to CBM2a, (5) although both orientations of the V_HH-CBM2a fusion protein were able to detect RV, detecting RV with CBM2a at the V_HH C-terminus was significantly higher than with CBM2a at the V_HH N-terminus, (6) the fusion protein was successfully immobilized on cellulose filter paper and RV was specifically detected by the antibody-cellulose filter (7) both full-length IgG 26 and V_HH were successfully conjugated onto magnetic beads and able to detect RV, and (8) the developed antibody-cellulose filter system was able to retain much higher numbers of RV on the filter material (taken into account the non-specific binding on to the filter) in a primary step in comparison to the virus retention after secondary concentration step using other filter types (used in other studies) and the antibody-coupled beads system (used in this study). However, both antibody-based systems in this study were difficult to evaluate for the removal of the virus in water samples because of the non-specific binding thus more optimization steps are required.

6 CONCLUSIONS AND RECOMMENDATIONS

6.1 Conclusions

Given the limitations for current capture (e.g., filtration) and detection (e.g., cell culture and qPCR) technologies outlined in this Ph.D. thesis (Chapter 1), the demand for developing a novel technology for the capturing and the removal of viruses from water environment is increasing. To address those challenges, in this study, we developed a novel capturing technology that is specific, sensitive, and rapid for the direct isolation of RV from environmental water samples. This technology involves the immobilization of recombinant antibody fragments (sdAb "V_HH" and/or full-length IgG), which targeted a specific viral antigen, on a support surface (cellulose filter and/or magnetic bead).

Throughout this Ph.D. thesis, the capabilities of these recombinant antibody fragments to specifically detect RV were explored. These antibody fragments were further engineered for 2 capturing systems: antibody-cellulose filter using recombinant antibody and CBM-fusion technologies and antibody-magnetic bead using recombinant antibody engineering technology. The capability of these antibody-based systems to specifically capture RV in environmental water sources under different conditions was evaluated using qPCR assay.

Assessment of V_HH-CBM fusion protein activity found the protein capable of specifically binding human and bovine strains of RV group A by Western blot, ELISA, and on cellulose filter paper. This capturing system utilized a cellulose filter paper as a support surface and was shown to effectively attach antibody and specifically remove RV from water samples even under competitive conditions. The system was able to specifically remove RV by 27.44 ± 22.93% and 26.72 ± 19.66% from tap and river waters,

respectively, when the virus was present alone. When RV was present with 1000-fold more hAdenoV, the system was able to remove RV by 29.18 ± 2.38% and 32.66 ± 8.74% from tap and river waters, respectively. The system also was found to produce a visual colour on the cellulose filter paper in the presence of RV when a detecting antibody against the viral antigen (RV-IgG 26) was used. This system provides a good test for developing a rapid and an economical bioactive paper (biosensor) to capture a target in an environment.

On the other hand, assessment of RV-IgG 26-coupled and RV-V_HH-coupled beads were also found capable of specifically binding to RV-VP_6 and whole virus by SDS-PAGE and qPCR analyses. This capturing system utilized an expensive magnetic bead as a support surface and was shown to effectively capture and remove RV from water samples with competitive conditions. The RV-IgG 26-coupled bead system was able to specifically remove RV from river water by 1.85 ± 1.46% while RV-2KD1-couple bead system removed RV by 0.87 ± 0.4%. This system was difficult to evaluate because of the non-specific binding of the virus. This may be due to the low volume of the beads or concentration of the antibody used in this study.

The ability of the developed capturing technology (antibody-cellulose filter "i.e., bioactive-cellulose filter or paper" and antibody-coupled magnetic beads) to selectively remove RV from water samples was compared. The results from these developed capturing technologies indicated that both systems were rapid and selective for capturing the virus in complex water environments. Removal of RV from river water was higher with RV-HA-2KD1-$(G_4S)_{3x}$-CBM2a-cellulose filter system (32.66 ± 8.74%) than RV-IgG 26-coupled bead (1.85 ± 1.46%) and RV-2KD1-coupled bead (0.87 ± 0.4%). However, these

data were impacted by the non-specific binding which was the main challenge in this study, and it is a common problem in antibody-based assays. Also, RV-HA-2KD1-$(G_4S)_{3x}$-CBM2a-cellulose filter system is more economical and convenient than antibody-coupled bead system. Therefore, and based on the success of the V_HH-cellulose filter capturing system, several directions for future research can be considered.

6.2 Recommendations

Potential directions for future research on this work, based on the experiences gained from this thesis and from recent published literature may include:

6.2.1 Broader Use of Cellulose Filter Paper Capture System

This system can be used as a biosensor to detect a target in less time. Similarly to the direct labelling technique described above, RV-mAbs can be directly conjugated with an enzyme to reduce the detection time of the virus and/or to improve the signal on the antibody-cellulose filter paper for visual detection. Conjugation of RV-V_HHs and RV-IgG 26 with a HRP can be performed to reduce the detection time of the virus in ELISA and no-specific binding. Conjugation of RV-V_HHs and RV-IgG 26 with an AP, on the other hand, would be usable with visual detection of the virus on an antibody-cellulose paper (biosensor) by ELISA and on PVDF membrane by Western blot (i.e., improve the signal). A color in wells of ELISA plate and/or on the papers will be produced in the presence of the target virus in less time when a detecting antibody-coupled enzyme against specific antigen (e.g., RV-V_HH-conjugated or RV-IgG 26-conjugated HRP and RV-V_HH-conjugated or RV-IgG 26-conjugated AP) is further used, whereas no signal should be

produced in the absence of the virus. This assay can be used as a rapid screening method to evaluate water on-site. Furthermore, the filter can be used to extract the virus since the virus would remain attached on the filter materials for quantification in qPCR.

Although the antibody-cellulose filter developed in this study showed efficient removal of RV in water samples, the tests were conducted on a small scale to detect a specific target. Conducting the tests on a large scale (10 to 1000s L) to evaluate matrix affect, such as high turbidity and alkaline surface water (most natural waters for Ontario are often between 6.5 to 9.0 for pH) would give a better insight on the binding ability of the V_HH to capture the virus on an antibody-cellulose filter paper. This will also require scaling up the size of the filter (e.g., 79 mm^2 filter suits to filter up to 3 L sample) and optimization step for best fusion protein concentration to coat the filter. As the non-specific binding was the main issue with this antibody-filtration system, different optimization steps of buffers (e.g., blocking and washing) including, but not limited to, pH, components, temperature and conditions (i.e., exposure time) are essential to reduce the level of non-specific binding.

Another thought would be to develop a V_HH-cellulose filter that can capture multiple EVs. The wide antigenic variation among viruses is presently an obstacle to the effective use of antibodies in the detection of these viruses. If common antigen epitopes were to be revealed, then the use of high affinity antibodies against these epitopes could facilitate the capture of different antigenic variants. This can be accomplished by producing a fusion protein that consists of different V_HHs in which each V_HH targets a common protein for common viral gastroenteritis (e.g., RV-V_HH, NoroV-V_HH, AdenoV-V_HH and AstroV-V_HH (Cunliffe et al., 2010)). Each V_HH can be linked to CBM2a to create

5 fusion proteins which then can be linked together to create a pentameric, bispecific molecule. The final product (pentameric bispecific protein) can bind these viruses through 5 copies of V_HHs and cellulose through 5 CBM2a. Similar pentameric protein has been developed by Hussack et al. (2009) toward one pathogen (*S. aureus*). However, the suggested fusion protein with 5 different V_HHs (each V_HH against specific virus group) would be usable in diverse locations of the world to target different strains within a group of multiple EVs. In this regard, a multiplex-qPCR would be considered to simultaneously quantify the strain of the viruses.

6.2.2 Visualizing and Determining the Binding of RV-mAbs on the Virus

The use of antibodies to mark specific molecules or cells has been widely applied in electron microscopy. Visualization of the antibody-binding molecules by the electron microscopy, typically, requires labelling the antibody with an electron-dense particle. Colloidal gold nanoparticles with a diameter ranging between 15 to 30 nm are often used for this purpose because of their high electron density, which increases electron scatter to provide high contrast “black dots” in an EM image. The principle of this technique is very similar to the principle of ELISA. In this indirect labelling technique, gold nanoparticles are attached to secondary antibody which is ordinary attached to primary antibody designed to specifically bind a target (e.g., antigen or cell component). In this work, 3 RV-mAbs (produced in this work, RV-2KD1, RV-3B2 and RV-IgG 26) were used in ELISA as primary antibodies followed by commercial tagged antibodies as secondary antibodies to detect the recombinant RV-VP_6 or the whole virus. However, indirect labelling is not possible with these RV-mAbs as free-tagged secondary antibodies,

targeting RV-mAbs, that can be conjugated with gold nanoparticles is not available. In this regard, RV-mAbs can be directly labelled with gold nanoparticles to visualize the binding of these antibodies to their antigen (RV-VP_6) on the whole virus by electron microscopy.

Also, the results in this study indicated that RV-2KD1 was higher in binding to RV-VP_6 and RV particles than RV-3B2 (at concentrations of 10 and 100 ng). As it was mentioned previously (Chapter 5), this may be due to differences in the affinity of these V_HHs and differences of their binding patterns to VP_6-capside protein. Since the recognition sites of these V_HHs are unknown yet, a crystallography study can be performed to determine the structure of the peptide epitopes. This study will improve our understanding of antibody-antigen recognition and aid in the design of a fusion protein consisting of both V_HHs that can be immobilized on a cellulose filter paper to capture RV from water more efficiently. We are considering a collaborative work for this trial and publication. To initiate co-crystallization studies of RV-2KD1 and RV-3B2 in complex with RV-VP_6 capsid protein, both V_HHs and RV-VP_6 (produced by pETSUMO expression system) will produced as mentioned previously (Chapter 3) and provided at required concentration (usually preferred concentration ranges between 10 to 20 mg/ml, personal contact) to collaborators for x-ray crystallization trials.

In conclusion, currently access to clean drinking water is one of the greatest global challenges. This Ph.D. thesis was proposed to develop paper-based technology for the capture and rapid detection of human EVs in water sources. The results obtained from this thesis provide an antibody-cellulose filter capturing technology that was able to specifically detect RV by by 29.18 ± 2.38% in tap water and by 32.66 ± 8.74% in river

samples. This technology can help improving EVs monitoring and protection of drinking water. We anticipate that such development provides a powerful tool for scientists willing to use paper-based biosensors and would be suitable for analyzing samples from different environments thus ensuring safety of the consumers.

REFERENCES

Adeniji, J. A., Adewale, A. O., Faleye, T. O., & Adewumi, M. O. O. (2017). Isolation and Identification of Enteroviruses from Sewage and Sewage-contaminated Water Samples from Ibadan, Nigeria, 2012-2013. *bioRxiv*, 189902.

Afchangi, A., Jalilvand, S., Mohajel, N., Marashi, S., & Shoja, Z. (2019). Rotavirus VP6 as a Potential Vaccine Candidate. *Reviews in Medical Virology, 29*(2), N/a.

Ahmad, Z., Yeap, S., Ali, A., Ho, W., Alitheen, N., & Hamid, M. (2012). ScFv Antibody: Principles and Clinical Application. *Clinical and Developmental Immunology, 2012*, 15.

Aiyegbo, M., Sapparapu, G., Spiller, B., Eli, I., Williams, D., Kim, R., . . . Liu, Ding Xiang. (2013). Human Rotavirus VP6-Specific Antibodies Mediate Intracellular Neutralization by Binding to a Quaternary Structure in the Transcriptional Pore. *PLoS ONE, 8*(5), E61101.

Aladin, F., Einerhand, A., Bouma, J., Bezemer, S., Hermans, P., Wolvers, D., . . . Sestak, Karol. (2012). In Vitro Neutralisation of Rotavirus Infection by Two Broadly Specific Recombinant Monovalent Llama-Derived Antibody Fragments. *PLoS ONE, 7*(3), E32949.

Albinana-Gimenez, Clemente-Casares, Calgua, Huguet, Courtois, & Girones. (2009). Comparison of Methods for Concentrating Human Adenoviruses, Polyomavirus JC and Noroviruses in Source Waters and Drinking Water Using Quantitative PCR. *Journal of Virological Methods, 158*(1), 104-109.

Arnold, M., Patton, J. T., & McDonald, S. M. (2009). Culturing, Storage, and Quantification of Rotaviruses. *Current Protocols in Microbiology*, *15*(1), 15C-3.

Arola, S., & Linder, M. B. (2016). Binding of Cellulose Binding Modules Reveal Differences Between Cellulose Substrates. *Scientific Reports*, *6*, 35358.

Arraj, A., Bohatier, J., Aumeran, C., Bailly, J., Laveran, H., & Traoré, O. (2008). An Epidemiological Study of Enteric Viruses in Sewage with Molecular Characterization by RT-PCR and Sequence Analysis. *Journal of Water and Health, 6*(3), 351-358.

Babiuk, L A, Mohammed, K, Spence, L, Fauvel, M, & Petro, R. (1977). Rotavirus Isolation and Cultivation in the Presence of Trypsin. *Journal of Clinical Microbiology, 6*(6), 610-617.

Ball, L. (2004). The Universal Taxonomy of Viruses in Theory and Practice. In *Virus Taxonomy* (pp. 3-8).

Bányai, Kemenesi, Budinski, Földes, Zana, Marton, . . . Jakab. (2017). Candidate New Rotavirus Species in Schreiber's Bats, Serbia. *Infection, Genetics and Evolution, 48*, 19-26.

Bányai, Krisztián, László, Brigitta, Duque, Jazmin, Steele, A. Duncan, Nelson, E. Anthony S., Gentsch, Jon R., & Parashar, Umesh D. (2012). Systematic Review of Regional and Temporal Trends in Global Rotavirus Strain Diversity in the Pre Rotavirus Vaccine Era: Insights for Understanding the Impact of Rotavirus Vaccination Programs. *Vaccine, 30S1*, A122-A130.

Belfort, G., Paluszek, A., & Sturman, L. (1982). Enterovirus Concentration Using Automated Hollow Fiber Ultrafiltration. *Water Science and Technology, 14*(4-5), 257-272.

Bennett, H. B., O'Dell, H. D., Norton, G., Shin, G., Hsu, F. C., & Meschke, J. S. (2010). Evaluation of a Novel Electropositive Filter for the Concentration of Viruses from Diverse Water Matrices. *Water Science and Technology, 61*(2), 317-322.

Berry, M. J., Davis, P. J., & Gidley, M. J. (2001). *U.S. Patent No. 6,225,462*. Washington, DC: U.S. Patent and Trademark Office.

Bertolotti-Ciarlet, A., Ciarlet, M., Crawford, S., Conner, M., & Estes, M. (2003). Immunogenicity and Protective Efficacy of Rotavirus 2/6-virus-like Particles Produced by a Dual Baculovirus Expression Vector and Administered Intramuscularly, Intranasally, or Orally to Mice. *Vaccine, 21*(25-26), 3885-3900.

Bishop, R., Davidson, G. P., Holmes, I. H., & Ruck, B. J. (1973). Virus Particles in Epithelial Cells of Duodenal Mucosa from Children with Acute Non-Bacterial Gastroenteritis. *The Lancet, 302*(7841), 1281-1283.

Blacklow, N. R., & Greenberg, H. B. (1991). Viral gastroenteritis. *New England Journal of Medicine*, *325*(4), 252-264.

Block, J., & Schwartzbrod, L. (1989). Viruses in Water Systems: Detection and Identification. *VCH Publishers, New York, NY (USA).*

Bofill-Mas, S., Albinana-Gimenez, N., Clemente-Casares, P., Hundesa, A., Rodriguez-Manzano, J., Allard, A., ... & Girones, R. (2006). Quantification and Stability of Human Adenoviruses and Polyomavirus JCPyV in Wastewater Matrices. *Applied and Environmental Microbiology*, *72*(12), 7894-7896.

Boraston, A. B., Bolam, D. N., Gilbert, H. J., & Davies, G. J. (2004). Carbohydrate-binding Modules: Fine-tuning Polysaccharide Recognition. *Biochemical Journal*, *382*(3), 769-781.

Borchardt, M. A., Spencer, S. K., Kieke Jr, B. A., Lambertini, E., & Loge, F. J. (2012). Viruses in Nondisinfected Drinking Water from Municipal Wells and Community Incidence of Acute Gastrointestinal Illness. *Environmental Health Perspectives*, *120*(9), 1272-1279.

Borchardt, M. A., Haas, N. L., & Hunt, R. J. (2004). Vulnerability of Drinking-water Wells in La Crosse, Wisconsin, to Enteric Virus Contamination from Surface Water Contributions. *Applied and Environmental Microbiology*, *70*(10), 5937-5946.

Boyd, C. E. (2015). Water Quality: An Introduction. *Springer*.

Bradbury, K. R., Borchardt, M. A., Gotkowitz, M., Spencer, S. K., Zhu, J., & Hunt, R. J. (2013). Source and Transport of Human Enteric Viruses in Deep Municipal Water Supply Wells. *Environmental Science and Technology*, *47*(9), 4096-4103.

Brown, M. A. R. T. H. A. (1990). Laboratory Identification of Adenoviruses Associated with Gastroenteritis in Canada from 1983 to 1986. *Journal of Clinical Microbiology*, *28*(7), 1525-1529.

Bugli, F., Caprettini, V., Cacaci, M., Martini, C., Sterbini, F. P., Torelli, R., ... & Posteraro, B. (2014). Synthesis and Characterization of Different Immunogenic Viral Nanoconstructs from Rotavirus VP6 Inner Capsid Protein. *International Journal of Nanomedicine*, *9*, 2727.

Burke, B., & Desselberfer, U. (1996). Rotavirus Pathogenicity. *Virology*, *218*(2), 299-305.

Bustin, S. A., Benes, V., Garson, J. A., Hellemans, J., Huggett, J., Kubista, M., ... & Vandesompele, J. (2009). The MIQE Guidelines: Minimum Information for Publication of Quantitative Real-time PCR Experiments. *Clinical Chemistry*, *55*(4), 611-622.

Cannon, J. L., & Vinjé, J. (2008). Histo-blood Group Antigen Assay for Detecting Noroviruses in Water. *Applied and Environmental Microbiology*, *74*(21), 6818-6819.

Cashdollar, J. L., & Wymer, L. (2013). Methods for Primary Concentration of Viruses from Water Samples: A Review and Meta-analysis of Recent Studies. *Journal of Applied Microbiology*, *115*(1), 1-11.

Cashdollar, J. L., & Dahling, D. R. (2006). Evaluation of a Method to Re-use Electropositive Cartridge Filters for Concentrating Viruses from Tap and River Water. *Journal of Virological Methods*, *132*(1-2), 13-17.

Cecuk, D., Kruzic, V., Turkovic, B., & Grce, M. (1993). Human Viruses in the Coastal Environment of a Croatian Harbor. *Revue D'epidemiologie et de Sante Publique*, *41*(6), 487-493.

CDCP. Centers for Disease Control and Prevention. (2002). Norovirus Activity-United States, 2002. *MMWR. Morbidity and Mortality Weekly Report*, *52*(3), 41.

Chames, P., Van Regenmortel, M., Weiss, E., & Baty, D. (2009). Therapeutic Antibodies: Successes, Limitations and Hopes for the Future. *British Journal of Pharmacology*, *157*(2), 220-233.

Chang, S. L., Stevenson, R. E., Bryant, A. R., Woodward, R. L., & Kabler, P. W. (1958). Removal of Coxsackie and Bacterial Viruses in Water by Flocculation: II. Removal of Coxsackie and Bacterial Viruses and the Native Bacteria in Raw Ohio River Water by Flocculation with Aluminum Sulfate and Ferric Chloride. *American Journal of Public Health and the Nations Health*, *48*(2), 159-169.

Chen, D., Luongo, C. L., Nibert, M. L., & Patton, J. T. (1999). Rotavirus Open Cores Catalyze 5′-capping and Methylation of Exogenous RNA: Evidence that VP3 is a Methyltransferase. *Virology*, *265*(1), 120-130.

Chen, C. C., & Chang, H. M. (1998). Effect of Thermal Protectants on the Stability of Bovine Milk Immunoglobulin G. *Journal of Agricultural and Food Chemistry*, *46*(9), 3570-3576.

Chowdhary, R., & Dhole, T. N. (2008). Interrupting Wild Poliovirus Transmission Using Oral Poliovirus Vaccine: Environmental Surveillance in High-risks Area of India. *Journal of Medical Virology*, *80*(8), 1477-1488.

Clarke, N. A., & Lu Chang, S. (1959). Enteric Viruses in Water. *Journal (American Water Works Association)*, *51*(10), 1299-1317.

Cliver, D. O., & Yeatman, J. (1965). Ultracentrifugation in the Concentration and Detection of Enteroviruses. *Applied Microbiology*, *13*(3), 387-392.

Coin, L., Gomella, C., Hannoun, C., & Trimoreau, J. C. (1967). Inactivation by Ozone of Poliomyelitis Virus Present in Water. (Further Contribution). *La Presse Medicale*, *75*(38), 1883.

Collins, P. J., Martella, V., Buonavoglia, C., & O'Shea, H. (2010). Identification of a G2-Like Porcine Rotavirus Bearing a Novel VP4 Type, P [32]. *Veterinary Research*, *41*(5), 73.

Colomina, J., Gil, M. T., Codoñer, P., & Buesa, J. (1998). Viral Proteins VP2, VP6, and NSP2 are Strongly Precipitated by Serum and Fecal Antibodies from Children with Rotavirus Symptomatic Infection. *Journal of Medical Virology*, *56*(1), 58-65.

Cox, C., Cao, S., & Lu, Y. (2009). Enhanced Detection and Study of Murine Norovirus-1 Using a More Efficient Microglial Cell Line. *Virology Journal*, *6*(1), 196.

Craig, S. J., Shu, A., Xu, Y., Foong, F. C., & Nordon, R. (2007). Chimeric Protein for Selective Cell Attachment onto Cellulosic Substrates. *Protein Engineering, Design & Selection*, *20*(5), 235-241.

Cunliffe, N. A., Booth, J. A., Elliot, C., Lowe, S. J., Sopwith, W., Kitchin, N., ... & Regan, M. (2010). Healthcare-associated Viral Gastroenteritis Among Children in a Large Pediatric Hospital, United Kingdom. *Emerging Infectious Diseases*, *16*(1), 55.

Cunliffe, N., Witte, D., & Ngwira, B. (2009). History of Rotavirus Research in Children in Malawi: The Pursuit of a Killer. *Malawi Medical Journal*, *21*(3).

Dagel, D. J., Liu, Y. S., Zhong, L., Luo, Y., Himmel, M. E., Xu, Q., ... & Smith, S. (2010). In Situ Imaging of Single Carbohydrate-binding Modules on Cellulose Microfibrils. *The Journal of Physical Chemistry B*, *115*(4), 635-641.

Dahling, D. R. (2002). An Improved Filter Elution and Cell Culture Assay Procedure for Evaluating Public Groundwater Systems for Culturable Enteroviruses. *Water Environment Research*, *74*(6), 564-568.

De Buck, S., Nolf, J., De Meyer, T., Virdi, V., De Wilde, K., Van Lerberge, E., ... & Depicker, A. (2013). Fusion of an Fc Chain to a VHH Boosts the Accumulation Levels in A Aabidopsis Seeds. *Plant Biotechnology Journal*, *11*(8), 1006-1016.

Deffar, K., Shi, H., Li, L., Wang, X., & Zhu, X. (2009). Nanobodies-the New Concept in Antibody Engineering. *African Journal of Biotechnology*, *8*(12).

De Genst, E., Saerens, D., Muyldermans, S., & Conrath, K. (2006). Antibody Repertoire Development in Camelids. *Developmental and Comparative Immunology*, *30*(1-2), 187-198.

De Meyer, T., Muyldermans, S., & Depicker, A. (2014). Nanobody-based Products as Research and Diagnostic Tools. *Trends in Biotechnology*, *32*(5), 263-270.

Desselberger, U. (2014). Rotaviruses. *Virus Research*, *190*, 75-96.

de Roda Husman, A. M., & Bartram, J. (2007). Global Supply of Virus-safe Drinking Water. *Perspectives in Medical Virology*, *17*, 127-162.

Dewailly, E. R. I. C., Poirier, C., & Meyer, F. M. (1986). Health Hazards Associated with Windsurfing on Polluted Water. *American Journal of Public Health*, *76*(6), 690-691.

Ding, S. Y., Xu, Q., Ali, M. K., Baker, J. O., Bayer, E. A., Barak, Y., ... & Himmel, M. E. (2006). Versatile Derivatives of Carbohydrate-binding Modules for Imaging of Complex Carbohydrates Approaching the Molecular Level of Resolution. *Biotechniques*, *41*(4), 435-443.

Divizia, M., De Filippis, P., Di Napoli, A., Venuti, A., Perez-Bercoff, R., & Pana, A. (1989a). Isolation of Wild-type Hepatitis A Virus from the Environment. *Water Research*, *23*(9), 1155-1160.

Divizia, M., Santi, A. L., & Pana, A. (1989b). Ultrafiltration: An Efficient Second Step for Hepatitis A Virus and Poliovirus Concentration. *Journal of Virological Methods*, *23*(1), 55-62.

Droz, E., Taborelli, M., Descouts, P., Wells, T. N., & Werlen, R. C. (1996). Covalent Immobilization of Immunoglobulins G and Fab′ Fragments on Gold Substrates for Scanning Force Microscopy Imaging in Liquids. *Journal of Vacuum Science and*

Technology B: Microelectronics and Nanometer Structures Processing, Measurement, and Phenomena, *14*(2), 1422-1426.

Domínguez, E., Perez, M. D., Puyol, P., SÁnchez, L., & Calvo, M. (2001). Effect of pH on Antigen-binding Activity of IgG from Bovine Colostrum Upon Heating. *Journal of Dairy Research*, *68*(3), 511-518.

Dormitzer, P. R., Nason, E. B., Prasad, B. V., & Harrison, S. C. (2004). Structural Rearrangements in the Membrane Penetration Protein of a Non-enveloped Virus. *Nature*, *430*(7003), 1053.

Dowd, S. E., Pillai, S. D., Wang, S., & Corapcioglu, M. Y. (1998). Delineating the Specific Influence of Virus Isoelectric Point and Size on Virus Adsorption and Transport through Sandy Soils. *Applied and Environmental Microbiology*, *64*(2), 405-410.

Eftim, S. E., Hong, T., Soller, J., Boehm, A., Warren, I., Ichida, A., & Nappier, S. P. (2017). Occurrence of Norovirus in Raw Sewage-A Systematic Literature Review and Meta-analysis. *Water Research*, *111*, 366-374.

El-Galil, K. H. A., El Sokkary, M. A., Kheira, S. M., Salazar, A. M., Yates, M. V., Chen, W., & Mulchandani, A. (2005). Real-time Nucleic Acid Sequence-based Amplification Assay for Detection of Hepatitis A Virus. *Applied and Environmental Microbiology*, *71*(11), 7113-7116.

Elford, W.J. (1931). A New Series of Graded Collodion Membranes Suitable for General Bacteriological Use, Especially in Filterable Virus Studies. *The Journal of Pathology and Bacteriology*, *34*(4), 505-521.

Esteban, A., Frutos-Vivar, F., Muriel, A., Ferguson, N. D., Peñuelas, O., Abraira, V., ... & Violi, D. A. (2013a). Evolution of Mortality Over Time in Patients Receiving

Mechanical Ventilation. *American Journal of Respiratory and Critical Care Medicine*, *188*(2), 220-230.

Esteban, L. E., Temprana, C. F., Argüelles, M. H., Glikmann, G., & Castello, A. A. (2013b). Antigenicity and Immunogenicity of Rotavirus VP6 Protein Expressed on the Surface of *Lactococcus lactis*. *BioMed Research International*, *2013*.

Estes, M. K., Kang, G., Zeng, C. Q. Y., Crawford, S. E., & Ciarlet, M. (2001, January). Pathogenesis of Rotavirus Gastroenteritis. In *Novartis Foundation Symposium* (pp. 82-100). Chichester; New York; John Wiley; 1999.

Estes, M. K., & Cohen, J. E. A. N. (1989). Rotavirus Gene Structure and Function. *Microbiology and Molecular Biology Reviews*, *53*(4), 410-449.

Etsano, A. (2016). Environmental Isolation of Circulating Vaccine-derived Poliovirus after Interruption of Wild Poliovirus Transmission-Nigeria, 2016. *MMWR. Morbidity and Mortality Weekly report*, *65*.

Ewert, S., Cambillau, C., Conrath, K., & Plückthun, A. (2002). Biophysical Properties of Camelid VHH Domains Compared to those of Human VH3 Domains. *Biochemistry*, *41*(11), 3628-3636.

Farrah, S. R., & Bitton, G. (1979). Low Molecular Weight Substitutes for Beef Extract as Eluents for Poliovirus Adsorbed to Membrane Filters. *Canadian Journal of Microbiology*, *25*(9), 1045-1051.

Farrah, S. R., Goyal, S. M., Gerba, C. P., Wallis, C., & Melnick, J. L. (1978). Concentration of Poliovirus from Tap Water onto Membrane Filters with Aluminum Chloride at Ambient pH Levels. *Applied and Environmental Microbiology*, *35*(3), 624-626.

Feng, B., Huang, S., Ge, F., Luo, Y., Jia, D., & Dai, Y. (2011). 3D Antibody Immobilization on a Planar Matrix Surface. *Biosensors and Bioelectronics*, *28*(1), 91-96.

Finkbeiner, S. R., Kirkwood, C. D., & Wang, D. (2008). Complete Genome Sequence of a Highly Divergent Astrovirus Isolated from a Child with Acute Diarrhea. *Virology Journal*, *5*(1), 117.

Fleischer, J., Schlafmann, K., Otchwemah, R., & Botzenhart, K. (2000). Elimination of Enteroviruses, other Enteric Viruses, F-specific Coliphages, Somatic Coliphages and *E. coli* in Four Sewage Treatment Plants of Southern Germany. *Journal of Water Supply: Research and Technology-AQUA*, *49*(3), 127-138.

Fong, T. T., Griffin, D. W., & Lipp, E. K. (2005). Molecular Assays for Targeting Human and Bovine Enteric Viruses in Coastal Waters and Their Application for Library-independent Source Tracking. *Applied and Environmental Microbiology*, *71*(4), 2070-2078.

Fong, T. T., & Lipp, E. K. (2005). Enteric Viruses of Humans and Animals in Aquatic Environments: Health Risks, Detection, and Potential Water Quality Assessment Tools. *Microbiology and Molecular Biology Reviews*, *69*(2), 357-371.

Fout, G. S., Martinson, B. C., Moyer, M. W., & Dahling, D. R. (2003). A Multiplex Reverse Transcription-PCR Method for Detection of Human Enteric Viruses in Groundwater. *Applied and Environmental Microbiology*, *69*(6), 3158-3164.

Francy, D. S., Stelzer, E. A., Brady, A. M., Huitger, C., Bushon, R. N., Ip, H. S., ... & Lindquist, H. A. (2013). Comparison of Filters for Concentrating Microbial Indicators and Pathogens in Lake Water Samples. *Applied and Environmental Microbiology*, *79*(4), 1342-1352.

Fu, X., Gao, X., He, S., Huang, D., Zhang, P., Wang, X., ... & Yang, Z. (2013). Design and Selection of a Camelid Single-chain Antibody Yeast Two-hybrid Library Produced de Novo for the Cap Protein of Porcine Circovirus Type 2 (PCV2). *PLoS One*, *8*(3), e56222.

Fuglsang, C. C., & Tsuchiya, R. (2001). *U.S. Patent No. 6,264,925*. Washington, DC: U.S. Patent and Trademark Office.

Fujioka, R. S., & Yoneyama, B. S. (2002). Sunlight Inactivation of Human Enteric Viruses and Fecal Bacteria. *Water Science and Technology*, *46*(11-12), 291-295.

Fumian, T. M., Guimarães, F. R., Vaz, B. J. P., da Silva, M. T. T., Muylaert, F. F., Bofill-Mas, S., ... & Miagostovich, M. P. (2010). Molecular Detection, Quantification and Characterization of Human Polyomavirus JC from Waste Water in Rio De Janeiro, Brazil. *Journal of Water and Health*, *8*(3), 438-445.

Gajardo, R., Díez, J., Jofre, J., & Bosch, A. (1991). Adsorption-elution with Negatively and Positively-charged Glass Powder for the Concentration of Hepatitis A Virus from Water. *Journal of Virological Methods*, *31*(2-3), 345-351.

Ganesh, A., & Lin, J. (2013). Waterborne Human Pathogenic Viruses of Public Health Concern. *International Journal of Environmental Health Research*, *23*(6), 544-564.

Garaicoechea, L., Olichon, A., Marcoppido, G., Wigdorovitz, A., Mozgovoj, M., Saif, L., ... & Parreno, V. (2008). Llama-derived Single-chain Antibody Fragments Directed to Rotavirus VP6 Protein Possess Broad Neutralizing Activity in Vitro and Confer Protection Against Diarrhea in Mice. *Journal of Virology*, *82*(19), 9753-9764.

Gaertner, H. (1967). *Retention and Recovery of Polioviruses on a Soluble Ultrafilter*.

Gene, R. (2012). VHH Antibody Fragments Against Internalin B, a Virulence Factor of *Listeria monocytogenes*: Reagents for Biosensor Development *(Doctoral Dissertation)*.

Gerba, C. P., Betancourt, W. Q., Kitajima, M., & Rock, C. M. (2018). Reducing Uncertainty in Estimating Virus Reduction by Advanced Water Treatment Processes. *Water Research*, *133*, 282-288.

Gerba, C. P., & Betancourt, W. Q. (2017). Viral Aggregation: Impact on Virus Behavior in the Environment. *Environmental Science and Technology*, *51*(13), 7318-7325.

Gerba, C. P., & Bitton, G. (1984a). Microbial Pollutants: Their Survival and Transport Pattern to Groundwater. *Groundwater Pollution Microbiology, John Wiley and Sons, New York, New York 1984. p 65-88, 3 fig, 4 tab, 123 ref.*

Gerba, C. P. (1984b). Applied and Theoretical Aspects of Virus Adsorption to Surfaces. In *Advances in Applied Microbiology* (Vol. 30, pp. 133-168). Academic Press.

Gerba, C. P., Farrah, S. R., Goyal, S. M., Wallis, C. R. A. I. G., & Melnick, J. L. (1978). Concentration of Enteroviruses from Large Volumes of Tap Water, Treated Sewage, and Seawater. *Applied and Environmental Microbiology*, *35*(3), 540-548.

Gibbons, C. D., Rodriguez, R. A., Tallon, L., & Sobsey, M. D. (2010). Evaluation of Positively Charged Alumina Nanofibre Cartridge Filters for the Primary Concentration of Noroviruses, Adenoviruses and Male-specific Coliphages from Seawater. *Journal of Applied Microbiology*, *109*(2), 635-641.

Gibson, K. E., Schwab, K. J., Spencer, S. K., & Borchardt, M. A. (2012). Measuring and Mitigating Inhibition During Quantitative Real Time PCR Analysis of Viral Nucleic

Acid Extracts from Large-volume Environmental Water Samples. *Water Research*, *46*(13), 4281-4291.

Gibson, K. E., & Schwab, K. J. (2011). Tangential-flow Ultrafiltration with Integrated Inhibition Detection for Recovery of Surrogates and Human Pathogens from Large-volume Source Water and Finished Drinking Water. *Applied and Environmental Microbiology*, *77*(1), 385-391.

Gilkes, N. R., Henrissat, B., Kilburn, D. G., Miller, R. C., & Warren, R. (1991). Domains in Microbial Beta-1, 4-glycanases: Sequence Conservation, Function, and Enzyme Families. *Microbiological Reviews*, *55*(2), 303-315.

Gilkes, N. R., Warren, R., Miller, R. C., & Kilburn, D. G. (1988). Precise Excision of the Cellulose Binding Domains from Two *Cellulomonas fimi* Cellulases by a Homologous Protease and the Effect on Catalysis. *Journal of Biological Chemistry*, *263*(21), 10401-10407.

Giritch, A., Marillonnet, S., Engler, C., van Eldik, G., Botterman, J., Klimyuk, V., & Gleba, Y. (2006). Rapid High-yield Expression of Full-size IgG Antibodies in Plants Coinfected with Noncompeting Viral Vectors. *Proceedings of the National Academy of Sciences*, *103*(40), 14701-14706.

Girones, R., Ferrús, M. A., Alonso, J. L., Rodriguez-Manzano, J., Calgua, B., de Abreu Corrêa, A., ... & Bofill-Mas, S. (2010). Molecular Detection of Pathogens in Water-the Pros and Cons of Molecular Techniques. *Water Research*, *44*(15), 4325-4339.

Gjessing, E. T., Egeberg, P. K., & Håkedal, J. (1999). Natural Organic Matter in Drinking Water-The “NOM-typing Project”, Background and Basic Characteristics of

Original Water Samples and NOM Isolates. *Environment International*, *25*(2-3), 145-159.

Grabow, W. O. K. (1968). The Virology of Waste Water Treatment. *Water Research*, *2*(10), 675-701.

Graumann, K., & Premstaller, A. (2006). Manufacturing of Recombinant Therapeutic Proteins in Microbial Systems. *Biotechnology Journal: Healthcare Nutrition Technology*, *1*(2), 164-186.

Greenberg, H. B., & Estes, M. K. (2009). Rotaviruses: from Pathogenesis to Vaccination. *Gastroenterology*, *136*(6), 1939-1951.

Griffin, D. W., Donaldson, K. A., Paul, J. H., & Rose, J. B. (2003). Pathogenic Human Viruses in Coastal Waters. *Clinical Microbiology Reviews*, *16*(1), 129-143.

Griffin, D. W., Lipp, E. K., McLaughlin, M. R., & Rose, J. B. (2001). Marine Recreation and Public Health Microbiology: Quest for the Ideal Indicator: This Article Addresses the Historic, Recent, and Future Directions in Microbiological Water Quality Indicator Research. *AIBS Bulletin*, *51*(10), 817-825.

Grinstein, S., Melnick, J. L., & Wallis, C. (1970). Virus Isolations from Sewage and from a Stream Receiving Effluents of Sewage Treatment Plants. *Bulletin of the World Health Organization*, *42*(2), 291.

Goldman, E. R., Anderson, G. P., Liu, J. L., Delehanty, J. B., Sherwood, L. J., Osborn, L. E., ... & Hayhurst, A. (2006). Facile Generation of Heat-stable Antiviral and Antitoxin Single Domain Antibodies from a Semisynthetic Llama Library. *Analytical Chemistry*, *78*(24), 8245-8255.

Gómez-Sebastián, S., Nuñez, M. C., Garaicoechea, L., Alvarado, C., Mozgovoj, M., Lasa, R., ... & Escribano, J. M. (2012). Rotavirus A-specific Single-domain Antibodies Produced in Baculovirus-infected Insect Larvae are Protective in Vivo. *BMC Biotechnology*, *12*(1), 59.

Gómara, M. I., Wong, C., Blome, S., Desselberger, U., & Gray, J. (2002). Molecular Characterization of VP6 Genes of Human Rotavirus Isolates: Correlation of Genogroups with Subgroups and Evidence of Independent Segregation. *Journal of Virology*, *76*(13), 6596-6601.

Govaert, J., Pellis, M., Deschacht, N., Vincke, C., Conrath, K., Muyldermans, S., & Saerens, D. (2012). Dual Beneficial Effect of Interloop Disulfide Bond for Single Domain Antibody Fragments. *Journal of Biological Chemistry*, *287*(3), 1970-1979.

Greenberg, H B, Valdesuso, J, Van Wyke, K, Midthun, K, Walsh, M, McAuliffe, V, . . . Hoshino, Y. (1983). Production and Preliminary Characterization of Monoclonal Antibodies Directed at Two Surface Proteins of Rhesus Rotavirus. *The Journal of Virology, 47*(2), 267-275.

Gunneriusson, E., P. Samuelson, M. Uhlen, P. A. Nygren, & S. Stahl. (1996). Surface Display of a Functional Single-chain Fv Antibody on *Staphylococci*. *Journal of Bacteriology*, 178:1341-1346.

Guttman-Bass, N, & Nasser, A. (1984). Simultaneous Concentration of Four Enteroviruses from Tap, Waste, and Natural Waters. *Applied and Environmental Microbiology, 47*(6), 1311-1315.

Haas, C. N., Rose, J. B., Gerba, C., & Regli, S. (1993). Risk Assessment of Virus in Drinking Water. *Risk Analysis*, *13*(5), 545-552.

Hamza, I. A., Jurzik, L., Überla, K., & Wilhelm, M. (2011). Methods to Detect Infectious Human Enteric Viruses in Environmental Water Samples. *International Journal of Hygiene and Environmental Health*, *214*(6), 424-436.

Hamza, I. A., Jurzik, L., Stang, A., Sure, K., Überla, K., & Wilhelm, M. (2009). Detection of Human Viruses in Rivers of a Densly-populated Area in Germany Using a Virus Adsorption Elution Method Optimized for PCR Analyses. *Water Research*, *43*(10), 2657-2668.

Han, T. H., Kim, C. H., Chung, J. Y., Park, S. H., & Hwang, E. S. (2010). Genetic Characterization of Rotavirus in Children in South Korea from 2007 to 2009. *Archives of Virology*, *155*(10), 1663-1673.

Haramoto, E., Kitajima, M., Hata, A., Torrey, J. R., Masago, Y., Sano, D., & Katayama, H. (2018). A Review on Recent Progress in the Detection Methods and Prevalence of Human Enteric Viruses in Water. *Water Research*.

Haramoto, E., Kitajima, M., Katayama, H., & Ohgaki, S. (2010). Real-time PCR Detection of Adenoviruses, Polyomaviruses, and Torque Teno Viruses in River Water in Japan. *Water Research*, *44*(6), 1747-1752.

Haramoto, E., Katayama, H., Oguma, K., Yamashita, H., Tajima, A., Nakajima, H., & Ohgaki, S. (2006). Seasonal Profiles of Human Noroviruses and Indicator Bacteria in a Wastewater Treatment Plant in Tokyo, Japan. *Water Science and Technology*, *54*(11-12), 301-308.

Haramoto, E., Katayama, H., & Ohgaki, S. (2004). Detection of Noroviruses in Tap Water in Japan by Means of a New Method for Concentrating Enteric Viruses in Large Volumes of Freshwater. *Applied and Environmental Microbiology*, *70*(4), 2154-2160.

Harmsen, M. M., & De Haard, H. J. (2007). Properties, Production, and Applications of Camelid Single-domain Antibody Fragments. *Applied Microbiology and Biotechnology*, *77*(1), 13-22.

Harwood, V. J., Levine, A. D., Scott, T. M., Chivukula, V., Lukasik, J., Farrah, S. R., & Rose, J. B. (2005). Validity of the Indicator Organism Paradigm for Pathogen Reduction in Reclaimed Water and Public Health Protection. *Applied and Environmental Microbiology*, *71*(6), 3163-3170.

Hassanzadeh-Ghassabeh, G., Devoogdt, N., De Pauw, P., Vincke, C., & Muyldermans, S. (2013). Nanobodies and their Potential Applications. *Nanomedicine*, *8*(6), 1013-1026.

Health Canada. (2017). Enteric Viruses in Drinking Water. Document for Public Consultation. Prepared by the Federal Provincial Territorial Committee on Drinking Water.

Herrmann, J. E., Perron-Henry, D. M., Stobbs-Walro, D., & Blacklow, N. R. (1987). Preparation and Characterization of Monoclonal Antibodies to Enteric Adenovirus Types 40 and 41. *Archives of Virology*, *94*(3-4), 259-265.

Hill, V. R., Polaczyk, A. L., Kahler, A. M., Cromeans, T. L., Hahn, D., & Amburgey, J. E. (2009). Comparison of Hollow-fiber Ultrafiltration to the USEPA VIRADEL

Technique and USEPA Method 1623. *Journal of Environmental Quality*, *38*(2), 822-825.

Hill Jr, W. F., Akin, E. W., & Benton, W. H. (1971). Detection of Viruses in Water: A Review of Methods and Application. *Water Research*, *5*(11), 967-995.

Houen, G. (2019). Nonspecific Binding in Immunoassays for Autoantibodies. In *Autoantibodies* (pp. 13-17). *Humana Press, New York, NY*.

Hovi, T., Roivainen, M., & Blomqvist, S. (2007). Enteroviruses with Special Reference to Poliovirus and Poliomyelitis Eradication. *Perspectives in Medical Virology*, *17*, 69-89.

Hovi, T., Stenvik, M., Partanen, H., & Kangas, A. (2001). Poliovirus Surveillance by Examining Sewage Specimens. Quantitative Recovery of Virus after Introduction into Sewerage at Remote Upstream Location. *Epidemiology and Infection*, *127*(1), 101-106.

Hsu, G. G., Bellamy, A. R., & Yeager, M. (1997). Projection Structure of VP6, the Rotavirus Inner Capsid Protein, and Comparison with Bluetongue VP7. *Journal of Molecular Biology*, *272*(3), 362-368.

Huang, J. Y., Takizawa, S., & Fujita, K. (2000). Pilot-plant Study of a High Recovery Membrane Filtration Process for Drinking Water Treatment. *Water Science and Technology*, *41*(10-11), 77-84.

Hudson, P. J., & Kortt, A. A. (1999). High Avidity scFv Multimers; Diabodies and Triabodies. *Journal of Immunological Methods*, *231*(1-2), 177-189.

Hurst, C. J. (1988). Influence of Aerobic Microorganisms Upon Virus Survival in Soil. *Canadian Journal of Microbiology*, *34*(5), 696-699.

Hussack, G., Luo, Y., Veldhuis, L., Hall, J. C., Tanha, J., & MacKenzie, R. (2009). Multivalent Anchoring and Oriented Display of Single-domain Antibodies on Cellulose. *Sensors*, *9*(7), 5351-5367.

Hwang, Y. C., Leong, O. M., Chen, W., & Yates, M. V. (2007). Comparison of a Reporter Assay and Immunomagnetic Separation Real-time Reverse Transcription-PCR for the Detection of Enteroviruses in Seeded Environmental Water Samples. *Applied and Environmental Microbiology*, *73*(7), 2338-2340.

Ikner, L. A., Gerba, C. P., & Bright, K. R. (2012). Concentration and Recovery of Viruses from Water: A Comprehensive Review. *Food and Environmental Virology*, *4*(2), 41-67.

Ikner, L. A., Soto-Beltran, M., & Bright, K. R. (2011). New Method Using a Positively Charged Microporous Filter and Ultrafiltration for Concentration of Viruses from Tap Water. Applied and Environmental Microbiology, 77,3500.

Ismaili, A., Jalali-Javaran, M., Rasaee, M. J., Rahbarizadeh, F., Forouzandeh-Moghadam, M., & Memari, H. R. (2007). Production and Characterization of Anti-(mucin MUC1) Single-domain Antibody in Tobacco (*Nicotiana tabacum cultivar Xanthi*). *Biotechnology and Applied Biochemistry*, *47*(1), 11-19.

Jakubowski, W., Hoff, J. C., Anthony, N. C., & Hill Jr, W. F. (1974). Epoxy-fiberglass Adsorbent for Concentrating Viruses from Large Volumes of Potable Water. *Applied Microbiology*, *28*(3), 501.

Jain, S., Vashistt, J., & Changotra, H. (2014). Rotaviruses: Is their Surveillance Needed?. *Vaccine*, *32*(27), 3367-3378.

Jervis, E. J., Haynes, C. A., & Kilburn, D. G. (1997). Surface Diffusion of Celluloses and their Isolated Binding Domains on Cellulose. *Journal of Biological Chemistry*, *272*(38), 24016-24023.

Jeyachandran, Y. L., Mielczarski, J. A., Mielczarski, E., & Rai, B. (2010). Efficiency of Blocking of Non-specific Interaction of Different Proteins by BSA Adsorbed on Hydrophobic and Hydrophilic Surfaces. *Journal of Colloid and Interface Science*, *341*(1), 136-142.

Jiang, S. C. (2006). Human Adenoviruses in Water: Occurrence and Health Implications: A Critical Review. *Environmental Science and Technology*, *40*(23), 7132-7140.

Jiang, S., Noble, R., & Chu, W. (2001). Human Adenoviruses and Coliphages in Urban Runoff-impacted Coastal Waters of Southern California. *Applied and Environmental Microbiology*, *67*(1), 179-184.

Johne, R., Otto, P., Roth, B., Löhren, U., Belnap, D., Reetz, J., & Trojnar, E. (2011). Sequence Analysis of the VP6-encoding Genome Segment of Avian Group F and G Rotaviruses. *Virology*, *412*(2), 384-391.

Jothikumar, N., Cliver, D. O., & Mariam, T. W. (1998). Immunomagnetic Capture PCR for Rapid Concentration and Detection of Hepatitis A Virus from Environmental Samples. *Applied and Environmental Microbiology*, *64*(2), 504-508.

Julian, T. R., & Schwab, K. J. (2012). Challenges in Environmental Detection of Human Viral Pathogens. *Current Opinion in Virology*, *2*(1), 78-83.

Jung, Y., Jeong, J. Y., & Chung, B. H. (2008). Recent Advances in Immobilization Methods of Antibodies on Solid Supports. *Analyst*, *133*(6), 697-701.

Kallewaard, N. L., McKinney, B. A., Gu, Y., Chen, A., Prasad, B. V., & Crowe, J. E. (2008). Functional Maturation of the Human Antibody Response to Rotavirus. *The Journal of Immunology*, *180*(6), 3980-3989.

Karim, M. R., Rhodes, E. R., Brinkman, N., et al. (2009). New Electropositive Filter for Concentrating Enteroviruses and Noroviruses from Large Volumes of Water. *Applied and Environmental Microbiology, 75*, 2393.

Kashani, H. H., & Moniri, R. (2015). Expression of Recombinant pET22b-LysK-cysteine/histidine-dependent Amidohydrolase/peptidase Bacteriophage Therapeutic Protein in *Escherichia coli BL21 (DE3)*. *Osong Public Health and Research Perspectives*, *6*(4), 256-260.

Katayama, H., Shimasaki, A., & Ohgaki, S. (2002). Development of a Virus Concentration Method and its Application to Detection of Enterovirus and Norwalk Virus from Coastal Seawater. *Applied and Environmental Microbiology*, *68*(3), 1033-1039.

Kavoosi, M., Meijer, J., Kwan, E., Creagh, A. L., Kilburn, D. G., & Haynes, C. A. (2004). Inexpensive One-step Purification of Polypeptides Expressed in *Escherichia coli* as Fusions with the Family 9 Carbohydrate-binding Module of Xylanase 10A from *T. maritima*. *Journal of Chromatography B*, *807*(1), 87-94.

Kawai, K., O'Brien, M. A., Goveia, M. G., Mast, T. C., & El Khoury, A. C. (2012). Burden of Rotavirus Gastroenteritis and Distribution of Rotavirus Strains in Asia: A Systematic Review. *Vaccine*, *30*(7), 1244-1254.

Kelly, S. M. (1953). Detection and Occurrence of Coxsackie Viruses in Sewage. American Journal of Public Health and the Nations Health, 43(12), 1532-1538.

Kheyami, A. M., Areeshi, M. Y., Dove, W., Nakagomi, O., Cunliffe, N. A., & Hart, C. A. (2008). Characterization of Rotavirus Strains Detected Among Children and Adults with Acute Gastroenteritis in Gizan, Saudi Arabia. *Saudi Medical Journal*, *29*(1), 90-93.

Kittigul, L., Khamoun, P., Sujirarat, D., Utrarachkij, F., Chitpirom, K., Chaichantanakit, N., & Vathanophas, K. (2001). An Improved Method for Concentrating Rotavirus from Water Samples. *Memorias do Instituto Oswaldo Cruz*, *96*(6), 815-821.

Knight, A., Li, D., Uyttendaele, M., & Jaykus, L. A. (2013). A Critical Review of Methods for Detecting Human Noroviruses and Predicting their Infectivity. *Critical Reviews in Microbiology*, *39*(3), 295-309.

Kocwa-Haluch, R. (2001). Waterborne Enteroviruses as a Hazard for Human Health. *Polish Journal of Environmental Studies*, *10*(6), 485-488.

Kong, F., & Hu, Y. F. (2012). Biomolecule Immobilization Techniques for Bioactive Paper Fabrication. *Analytical and Bioanalytical Chemistry*, *403*(1), 7-13.

Koromyslova, A. D., & Hansman, G. S. (2015). Nanobody Binding to a Conserved Epitope Promotes Norovirus Particle Disassembly. *Journal of Virology*, *89*(5), 2718-2730.

Krikelis, V., Markoulatos, P., Spyrou, N., & Serie, C. (1985). Detection of Indigenous Enteric Viruses in Raw Sewage Effluents of the City of Athens, Greece, during a Two Year Survey. *Water Science and Technology*, *17*(10), 159-164.

Kuby, J. (2007). Kuby Immunology. New York, NY, USA: W.H. Freeman and Company.

Kunze, A., Pei, L., Elsässer, D., Niessner, R., & Seidel, M. (2015). High Performance Concentration Method for Viruses in Drinking Water. *Journal of Virological Methods*, *222*, 132-137.

Lambertini, E., Spencer, S. K., Bertz, P. D., Loge, F. J., Kieke, B. A., & Borchardt, M. A. (2008). Concentration of Enteroviruses, Adenoviruses, and Noroviruses from Drinking Water by Use of Glass Wool Filters. *Applied and Environmental Microbiology*, *74*(10), 2990-2996.

Langlet, J., Gaboriaud, F., Duval, J. F., & Gantzer, C. (2008). Aggregation and Surface Properties of F-specific RNA Phages: Implication for Membrane Filtration Processes. *Water Research*, *42*(10-11), 2769-2777.

La Rosa, G., Fratini, M., della Libera, S., Iaconelli, M., & Muscillo, M. (2012). Emerging and Potentially Emerging Viruses in Water Environments. *Annali dell'Istituto Superiore di sanità*, *48*, 397-406.

Lee, D. Y., Leung, K. T., Lee, H., & Habash, M. B. (2016). Simultaneous Detection of Selected Enteric Viruses in Water Samples by Multiplex Quantitative PCR. *Water, Air and Soil Pollution*, *227*(4), 107.

Lee, S. H., & Kim, S. J. (2002). Detection of Infectious Enteroviruses and Adenoviruses in Tap Water in Urban Areas in Korea. *Water Research*, *36*(1), 248-256.

Lee, T. W., & Kurtz, J. B. (1982). Human Astrovirus Serotypes. *Epidemiology and Infection*, *89*(3), 539-540.

Le Guyader, F., Haugarreau, L., Miossec, L., Dubois, E., & Pommepuy, M. (2000). Three-year Study to Assess Human Enteric Viruses in Shellfish. *Applied and Environmental Microbiology*, *66*(8), 3241-3248.

Le Guyader, F., Menard, D., Pommepuy, M., & Kopecka, H. (1995). Use of RT Seminested PCR to Assess Viral Contamination in Caribbean Rivers (Martinique). *Water Science and Technology*, *31*(5-6), 391-394.

Lei, Y., Chen, W., & Mulchandani, A. (2006). Microbial Biosensors. *Analytica Chimica Acta*, *568*(1-2), 200-210.

Leon, J., & Moe, C. L. (2006). Role of Viruses in Foodborne Disease. In *Food Consumption and Disease Risk* (pp. 309-342).

Leung, A. K., Kellner, J. D., & Davies, H. D. (2005). Rotavirus Gastroenteritis. *Advances in Therapy*, *22*(5), 476-487.

Levy, I., & Shoseyov, O. (2002). Cellulose-binding Domains: Biotechnological Applications. *Biotechnology Advances*, *20*(3-4), 191-213.

Li, T., Lin, H., Zhang, Y., Li, M., Wang, D., Che, Y., ... & Zhao, Q. (2014). Improved Characteristics and Protective Efficacy in an Animal Model of *E. coli*-derived Recombinant Double-layered Rotavirus Virus-like Particles. *Vaccine*, *32*(17), 1921-1931.

Li, D., He, M., & Jiang, S. C. (2010). Detection of Infectious Adenoviruses in Environmental Waters by Fluorescence-activated Cell Sorting Assay. *Applied and Environmental Microbiology*, *76*(5), 1442-1448.

Linder, M., Nevanen, T., Söderholm, L., Bengs, O., & Teeri, T. T. (1998). Improved Immobilization of Fusion Proteins via Cellulose-binding Domains. *Biotechnology and Bioengineering*, *60*(5), 642-647.

Lindesmith, L., Moe, C., Marionneau, S., Ruvoen, N., Jiang, X. I., Lindblad, L., ... & Baric, R. (2003). Human Susceptibility and Resistance to Norwalk Virus Infection. *Nature Medicine*, *9*(5), 548.

Lipp, E. K., Lukasik, J., & Rose, J. B. (2001). Human Enteric Viruses and Parasites in the Marine Environment. *Methods in Microbiology*, *30*, 559-588.

Lipp, E. K., & Rose, J. B. (1997). The Role of Seafood in Foodborne Diseases in the United States of America. *Revue Scientifique et Technique-Office International des Epizooties*, *16*(2), 620-640.

Liu, M., Mattion, N. M., & Estes, M. K. (1992). Rotavirus VP3 Expressed in Insect Cells Possesses Guanylyltransferase Activity. *Virology*, *188*(1), 77-84.

Liu, O. C., Brashear, D. A., Seraichekas, H. R., Barnick, J. A., & Metcalf, T. G. (1971). Virus in Water I. A Preliminary Study on a Flow-Through Gauze Sampler for Recovering Virus from Waters. *Applied Microbiology*, *21*(3), 405-410.

Lodder, W. J., Schijven, J. F., Rutjes, S. A., de Roda Husman, A. M., & Teunis, P. F. M. (2015). Entero-and Parechovirus Distributions in Surface Water and Probabilities of Exposure to these Viruses during Water Recreation. *Water research*, *75*, 25-32.

Logrippo, G. A., & Berger, B. (1952). Use of Ion Exchange Resins in Partial Purification and Concentration of Poliomyelitis Virus. *The Journal of Laboratory and Clinical Medicine*, *39*(6), 970-973.

Lukasik, J., Scott, T. M., Andryshak, D., & Farrah, S. R. (2000). Influence of Salts on Virus Adsorption to Microporous Filters. *Applied Environmental Microbiology*, *66*(7), 2914-2920.

Maffey, L., Vega, C. G., Miño, S., Garaicoechea, L., & Parreño, V. (2016). Anti-VP6 VHH: an Experimental Treatment for Rotavirus A-associated Disease. *PloS one*, *11*(9), e0162351.

Mathieu, M., Petitpas, I., Navaza, J., Lepault, J., Kohli, E., Pothier, P., ... & Rey, F. A. (2001). Atomic Structure of the Major Capsid Protein of Rotavirus: Implications for the Architecture of the Virion. *The Embo Journal*, *20*(7), 1485-1497.

Matthijnssens, J., Otto, P. H., Ciarlet, M., Desselberger, U., Van Ranst, M., & Johne, R. (2012). VP6-sequence-based Cutoff Values as a Criterion for Rotavirus Species Demarcation. *Archives of Virology*, *157*(6), 1177-1182.

Matthijnssens, J., Heylen, E., Zeller, M., Rahman, M., Lemey, P., & Van Ranst, M. (2010). Phylodynamic Analyses of Rotavirus Genotypes G9 and G12 Underscore their Potential for Swift Global Spread. *Molecular Biology and Evolution*, *27*(10), 2431-2436.

Matthijnssens, J., Ciarlet, M., Heiman, E., Arijs, I., Delbeke, T., McDonald, S. M., ... & Rahman, M. (2008). Full Genome-based Classification of Rotaviruses Reveals a Common Origin between Human Wa-like and Porcine Rotavirus Strains and Human DS-1-like and Bovine Rotavirus Strains. *Journal of Virology*, *82*(7), 3204-3219.

Mattison, K., & Bidawid, S. (2009). Analytical Methods for Food and Environmental Viruses. *Food and Environmental Virology*, *1*(3-4), 107-122.

Maurice, S., Dekel, M., Shoseyov, O., & Gertler, A. (2003). Cellulose Beads Bound to Cellulose Binding Domain-fused Recombinant Proteins; An Adjuvant System for Parenteral Vaccination of Fish. *Vaccine*, *21*(23), 3200-3207.

Maynard, J., & Georgiou, G. (2000). Antibody Engineering. *Annual Review of Biomedical Engineering*, *2*(1), 339-376.

McLean, B. W., Boraston, A. B., Brouwer, D., Sanaie, N., Fyfe, C. A., Warren, R. A. J., ... & Haynes, C. A. (2002). Carbohydrate-binding Modules Recognize Fine Substructures of Cellulose. *Journal of Biological Chemistry*, *277*(52), 50245-50254.

McLean, B. W., Bray, M. R., Boraston, A. B., Gilkes, N. R., Haynes, C. A., & Kilburn, D. G. (2000). Analysis of Binding of the Family 2a Carbohydrate-binding Module from *Cellulomonas fimi* Xylanase 10A to Cellulose: Specificity and Identification of Functionally Important Amino Acid Residues. *Protein Engineering*, *13*(11), 801-809.

McQuaig, S. M., & Noble, R. T. (2011). Viruses as Tracers of Fecal Contamination. In *Microbial Source Tracking: Methods, Applications, and Case Studies* (pp. 113-135). Springer, New York, NY.

Melnick, J. L., Gerba, C. P., & Berg, G. (1980). The Ecology of Enteroviruses in Natural Waters. *Critical Reviews in Environmental Science and Technology*, *10*(1), 65-93.

Metcalf, T. G., Melnick, J. L., & Estes, M. K. (1995). Environmental Virology: from Detection of Virus in Sewage and Water by Isolation to Identification by Molecular Biology-a Trip of over 50 Years. *Annual Reviews in Microbiology*, *49*(1), 461-487.

Mihalov-Kovács, E., Gellért, Á., Marton, S., Farkas, S. L., Fehér, E., Oldal, M., ... & Bányai, K. (2015). Candidate New Rotavirus Species in Sheltered Dogs, Hungary. *Emerging Infectious Diseases*, *21*(4), 660.

Moe, K., & Shirley, J. A. (1982). The Effects of Relative Humidity and Temperature on the Survival of Human Rotavirus in Faeces. *Archives of Virology*, *72*(3), 179-186.

Morris, R., & Waite, W. M. (1980). Evaluation of Procedures for Recovery of Viruses from Water-1 Concentration Systems. *Water Research*, *14*(7), 791-793.

Muscillo, M., Aulicino, F. A., Patti, A. M., Orsini, P., Volterra, L., & Fara, G. M. (1994). Molecular Techniques for the Identification of Enteric Viruses in Marine Waters. *Water Research*, *28*(1), 1-7.

Muyldermans, S. (2013). Nanobodies: Natural Single-domain Antibodies. *Annual Review of Biochemistry*, *82*, 775-797.

Muyldermans, S. (2001). Single Domain Camel Antibodies: Current Status. *Reviews in Molecular Biotechnology*, *74*(4), 277-302.

Myrmel, M., Rimstad, E., & Wasteson, Y. (2000). Immunomagnetic Separation of a Norwalk-like Virus (Genogroup I) in Artificially Contaminated Environmental Water Samples. *International Journal of Food Microbiology*, *62*(1-2), 17-26.

Nahálka, J., & Gemeiner, P. (2006). Thermoswitched Immobilization-a Novel Approach in Reversible Immobilization. *Journal of Biotechnology*, *123*(4), 478-482.

Nelson, P. N., Reynolds, G. M., Waldron, E. E., Ward, E., Giannopoulos, K., & Murray, P. G. (2000). Demystified: Monoclonal Antibodies. *Molecular Pathology*, *53*(3), 111

Nguyen, V. K., Muyldermans, S., & Hamers, R. (1998). The Specific Variable Domain of Camel Heavy-chain Antibodies is Encoded in the Germline1. *Journal of Molecular Biology*, *275*(3), 413-418.

Nupen, E. M. (1970). Virus Studies on the Windhoek Waste-water Reclamation Plant (South-West Africa). *Water Research*, *4*(10), 661-672.

Okoh, A. I., Sibanda, T., & Gusha, S. S. (2010). Inadequately Treated Wastewater as a Source of Human Enteric Viruses in the Environment. *International Journal of Environmental Research and Public Health*, *7*(6), 2620-2637.

Ogorzaly, L., Bonot, S., El Moualij, B., Zorzi, W., & Cauchie, H. M. (2013). Development of a Quantitative Immunocapture Real-time PCR Assay for Detecting Structurally Intact Adenoviral Particles in Water. *Journal of Virological Methods*, *194*(1-2), 235-241.

Oliveira, C., Carvalho, V., Domingues, L., & Gama, F. M. (2015). Recombinant CBM-Fusion Technology-applications Overview. *Biotechnology Advances*, *33*(3-4), 358-369.

Olszewski, J., Winona, L., & Oshima, K. H. (2005). Comparison of 2 Ultrafiltration Systems for the Concentration of Seeded Viruses from Environmental Waters. *Canadian Journal of Microbiology*, *51*(4), 295-303.

Ong, E., Gilkes, N. R., Miller Jr, R. C., Antony, R., Warren, J., & Kilburn, D. G. (1991). Enzyme Immobilization Using a Cellulose-binding Domain: Properties of a β-glucosidase Fusion Protein. *Enzyme and Microbial Technology*, *13*(1), 59-65.

Otani, H., Matsumoto, K., Saeki, A., & Hosono, A. (1991). Comparative Studies on Properties of Hen Egg Yold IgY and Rabbit Serum IgG Antibodies. *Lebensmittel-Wissenschaft + Technologie= Food Science+ Technology*, 24(2),153-158.

Pala, H., Lemos, M. A., Mota, M., & Gama, F. M. (2001). Enzymatic Upgrade of Old Paperboard Containers. *Enzyme and Microbial Technology*, *29*(4-5), 274-279.

Pang, X., Qiu, Y., Gao, T., Zurawell, R., Neumann, N. F., Craik, S., & Lee, B. E. (2019). Prevalence, Levels and Seasonal Variations of Human Enteric Viruses in Six Major Rivers in Alberta, Canada. *Water Research*, *153*, 349-356.

Pang, X. L., Lee, B. E., Pabbaraju, K., Gabos, S., Craik, S., Payment, P., & Neumann, N. (2012). Pre-analytical and Analytical Procedures for the Detection of Enteric Viruses and Enterovirus in Water Samples. *Journal of Virological Methods*, *184*(1-2), 77-83.

Pang, L. (2009). Microbial Removal Rates in Subsurface Media Estimated from Published Studies of Field Experiments and Large Intact Soil Cores. *Journal of Environmental Quality*, *38*(4), 1531-1559.

Papafragkou, E., Plante, M., Mattison, K., Bidawid, S., Karthikeyan, K., Farber, J. M., & Jaykus, L. A. (2008). Rapid and Sensitive Detection of Hepatitis A Virus in Representative Food Matrices. *Journal of Virological Methods*, *147*(1), 177-187.

Park, S., Kim, H., Paek, S. H., Hong, J. W., & Kim, Y. K. (2008). Enzyme-linked Immuno-Strip Biosensor to Detect *Escherichia coli O157: H7*. *Ultramicroscopy*, *108*(10), 1348-1351.

Parshionikar, S. U., Willian-True, S., Fout, G. S., Robbins, D. E., Seys, S. A., Cassady, J. D., & Harris, R. (2003). Waterborne Outbreak of Gastroenteritis Associated with a Norovirus. *Applied and Environmental Microbiology*, *69*(9), 5263-5268.

Patti, A. M., Aulicino, F. A., Santi, A. L., Muscillo, M., Orsinv, P., Bellucci, C., ... & Volterra, L. (1996). Enteric Virus Pollution of Tyrrhenian Areas. *Water, Air, and Soil Pollution*, *88*(3-4), 261-267.

Payment, P., Morin, E., & Trudel, M. (1988). Coliphages and Enteric Viruses in the Particulate Phase of River Water. *Canadian Journal of Microbiology*, *34*(7), 907-910.

Payment, P, Assaf, R, Trudel, M, & Marois, P. (1979). Enzyme-linked Immunosorbent Assay for Serology of Infectious Bovine Rhinotracheitis Virus Infections. *Journal of Clinical Microbiology, 10*(5), 633-636.

Petitpas, I., Lepault, J., Vachette, P., Charpilienne, A., Mathieu, M., Kohli, E., ... & Rey, F. A. (1998). Crystallization and Preliminary X-ray Analysis of Rotavirus Protein VP6. *Journal of Virology*, *72*(9), 7615-7619.

Petterson, S., Grøndahl-Rosado, R., Nilsen, V., Myrmel, M., & Robertson, L. J. (2015). Variability in the Recovery of a Virus Concentration Procedure in Water: Implications for QMRA. *Water research*, *87*, 79-86.

Pelton, R. (2009). Bioactive Paper Provides a Low-cost Platform for Diagnostics. *TrAC Trends in Analytical Chemistry*, *28*(8), 925-942.

Pêra, F. F., Mutepfa, D. L., Khan, A. M., Els, J. H., Mbewana, S., van Dijk, A. A., ... & Hitzeroth, I. I. (2015). Engineering and Expression of a Human Rotavirus Candidate Vaccine in *Nicotiana benthamiana*. *Virology Journal*, *12*(1), 205.

Pieper, A. P., Ryan, J. N., Harvey, R. W., Amy, G. L., Illangasekare, T. H., & Metge, D. W. (1997). Transport and Recovery of Bacteriophage PRD1 in a Sand and Gravel Aquifer: Effect of Sewage-derived Organic Matter. *Environmental Science and Technology*, *31*(4), 1163-1170.

Pintó, R. M., & Saiz, J. C. (2007). Enteric Hepatitis Viruses. *Perspectives in Medical Virology*, *17*, 39-67.

Pisano, M. B., Lugo, B. C., Poma, R., Cristóbal, H. A., Raskovsky, V., Martínez Wassaf, M. G., ... & Ré, V. E. (2018). Environmental Hepatitis E Virus Detection Supported by Serological Evidence in the Northwest of Argentina. *Transactions of The Royal Society of Tropical Medicine and Hygiene*, *112*(4), 181-187.

Powell, K. L., Taylor, R. G., Cronin, A. A., Barrett, M. H., Pedley, S., Sellwood, J., ... & Lerner, D. N. (2003). Microbial Contamination of Two Urban Sandstone Aquifers in the UK. *Water Research*, *37*(2), 339-352.

Prasad, B. V., Rothnagel, R., Zeng, C. Y., Jakana, J., Lawton, J. A., Chiu, W., & Estes, M. K. (1996). Visualization of Ordered Genomic RNA and Localization of Transcriptional Complexes in Rotavirus. *Nature*, *382*(6590), 471.

Prasad, B. V., Wang, G. J., Clerx, J. P., & Chiu, W. (1988). Three-dimensional Structure of Rotavirus. *Journal of Molecular Biology*, *199*(2), 269-275.

Ramírez, C., Fung, J., Miller Jr, R. C., Antony, R., Warren, J., & Kilburn, D. G. (1993). A Bifunctional Affinity Linker to Couple Antibodies to Cellulose. *Nature Biotechnology*, *11*(12), 1570.

Rao, N. U., & Labzoffsky, N. A. (1969). A Simple Method for the Detection of Low Concentration of Viruses in Large Volumes of Water by the Membrane Filter Technique. *Canadian Journal of Microbiology*, *15*(5), 399-403.

Raymaekers, M., Smets, R., Maes, B., & Cartuyvels, R. (2009). Checklist for Optimization and Validation of Real-time PCR Assays. *Journal of Clinical Laboratory Analysis*, *23*(3), 145-151.

Reese, E. T., Siu, R. G., & Levinson, H. S. (1950). The Biological Degradation of Soluble Cellulose Derivatives and its Relationship to the Mechanism of Cellulose Hydrolysis. *Journal of Bacteriology*, *59*(4), 485.

Regnery, J., Gerba, C. P., Dickenson, E. R., & Drewes, J. E. (2017). The Importance of Key Attenuation Factors for Microbial and Chemical Contaminants during

Managed Aquifer Recharge: A Review. *Critical Reviews in Environmental Science and Technology*, *47*(15), 1409-1452.

Reynolds, K. S., Gerba, C. P., & Pepper, I. L. (1997). Rapid PCR-based Monitoring of Infectious Enteroviruses in Drinking Water. *Water Science and Technology*, *35*(11-12), 423-427.

Rosa, A. M., Louro, A. F., Martins, S. A., Inácio, J., Azevedo, A. M., & Prazeres, D. M. F. (2014). Capture and Detection of DNA Hybrids on Paper via the Anchoring of Antibodies with Fusions of Carbohydrate Binding Modules and ZZ-domains. *Analytical Chemistry*, *86*(9), 4340-4347.

Rose, J. B. (2005). Reduction of Pathogens, Indicator Bacteria, and Alternative Indicators by Wastewater Treatment and Reclamation Processes. IWA Publishing.

Rotem-Borensztajn, Y., Belfort, G., & Katzenelson, E. (1979). Virus Concentration by Ultrafiltration. *Journal of the Environmental Engineering Division*, *105*(2), 401-407.

Rutjes, S. A., Italiaander, R., van den Berg, H. H., Lodder, W. J., & de Roda Husman, A. M. (2005). Isolation and Detection of Enterovirus RNA from Large-volume Water Samples by Using the NucliSens miniMAG System and Real-time Nucleic Acid Sequence-based Amplification. *Applied and Environmental Microbiology*, *71*(7), 3734-3740.

Rzeżutka, A., & Cook, N. (2004). Survival of Human Enteric Viruses in the Environment and Food. *FEMS Microbiology Reviews*, *28*(4), 441-453.

Saerens, D., Huang, L., Bonroy, K., & Muyldermans, S. (2008). Antibody Fragments as Probe in Biosensor Development. *Sensors*, *8*(8), 4669-4686.

Salim, A. F. M., Phillips, A. D., & Farthing, M. J. G. (1990). Pathogenesis of Gut Virus Infection. *Baillière's Clinical Gastroenterology*, *4*(3), 593-607.

Scandura, J. E., & Sobsey, M. D. (1997). Viral and Bacterial Contamination of Groundwater from On-site Sewage Treatment Systems. *Water Science and Technology*, *35*(11-12), 141-146.

Schijven, J. F., & Hassanizadeh, S. M. (2000). Removal of Viruses by Soil Passage: Overview of Modeling, Processes, and Parameters. *Critical Reviews in Environmental Science and Technology*, *30*(1), 49-127.

Schotte, L., Strauss, M., Thys, B., Halewyck, H., Filman, D. J., Bostina, M., ... & Rombaut, B. (2014). Mechanism of Action and Capsid Stabilizing Properties of VHHs with an in vitro Anti-polioviral Activity. *Journal of Virology*, JVI-03402.

Schrader, C., Schielke, A., Ellerbroek, L., & Johne, R. (2012). PCR Inhibitors-occurrence, Properties and Removal. *Journal of Applied Microbiology*, *113*(5), 1014-1026.

Schvoerer, E., Ventura, M., Dubos, O., Cazaux, G., Serceau, R., Gournier, N., ... & Lafon, M. E. (2001). Qualitative and Quantitative Molecular Detection of Enteroviruses in Water from Bathing Areas and from a Sewage Treatment Plant. *Research in Microbiology*, *152*(2), 179-186.

Schwab, K. E., & Gargett, C. E. (2007). Co-expression of Two Perivascular Cell Markers Isolates Mesenchymal Stem-like Cells from Human Endometrium. *Human Reproduction*, *22*(11), 2903-2911.

Schwab, K. J., De Leon, R., & Sobsey, M. D. (1996). Immunoaffinity Concentration and Purification of Waterborne Enteric Viruses for Detection by Reverse Transcriptase PCR. *Applied and Environmental Microbiology*, *62*(6), 2086-2094.

Shani, Z., & Shoseyov, O. (2001). Process of Expressing and Isolating Recombinant Proteins and Recombinant Protein Products from Plants, Plant Derived Tissues or Cultured Plant Cells. *Patent NumberUS Patent: 6331416*.

Shen, H., Schmuck, M., Pilz, I., Gilkes, N. R., Kilburn, D. G., Miller, R. C., & Warren, R. A. (1991). Deletion of the Linker Connecting the Catalytic and Cellulose-binding Domains of Endoglucanase A (CenA) of *Cellulomonas fimi* Alters its Conformation and Catalytic Activity. *Journal of Biological Chemistry*, *266*(17), 11335-11340.

Shimizu, M., Nagashima, H., & Hashimoto, K. (1993). Comparative Studies in Molecular Stability of Immunoglobulin G from Different Species. *Comparative Biochemistry and Physiology. B, Comparative Biochemistry*, *106*(2), 255-261.

Shoseyov, O., Shani, Z., & Levy, I. (2006). Carbohydrate Binding Modules: Biochemical Properties and Novel Applications. *Microbiology and Molecular Biology Reviews*, *70*(2), 283-295.

Shoseyov, O., Shpiegl, I., Goldstein, M. A., & Doi, R. H. (1999). Methods of Detection Using a Cellulose Binding Domain Fusion Product (No. US 5,856,201/A/). University of California.

Shpigel, E., Goldlust, A., Eshel, A., Ber, I. K., Efroni, G., Singer, Y., ... & Shoseyov, O. (2000). Expression, Purification and Applications of Staphylococcal Protein A Fused to Cellulose-binding Domain. *Biotechnology and Applied Biochemistry*, *31*(3), 197-203.

Shuval, H. I., Cymbalista, B. F. S., & Goldblum, N. (1969). The Phase-separation Method for the Concentration and Detection of Viruses in Water. *Water Research, 3*,225-240.

Shuval, H. J., Cymbalista, S., Fatal, B., & Goldblum, N. (1967). Concentration of Enteric Viruses in Water by Hydro-extraction and Two Phase Separation. In G. Berg (Ed.), *Transmission of Viruses by the Water Route* (pp. 45–55). London: Interscience.

Simpson, P. J., Xie, H., Bolam, D. N., Gilbert, H. J., & Williamson, M. P. (2000). The Structural Basis for the Ligand Specificity of Family 2 Carbohydrate-binding Modules. *Journal of Biological Chemistry*, *275*(52), 41137-41142.

Sinclair, T. R., Patil, A., Raza, B. G., Reurink, D., van den Hengel, S. K., Rutjes, S. A., ... & de Vos, W. M. (2019). Cationically Modified Membranes Using Covalent Layer-by-layer Assembly for Antiviral Applications in Drinking Water. *Journal of Membrane Science*, *570*, 494-503.

Singh-Naz, N., & Naz, R. (1986). Development and Application of Monoclonal Antibodies for Specific Detection of Human Enteric Adenoviruses. *Journal of Clinical Microbiology, 23*(5), 840-842.

Sobsey, M. D. (1995). Male-specific Coliphages as Indicators of Viral Contamination of Drinking Water. *AWWA Reserch Foudation Report*.

Sobsey, M. D., Wallis, C., Henderson, M., & Melnick, J. L. (1973). Concentration of Enteroviruses from Large Volumes of Water. *Applied Microbiology*, *26*(4), 529-534.

Sommer, R., Pribil, W., Appelt, S., Gehringer, P., Eschweiler, H., Leth, H., ... & Haider, T. (2001). Inactivation of Bacteriophages in Water by Means of Non-ionizing (UV-253.7 nm) and Ionizing (Gamma) Radiation: A Comparative Approach. *Water Research*, *35*(13), 3109-3116.

Song, L., & Elimelech, M. (1994). Transient Deposition of Colloidal Particles in Heterogeneous Porous Media. *Journal of Colloid and Interface Science*, *167*(2), 301-313.

Spinelli, S., Frenken, L. G., Hermans, P., Verrips, T., Brown, K., Tegoni, M., & Cambillau, C. (2000). Camelid Heavy-chain Variable Domains Provide Efficient Combining Sites to Haptens. *Biochemistry*, *39*(6), 1217-1222.

Stahl, S., and M. Uhlen. (1997). Bacterial Surface Display: Trends and Progress. Trends Biotechnol. 15:185-192.

Strauss, M., Schotte, L., Thys, B., Filman, D. J., & Hogle, J. M. (2016). Five of Five VHHs Neutralizing Poliovirus Bind the Receptor-binding Site. *Journal of Virology*, JVI-03017.

Svec, D., Tichopad, A., Novosadova, V., Pfaffl, M. W., & Kubista, M. (2015). How Good is a PCR Efficiency Estimate: Recommendations for Precise and Robust qPCR Efficiency Assessments. *Biomolecular Detection and Quantification*, *3*, 9-16.

Tambini, G., Andrus, J. K., Marques, E., Boshell, J., Pallansch, M., de Quadros, O. A., & Kew, O. (1993). Direct Detection of Wild Poliovirus Circulation by Stool Surveys of Healthy Children and Analysis of Community Wastewater. *Journal of Infectious Diseases*, *168*(6), 1510-1514.

Tang, B., Gilbert, J. M., Matsui, S. M., & Greenberg, H. B. (1997). Comparison of the Rotavirus Gene 6 from Different Species by Sequence Analysis and Localization of Subgroup-specific Epitopes Using Site-directed Mutagenesis. *Virology*, *237*(1), 89-96.

Taylor, M. B., Becker, P. J., Van Rensburg, E. J., Harris, B. N., Bailey, I. W., & Grabow, W. O. K. (1995). A Serosurvey of Water-borne Pathogens Amongst Canoeists in South Africa. *Epidemiology and Infection*, *115*(2), 299-307.

Tcheremenskaia, O., Marucci, G., De Petris, S., Ruggeri, F. M., Dovecar, D., Sternak, S. L., ... & Fiore, L. (2007). Molecular Epidemiology of Rotavirus in Central and Southeastern Europe. *Journal of Clinical Microbiology*, *45*(7), 2197-2204.

Teunis, P. F., Moe, C. L., Liu, P., E. Miller, S., Lindesmith, L., Baric, R. S., ... & Calderon, R. L. (2008). Norwalk Virus: How Infectious Is It?. *Journal of Medical Virology*, *80*(8), 1468-1476.

Thurston-Enriquez, J. A., Haas, C. N., Jacangelo, J., Riley, K., & Gerba, C. P. (2003). Inactivation of Feline Calicivirus and Adenovirus Type 40 by UV Radiation. *Applied and Environmental Microbiology*, *69*(1), 577-582.

Thys, B., Schotte, L., Muyldermans, S., Wernery, U., Hassanzadeh-Ghassabeh, G., & Rombaut, B. (2010). In Vitro Antiviral Activity of Single Domain Antibody Fragments Against Poliovirus. *Antiviral Research*, *87*(2), 257-264.

Tischenko, V. M., Abramov, V. M., & Zav'yalov, V. P. (1998). Investigation of the Cooperative Structure of Fc Fragments from Myeloma Immunoglobulin G. *Biochemistry*, *37*(16), 5576-5581.

Toldrà, A., Andree, K. B., Bertomeu, E., Roque, A., Carrasco, N., Gairín, I., ... & Campàs, M. (2018). Rapid Capture and Detection of Ostreid Herpesvirus-1 from Pacific Oyster Crassostrea Gigas and Seawater Using Magnetic Beads. *PloS one*, *13*(10), e0205207.

Tomme, Van Tilbeurgh, Pettersson, Van Damme, Vandekerckhove, Knowles, . . . Tomme, P. (1988). Studies of the Cellulolytic System of *Trichoderma reesei QM 9414*. Analysis of Domain Function in Two Cellobiohydrolases by Limited Proteolysis. *European Journal of Biochemistry, 170*(3), 575-581.

USEPA. Environmental Protection Agency. (1992). Manual on Guidelines for Water Reuse. EPA/625/R-92/004. Center for Environmental Reservation Information, Cincinnati, Ohio.

USEPA. Environmental Protection Agency (1996). Information Collection Rule Technical Summary.

USEPA. Environmental Protection Agency. (1984). Final Report: The Cost of Clean Air and Water, Report to Congress. *Washington, D.C., May 1984. 31.*

Valenzuela, S., Pizarro, J., Sandino, A. M., Vásquez, M., Fernández, J., Hernández, O., ... & Spencer, E. (1991). Photoaffinity Labeling of Rotavirus VP1 with 8-azido-ATP: Identification of the Viral RNA Polymerase. *Journal of Virology*, *65*(7), 3964-3967.

van der Linden, R. H. J., Frenken, L. G. J., De Geus, B., Harmsen, M. M., Ruuls, R. C., Stok, W., ... & Verrips, C. T. (1999). Comparison of Physical Chemical Properties of Llama VHH Antibody Fragments and Mouse Monoclonal Antibodies. *Biochimica et Biophysica Acta (BBA)-Protein Structure and Molecular Enzymology*, *1431*(1), 37-46.

van der Vaart, J. M., Pant, N., Wolvers, D., Bezemer, S., Hermans, P. W., Bellamy, K., ... & Hammarstrom, L. (2006). Reduction in Morbidity of Rotavirus Induced Diarrhoea in Mice by Yeast Produced Monovalent Llama-derived Antibody Fragments. *Vaccine*, *24*(19), 4130-4137.

Van Tilbeurgh, H., Tomme, P., Claeyssens, M., Bhikhabhai, R., & Pettersson, G. (1986). Limited Proteolysis of the Cellobiohydrolase I from *Trichoderma reesei*: Separation of Functional Domains. *FEBS Letters*, *204*(2), 223-227.

Vega, C. G., Bok, M., Vlasova, A. N., Chattha, K. S., Gómez-Sebastián, S., Nuñez, C., ... & Fernandez, F. (2013). Recombinant Monovalent Llama-derived Antibody Fragments (VHH) to Rotavirus VP6 Protect Neonatal Gnotobiotic Piglets Against Human Rotavirus-induced Diarrhea. *PLoS Pathogens*, *9*(5), e1003334.

Ver, B. A., Melnick, J. L., & Wallis, C. (1968). Efficient Filtration and Sizing of Viruses with Membrane Filters. *Journal of Virology*, *2*(1), 21-25.

Vermeer, A. W., Norde, W., & van Amerongen, A. (2000). The Unfolding/denaturation of Immunogammaglobulin of Isotype 2b and its Fab and Fc Fragments. *Biophysical Journal*, *79*(4), 2150-2154.

Vikholm-Lundin, I. (2005). Immunosensing Based on Site-directed Immobilization of Antibody Fragments and Polymers that Reduce Nonspecific Binding. *Langmuir*, *21*(14), 6473-6477.

Vilaginès, P., Sarrette, B., Champsaur, H., Hugues, B., Dubrou, S., Joret, J. C., ... & Oger, C. (1997). Round Robin Investigation of Glass Wool Method for Poliovirus Recovery from Drinking Water and Sea Water. *Water Science and Technology*, *35*(11-12), 445-449.

Vincke, C., & Muyldermans, S. (2012). Introduction to Heavy Chain Antibodies and Derived Nanobodies. In *Single Domain Antibodies* (pp. 15-26). Humana Press, Totowa, NJ.

Vu, K. B., Ghahroudi, M. A., Wyns, L., & Muyldermans, S. (1997). Comparison of Llama VH Sequences from Conventional and Heavy Chain Antibodies. *Molecular Immunology*, *34*(16-17), 1121-1131.

Walshe, G. E., Pang, L., Flury, M., Close, M. E., & Flintoft, M. (2010). Effects of pH, Ionic Strength, Dissolved Organic Matter, and Flow Rate on the Co-transport of MS2 Bacteriophages with Kaolinite in Gravel Aquifer Media. *Water Research*, *44*(4), 1255-1269.

Wallis, C., Henderson, M., & Melnick, J. L. (1972). Enterovirus Concentration on Cellulose Membranes. *Applied Microbiology*, *23*(3), 476-480.

Wallis, C., & Melnick, J. L. (1967a). Concentration of Viruses on Aluminum and Calcium Salts. *American Journal of Epidemiology*, *85*(3), 459-68.

Wallis, C., & Melnick, J. L. (1967b). Concentration of Enteroviruses on Membrane Filters. *Journal of Virology*, *1*(3), 472-477.

Wallis, C., & Melnick, J. L. (1967c). Concentration of Viruses from Sewage by Adsorption on Millipore Membranes. *Bulletin of the World Health Organization*, *36*(2), 219.

Wang, X. D., & Wolfbeis, O. S. (2012). Fiber-optic Chemical Sensors and Biosensors (2008–2012). *Analytical Chemistry*, *85*(2), 487-508.

Ward, R.L. & McNeal, M.M., 2010. VP6: A Candidate Rotavirus Vaccine. *The Journal of Infectious Diseases*, 202 (1), pp.101–107.

Ward, R. L. (2008). Rotavirus Vaccines: How they Work or Don't Work. *Expert Reviews in Molecular Medicine*, *10*.

Weitkamp, J. H., Kallewaard, N., Kusuhara, K., Feigelstock, D., Feng, N., Greenberg, H. B., & Crowe Jr, J. E. (2003). Generation of Recombinant Human Monoclonal

Antibodies to Rotavirus from Single Antigen-specific B Cells Selected with Fluorescent Virus-like Particles. *Journal of Immunological Methods*, *275*(1-2), 223-237.

Widdowson, M. A., Sulka, A., Bulens, S. N., Beard, R. S., Chaves, S. S., Hammond, R., ... & Mead, P. S. (2005). Norovirus and Foodborne Disease, United States, 1991-2000. *Emerging Infectious Diseases*, *11*(1), 95.

Winichayakul, S., Pernthaner, A., Scott, R., Vlaming, R., & Roberts, N. (2009). Head-to-tail Fusions of Camelid Antibodies Can Be Expressed in Planta and Bind in Rumen Fluid. *Biotechnology and Applied Biochemistry*, *53*(2), 111-122.

Wood, S. (2011). Engineering Single-domain Antibodies for Bioactive Paper Applications (Doctoral Dissertation).

World Health Organization. (2017). Diarrhoeal disease. https://www.who.int/en/news-room/fact-sheets/detail/diarrhoeal-disease. Published May 2, 2017. Accessed July 9, 2019.

World Health Organization. (2003). Guidelines for Environmental Surveillance of Poliovirus Circulation. Geneva, Switzerland.

Wu, Y., Jiang, S., & Ying, T. (2017). Single-domain Antibodies as Therapeutics Against Human Viral Diseases. *Frontiers in Immunology*, *8*, 1802.

Wyn-Jones, A. P., & Sellwood, J. (2001). Enteric Viruses in the Aquatic Environment. *Journal of Applied Microbiology*, *91*(6), 945-962.

Xu, Z., Bae, W., Mulchandani, A., Mehra, R. K., & Chen, W. (2002). Heavy Metal Removal by Novel CBD-EC20 Sorbents Immobilized on Cellulose. *Biomacromolecules*, *3*(3), 462-465.

Xu, G. Y., Ong, E., Gilkes, N. R., Kilburn, D. G., Muhandiram, D. R., Harris-Brandts, M., ... & Harvey, T. S. (1995). Solution Structure of a Cellulose-binding Domain from *Cellulomonas fimi* by Nuclear Magnetic Resonance Spectroscopy. *Biochemistry*, *34*(21), 6993-7009.

Yang, W., Gu, A. Z., Zeng, S. Y., Li, D., He, M., & Shi, H. C. (2011). Development of a Combined Immunomagnetic Separation and Quantitative Reverse Transcription-PCR assay for Sensitive Detection of Infectious Rotavirus in Water Samples. *Journal of Microbiological Methods*, *84*(3), 447-453.

Yeager, M., Dryden, K. A., Olson, N. H., Greenberg, H. B., & Baker, T. S. (1990). Three-dimensional Structure of Rhesus Rotavirus by Cryoelectron Microscopy and Image Reconstruction. *The Journal of Cell Biology*, *110*(6), 2133-2144.

Zav'yalov, V. P., & Tishchenko, V. M. (1991). Mechanisms of Generation of Antibody Diversity as a Cause for Natural Selection of Homoiothermal Animals in the Process of Evolution. *Scandinavian Journal of Immunology*, *33*(6), 755-762.

Zeng, X., Shen, Z., & Mernaugh, R. (2012). Recombinant Antibodies and their Use in Biosensors. *Analytical and Bioanalytical Chemistry*, *402*(10), 3027-3038.

Zhao, X., Lin, C. W., Wang, J., & Oh, D. H. (2014). Advances in Rapid Detection Methods for Foodborne Pathogens. *Journal of Microbial Biotechnology*, *24*(3), 297-312.

APPENDICES

APPENDIX 1. COMPOSITION AND PREPARATION OF REAGENTS

1. Antibiotics and Solutions

- **Kanamycin (50 mg/ml)**

  • Dissolve 0.5 g of kanamycin into 9.5 ml of distilled water. Tap up the volume to 10 ml with distilled water and filter-sterilize using a 0.22-µm syringe filter. Store in 1-ml aliquots at −20°C.

- **Ampicillin (100 mg/ml)**

  • Dissolve 1 g of ampicillin into 9.5 ml of distilled water. Tap up the volume to 10 ml with distilled water and filter-sterilize using a 0.22-µm syringe filter. Store in 1-ml aliquots at −20°C.

- **Rifampicin (50 mg/ml)**

  • Dissolve 0.5 g of rifampicin into 9.5 ml of 100% methanol. Tap up the volume to 10 ml with 100% methanol and filter-sterilize using a 0.22-µm syringe filter. Store in 1-ml aliquots at −20°C.

- **Carbenicillin (50 mg/ml)**

  • Dissolve 0.5 g of disodium carbenicillin into 9.5 ml of distilled water. Top up the volume to 10 ml with distilled water and filter-sterilize using a 0.22-µm filter. Store in 1-ml aliquots at −20°C.

- **IPTG (1 M)**

• Dissolve 2.38 g of IPTG into into 8 ml of distilled water. Top up the volume to 10 ml with distilled water and filter-sterilize using a 0.22-µm filter. Store in 1-ml aliquots at −20°C.

- **Sodium Dodecyl Sulfate (SDS, 10%)**

• Dissolve 5 g of SDS into 40 ml of distilled water. Top up the volume to 50 ml with distilled water. Filter-sterilize and store at 24°C.

- **Ammonium Presulfate (APS, 10%)**

• Dissolve 50 mg of ammonium presulfate into 3 ml of distilled water. Top up the volume to 5 ml with distilled water. Filter-sterilize and store in 1-ml aliquots at −20°C.

- **SDS-PAGE Non-Reducing Solution (5x, 10 ml)**

• Combine 0.6 ml of Tris-HCl (1 M, pH 6.8), 5 ml of glycerol (50%), 2 ml of SDS (10%) and 1 ml of bromophenol blue (1%, 10 mg into 1 ml of distilled water). Top up the volume to 10 ml with distilled water. Store in 1-ml aliquots at −20°C.

- **SDS-PAGE Reducing Solution (5x, 10 ml)**

• Combine 0.6 ml of Tris-HCl (1 M, pH 6.8), 5 ml of glycerol (50%), 2 ml of SDS (10%) and 1 ml of bromophenol blue (1%, 10 mg into 1 ml of distilled water). Add 500 µl beta-mercaptoethanol then top up the volume to 10 ml with distilled water. Store in 1-ml aliquots at −20°C.

- **Coomassie Blue Staining Solution**

• First, prepare Coomassie stock by dissolving 24 g of Coomassie brilliant blue R-250 into 600 ml of 100% methanol and 120 ml of acetic acid. Store at RT.

• Second, make Coomassie blue staining solution (2x) by combining 60 ml of Coomassie stock with 500 ml methanol, 100 ml acetic acid and 400 ml of distilled water. Store at RT.

- **Stop Solution (H_2SO_4, 1 M)**

• Combine 28 ml of 95% sulfuric acid and 972 ml of distilled water. Store at RT.

2. Buffers

- **TAE Agarose Electrophoresis Buffer**

• First, prepare a 50x TAE buffer stock by dissolving 242 g of Tris-base into 57.1 ml acetic acid and 100 ml of 0.5 M EDTA (pH 8). Adjust pH to 7.4 with 10% HCl. Top up the volume to 1 L with distilled water. Filter-sterilize and store at RT.

• Second, make 1x TAE buffer by combining 20 ml of 50x TAE buffer with 980 ml of distilled water. Filter-sterilize and store at RT.

- **Phosphate Buffered Saline (PBS, pH 7.6)**

• First, prepare a 10x PBS stock concentration by dissolving 80 g of sodium chloride (NaCl), 2 g of potassium chloride (KCl), 14.2 g of disodium phosphate (Na_2HPO_4) and 2.4 g of monopotassium phosphate (KH_2PO_4) into 500 ml of distilled water.

Adjust pH to 7.6 with 10% HCl and top up the volume to 1 L with distilled water. Filter-sterilize and store at RT.

- Second, make 1x PBS buffer by combining 100 ml of 10x PBS with 900 ml of distilled water. Filter-sterilize and store at RT.

- **Phosphate Buffered Saline with Tween (PBST)**

- Add 500 µl of Tween 20 to 1 L of 1x PBS (i.e., 0.05% v/v). Filter-sterilize and store at RT.

- **Tris-HCl (0.5 M, pH 6.8, 250 ml)**

- Dissolve 15.143 g of Tris-base into 100 ml of distilled water. Adjust to pH 6.8 with 10% HCl and top up the volume to 250 ml with distilled water. Filter-sterilize and store at RT.

- **Tris-HCL (1 M, pH 6.8, 200 ml)**

- Dissolve 24.1 g of Tris-base into 100 ml of distilled water. Adjust to pH 8.8 with 10% HCl and top up the volume to 200 ml with distilled water. Filter-sterilize and store at RT.

- **Tris-HCl (1.5 M, pH 8.8, 500 ml)**

- Dissolve 90.855 g of Tris-base into 100 ml of distilled water. Adjust to pH 8.8 with 10% HCl and top up the volume to 500 ml with distilled water. Filter-sterilize and store at RT.

- **SDS-PAGE Running Buffer**

• First, prepare a 10x running buffer stock concentration by dissolving 30.2 g of Tris-base, 10 g of SDS and 144 g of glycine into 500 ml of distilled water. Top up the volume to 1 L with distilled water. Store at RT.

• Second, make 10x running buffer by combining 100 ml of 10x running buffer with 900 ml of distilled water. Store at RT.

- **Western Blotting Transfer buffer**

• Dissolve 3.03 g of Tris-base and 14.42 g of glycine into 40 ml of methanol and 200 ml of distilled water. Top up the volume to 1 L with distilled water. Store at 4°C.

- **Skim Milk Blocking Buffer (4%)**

• Dissolve 2 g of skim milk into 50 ml of 1 x PBST buffer. Use immediately.

- **De-staining Buffer**

• Combine 100 ml of methanol, 50 ml of acetic acid and 350 ml of distilled water. Store at RT.

3. Gels

- **Agarose Gel (1%) for Electrophoresis**

• Add 0.5 g agarose powder and 50 ml 1x TAE buffer to a conical flask. Microwave for ~1 min with regular swirling until melted; no solid should be visible. Cool conical flask and swirling the contents until the flask can be held comfortably. Add 10 µl of

cyber-safe dye to the flask and swirl to mix. Pour the gel into the gel tray with combo with care not not produce bubbles. Leave until set (solid).

- **Polyacrylamide Resolving Gel (12%) for SDS-PAGE**

• Combine 3.2 ml of 30% acrylamide (Cat. #1610158, Bio-Rad Laboratories, Inc., Hercules, CA, USA), 2 ml of 1.5 M Tris-HCl (pH 8.8), 2.6 ml of distilled water, 80 µl of 10% SDS solution, 80 µl of 10% APS solution and 8 µl of Tetramethylethylenediamine (TEMED; Cat. #161-0801, Bio-Rad Laboratories, Inc., Hercules, CA, USA). Mix gently and pipette 7.5 ml of the gel solution between the glass plates. Top up with 70% ethanol and leave until set (solid).

- **Polyacrylamide Stacking Gel (6%) for SDS-PAGE**

• Combine 1 ml of 30% acrylamide, 1.25 ml of 0.5 M Tris-HCl (pH 6.8), 2.6 ml of distilled water, 50 µl of 10% SDS solution, 50 µl of 10% APS solution and 6 µl of TEMED. Mix gently and pour on the top of resolving gel after discarding the ethanol. Add a combo and leave until set (solid).

4. Bacterial Culture Media

Note: add the same number of µl of antibiotic stock as the ml volume of media.

- **Luria-Bertani (LB)**

• For LB broth, dissolve 10 g tryptone, 5 g yeast extract and 10 g NaCl in distilled water and adjust pH to 7.0 with sodium hydroxide (NaOH). Make up to a final volume of 1,000 ml with distilled water. Autoclave for 15 min at 121°C.

• For LB agar plates, add 15 g agar to 1 L of LB broth (adjusted pH to 7.0 with NaOH) and autoclave. Allow the medium to cool to 45°C before adding a suitable antibody at a required concentration (e.g., 50 µg/ml for Kan and 100 µg/ml for Amp). Pour 30-35 ml of medium into 85 mm petri dishes. Let the agar harden. Store at 4°C for up to a month.

• For LB agar plates with ampicillin/IPTG/X-Gal, make the LB plates with ampicillin as above; then supplement with 0.5 mM IPTG and 80 µg/ml X-Gal (Cat. #V394A, Promega, Madison, WI, USA) and pour the plates. Alternatively, 100 µl of 100 mM IPTG and 20 µl of 50 mg/ml X-Gal may be spread over the surface of an LB-Amp plate and allowed to absorb for 30 min at 37°C prior to use.

- **SuperBroth Medium**

• Dissolve 35 g of tryptone, 20 g of yeast extract and 5 g of 0.5% NaCl into 500 ml of distilled water. Add 1 ml of 1 N NaOH and top up the volume to 1 L with distilled water. Autoclave to sterilize.

- **2x YT medium**

• Dissolve 16 g of tryptone, 10 g of yeast extract and 5 g of 0.5% NaCl into a final volume of 1 L distilled water. Autoclave to sterilize.

- **Terrific Broth Nutrient (TB, 10x)**

• Dissolve 12 g of tryptone, 24 g of yeast extract and 5 ml of glycerol into a final volume of 100 ml distilled water or 10x TB salts. Autoclave to sterilize.

• For 10x TB salts (100 ml), prepare phosphate buffer by dissolving 2.31 g of monopotassium phosphate (KH_2PO_4) and 12.54 g of dipotassium phosphate (K_2HPO_4) into a final volume of 100 ml distilled water. Autoclave to sterilize.

APPENDIX 2. CLONING AND TRANSFORMATION OF EXPRESSION CASSETTES

In the following pages, the results from gene cloning and DNA analysis experiments are presented. Specifically, RV-V_HHs, RV-CBM2a-V_HHs, RV-V_HH-CBM2a, RV-IgG 26 and RV-VP_6 were all introduced in bacteria.

1. Competent Bacterial Cells

After transforming 100 µl of competent cells with 0.1 ng of uncut plasmid DNA, the transformation reaction was added to 900 µl of LB medium. From that volume, a 1:10 dilution with LB medium (0.01 ng DNA/µl) was made and 100 µl plated on 2 plates (0.001 ng DNA/100µl). An average of around 80-120 colonies were obtained and the transformation efficiency was calculated to be about $15x10^6$ cfu/ng DNA.

2. Recombinant RV-V_HHs and RV-V_HHs with CBM2a

The nucleotide sequences encoding 2KD1 and 3B2 V_HH genes as well as V_HHs linked to a native CBM2a were all synthesized for prokaryotic (*E. coli*) expression system by GeneWiz. The restriction enzyme sites NcoI and NotI were added at the 5' and 3' ends, respectively, to facilitate cloning into the pITKan expression vector. However, to prevent the expression of the 6x-His tag hence avoiding cross reactivity with anti-his antibody in ELISAs, templates of HA-2KD1-$([PT]_3T)_{3x}$S-CBM2a, HA-CBM2a-$(G_4S)_{3x}$-2KD1 and HA-2KD1-$(G_4S)_{3x}$-CBM2a were designed to contain a stop codon before the 6x-His and NotI site at the C-terminal of pITKan vector.

After synthesis of the genes for 2KD1 (382 bp), 3B2 (385 bp), HA-CBM2a-$([PT]_3T)_{3x}$S-2KD1-His (802 bp), HA-CBM2a-$([PT]_3T)_{3x}$S-3B2-His (805 bp), HA-2KD1-$([PT]_3T)_{3x}$S-CBM2a (805 bp), HA-CBM2a-$(G_4S)_{3x}$-2KD1 (787 bp) and HA-2KD1-$(G_4S)_{3x}$-CBM2a (787 bp), each DNA was subcloned into the pITKan expression vector (4,453 bp) via NcoI and NotI restriction enzyme sites. This resulted in seven vectors 2KD1 (4,838 bp), 3B2 (4,835 bp), HA-CBM2a-$([PT]_3T)_{3x}$S-2KD1-His (5,255 bp), HA-CBM2a-$([PT]_3T)_{3x}$S-3B2-His (5,258 bp), HA-2KD1-$([PT]_3T)_{3x}$S-CBM2a (5,258 bp), HA-CBM2a-$(G_4S)_{3x}$-2KD1 (5,240 bp) and HA-2KD1-$(G_4S)_{3x}$-CBM2a (5,240 bp). The cloning of these seven genes into pITKan vector was performed by GeneWis while transformation was successfully done into a home-made electro-competent *E. coli HB2151* using a MicroPulser™ electroporator by the researcher of this project. Several colonies appeared on LB agar plates containing Kan antibiotic while six clones from each transformation were screened by colony PCR using each primer set and reaction conditions indicated previously (Methods Chapter) and found to contain the constructs. The expected sizes for PCR products of pITKan comprising 2KD1 (584 bp), 3B2 (587 bp), HA-CBM2a-$([PT]_3T)_{3x}$S-2KD1-His (1,004 bp) and HA-CBM2a-$([PT]_3T)_{3x}$S-3B2-His (1,007 bp), HA-2KD1-$([PT]_3T)_{3x}$S-CBM2a (1,004 bp), HA-CBM2a-$(G_4S)_{3x}$-2KD1 (986 bp) and HA-2KD1-$(G_4S)_{3x}$-CBM2a (986 bp) (Appendices 2.1-2.3).

Once positive clones were confirmed, only one colony was selected for plasmid DNA extraction, digestion and sequence analysis. The expected sizes of 2KD1 (382 bp), 3B2 (385 bp), HA-CBM2a-$([PT]_3T)_{3x}$S-2KD1-His (802 bp), HA-CBM2a-$([PT]_3T)_{3x}$S-3B2-His (805 bp), HA-2KD1-$([PT]_3T)_{3x}$S-CBM2a (805 bp), HA-CBM2a-$(G_4S)_{3x}$-2KD1 (787 bp)

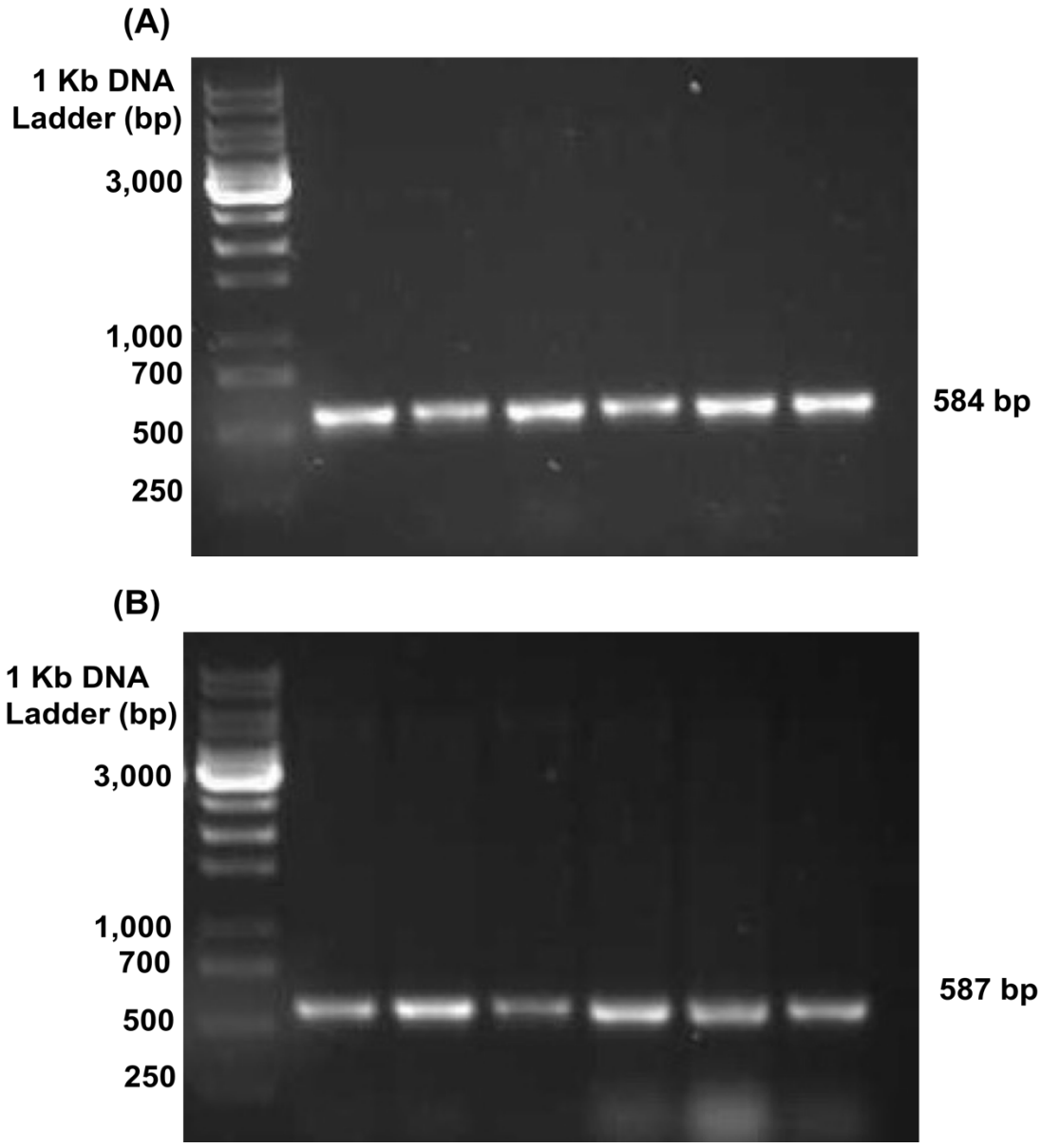

Appendix 2.1. Colony PCR of anti-rotavirus group A single domain antibody "V_HH" into the pITKan bacterial expression vector to confirm putative transformants using vector specific primers. (A) A 1% DNA agarose gel showing the PCR amplification of six selected colonies containing 2KD1 (584 bp). (B) A 1% DNA agarose gel showing the PCR amplification of six selected colonies containing 3B2 (587 bp). Selected colonies of the transformants grown on LB with kanamycin agar plate.

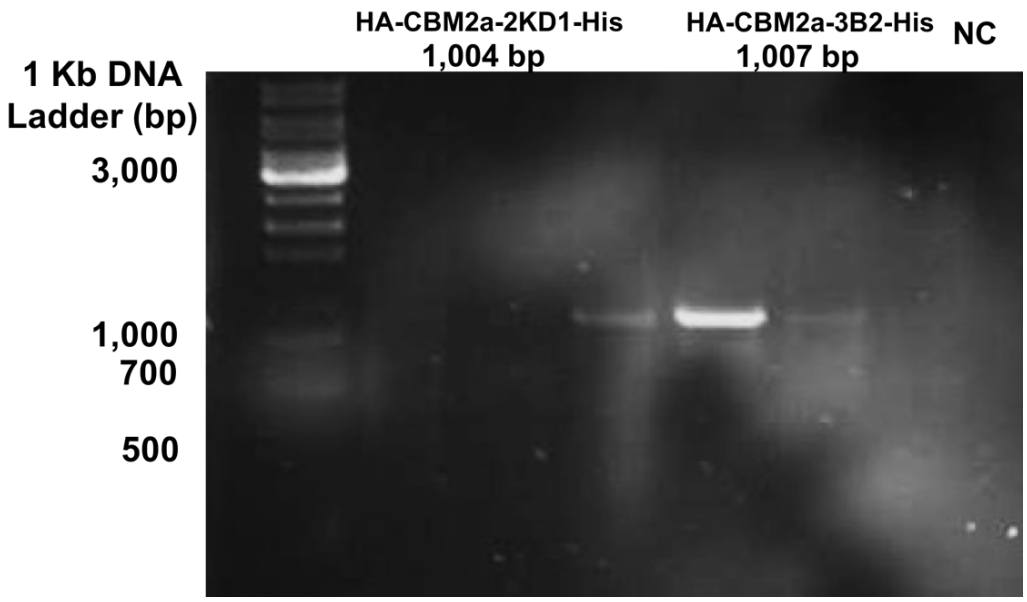

Appendix 2.2. Colony PCR of anti-rotavirus group A single domain antibody "V_HH" linked to CBM2a at C-terminal via a proline-threonine linker into the pITKan bacterial expression vector on a 1% agarose gel to confirm putative transformants using vector specific primers. Selected colonies of the transformants grown on LB with kanamycin agar plate. Lane 1, 1 Kb DNA standard. NC: negative control.

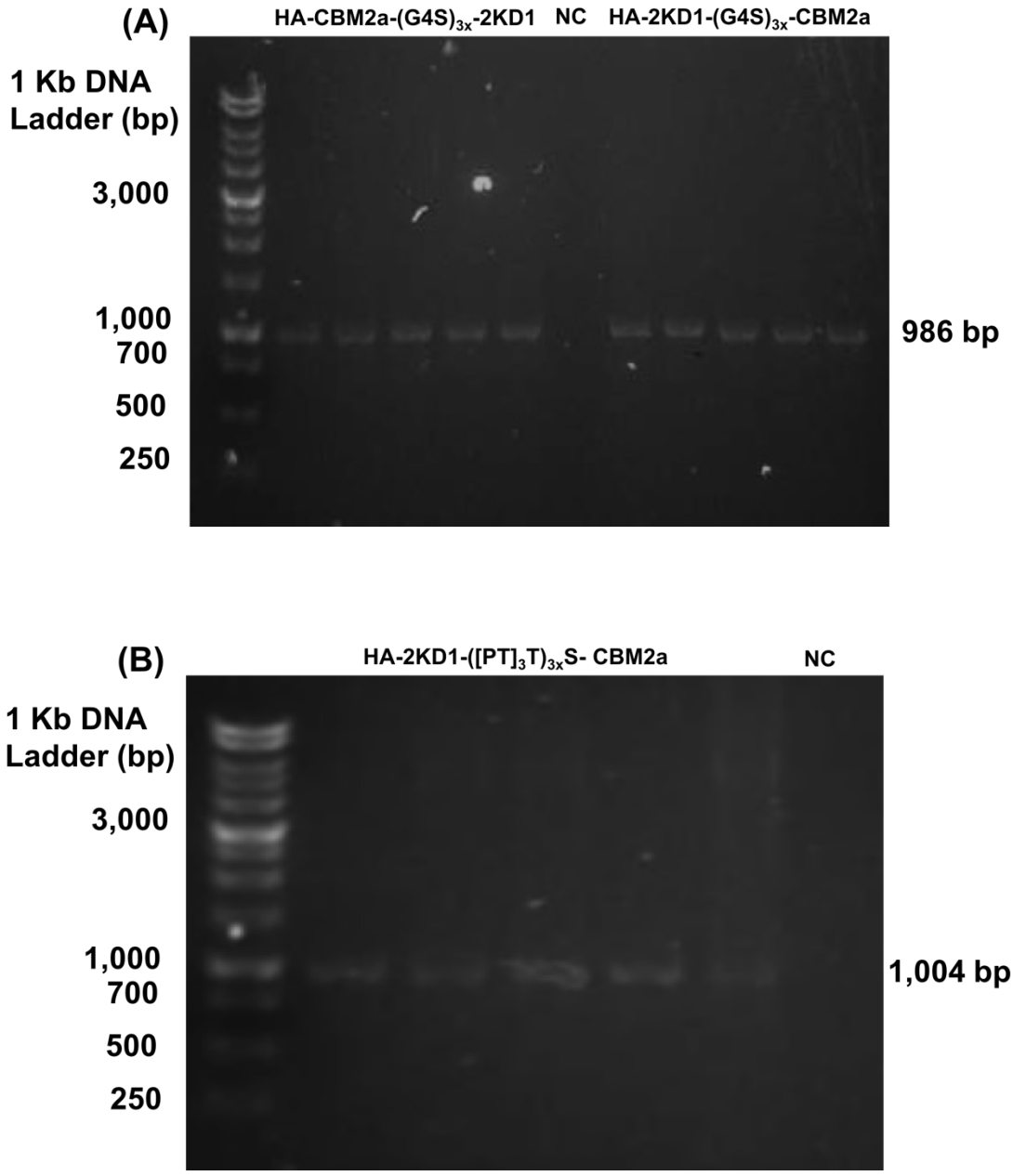

Appendix 2.3. Colony PCR of anti-rotavirus group A single domain antibody "V_HH" linked at C and N-terminals to CBM2a via two flexible linkers into the pITKan bacterial expression vector. (A) A 1% DNA agarose gel showing the PCR amplification of selected colonies containing HA-CBM2a-$(G_4S)_{3x}$-2KD1 (986 bp) and HA-2KD1-$(G_4S)_{3x}$-CBM2a (986 bp), respectively. (B) A 1% DNA agarose gel showing the PCR amplification of selected colonies containing HA-2KD1-$([PT]_3T)_{3x}$S-CBM2a (1,004 bp). Selected colonies of the transformants grown on LB with kanamycin agar plate. NC: negative control.

and HA-2KD1-$(G_4S)_{3x}$-CBM2a (787 bp) and vector (4,453 bp) after digestion with NcoI and NotI are shown in Appendix 2.4. The DNA sequencing results indicated a 100% match to the predicted nucleotide sequences.

3. Recombinant RV-HA-CBM2a

Similarly, to prevent the expression of the 6x-His tag hence avoiding cross reactivity with anti-His antibody in ELISAs, a stop codon was created before the linker region followed by NotI at the C-terminal of HA-CBM2a-$([PT]_3T)_{3x}$S-2KD1-His (1004 bp) template. The resulting construct named HA-CBM2a was used as a negative control antibody throughout experiments in this research. The plasmid pITKan HA-CBM2a (376 bp) was prepared using a PCR product amplified from DNA extracted from a 25% glycerol stocks of HA-CBM2a-$([PT]_3T)_{3x}$S-2KD1-His (1,004 bp) using each primer set and reaction conditions indicated previously (Appendix 2.5 A). The PCR product was cloned into the pGEM® -T Easy vector (3,000 bp) and transformed into competent *E. coli DH5α* cells, as per the manufacturer's instructions. Putative transformants were selected on LB agar plates containing 100 µg/ml Amp, 0.5 mM IPTG, and 80 µg/ml X-Gal. Successful cloning of an insert into the pGEM®-T vector interrupts the coding sequence of β-galactosidase; recombinant clones can be identified by color screening on a plate. Usually clones containing the gene produce white colonies, but blue colonies can result from inserted fragments that are cloned in-frame with the lac Z gene within the vector. Such fragments are usually a multiple of 3 base pairs long (including the 3'-A overhangs) and do not contain in-frame stop codons. The plasmid was screened for presence of the target gene

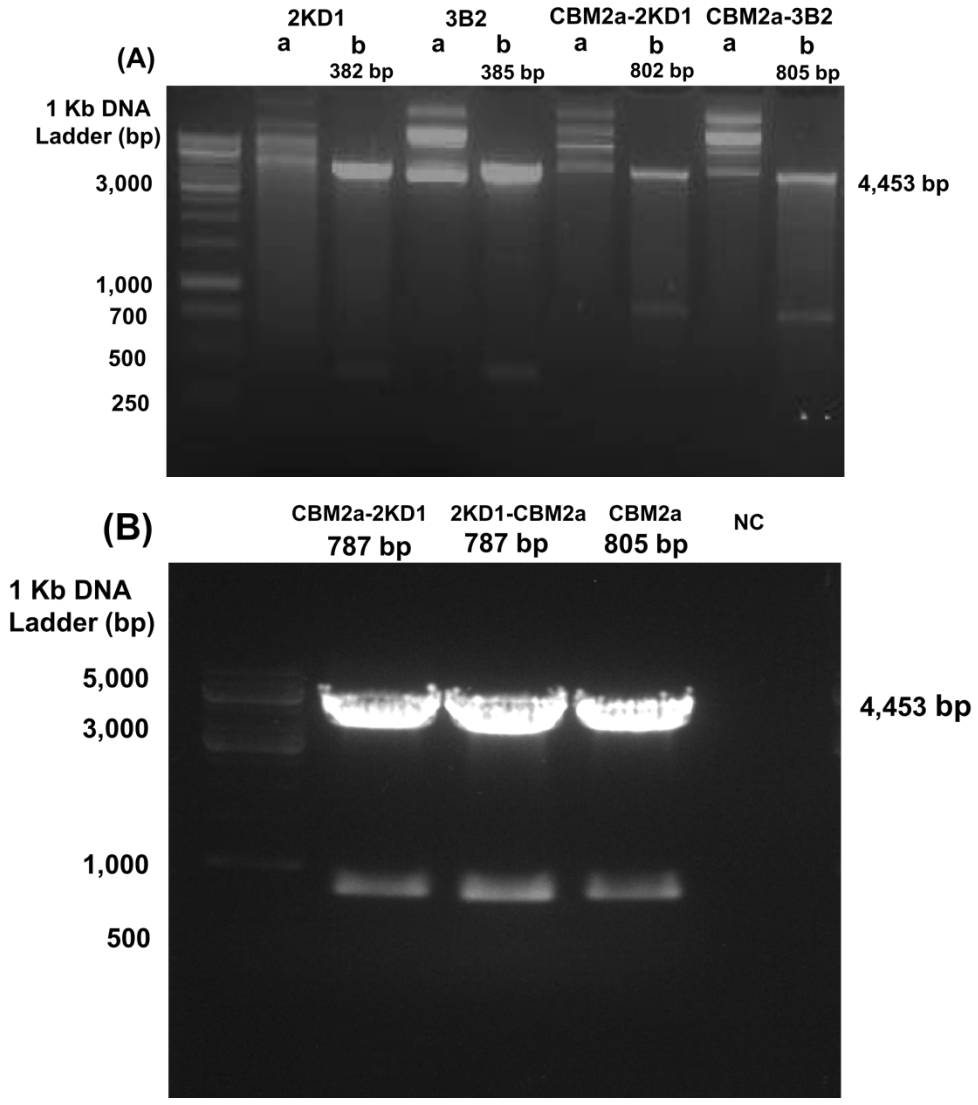

Appendix 2.4. Linearization of pITKan/V_HHs constructs with and without CBM2a by restriction enzymes NcoI and NotI for *E. coli HB2151* transformants. (A) A 1% DNA agarose gel illustrating a diagnostic double-digest of 2KD1 (383 bp), 3B2 (385 bp) and HA-CBM2a-$([PT]_3T)_{3x}$S-2KD1-His (802 bp) clones. Letter a, undigested DNA. Letter b, digested DNA with NocI and NotI restriction enzymes. (B) A 1% DNA agarose gel illustrating a diagnostic double-digest of HA-CBM2a-$(G_4S)_{3x}$-2KD1 (787 bp), HA-2KD1-$(G_4S)_{3x}$-CBM2a (787 bp) and HA-2KD1-$([PT]_3T)_{3x}$S-CBM2a (805 bp). NC: negative control.

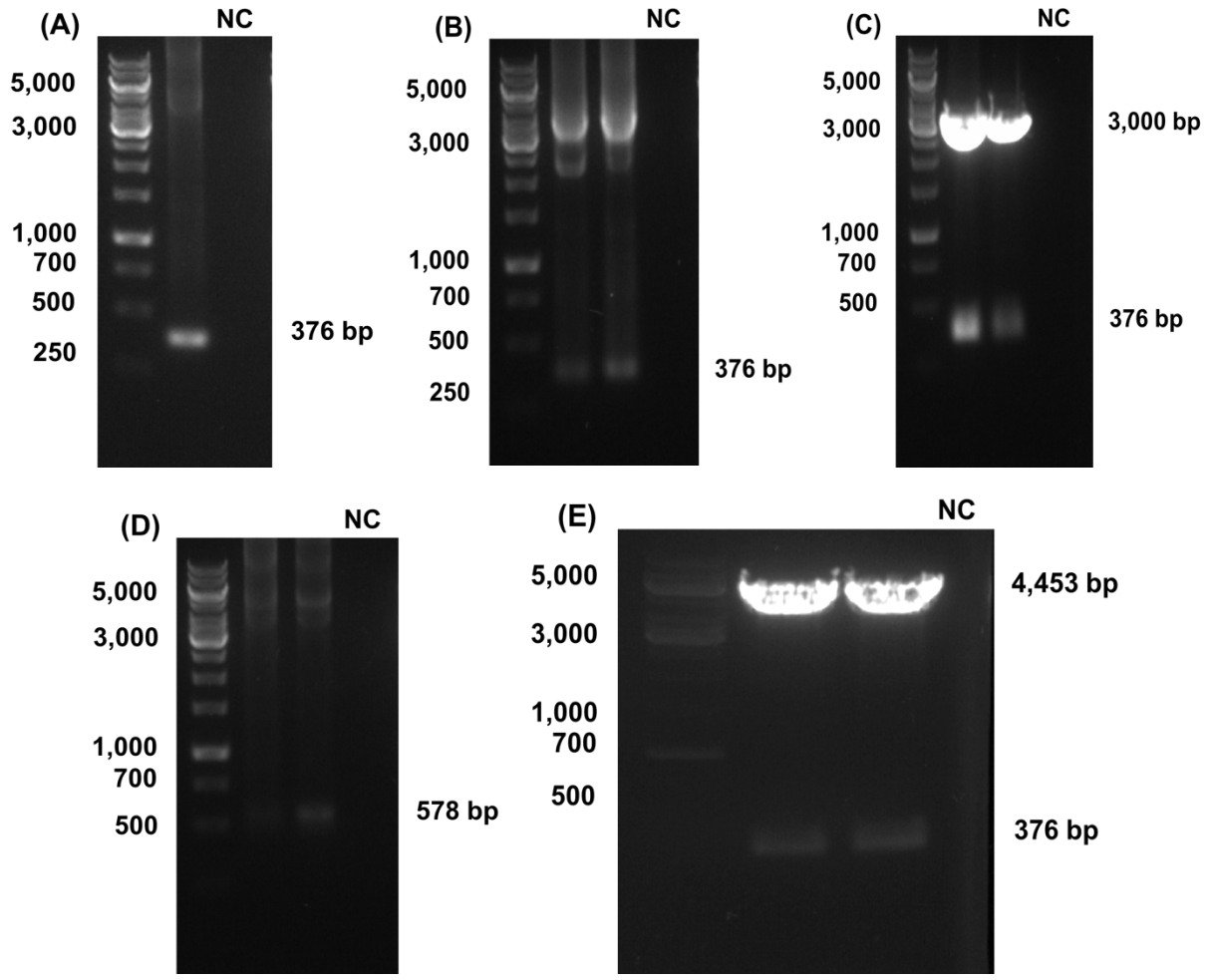

Appendix 2.5. A 1% DNA agarose gel showing cloning and transformation procedure of HA-CBM2a into pGEM®-T and pITKan vectors to createe pITKan/HA-CBM2a. (A) Gene HA-CBMa amplification (376 bp) from HA-CBM2a-$([PT]_3T)_{3x}$S-2KD1 (802 bp) template. (B) Colony PCR of selected colonies containing pGEM®-T-HA-CBM2a. (C) Diagnostic double-digest of pGEM®-T-HA-CBM2a (376 bp) with restriction enzymes NcoI and NotI for transformation into *E. coli DH5α* cloning cells. (D) Colony PCR of selected colonies containing pITKan/HA-CBM2a (578 bp). (E) Diagnostic double-digest of pITKan/HA-CBM2a (376 bp) with restriction enzymes NcoI and NotI for transformation into *E. coli HB2151* expression cells. Lane 1: 1 Kb DNA standard. NC: negative control.

by colony PCR. Positive clones that found to have the target gene, resulted in vector pGEM®-T- HA-CBM2a (Appendix 2.5 B). Transformed *E. coli* cells were then propagated in LB broth with Amp, plasmids were extracted using the Gene JET Plasmid Miniprep and were sent for sequencing. Plasmid DNA concentrations were determined at 260 nm using a Nanodrop spectrophotometer and digested with NcoI and NotI restriction enzymes for overnight at 37ºC. The expected size of pGEM®-T comprising HA-CBM2a (376 bp) for PCR product and after digestion with NcoI and NotI is shown in Appendix 2.5 C.

Once the sequence of the gene confirmed, the gene was gel purified using the Gene JET gel extraction kit and subcloned into a linearized pITKan digested with NcoI and NotI. The gene was then successfully transformed into electro competent *E. coli HB2151* and plated on selective LB plates with 50 µg/ml kan antibiotic. Putative transformants were confirmed by colony PCR using each primer set and reaction conditions indicated previously. The expected sizes for PCR product of pITKan comprising HA-CBM2a and for DNA after digestion with NcoI and NotI are 578 and 376 bp, respectively (Appendix 2.5 D-E).

The DNA sequencing results indicated a 100% match to the predicted nucleotide sequences.

4. Recombinant RV-IgG 26

The codon optimized H_C (1,433 bp) and L_C (725 bp) fragments for expression in plant were synthesized and subcloned into a plant expression vector (pPFC0205) via SacI and BamHI restriction enzymes. This resulted into plasmid named pPFC0205-RV-IgG (11,110

bp), known as RV-VP_6-IgG 26 RV-IgG. Genes synthesis and subcloning was performed by GeneWiz.

In plant research, usually, an *A. tumefaciens*-mediated transformation procedure is used to generate transgenic plants. In this procedure, the bacteria (*A. tumefaciens*) carries an engineered binary plasmid harboring the gene of interest for integration into the plant genome. To confirm the *Agrobacterium* harboring the expression plasmid, miniprep plasmid extraction was performed. However, due to the low plasmid copy number in *Agrobacterium* and the recalcitrance of the bacteria strain to cell lysis, the extraction of the binary plasmid from *A. tumefaciens* is extremely problematic. Therefore, to verify the correct construct prior to plant transformation, the pPFC0205-RV-IgG 26 plasmid was first transformed into a chemical competent cells of *E. coil DH5a* cell to propagate. Several colonies appeared on LB agar plates containing 50 µg/ml Carb or Amp antibiotic from transformation and few colonies were selected for DNA analysis. Then DNA was extracted from a 5 ml overnight culture supplemented with Carb or Amp using the Gene JET Plasmid Miniprep and subjected to restriction digestion verification by SacI and BamHI restriction enzymes (Appendix 2.6). The DNA was linearized with SacI and BamHI and separated on 1% 1x TA EDTA agarose gel resulted in four fragments at expected size of whole plasmid cut from onset of BamHI-H_C to the end of SacI-L_C sites (9,662 bp), cut between SacI-H_C and BamHI-L_C genes (7,530 bp), cut of BamHI-H_C to SacI-H_C (1,433 bp) and cut of BamHI-L_C to SacI-L_C (725 bp) (Appendix 2.6). Single DNA digestion with either SacI or BamHI, however, showed two fragments in which one fragment represents a cut of whole plasmid containing H_C and L_C (9,662 bp) while the other fragment represents a cut from SacI-HC to SacI-LC (2,868 bp) or a cut from BamHI-

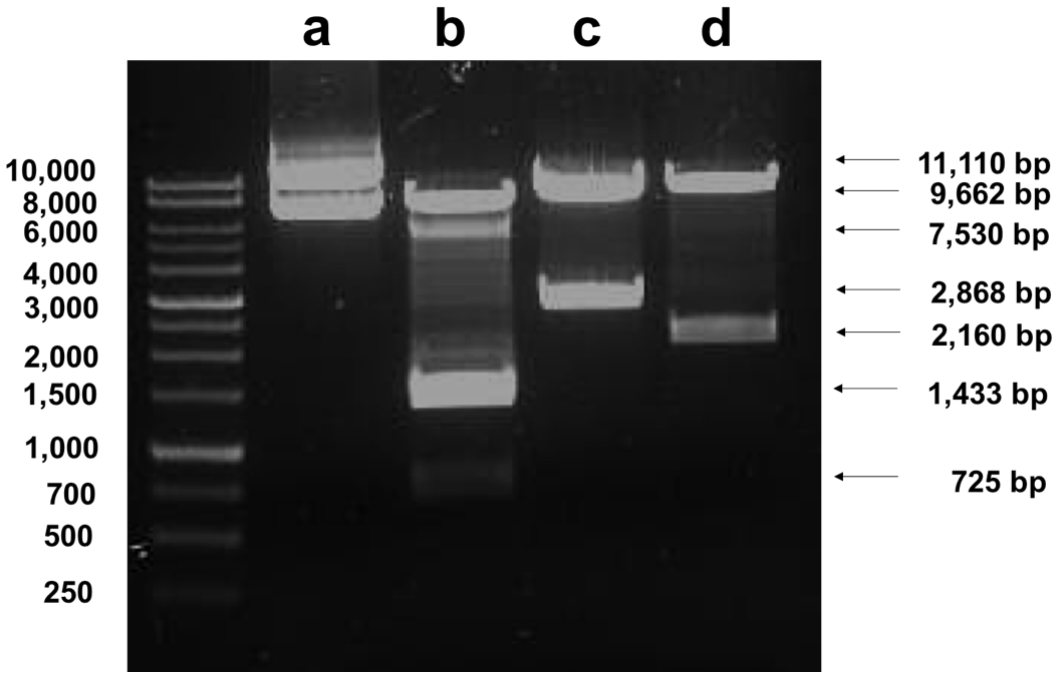

Appendix 2.6. Diagnostic digest of pPFC0205-IgG 26 (11,110 bp) with restriction enzymes SacI and BamHI from transformation into *E. coli DH5α* cloning cells. Lane 1: 1 Kb DNA standard. Lane labelled "a" present undigested DNA. Lane labelled "b" represent double digested DNA with SacI and BamHI. Lane labelled "c" represent single digest DNA with SacI. Lane labelled "d" represent single digest DNA with BamHI. Arrows on the left of picture represent size of each fragment in bp.

H_C to BamHI-L_C (2,160 bp), respectively. Once correct size was confirmed, the RV-IgG 26 plasmid was then transformed into into *A. tumefaciens* for expression in plant's leaves (*N. benthamiana*) without a need to confirm the sequence of the gene.

5. Recombinant Protein RV-VP_6

The nucleotides encoding the VP_6 gene was optimized and synthesized for prokaryotic (*E. coli*) expression system by GeneWiz. The restriction enzyme sites NcoI and NotI were added at the 5' and 3' ends, respectively, to facilitate cloning into the pITKan expression vector. After synthesis, the DNA (1,201 bp) was subcloned into the pITKan expression vector (4,453 bp) via NcoI and NotI restriction enzyme sites resulted in vector pITKan/VP_6 (5,654 bp). Cloning of RV-VP_6 gene into pITKan vector (4,453 bp) was performed by GeneWis while subcloning of RV-VP_6 gene into pET22b$^{(+)}$ (5,493 bp) and pET-SUMO (5,628 bp) vectors were done by PCR amplification using gene specific primers from the template pITKan/VP_6. The expected sizes of amplified VP_6 were 1,205 and 1,225 bp for pET22b$^{(+)}$/VP_6 and pET-SUMO/VP_6, respectively (Appendix 2.7 A). Upon transformation of a suitable *E. coli* cloning host with each corresponding vector, several clones appeared on LB agar plates supplemented with suitable antibiotic. Clones from each transformation were screened by colony PCR, using primers reported in previous chapter, and found to express VP_6 in *E. coli*. The expected sizes of pET22b$^{(+)}$/VP_6 and pET-SUMO/VP_6 from colony PCR are 1,205 and 1,446 bp, respectively (Appendix 2.7 B-E). Once positive clones were confirmed, only one clone from the expression host of the *E. coli HB 2125* and *LB21* was selected for plasmid DNA extraction, digestion and sequence analysis. The expected size of RV-VP_6 within pITKan and pET22b$^{(+)}$ after digestion with NcoI and

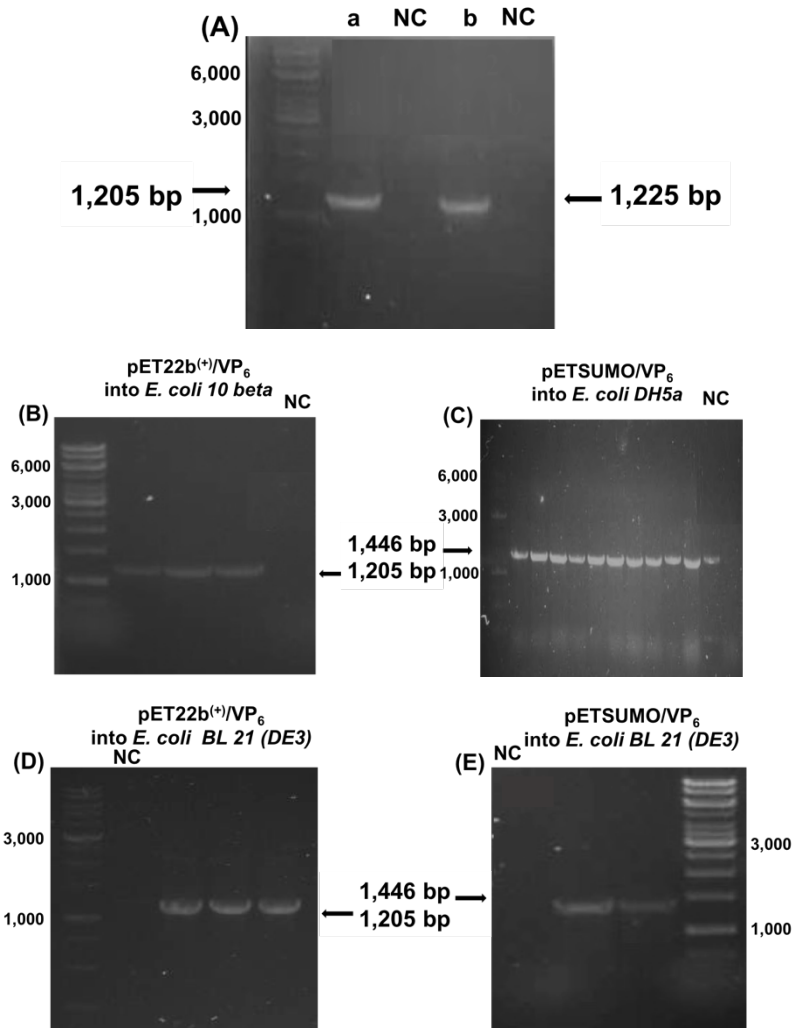

Appendix 2.7. A 1% DNA agarose gel showing cloning and transformation procedure of RV-VP6 capsid protein into pET22b$^{(+)}$ and pET-SUMO vectors to create pET22b$^{(+)}$/VP6 and pET-SUMO/VP6. (A) Gene VP6 amplification from pITKan/VP6 template (1,201 bp) for (1) pET22b$^{(+)}$ (1,205 bp) and (2) pET-SUMO (1,225 bp). (B-C) Colony PCR of selected colonies of *E. coli DH5α* containing pET22b$^{(+)}$/VP6 (B; 1,205 bp) and *E. coli 10 beta* containing pET-SUMO/VP6 (C; 1,446 bp). (D-E) Colony PCR of selected colonies of *E. coli LB21* containing pET22b$^{(+)}$/VP6 (D; 1,205 bp) and pET-SUMO/VP6 (C; 1,446 bp). Lane 1: 1 Kb DNA standard. Lanes labelled "a" and "b" represent PCR product. NC: negative control.

NotI is 1,201 bp (Appendix 2.8). The DNA sequence results indicated a 100% match to the predicted nucleotide sequences for all plasmids.

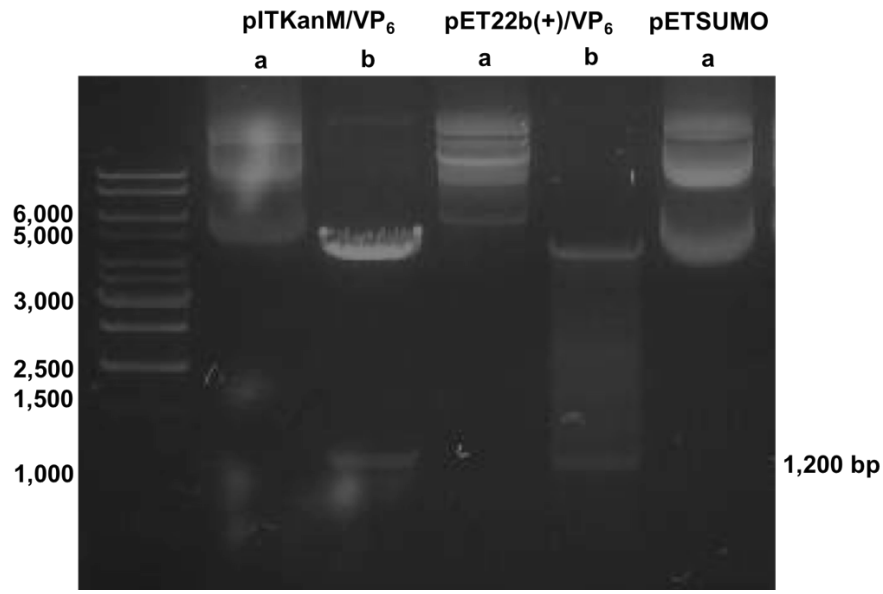

Appendix 2.8. A 1% DNA agarose gel illustrating a diagnostic double digest of VP6 gene cloned into pITKan (4,453 bp) and pET22b$^{(+)}$ (5,493 bp) with restriction enzyme/s NcoI and NotI whereas BsaI digestion of pET-SUMO vector (5,628 bp). The size of VP6 gene (1,200 bp) is noted. Lane 1: 1 Kb DNA standard. Lane labelled "a" represent undigested DNA. Lane labelled "b" represent digested DNA with restriction enzyme/s.

APPENDIX 3. PURIFICATION OF RV-V_HHS FROM LONG EXPRESSION PROTOCOL

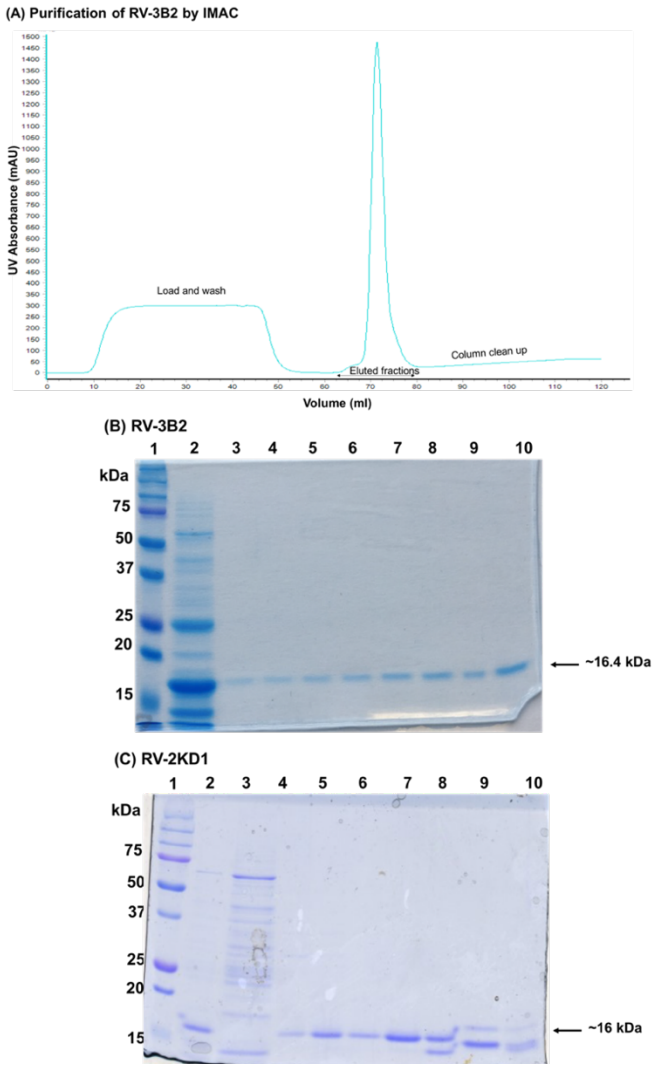

Appendix 3.1. Expression and purification of RV-V_HHs expressed with long protocol (*E. coli HB2151* (pITKan/2KD1) culture induced with 0.1 mM IPTG at 24^{0}C for 60 h). The periplasmic protein was extracted via sucrose shock protocol and applied to Ni^2-resin. After column washing, RV-V_HH was eluted over 500 mM imidazole in 1 ml fractions. (A) Affinity 6x-His tag chromatography purification profile illustrating the absorbance at 280 nm and collection of eluted fractions (blue line). (B) A 12% SDS-PAGE gel indicating expression and purification of RV-3B2 (1.5 µl of protein observed at about 16.4 kDa). (C) A 12% SDS-PAGE gel indicating expression and purification of RV-2KD1 (1.5 µl of protein observed at about 16 kDa). Lane 1: protein standard. Lane 2: Total soluble protein (TSP) from un-induced *E. coli HB2151* (pITKan/2KD1) culture. Lane 3: TSP from induced *E. coli HB2151* (pITKan/2KD1) culture, Lane 4: column wash. Lanes 5-10: eluted fractions of RV-2KD1.

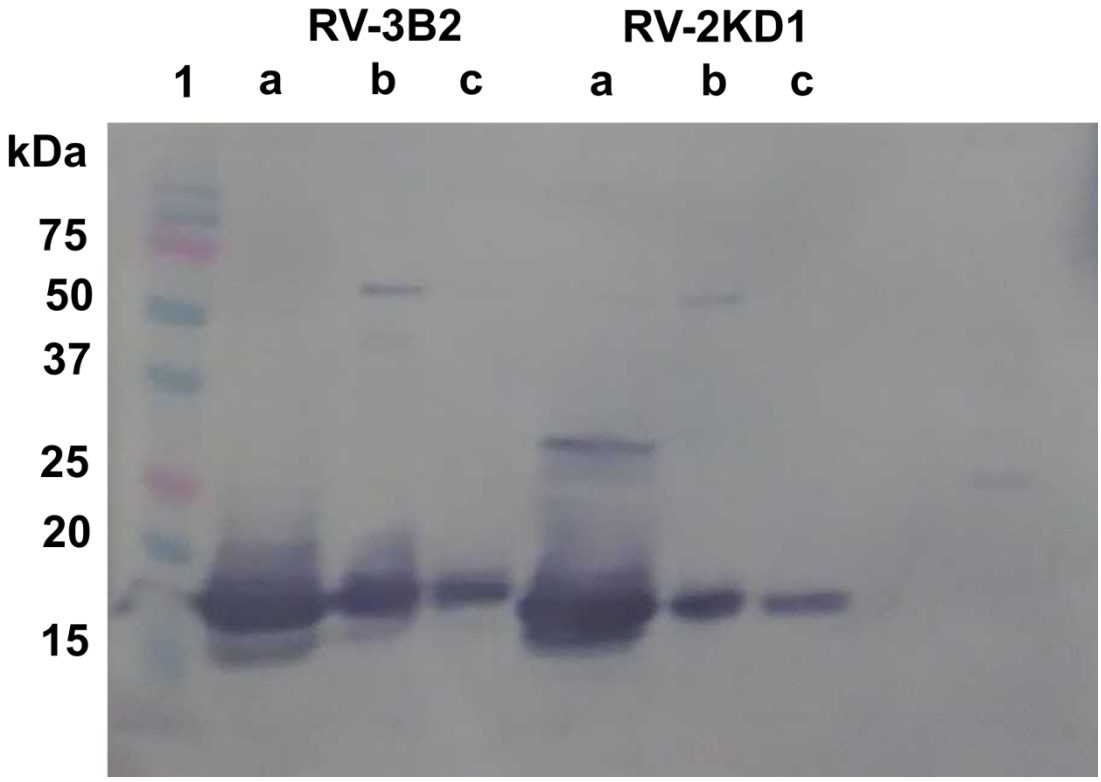

Appendix 3.2. Western blot analysis of expressed and purified RV-3B2 and RV-2KD1 as presented in Appendix 3.1. Total soluble proteins (TSP) and pooled purified proteins were run on 12% SDS-PAGE gel before transferring to PVDF membrane and probed with a polyclonal anti-His antibody conjugated to alkaline phosphate. Lane 1: protein standard. Lanes labeled "a" represent TSP of RV-V_HHs (diluted to 1:10). Lanes labeled "b" represent pooled purified of RV-V_HHs (diluted to 1:5). Lanes labeled "c" represent pooled purified of RV-V_HHs (diluted to 1:3)

APPENDIX 4. ANALYSIS OF RV-VP_6 EXPRESSION AND PURIFICATION

1. Analysis of Recombinant RV-VP_6

The fusion protein VP_6 was expressed in two strains of *E. coli* using 3 different vectors. The *E. coli HB2151* strain was used with pITKan vector while *E. coli BL21 (DE3)* strain was used with pET22b$^{(+)}$ and pET-SUMO vectors. The pITKan and pET22b$^{(+)}$ vectors contain a C-terminal 6x-His tag while pET-SUMO vector contains an N-terminal 6x-His tag followed by a SUMO tag. The expression levels of VP_6 from 2 different *E. coli* strains transformed with corresponding plasmid were subjected to a pilot expression test. The proteins were expressed in a small scale of 250 ml LB broth with 1 mM of IPTG for 3 h at 37°C and with 0.25 mM of IPTG for 12 h at 24°C. The expression conditions that were tested included inducer concentration of IPTG in both expression cells (*E. coli HB2151* and *E. coli BL21*) using different His-tag expression vectors, post-induction growth temperature and time. The cell cultures were harvested and bacterial masses were estimated. Bacterial biomasses from 250 ml cultures transformed with pITKan/VP_6, pET22b$^{(+)}$/VP_6 and pET-SUMO/VP_6 plasmids and induced cultures at 1 mM IPTG for 3 h were estimated to be 9.20, 6.30 and 7.68 mg, respectively. On the other hand, bacterial masses from 250 ml cultures transformed with pITKan/VP_6, pET22b$^{(+)}$/VP_6 and pET-SUMO/VP_6 and induced cultures at 0.25 mM IPTG for 12 h were estimated to be 10.12, 7.36 and 8, respectively.

The fusion proteins were extracted using lysozyme and sonication protocols. Soluble and inclusion body fractions of un-induced and induced bacteria with IPTG were assessed by SDS-PAGE (Appendix 4.1). The expected sizes of the His-tag fusion protein

VP_6 were estimated to be 47.5 kDa for pITKan and pET22b$^{(+)}$ and 60 kDa for pET-SUMO with a theoretical pI of 5.83. The high molecular weight of SUMO/VP_6 was due to the presence of histidine residues along with extra amino acids from SUMO tag. The SDS-PAGE gels for soluble and insoluble RV-VP_6 fusion protein (Appendix 4.1) showed no big difference in the expression among different induction conditions (e.g., IPTG concentration, induction- growth temperature and time). As SDS-PAGE gel for soluble RV-VP_6 (Appendix 4.1 A) shown, RV-VP_6 was slightly expressed by *E. coli HB2151* transformed with pITKan/VP_6 plasmid and reasonably by well *E. coli BL 21 (DE3)* transformed with pET-SUMO/VP_6 while no expression was observed when *E. coli BL 21* (*DE3*) transformed with pET22b$^{(+)}$/VP_6 was used. However, total amount of VP_6 fusion protein production was insoluble (Appendix 4.1 B). A better expression of RV-VP_6 in the whole cell lysates was observed when lower concentration of IPTG used in the induction and growth at lower temperature for longer time. Also, there was a degradation of soluble RV-VP_6 fusion protein produced by *E. coli HB2151* transformed with pITKan/VP_6 (Appendix 4.2 A) and complete loss of the fusion protein after purification “very unpure” (Appendix 4.2 B-C).

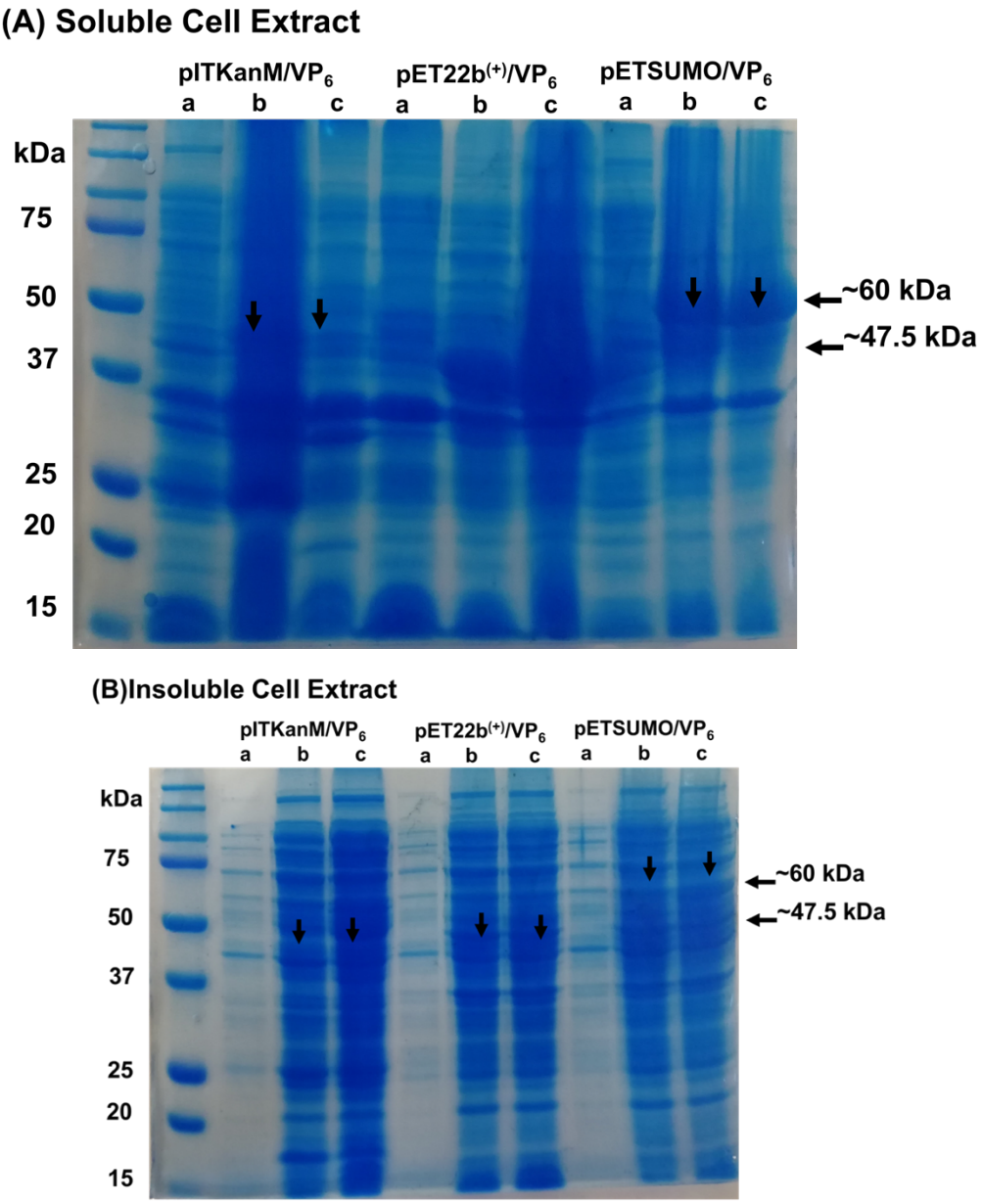

Appendix 4.1. A 12% Sodium dodecyl sulfate polyacrylamide gel electrophoresis (SDS-PAGE; Coomassie blue staining) analysis of RV-VP$_6$ fusion proteins expression in *Escherichia coli*. (A) Soluble cell extract of the induced culture transformed with pITKan/VP$_6$ (*E. coli HB2151*), pET22b$^{(+)}$/VP$_6$ (*E. coli BL21*) and pETSUMO/VP$_6$ (*E. coli BL21*). (B) Insoluble cell extract of the induced culture transformed with pITKan/VP$_6$, pET22b$^{(+)}$/VP$_6$ and pETSUMO/VP$_6$. Note: protein sample loaded on SDS gel in figure B was diluted. Lane 1: protein standard. Lanes labelled "a" represent cell extract from un-induced culture. lanes labelled "b" represent cell extract from induced culture with 1mM IPTG grown at 37ºC for 3 h. Lanes labelled "c" represent cell extract from induced culture with 0.25 mM IPTG grown at 24ºC for 12 h. Arrows refer to RV-VP$_6$ fusion protein (47.5 kDa and 60 kDa).

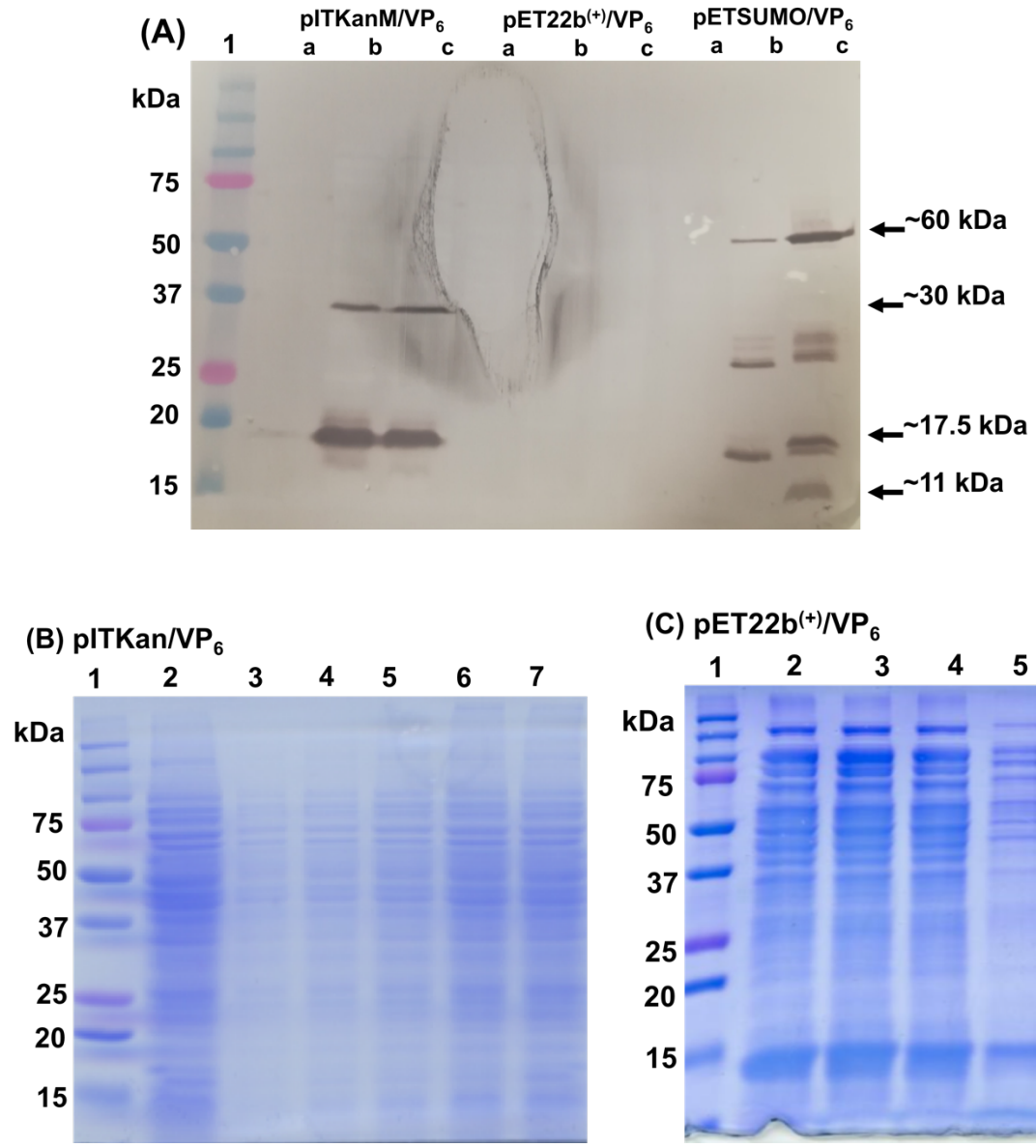

Appendix 4.2. Analysis of RV-VP_6 fusion proteins expression in *E. coli* and purification. (A) Soluble cell extract of the induced culture transformed with pITKan/VP_6 (*E. coli HB2151*), pET22b$^{(+)}$/VP_6 (*E. coli BL21*) and pETSUMO/VP_6 (*E. coli BL21*). (B) Purification trail for soluble RV-VP_6 extracted from induced culture transformed with pITKan/VP_6 (*E. coli HB2151*). (C) Purification trail for soluble RV-VP_6 extracted from induced culture transformed with pET22b$^{(+)}$/VP_6 (*E. coli BL21*). Lane 1: protein standard. Lanes labelled "a" present cell extract from uninduced culture. Lanes labelled "b" represent cell extract from induced culture with 1mM IPTG grown at 37ºC for 3 h. Lanes labelled "c" represent cell extract from induced culture with 0.25 mM IPTG grown at 24ºC for 12 h. Lane 2: total soluble protein. Lane 3: flow through. Lane 4: wash. Lanes 5-7: eluted fractions. Arrows refer to the expected molecular size of detected bands.

2. Discussion

To ensure that these mAb fragments (RV-V_HHs and RV-IgG 26) are not cross reactive with other proteins or other EVs, RV-VP_6 was synthesized for expression in *E. coli* and was aimed to be used as a positive control. The RV-VP_6 plays an important role in the replication cycle of the virus in which makes VP_6 an appropriate vaccine candidate (Bertolotti-Ciarlet et al. 2003). In this regards, different expression systems have been used to produce this protein in a cost-effective manner as a vaccine nevertheless there was no success in the protein production. For example, a study by Pêra et al. (2015) failed to observe VP_6 using a plant expression system (*N. benthamiana*). Bacterial expression systems have also been used as an easy and inexpensive system for the production of RV-VP_6 although recombinant protein was repeatedly found to be insoluble. This result was reported when a gram negative bacterium (*E. coli BL21* strain) was used as an expression host with pETL (Zhao *et al.,* 2011), pET15-b and pTRX (Bugli et al., 2014) bacterial expression vectors. Esteban et al. (2013b), on the other hand, reported an efficient expression of VP_6 on the surface of a gram positive bacterium (*Lactococcus lactis*) with nisin-controlled expression system. Also, a successful expression of soluble VP_6 fusion protein (although most of the VP_6 was insoluble) was reported by Bugli et al. (2014) when an *E. coli BL21* strain with pET-SUMO was used. In this study, the expression of RV-VP_6 was compared in *E. coli BH2151* using pIT vector and in *E. coli BL21* using pET22b$^{(+)}$ and pET-SUMO. Although all these vectors have a His-tag affinity, they differ in a few points. The pIT system has an N-terminal pelB leader sequence, which directs expression of fusion protein to the periplasm, and a His-tag followed by a M-cyc-tag at the C-terminus. The pET22b$^{(+)}$ system also has a His-tag at the C-terminus, but

does not contain a pelB sequence. Although pET-SUMO is compatible with the pET system, it contains an N-terminus His-tag followed by SUMO-tag (cleavage site) that enhances the expression and solubility of fusion proteins. Some of the VP_6 was observed to be degraded on Western blot when pIT was used whereas no soluble protein was observed when pET22b$^{(+)}$ was used. However, pET-SUMO was the only system produced high yield of RV-VP_6. Despite of the expression system, most of the RV-VP_6 fusion protein was insoluble. The practical success of producing a soluble VP_6 with the pIT vector may be due to the pelB leader sequence in the vector or to the *E. coil* strain. The results obtained from pET22b$^{(+)}$ system was in agreement with Kashani and Moniri (2015) who could not produce lysins (phage-encoded peptidoglycan hydrolases) by using this system. However, the result obtained from pET-SUMO was in agreement with the findings reported by Bugli et al. (2014).

APPENDIX 5. EXPRESSION AND PURIFICATION OF SUMO-PROTEASE

The SUMO-protease was expressed in *E. coli Rosetta*. The culture was grown for 3 h at 37°C after induction with final concentration of 1 mM IPTG. The bacterial biomass of SUMO-protease was 9.19 g/L. Total soluble protein was extracted in a lysis buffer by sonication then purified using HisTrap™ Chelating HP IMAC column on FPLC (Appendix 5.1 A). The purity of the protein was analyzed by SDS-PAGE with expected molecular weight of about 25 kDa (Appendix 5.1 B) and theoretical pI of 5.76 for SUMO-protease. The pure enzyme was dialyzed against 20 mM Tris pH 8.0, 200 mM NaCl, 1 mM DTT, 5% glycerol at 4ºC, concentrated on PEG to 1 mg/ml, diluted to 0.5 mg/ml, aliquoted into 200 µl and stored at -80ºC until needed.

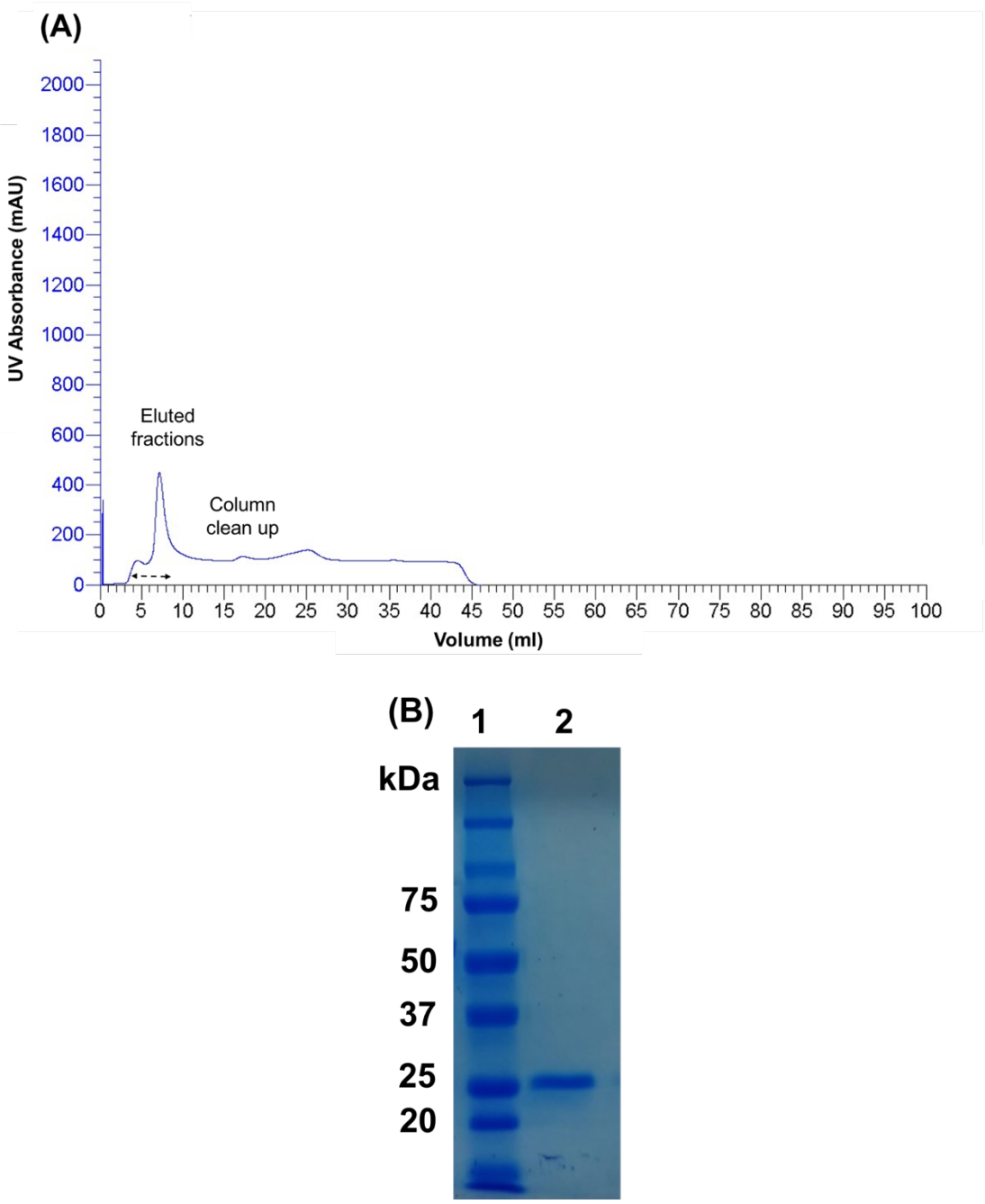

Appendix 5.1. Affinity 6x-His tag chromatography purification of SUMO-Protease. (A) Elution chromatographic profile illustrating the absorbance at 280 nm (blue line) and SUMO-Protease eluted fractions collected with a 250 mM imidazole. (B) A 12% SDS-PAGE gel run under reducing condition indicating the expression and the purity of SUMO-Protease (2 µl loaded) at a molecular weight of about 25 kDa. The fusion protein was expressed in super broth medium and induced with 1 mM IPTG at 37°C for 3 h. The periplasmic protein was extracted via lysozyme protocol and further purified via IMAC. Lane 1: protein standard. Lane 2: eluted fraction of SUMO-Protease.

APPENDIX 6. QUANTIFICATION OF ENTERIC VIRUSES

The results to quantify the virus from molecular methods (qPCR) provide an estimation of both infectious and non infectious particles whereas cell culture-based methods provide an estimation of infectious particles. Cell culture-based methods may be carried out in either solid culture (plaque assay) or liquid culture (tissue culture infective dose TCID 50%; known also as endpoint dilution assay) in which several dilutions of the virus are used for inoculation of the cell culture. After few days of incubation, the quantification of the virus is calculated as pfu in plaque assay and as the logarithm of the dilution of the virus producing CPE of the cultures in the TCID50% assay.

1. Plaque Assay

This test was conducted with all RV strains and mNV only. In this study, it was challenging for RV to form clear and countable plaques with all overlays ((1) SFM supplemented with0.8% agarose, (2) MEM supplemented with 4% sephadex G-75, 200 mM glutamine and 2.5% pancreatin and (3) SFM supplemented with 1% methyl cellulose) that were used. The sizes of the plaques for RV were extremely small to observe and to count by eye at 5 days post-infection. However, mNV was successfully quantified using methyl cellulose overlay at $1.5x10^8$ pfu/ml (Appendix 6.1). Plaque formation was noted at 6 days of post-infection with the virus (RV and mNV).

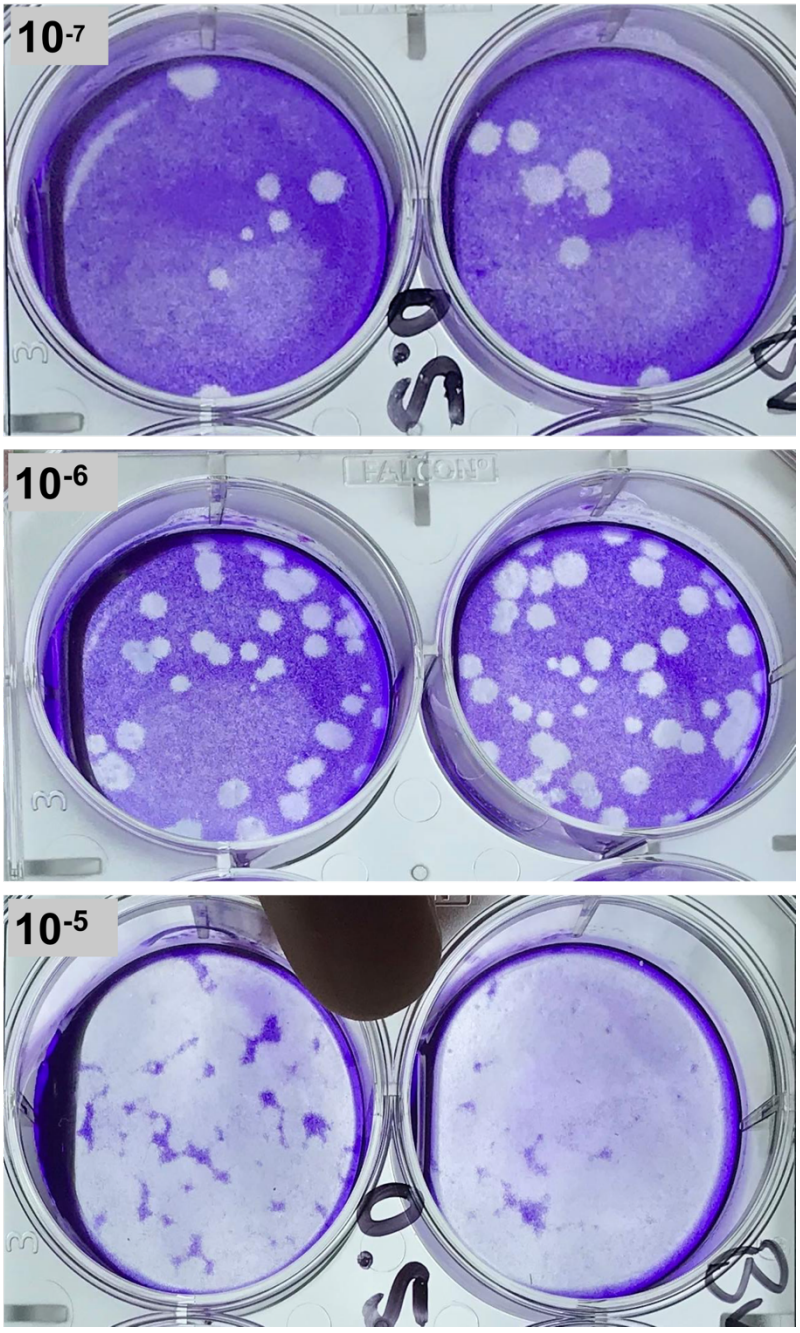

Appendix 6.1. A Plaque assay result using 0.5 mL of mNV strain at 10^{-7}, 10^{-6} and 10^{-5} dilutions on BV2 monolayer at 6-days post infection. Clear zones represent plaques for the virus calculated at $1.5x10^{8}$ pfu/ml.

2. Tissue Culture Infective Dose (TCID) 50%

This test was done on RV strains only. The virus was quantified based on the traditional TCID 50% method, where visible cell rounding, shrinking or floating were considered symptoms of CPE. The CPE were observed in all wells in a virus dilution-dependent manner. The microscopic analysis clearly showed damage to the monolayers due to viral infection. The amount of damage to the monolayer in any sample corresponded to the amount of virus present (0.025 ml). Analysis after removing the supernatant and staining wells with crystal violet showed greatest damage to the monolayer with few or no adhered cells due to viral infection, while the uninfected control displayed healthy monolayers (Appendix 6.2). The estimated TCID 50% for each RV strain are presented in Appendix 6.3.

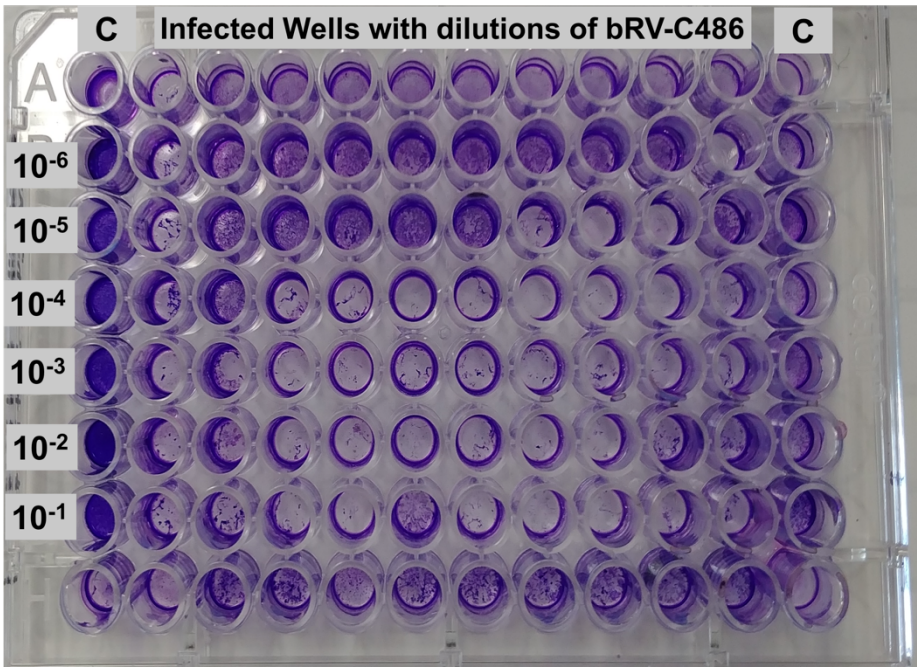

Appendix 6.2. Estimation the titer of bovine rotaviruses strain bRV-C486 by TCID 50%. The MA-104 monolayers were infected with serial dilutions of the virus. After 6-days of post infection, cytopathic effect was visualized under light microscopy. Monolayers were stained with crystal violet, however, monolayers were often washed off. The virus calculated a 9.70E+05 pfu/ml. Left and right columns (C) represent healthy cells.

Appendix 6.3. Quantification of rotavirus strains and murine norovirus by plaque assay and tissue culture infective does in 50% (TCID 50%). Pfu: plaque forming unit. NA: not applied. ND: not determined.

Virus	Plaque Assay (pfu/ml)	TCID50%	
		Log of the dilution in 50%	(pfu/ml)
Murine norovirus	$1.5x10^{8}$	NA	NA
Bovine rotavirus-B223	ND	$9.58x10^{4}$	$6.61x10^{4}$
Bovine rotavirus-C486	ND	$1.41x10^{6}$	$9.7x10^{5}$
Human rotavirus-Wa	ND	$9.57x10^{7}$	$6.6x10^{7}$